The load-bearing capacity of screw piles in silty soils based on mechanical, piezocone and seismic soundings

Lehar Leetsaar

The load-bearing capacity of screw piles in silty soils based on mechanical, piezocone and seismic soundings

Lehar Leetsaar

A doctoral thesis completed for the degree of Doctor of Science (Technology) to be defended, with the permission of the Aalto University School of Engineering, at a public examination held at the lecture hall M1 at Aalto University (Otakaari 1, Espoo, Finland) on 18 October 2024 at 12 noon.

Aalto University
School of Engineering
Deparment of Civil Engineering

Supervising professor

Prof. Leena Korkiala-Tanttu, Aalto University, Finland

Thesis advisor

Prof. Jarek Kurnitski, Tallinn University of Technology, Estonia

Preliminary examiners

Prof. Kenneth Gavin, Delft Universty of Technology, Netherlands
Prof. Priscilla Paniagua, Norwegian University of Science and Tehchnology, Norway

Opponent

Prof. Kenneth Gavin, Delft University of Technology, Netherlands

NORDIC SWAN ECOLABEL

Printed matter
4041-0619

A” Abstract

Author
Lehar Leetsaar

Name of the doctoral thesis
The load-bearing capacity of screw piles in silty soils based on mechanical, pie-zocone and seismic soundings

Publisher School of Engineering

Unit Deparment of Civil Engineering

Series Aalto University publication series DOCTORAL THESES 192/2024

Field of research

Manuscript submitted 13 September 2024   **Date of the defence** 18 October 2024

Permission for public defence granted (date) 8 August 2024   **Language** English

☐ **Monograph**   ☒ **Article thesis**   ☐ **Essay thesis**

Abstract

To accurately determine how piles behave in a particular situation, a static pile loading test is considered the most reliable method, although its implementation is restricted to special cases due to its high cost. In Estonia, the estimation of pile capacity is commonly based on dynamic probing data, specifically collected using the DPSH-A method. Furthermore, certain Estonian investigation companies have started to adopt static-dynamic probing tests. Cone penetration testing and piezocone penetration testing have been used in a limited number of site investigations in Estonia. The direct application of sounding outcomes for the determination of pile load-bearing capacity has emerged as a preferred approach. These methods are called direct methods. Such methods may encounter a drawback when relying on cone penetration testing or standard penetration testing data, as they may provide limited support in identifying the connections between load and settlement relation of the pile. When evaluating the load capacity of piles, it is essential to consider the relationship between load and settlement. Researchers have extensively studied analytical soil models based on stress, strain, and strength data obtained from practical experiments to better understand this connection. The small strain shear modulus is a key parameter in these models, and its determination is often done through the seismic cone penetration test. The load-bearing capacity of screw piles in silty soils has been assessed using mechanical, piezocone, and seismic soundings.

The findings indicated that there was a significant reduction in the variability of the computed outcomes when the sounding was carried out at a depth greater than several meters below the pile base. In terms of the direct methods relying on the cone penetration test, it was discovered that the LCPC method produced the most satisfactory outcomes for Fundex piles. The Briaud and Tucker (1988) method is distinguished among the different standard penetration test methods for its remarkable ability to accurately predict outcomes for Fundex piles. Comparing values from the cone penetration test and static-dynamic probing test for displacement piles and full displacement piles, it was found that the Eurocode 7 method demonstrated the most favorable performance. These studies provide evidence that the three direct methods (Briaud and Tucker (1988), LCPC, and Eurocode 7) all incorporate the s/B=10% failure criterion and have shown satisfactory outcomes. A comprehensive analysis was conducted to investigate the relationship between normalized operative shear stiffness and normalized pseudo-strain for screw piles in silty soil, leading to a highly significant correlation. The load-bearing capacity of screw piles in silty soils exceeds that of other types of piles, particularly in situations with low strain.

The Load-Bearing Capacity of Screw Piles in Silty Soils Based on Mechanical, Piezocone and Seismic Soundings

LEHAR LEETSAAR

TALLINN UNIVERSITY OF TECHNOLOGY
School of Engineering
Department of Civil Engineering and Architecture
This dissertation was accepted for the defence of the degree 08/08/2024

Supervisor: Prof. Leena Korkiala-Tanttu
Dep. of Civil Engineering
Aalto University
Espoo, Finland

Co-supervisor: Prof. Jarek Kurnitski
Dep. of Civil Engineering and Architecture
Tallinn University of Technology
Tallinn, Estonia

Opponent: Prof. Kenneth Gavin
Faculty of Civil Engineering and Geosciences
Dep. of Geoscience & Engineering
Delft University of Technology
Delft, Netherlands

Defence of the thesis: 18/10/2024, Espoo

Declaration:
Hereby I declare that this doctoral thesis, my original investigation and achievement, submitted for the double doctoral degree at Aalto University and at Tallinn University of Technology has not been submitted for doctoral or equivalent academic degree.

Lehar Leetsaar

----
signature

European Union
European Regional
Development Fund

Investing
in your future

Kruvivaiade kandevõime määramine möllides mehaaniliste, piesokoonuste ja seismiliste sondeerimistega

LEHAR LEETSAAR

Kokkuvõte

Vaiade käitumise täpseks määramiseks konkreetsetes olukordades peetakse staatilist vaiakatset kõige usaldusväärsemaks meetodiks, kuigi selle rakendamine on kõrge kulu tõttu piiratud erijuhtudega. Eestis põhinevad vaiade kandevõime hinnangud tavaliselt löökpenetratsioonikatse andmetel, mis on kogutud enamasti DPSH-A löökpenetromeetriga. Lisaks on mõned Eesti uurimisettevõtted hakanud tegema suru-löökpenetromeeterkatseid. Surupenetromeeterkatseid ja piesokoonuskatseid on Eestis geotehnilistes uuringutes teostatud piiratud juhtudel. Otseste sondeerimistulemuste rakendamisest vaiade kandevõime määramisel on saanud eelistatud lähenemisviis. Need meetodid on tuntud ka kui otsesed meetodid. Sellised meetodid võivad surupenetromeeterkatse või standardse penetratsioonikatse andmete kasutamisel pakkuda aga piiratud abi, kuna ei võimalda määrata vaia koormuse ja vajumi seoseid täpselt. Vaiade kandevõime hindamisel on oluline arvestada koormuse ja vajumi vahelist seost. Teadlased on põhjalikult uurinud analüütilisi pinnase mudeleid, mis põhinevad pinge, suhtelise deformatsiooni (pine) ja tugevuse andmetel, mis on saadud praktilistest katsetest, et paremini mõista seda seost. Väikeste deformatsioonide nihkemoodul on nende mudelite oluline parameeter, mille määramine toimub sageli seismilise koonuse sondeerimisel pinnasesse. Möllides on kruvivaiade kandevõimet hinnatud mehaaniliste, piesokoonuskatsete ja seismiliste sondeerimistega.

Uuringud näitasid, et surupenetromeeterkatse või löökpenetromeeterkatse läbiviimisel sügavusel, mis ületab vaia põhja tasapinda mitmed meetrid, vähenes arvutatud vaia kandevõime tulemuste varieeruvus oluliselt. Otseste meetodite osas, mis põhinevad surupenetromeeterkatsel, selgus, et LCPC-meetod pakkus Fundex vaiade analüüsimiseks kõige paremaid tulemusi. Briaudi ja Tuckeri (1988) meetod eristub erinevate standardsete penetratsioonikatsete andmetel põhinevate otseste meetodite seas oma erakordse võime poolest täpselt ennustada Fundex vaiade kandevõime tulemusi. Kui võrrelda surupenetromeeterkatse ja suru-löökpenetromeeterkatse põhjal arvutatud vaia kandevõime väärtusi pinnast tõrjuvate ja pinnast täielikult tõrjuvate vaiade puhul, leiti, et Eurocode 7 meetod näitas kõige paremaid tulemusi. Need uuringud viitavad asjaolule, et kolm otsest meetodit (Briaud ja Tucker (1988) meetod, LCPC-meetod ja Eurocode 7 meetod) sisaldavad kõik s/B=10% vaia kandevõime piiri kriteeriumit ning pakkusid rahuldavaid vaia kandevõime tulemusi. Uuringus analüüsiti kruvivaiade normaliseeritud operatiivse lõikejäikuse ja normaliseeritud

pseudo-pine suhet möllides, mille tulemusena esitati töös väga oluline korrelatsioon. Kruvivaiade kandevõime ületab teiste vaiatüüpide kandevõimet möllides, eriti madala pine tingimustes.

Acknowledgements

Contents

List of Abbreviations and Symbols

a	net cone area ratio
A_b	pile base area
A_c	cross sectional area of CPT cone
A_n	cross-sectional area of the load cell or shaft of CPTu cone
A_s	surface area of pile or sleeve area of CPT cone
$A_{s,i}$	outer pile shaft area
A_t	cross-section area of pile
C	factor of pile end bearing resistance
C_1	factor of pile end bearing resistance
C_2	factor of pile end bearing resistance
C_c	compression index
COV	coefficient of variation
CPT	cone penetration test
CPTu	piezocone penetration test
C_{se}	factor of pile unit shaft friction
C_{te}	factor of pile end bearing resistance
c_v	coefficient of consolidation
d	diameter of the pile
d	diameter of the sounding probe
D	diameter of the pile
d_b	pile base diameeter
D_b	pile base diameeter
DCPT	dynamic cone penetration test

D_{eg}	equivalent diameeter of the pile base
DMT	dilatometer test
DP	dynamic probing
DPH	dynamic probing heavy
DPL	dynamic probing light
DPM	dynamic probing medium
DPSH	dynamic probing super heavy
DPSH-A	dynamic probing super heavy type A
DPSH-B	dynamic probing super heavy type B
D_r	relative density of sand
d_s	pile shaft diameeter
D_s	pile shaft diameeter
DSP	displacement pile
d_t	diameter of the rod of the sounding probe
d_t	outer diameeter of the sounding rod
E	Young's modulus
E_p	elastic modulus of pile
f	factor of modified hyperbola of soil stiffness
FDP	full displacement pile
f_{pi}	unit shaft resistance of the pile
FS	factor of safety
f_s	measured cone sleeve friction
FVT	field vane test
g	factor of modified hyperbola of soil stiffness
G	operative shear modulus
G/G_{max}	operative shear stiffness
G_o	operative soil shear modulus at the pile top
G_o	small strain shear modulus
G_b	soil shear modulus below pile base
G_L	operative soil shear modulus at pile base

G_M	operative soil shear modulus at mid of pile embedment depth
G_{max}	small strain shear modulus
HfA	Swedish ram-sounding
K	factor of pile end bearing resistance
K	permeability
K_o	lateral stress ceofficient
k_b	factor of pile end bearing resistance
K_f	function of the CPT cone sleeve resistance
k_n	statistical coefficient
K_p	standard factor for SDT
k_s	factor of pile unit shaft friction
L	length of pile
L_1	first distance between SCPTu geophone and steel plate
L_2	second distance between SCPTu geophone and steel plate
M	constrained modulus
MCS	Monte Carlo simulation
M_{tot}	total torgue value of SDT
n	number of sounding measurements
N_{20}	number of blows required to drive the penetrometer over 20 centimeters
N_{30}	number of blows required to drive the penetrometer over 30 centimeters
N_b	factor of pile end bearing resistance
N_c	factor of pile end bearing resistance
N_{gb}	geometric average of N values between 8d above and 4b below pile base
N_{gs}	geometric average of N values along the pile
N_{kt}	factor of pile end bearing resistance and unit shaft friction
N_n	net stroke rate [l/0.2 m] of SDT
n_s	factor of pile type
N_s	factor of pile unit shaft friction

OCR	over-consolidation ration
p	perimeter of pile
PMT	pressuremeter test
Q	load applied at the pile top
Q_b	pile base load
q_b	unit base resistance of the pile
q_c	measured cone tip resistance
$Q_{c,CPT}$	cone tip resistance of CPT
q'_{ca}	is the mean value of q_c between 1.5d above and below pile base
q_E	effective cone resistance
q_{Eq}	is the geometric average of q_c
$q_{eq(tip)}$	is the average of q_c values
$Q_{n,SDT}$	net resistance to static pressure penetration of SDT
Q_s	pile shaft load
q_s	unit skaft friction of the pile
$q_{s,i}$	unit shaft friction of the pile
$q_{s,k}$	ultimate limit state value of pile skin friction
$q_s(z)$	unit skin friction of the pile
Q_t	applied top load on pile
q_t	total cone resistance
Q_{tot}	total compressive force of SDT
Q_{ult}	load equal to the ultimate bearing capacity of the pile
r_o	radius of pile shaft
R^2	R-squared (coefficient of determination)
r_b	pile base radius for underreamed piles
R_b	pile base resistance
R_c	axial static compression resistance of a single pile
R_f	friction ration of CPT cone
r_m	maximum radius of influence around the pile
R_s	pile shaft resistance

r_t	unit pile base rsistance
s	factor that takes into account the shape of the bottom of the pile
S	shear waves
SCPT	seismic cone penetration test
SCPTu	seismic piezocone penetration test
SDMT	seismic dilatometer test
SDT	static-dynamic probing test
SPT	standard penetration test
s_g	limit settlement of pile
s_u	undrained shear strength
s_x	standard deviation of the n sample test results
z	depth below the ground surface
t_1	time interval in the first SCPTu test
t_2	time interval in the second SCPTu test
u_o	hydrostatic (porewater) pressure
u_1	porewater pressures measured midface of cone tip
u_2	porewater pressure measured at shoulder position
u_3	porewater pressure measured behind the sleeve
w	settlement at the pile top
V_s	shear wave velocity
w_t	displacement at pile top
V_x	coefficient of variation of the parameter X
X_k	characteristic value of the parameter X
X_{mean}	arithmetical mean value of the parameter X

Greek Letters

α	factor of pile unit shaft friction
α1	coefficient of pile typology and intallation method
$α_p$	factor of pile end bearing resistance
$α_s$	factor of pile unit shaft friction

β	factor of pile unit shaft friction
β	factor that takes into account the shape of the pile base in EC7 method
β_1	exponent of pile typology and intallation method
γ	shear strain
$\gamma_p/\gamma_{p\text{-}ref}$	normalized pseudo-strain
γ_s	shear strain
γ_t	total unit weight
ΔL	change of geophone position in SCPTu test
Δt	time interval in SCPTu test
ε	strain
ζ	measure of influence radius
η	factor for underreamed piles that take greater loads at the pile base
λ	pile-soil stiffness ratio
μ_1	device-specific constant for SDT
ν'	Poisson's ratio of soil in drained conditions
ν_s	Poisson's ratio of soil
ξ	factor for end bearing piles resting on stiffer stratum
ρ	total mass density of the soil
ρ_E	modulus variation factor
σ	stress
τ	shear stress
τ_{max}	maximum shear stress
φ'	peak friction angle
ψ	soil state parameeter

List of Publications

This doctoral dissertation consists of a summary of the following publications, which are referred to in the text by their numerals.

1. Leetsaar, Lehar; Korkiala-Tanttu, Leena; Kurnitski, Jarek. 2022. CPT, CPTu and DCPT Methods for Predicting the Ultimate Bearing Capacity of Cast In Situ Displacement Piles in Silty Soils. Springer. *Geotechnical and Geological Engineering*. 10.1007/s10706-022-02292-6.

2. Leetsaar, Lehar; Korkiala-Tanttu, Leena. 2023. Deterministic and Probabilistic Analyses of the Bearing Capacity of Screw Cast in Situ Displacement Piles in Silty Soils as Measured by CPT and SDT. *The Baltic Journal of Road and Bridge Engineering*. 10.7250/bjrbe.2023-18.600.

3. Leetsaar, Lehar; Korkiala-Tanttu, Leena. 2024. Advantages of using a seismic piezocone penetration test for analysis of a single screw in situ displacement pile in silty soils. *Indian Geotechnical Journal*. 10.1007/s40098-024-00942-5.

Author's Contribution

Publication 1: CPT, CPTu and DCPT Methods for Predicting the Ultimate Bearing Capacity of Cast In Situ Displacement Piles in Silty Soils

The author collected the data, performed the statistical analysis, and wrote the article. Korkiala-Tanttu commented on the article and supervised the research. Kurnitski commented on the article.

Publication 2: Deterministic and Probabilistic Analyses of the Bearing Capacity of Screw Cast in Situ Displacement Piles in Silty Soils as Measured by CPT and SDT

The author collected the data, performed the statistical analysis, and wrote the article. Korkiala-Tanttu commented on the article and supervised the research.

Publication 3: Advantages of using a seismic piezocone penetration test for analysis of a single screw in situ displacement pile in silty soils

The author collected the data, performed the statistical analysis, and wrote the article. Korkiala-Tanttu commented on the article and supervised the research.

1. Introduction

1.1 Background and motivation

Soil, unlike other building materials such as concrete or steel, is an anisotropic material. Soil properties vary very much between different layers and even inside one layer. Before starting construction upon or inside ground sufficient information of soil behaviour is needed. There are always the questions about how much and what kind of investigations should be made. For buildings constructed onto soft soils commonly pile foundation would be the only and the right solution. The most accurate information how pile behaves in a certain case could be figured out using a static pile loading test. As the test is expensive it is used only in special cases. In Estonia pile capacity calculations are often based on sounding data obtained by dynamic probing (DP), especially by the DPSH-A method. This sounding technique is quick, and it can reach significant depths by using small-sized devices. In addition, Estonian geotechnical companies refer to the fact that DPSH-A complies with Swedish standard EVN 1997-3; 1005 for Swedish ram-sounding (HfA). According to Bergdahl and Ottosson (1998), the literature reports on HfA, stating that the device receives the same number of blows, N_{20}, as the standard penetration test (SPT) device records blows, N_{30}. Unfortunately, no local tests have been conducted to substantiate the accuracy of the correlation. Therefore, standard penetration test (SPT) correlations with DPSH-A sounding data are used in Estonia. However, erroneous outcomes may arise when employing DPSH-A in fine-grained soils or below the groundwater level (Gadeikis et al., 2010; Žaržojus, 2010). There are many example cases where this approach has led to over-designed foundations.

Cone penetration testing (CPT) or even piezocone penetration testing (CPTu) has been employed in Estonia for a limited number of site investigations. This method offers consistent, replicable and dependable data. Nevertheless, in certain instances, the utilization of anchoring or a larger reaction mass becomes necessary to penetrate deeper layers during CPT. Compared to DPSH-A sounding, CPT is relatively slower, and the required equipment is more expensive. Additionally, both customers and designers lack comprehensive understanding of the extent to which CPT can yield better soil data in comparison to DPSH-A.

Also the static-dynamic probing test (SDT) has been adopted by some Estonian investigation companies. This method, commonly used in the Nordic countries, combines both static and dynamic penetration tests. In the SDT method, the probe is pushed until it reaches the upper anchoring resistance. Once this resistance is reached, the denser layers are penetrated using dynamic blows. If

there is a weaker layer beneath the denser layer and the anchoring is sufficient, the probing can be continued by pushing the probe further. Furthermore, Rantala and Halkola (1997) established correlations between SDT and CPT results. This makes SDT a viable alternative in cases where the CPT method is unable to penetrate the required depth, particularly in fine-grained soils.

As in Tallinn, the capital city of Estonia, many buildings, including those with several dozen storeys, are erected, the survey areas were selected from Tallinn. The geological conditions in the Tallinn area exhibit significant variations. In some regions the average thickness of soil layers is only one metre above a hard limestone stratum. Conversely, other areas feature a complex network of ancient valleys that intersect with the hard stratum. These valleys are concealed beneath dense fluvioglacial sands as well as soft limnoglacial and marine clayey sediments, which can reach thicknesses of several tens of metres (Arbeiter, 1962; Map applications of the Estonian Land Board, 2020). Two ancient valley areas were included in the research. Mostly in such geological conditions, it is necessary to use piles beneath buildings. Bored piles and displacement piles are commonly utilized in Estonia (Mets et al., 2016). Due to the variety of soil types and pile installation techniques, predicting the vertical bearing capacity of the pile is typically difficult.

Niazi (2014) presented four alternatives for interpreting the pile axial geotechnical capacity based on in situ investigations (Figure 1). In this research, three of the four alternatives have been used in the analysis: correlation (empirical methods), statistics (analytical methods) and full-scale load test (experimental tests). Numerical methods should be included in subsequent research.
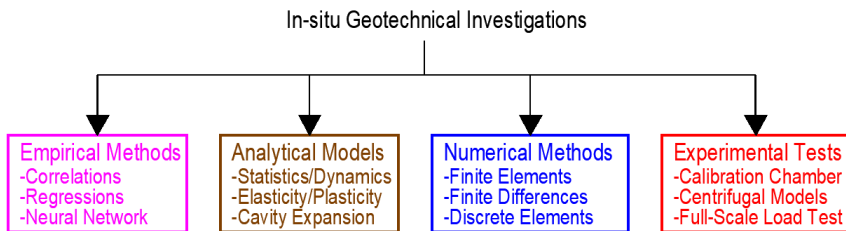
Figure 1. Alternatives to interpret axial pile response from in situ geotechnical investigations (Niazi, 2014).

With the analytical method, the axial static compression resistance of a single pile (R_c) is determined by summarizing the pile base resistance (R_b) and shaft resistance (R_s), Formula 1 is specified in (EN 1997-2:2007):

$$R_c = R_b + R_s = q_b \cdot A_b + \sum_{i=1}^{n} q_{s,i} \cdot A_{s,i} \tag{1}$$

The value of R_b is found by multiplying the unit end bearing or base resistance (q_b) by the pile base area (A_b). The value of R_s is obtained by summing up the product of the unit shaft friction ($q_{s,i}$) and the outer pile shaft area (A_{si}) for each

soil layer. Finally, the pile's own weight load is subtracted from the design value of pile capacity.

To find out the geological conditions for construction, The number of in situ tests has increased over the years compared to laboratory tests. Simultaneously, there has also been an increase in the use of empirical load-bearing capacity methods of the piles based on the results of soundings performed on the site (Eslami et al., 1997; Cai et al., 2012; Moshfeghi et al., 2016). Methods in which the results of sounding are used directly to calculate the load-bearing capacity of the pile have become preferable. Such methods are called direct methods (Niazi et al., 2013). Most of all, direct methods are composed for CPT results (e.g., Nottingham, 1975; Schmertmann, 1978; de Ruiter and Beringen, 1979; Bustamante and Gianeselli, 1982; Eslami and Fellenius, 1997; Kempfert and Becker, 2010). One of the reasons for this is that the cone penetrometer can be regarded as a mini-pile foundation (Bandini and Salgado, 1998; Mayne, 2007; Jardine et al., 2013). Several direct methods have also been proposed for the standard penetration test (SPT). One drawback of direct methods based on CPT(u) or SPT data can be highlighted as limited assistance in identifying the relations of load and settlement of the pile.

The load–settlement (Q–w) relationship of piles is a crucial factor to consider when determining the pile load capacity. Researchers are increasingly investigating the potential of using in situ test results to analyse pile Q–w relationships. To achieve this, many researchers have studied analytical stress–strain–strength soil models that are derived from actual measurements. Some of these researchers include Mayne and Poulos (2001), Berardi and Bovolenta (2005) and Niazi (2014).

The relationship between piles and Q–w performance is significantly influenced by soil heterogeneity. According to Cooke et al. (1979), the operative shear modulus (G) is the most important factor that affects the Q–w performance of a pile under loading. In addition, the use of shear modulus (G) is preferred over Young's modulus (E) in pile Q–w analysis due to two reasons: (1) the shear modulus is often not affected by whether the loading is in undrained or drained conditions, and (2) the soil mainly deforms in shear along the pile shaft (Niazi, 2014).

The determination of a small strain shear modulus (G_{max} or G_o) is commonly achieved by using the measured shear wave velocity (V_s). The assessment of V_s in situ is predominantly conducted applying seismic non-destructive tests such as multi-channel analysis of surface waves, crosshole seismic testing, or uphole and downhole methods. An alternative method for measuring V_s is the implementation of the seismic cone penetration test with the option of employing either crosshole or downhole testing techniques.

The utilization of V_s values in soil calculations is becoming increasingly prevalent. Due to the limited use of the seismic piezocone penetration test (SCPTu) in numerous countries, establishing correlations between CPTu and V_s would be highly beneficial. Extensive research conducted by various scientists (Hegazy

and Mayne, 1995; Mayne, 2006; Trevor et al., 2010; Holmsgaard et al., 2016) across the globe has resulted in the development of correlations between CPTu readings and V_s values. These correlations have been proposed for different types of soils or specific soil conditions. However, it is imperative to assess the effectiveness of these existing correlations in diverse soil conditions and, if necessary, formulate new correlations.

Mayne (2013) suggests adopting nonlinear load-displacement-capacity behaviour for bored pile foundation calculations. For geotechnical parameter input, seismic piezocone penetration tests (SCPTu) are a most efficient and economical means because the penetrometer readings provide data for assessing the capacity of side and base components, while the shear wave velocity provides the fundamental stiffness for displacement analyses. Nonlinear stiffness parameters are obtained and used in foundation design involving shallow footings and pile foundations. Niazi and Mayne (2013) concluded that any future work on pile–CPT correlations must attempt to include all soil types in general and clays, silts and mixed soil types, in particular. Optimal use of all the readings of SCPTu must be exploited for tying them together with the complete axial pile response. During the last decade SCPTu has been more and more often successfully used worldwide in very many different soils (Hegazy and Mayne, 1995; Mayne, 2000; Mayne, 2006; Trevor et al., 2010; Tonni et al., 2013; Niazi et al., 2015; Holmsgaard et al., 2016; Duan et al., 2018; Molina-Gómez et al., 2021; Zhang et al., 2022). The applicability and usefulness of DP, CPT, CPTu and SCPTu are provided in Table 1.

Table 1. The applicability and usefulness of in situ tests (Lunne et al., 1997; updated by Robertson, 2012).

Group	In-situ Test	Geotechnical Parameter												Ground Type					
		Soil type	Profile	u_0	OCR	$D_R\text{-}\psi$	ϕ'	s_u	$G_0\text{-}E$	$\sigma\text{-}\varepsilon$	$M\text{-}C_c$	k	c_v	hard rock	soft rock	gravel	sand	silt-clay	peat-organic
Penetrometer/ Direct Push	Dy. Probing (DP)	C	B	-	C	C	C	C	C	-	-	-	-	-	C	B	A	B	B
	SPT	B	B	-	C	B	C	B	C	-	-	-	-	-	C	B	A	B	B
	CPT	B	A	-	B	B	B	B	B	C	C	-	-	-	B	B	A	A	A
	CPTu	A	A	A	B	B	B	A	B	C	B	A	A	-	B	B	A	A	A
	SCPTu	A	A	A	A	A	B	A	A	B	B	A	A	-	B	B	A	A	A
	DMT	B	B	B	B	C	B	B	B	C	B	C	B	-	C	C	A	A	A
	SDMT	B	B	B	A	B	B	B	A	B	B	C	B	-	C	C	A	A	A
	Full-flow (T/ball)	C	B	B	B	C	C	A	C	C	C	C	C	-	-	-	C	B	A
	Field vane (FVT)	B	C	-	B	-	-	A	-	-	-	-	-	-	-	-	C	A	A
Pressuremeter	Pre-bored	B	B	-	C	C	C	B	B	C	C	-	C	A	A	B	B	B	B
	Self-bored	B	B	A[1]	B	B	B	B	A	A	B	B	A[1]	A	C	B	B	A	B
	Full-displacement	B	B	B	C	C	C	B	A	A	B	B	A	C	C	-	B	A	A
Other	Screw/plate load	C	-	-	B	C	C	B	B	B	B	C	C	C	A	B	C	C	B
	Borehole shear	C	-	-	-	-	B	C	-	-	-	-	B	C	B	C	C	C	-
	Permeameter	C	-	A	-	-	-	-	-	C	-	A	-	A	A	A	A	A	B
	Borehole seismic	C	C	-	B	C	-	-	A	C	-	-	-	A	A	A	A	A	B
	Surface seismic	-	C	-	B	C	-	-	A	C	-	-	-	A	A	A	A	A	A
	Hydraulic fracture	-	-	B	-	-	-	-	-	-	-	C	C	B	B	-	-	B	C

Applicability: A = high, B = moderate, C = low, - = none

Geotechnical parameters: u_0 = in-situ static pore pressure, OCR = over-consolidation ratio, D_R-ψ = relative density and/or state parameter, ϕ' = peak friction angle, s_u = undrained shear strength (peak and/or remolded), G_0-E = small strain shear and/or Young's modulus, σ-ε = stress-strain relationship, M-C_c = constrained modulus and/or compression index, k = permeability, c_v = coefficient of consolidation

ϕ' will depend on soil type; [1] only when pore pressure sensor fitted

With the growing significance of reliability and economic considerations in design, particularly in relation to the latest design codes worldwide, the application of the reliability-based design (RBD) method has gained prominence in assessing the load-bearing capacity of piles. To determine the load-bearing capacity of pile using the RBD method, a Monte Carlo simulation (MCS) approach was employed, involving 10,000 simulations. This methodological approach allows for a comprehensive analysis of the pile design's reliability and economic requirements.

In conclusion, it is essential to figure out how DPT, SDT, CPT and SCPTu data correlate to real behaviour of piles in Estonia. This study focused on three research sites in Tallinn dominated by silty soils. Eleven statically tested casts in place displacement piles (screw piles) were included in the study. The study examined seven Fundex piles, two displacement piles (DSP) and two full displacement piles (FDP). The investigation of the benefits offered by contemporary sounding techniques in assessing the load-bearing capacity of a pile compared to traditional methods is imperative. It is crucial to ascertain the extent to which newer sounding methods outperform older techniques in this regard. After conducting numerous static pile load tests and soundings in parallel, it could be enough to do only soundings to get sufficient data for predicting $Q–w$ performance of the piles in the future.

1.2 Research problem

The utilization of in situ tests to ascertain the load-bearing capacity of piles is a widely employed method. However, in Estonia, there is a lack of correlations between the load-bearing capacity of piles and the sounding data obtained. This discrepancy is particularly evident in challenging soil conditions, such as those found in ancient valleys, where accurately determining the load-bearing capacity of a pile remains a significant challenge. To achieve this goal, the following Research Questions regarding CPT, CPTu, SCPTu, DCPT and SDT sounding data and static pile load data based on three types of cast in situ displacement piles (screw piles) such as Fundex, DSP and FDP piles in silty soils were defined:

1. Do the results obtained from sounding the CPT using a truck-mounted 200kN CPT unit and an anchored-type light CPT unit yield similar outcomes? Moreover, which of these devices has the capability to penetrate to greater depths?
2. Is it feasible to use CPT devices in Estonia to reach the depths, or potentially deeper, of the bottom of piles situated in silty soils above primeval valleys?
3. What are the alternative sounding methods for determining the load-bearing capacity of the pile next to the CPT for piles longer than 10 m in silty soils?

4. Can SDT probing data be converted to CPT q_c readings in silty soils?
5. What pile load capacity results are provided by the direct CPT methods based on CPT, CPTu and SDT sounding data compared to pile static test results of screw piles in silty soils?
6. Could DCPT probing data be used in SPT's direct methods for determining pile load capacity of screw piles in silty soils?
7. Do the direct methods of CPT and SPT offer comparable results for three different screw piles (Fundex, DSP and FDP) in silty soils?
8. How much do the load-bearing capacities of the pile differ from reliability-based design and statistical determination based on the LCPC direct method of the DSP and FDP piles?
9. What advantages does SCPTu sounding offer compared to CPT and CPTu soundings in determining pile load-bearing capacity?
10. What dependence of the reduction of the G modulus on the increase in strain could be used for screw piles in silty soils?
11. Which V_s values dominate in silty soils at the three study points, and do these values overlap with those proposed by other researchers?
12. Which CPT$-V_s$ correlation provides the best results for the silty soils in Estonia?

1.3 Objectives and scope

To address the research questions, a set of objectives were formulated:

1. Compare CPT readings of a truck-mounted 200 kN unit and an anchored lightweight CPT device applied at the same study site.
2. Compare CPT sounding depths with parallel tested piles on three sites above primeval valleys in silty soils in Estonia.
3. Apply CPT, CPTu and SDT readings to direct CPT methods and apply DPSH-A readings in SPT direct methods to determine pile load-bearing capacity and compare results with static pile load test results.
4. Compare the load-bearing capacities of DSP and FDP piles using the LCPC direct method and MCS in parallel with statistical methods for processing sounding data.
5. Analyse $Q-w$ relation curves based on G values and analytical elastic solution proposed by Randolph and Wroth (1978, 1979) for pile$-$soil interaction.
6. Compare the results of four CPT$-Vs$ correlations in three test sites in parallel with the three new correlations proposed in the current study.

Finding the load-bearing capacity of three types of screw piles (Fundex, DSP and FDP) by direct methods of CPT and SPT and comparing the results with the results of the static pile load test in silty soils above primeval valleys is the main

topics of the dissertation. This topic also explores whether DPSH-A readings can be used in SPT's direct methods for determining the load-bearing capacity of a screw pile in silty soils. The advantages of the SCPTu probe in predicting the load-bearing capacity of the screw pile compared to the probing methods mainly used in Estonia such as DPSH-A, SDT and CPT, are the second main topic of the dissertation. The analysis is limited to an analytical elastic solution based on the theory of Randolph and Wroth (1978, 1979). In addition, the correlation between normalised operative shear stiffness (G/G_{max}) and normalised pseudo-strain (γ_p/γ_{p-ref}) is found in pile back-calculations. A secondary topic is finding the load-bearing capacity of the screw piles based on reliability design and statistical determination of sounding data according to Eurocode 7 (EN 1997-2:2007). Monte Carlo simulation is the only Reliability-based design method.

1.4 Dissertation structure

This dissertation is structured as follows:

Chapter 2:   Axial pile capacity evaluation from CPT and SPT data (Publications 1 and 2).

Chapter 3:   Settlement analysis for screw piles based on SCPTu data (Publication 3).

Chapter 4:   Probabilistic and deterministic analyses of the bearing capacity of screw piles in silty soils (Publication 2).

Chapter 5:   Empirical correlations between V_s and CPTu (Publication 3).

Chapter 6:   Test data and data analysis. The results provide answers to Research Question 3 (Publications 1–3).

Chapter 7:   Test sites. The results provide answers to Research Questions 1 to 4 and 11 (Publications 1–3).

Chapter 8:   Comparison of axial capacity of the piles based on CPT and SPT direct methods. The results provide answers to Research Questions 4 to 8 (Publications 1 and 2).

Chapter 9:   Axial elastic response of a single screw pile in silty soils based on SCPTu data. The results provide answers to Research Questions 9 and 10 (Publication 3).

Chapter 10:   Empirical correlation results between V_s and CPTu in silty soils. The results provide answers to Research Question 12 (Publication 3).

Chapter 11:   Discussion.

Chapter 12:   Conclusions and recommendations for future work.

2. Axial pile capacity evaluation from CPT and SPT data

2.1 Direct approaches to define pile capacity

There are two primary methodologies that have emerged for determining the pile capacity based on CPT/CPTu or SPT readings: indirect and direct methods. In order to estimate pile bearing capacity indirect penetration methods at first employ soil parameters, for instance friction angle and undrained shear strength achieved from cone data. Then these strength parameters with formulas of semiempirical and theoretical methods are used to calculate the unit end bearing capacity of the pile (q_b) and the unit skin friction of the pile (q_s). Indirect methods are considered as more rational as their formulation has been founded on well-developed theories. However, direct methods offer more convenience in their straightforward approach (Niazi, 2014). Many researchers have pointed out that indirect methods are rarely used and particularly are not suitable for use in engineering practice (Eslami 1997; Cai et al., 2009, 2011; Benali et al., 2013; Wrana 2015). Indirect methods will no longer be referred to by the author.

In direct cone penetration methods based on CPT readings, the cone sleeve friction is utilized to calculate the unit shaft resistance, whereas the cone resistance is employed to determine pile axial bearing capacity (Mayne, 2007). Direct SPT methods apply N values with some modification factors to ascertain the unit shaft resistance and unit end bearing resistance of the pile (Publications 1 and 2).

2.1.1 Direct approaches for CPT and CPTu soundings

The CPT cone and pile are influenced in a similar manner by the mean effective stress, compressibility and rigidity of the surrounding soil medium (Eslami and Fellenius, 1997; Ardalan et al., 2009). In the process of establishing direct methods CPT readings are simply scaled up and used to evaluate the load-bearing capacity of full-scale piles (Niazi and Mayne, 2013). This concept draws an analogy between the cone penetrometer and a model pile. And it has led to the development of many direct CPT methods around the world. Over 30 distinct direct methods based on CPT and CPTu have been developed (Niazi and Mayne, 2013). In the current investigation, six direct methods were employed: five CPT methods and the Unicone method, which is based on CPTu results. The CPT methods are

- the Nottingham and Schmertmann method (1975, 1978),
- de Ruiter and Beringen method (1979),
- LCPC method (1982; 1997),
- Eurocode 7 (EN 1997-2:2007) method and
- German method (EA-Pfähle, 2014).

The Unicone method (Eslami and Fellenius 1995, 1996, 1997; Fellenius and Eslami 2000; Eslami 1996; Fellenius 2020) stands out as an exceptional technique due to its utilization of all three readings of the CPTu sounding (q_c is cone tip resistance, f_s is cone sleeve friction and u_2 is porewater pressure measured at shoulder position) in the analysis of pile load-bearing capacity. Furthermore, the Unicone method has introduced a novel soil profiling chart.

The selection of these methods was based on their suitability for various soil types and a broad range of piles, except for the German method (EA-Pfähle, 2014), which is specifically designed for sandy soils. In this study, these methods were applied to piles installed in silty soils. A summary of CPT(u) methods used is presented in Table 2.

Nottingham (1975) provided calculation formulas and charts for different types of piles in sand and clay. His studies were based on 108 load tests on large model piles. In addition, he investigated the applicability of both mechanical and electrical penetrometers to determine the bearing capacity of displacement piles. Schmertmann (1978) clarified the method by adding some refinements to limiting q_b values for different soil types and some non-displacement piles. The resistance unit, r_t, represents an average value obtained from the cone resistance within a specific influence zone. This zone extends to a distance of 8 times the pile diameter above the pile base. The exact range within this influence zone is either 0.7 times the pile diameter or 4 times the pile diameter, as illustrated in Figure 2.

Table 2. Summary of direct CPT-based pile design methods (modified after Publication 1).

Method/reference	Design formulas	
	Pile unit shaft friction	Pile end bearing resistance
	(q_s)	(q_b)
Nottingham (1975) and Schmertmann (1978) (for driven concrete, steel and timber piles, and drilled shafts in all soil types)	In clay: $q_s = K_f \cdot f_s \leq 120$ kPa, $K_f = 0.2$–1.25 K_f is a function of the sleeve resistance In sand: $q_s = c_s \cdot q_c$ or $f_p = k \cdot f_s$	$q_b = C \cdot q_{ca} \leq 15$ MPa (in sands) and 10 MPa (in very silty sands) $C = 0.5$–1.0 depending on overconsolidation rate (OCR) $q_{ca} = (q_{c1} + q_{c2})/2$

	c_s = 0.8–1.8%, k = 0.8–2.5	
Dutch method (de Ruiter and Beringen, 1979) (for offshore piles in all soil types)	In clay: $q_s = \alpha \cdot s_u \leq 120$ kPa; α = 1 for NC clay and 0.5 for OC clay; $s_u = q_{ca}/N_{kt}$; N_{kt} = 15–20 In sand: $q_s = \min[f_s, q_c/300$ for compression, $q_c/400$ for tension, 120 kPa]	In clay: $q_b = N_c\, s_u \leq 15$ MPa, $s_u = q_{ca}/N_{kt}$, N_c = 9; N_{kt} = 15–20; $q_{ca} = (q_{c1} + q_{c2})/2$ In sand: similar to Nottingham (1975) and Schmertmann (1978) method
LCPC or French method (Bustamante and Gianeselli. 1982; Bustamante and Frank, 1997) (for all pile types in all soil types). Failure criteria: penetration of pile head equal 10% of pile diameter	$q_s = q_{side}/k_s \leq f_{p(max)}$ k_s = 30–150 depending on soil type, pile type and installation procedure	$q_b = k_b \cdot q_{eq}$ depending on soil types: k_b = 0.15–0.375 for non-displacement piles k_b = 0.375–0.60 for displacement piles
EUROCODE 7 (EN 1997-2:2007) (for all pile types in all soil types). Failure criteria: penetration of pile head equal 10% of pile diameter	$q_s = \alpha_s \cdot q_{c,z}$ α_s = 0.005–0.030 depending on soil type or pile type and installation procedure	$$q_b = 0.5 \cdot \alpha_p \cdot \beta \cdot s \left\{ \frac{q_{c,I,mean} + q_{c,II,mean}}{2} + q_{c,III,mean} \right\}$$ $q_{b,max} \leq 15$ MPa; α_p = 0.6–1.0 depending on soil type, pile type and installation procedure; β factor that takes into account the shape of the pile base; s factor that takes into account the shape of the bottom of the pile

German method (EA-Pfähle, 2014) (for piles in sandy soils)	Provides upper and lower bound estimates of q_s (kPa) based on q_c (measured in MPa)	Provides upper and lower bound estimates of q_b (MPa) based on q_c (measured in MPa)
Unicone method (Eslami and Felle-nius, 1995, 1996; Fellenius and Es-lami, 2000; Eslami 1996; Fellenius, 2020)	$q_s = C_{se} \cdot q_E$ $q_E = q_t - u_2$ $C_{se} = 0.8–8\%$ (see Fig. 4 for C_{se}) $q_s = C_{se} \cdot q_E$	$q_b = C_{te} \cdot q_{Eg}$; q_{Eg} is the geometric average of q_c C_{te} is generally taken as 1; for pile diameter $d >$ 0.4 m $C_{te} = 1/(3d)$

$$q_{ca} = \frac{q_{c1} + q_{c2}}{2}$$

q_{c1} = Average q_c over a distance of yD below the pile tip (path a-b-c). Sum q_c values in both the downward (path a-b) and upward (path b-c) directions. Use actual q_c values along path a-b and the minimum path rule along path b-c. Compute q_{c1} for y values from 0.7 and 4.0 and use the minimum q_{c1} values obtained.

q_{c2} = Average q_c over a distance of 8D above the pile tip (path c-e). Use the minimum path rule as for path b-c in the q_{c1} computations. Ignore any minor 'x' peak depressions if in sand, but include in minimum path if in clay.
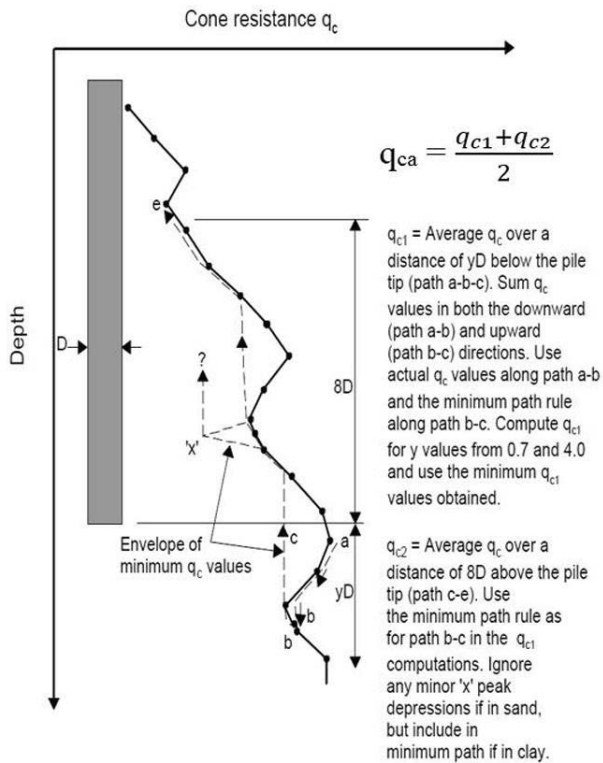
Figure 2. Scmertmann's rules for determining the influence zone for toe resistance adapted from Titi and Murad (1999).

De Ruiter and Beringen (1979) proposed a CPT-method based on pile foundations in the North Sea. This method is also known as the Dutch method or the European method. In sand the pile q_b is calculated similarly to the Scmertmann method, while q_s is calculated using the shaft resistance values of the soil layers f_s and q_c. In clay, pile calculations are based on undrained shear strength (s_u) which is first determined from q_c values. Upper limits for q_b and q_s are imposed.

The method of Bustamante and Gianeselli (1982) is based on 197 full-scale static load tests in different soils including silts. Tests were performed on both non-displacement and displacement piles. This method is generally known as the Laboratoire Central des Ponts et Chausées (LCPC) method or the French method. In this method only q_c readings are employed to calculate the toe and shaft resistance of the pile. Upper limits for q_s are solely imposed depending on the soil type, pile type and pile installation method. The determination of the unit end bearing capacity of the pile, r_t, is based on the cone resistance within a specific influence zone located 1.5 times the pile base diameter above and below the pile base. This concept is visually depicted in Figure 3 (d is the pile diameter). CPT cone sleeve friction f_s is not used in this method.
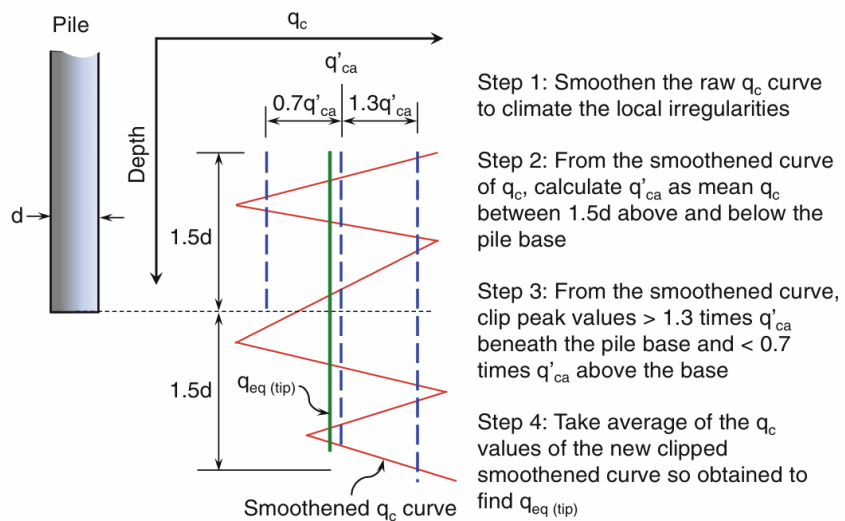
Figure 3. Determining the influence zone for the pile base resistance in the LCPC method adapted from Niazi and Mayne (2013).

The EUROCODE-7 method (EN 1997-2:2007) allows calculating pile bearing capacity of different piles in different soils including silts. q_b and q_s of the pile are calculated based entirely on q_c values. The method takes into account the shape of the pile base, the shape of the pile cross-section, the type of the pile and the installation method of the pile. The vale of pile base resistance is derived based on three mean q_c values of adequate ranges explained in Figure 4. Upper

values of the calculated pile base resistance are limited. The CPT cone sleeve friction f_s is not used in this method.

To calculate pile q_b according to the formula in Table 2, it is necessary to pre-determine three $q_{c,mean}$ values. Here $q_{c,I,mean}$ is the mean of the $q_{c,I}$ value calculated within a specific depth range, starting from the pile base level and extending to a level that is at least 0.7 times and at most 4 times in diameter of the equivalent pile base (D_{eq}) below the base level; $q_{c,II,mean}$ denotes the mean of the lowest $q_{c,II}$ values observed from the critical depth to the pile base, while considering the depth in an upward direction; the mean value of $q_{c,III}$ is determined by averaging the $q_{c,III}$ values over a depth interval that extends from the pile base level to a level that is 8 times as high as the pile base diameter, or, in case b (the length of the shorter side of the pile base) > 1.5 x a (the length of the longer side of the pile base) to 8 x a higher. This procedure starts with the lowest $q_{c,II}$ value used for the computation of $q_{c,II,mean}$. The unit of all three values is MPa. An explanation for determining $q_{c,I,mean}$, $q_{c,II,mean}$ and $q_{c,III,mean}$ for a 18.5 metre-long pile with a diameter of 0.4 metres is given in Figure 4.

The Eurocode-7 method does not establish any upper limits for the pile unit shaft friction. However, in the current investigation, modifications have been made to the Eurocode-7 method, introducing a maximum threshold of 120 kPa for the pile unit shaft friction.
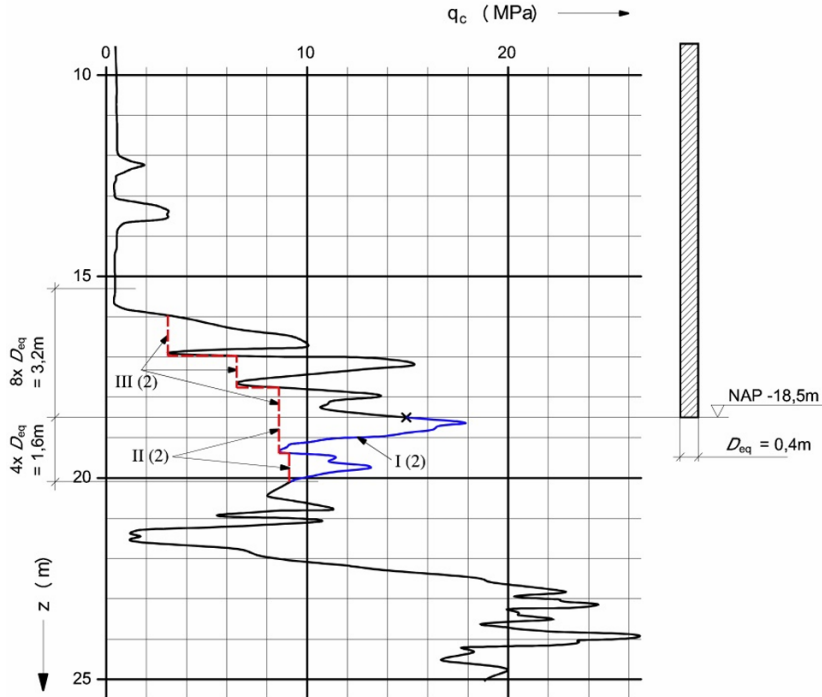

Figure 4. Explanation of the method for the determination of $q_{c,I,mean}$, $q_{c,II,mean}$ and $q_{c,III,mean}$ values in the Eurocode-7 method adapted from Reinders et al. (2016).

The German method relies on empirical pile end bearing capacity and pile shaft friction data for various pile systems including Fundex piles. Kempfert and Becker (2010) developed correlations for piles $q_s(z)$ and q_b from CPT q_c and s_u. They relied on the load test database of up to 1000 piles featuring screw cast-in-place, cast-in-place concrete, precast concrete, steel pipe and micro piles. They presented empirical results for five pile types in the form of lower and upper bound charts (Figure 5). In addition, they introduced tables of empirical data ranges for the characteristic toe resistance depending on the relative pile head settlement in three ranges and shaft resistance for different piles. Fundex piles are taken as screw piles and tables are given for non-cohesive soils (see Tables 3 and 4).
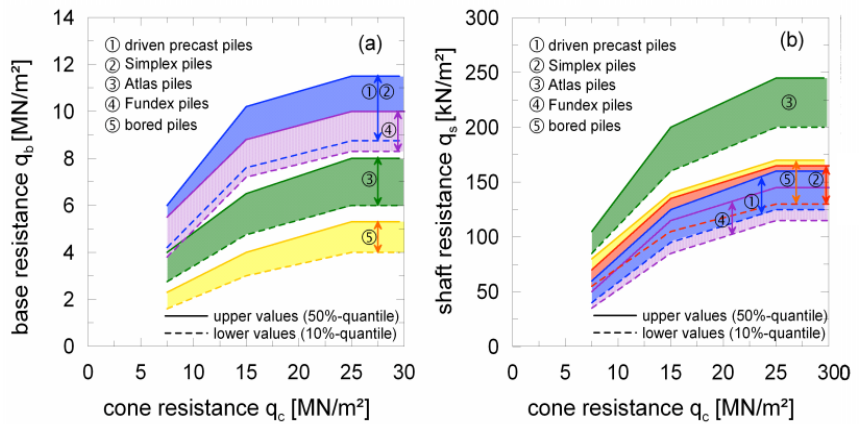
Figure 5. Upper and lower empirical values of different piles (including Fundex piles) in coarse-grained soils for (a) $q_s(z)$ and for (b) q_b (Kempfert and Becker, 2010).

Table 3. Empirical data ranges for the characteristic skin friction $q_{s,k}$ for Fundex piles in non-cohesive soils (EA-Pfähle, 2014).

Mean CPT cone resistance q_c [MN/m²]	Ultimate limit state value $q_{s,k}$ of pile skin friction [kN/m²]
7.5	35–50
15	85–115
≥25	115–145

Table 4. Empirical data ranges for the characteristic base resistance $q_{b,k}$ for Fundex piles in non-cohesive soils (EA-Pfähle, 2014).

Relative pile head settlement	Pile base resistance $q_{b,k}$ [kN/m²] for a mean CPT cone resistance q_c [kN/m²]		
s/D_b	7.5	15	25
0.02	1300 – 1900	2500–3100	3650–4350
0.03	1650 – 2500	3250–3950	4650–5550
0.10 (s_g)	3800 – 5500	7200–8800	8300–10000

Intermediate values may be linearly interpolated

The Eslami and Fellenius method (1997) is based on 142 pile load tests on a considerable assortment of piles installed in various soils including silts. This method, mainly known as the Unicone method, was the first to introduce all three CPTu readings (q_c, f_s, u_2). While the other methods described above use an arithmetic mean of cone resistance the Unicone method uses a geometric mean value. Additionally, this method developed a new soil profiling chart applying effective cone resistance q_E and sleeve friction f_s. A profiling chart is exerted to calculate shaft resistance of piles (Figure. 6).

The Unicone method offers two alternatives for determining the zone of influence of the pile's toe, which vary depending on the arrangement of the soil layers. In the case of installing a pile through a weak soil into a dense soil, the average is calculated over a zone of influence that extends from 4d below the pile base to a height of 8d above the pile base. However, when a pile is installed through a dense soil into a weak soil, the average above the pile base is determined over a zone of influence with a height of 2d above the pile base, which is different from the 8d height in the previous scenario.
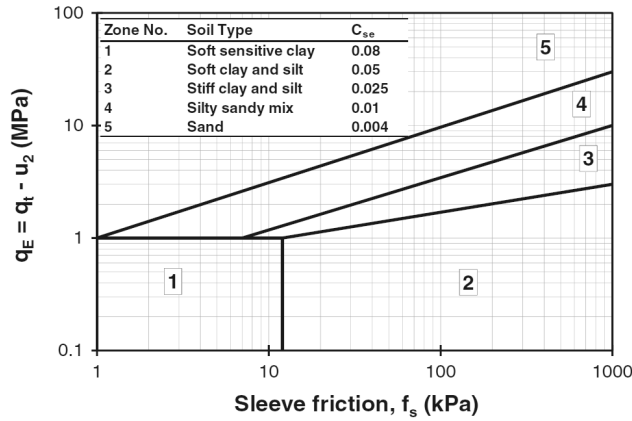
Figure 6. Unicone chart for zone numbers and soil types (Eslami and Fellenius, 1997).

2.1.2 Direct approaches for DCPT based on SPT methods

The DCPT device DPSH-A adheres to the Swedish standard EVN 1997-3; 1995 for HfA. According to the literature (Bergdahl and Ottosson, 1988), HfA states that the number of blows N20 received by the DCPT device is equivalent to the number of shots N30 recorded by the SPT device. This correlation allows for the utilization of soil properties developed for SPT in the evaluation process. In Estonia, site investigations often refer to this correlation. However, no local tests have been conducted to validate the accuracy of this correlation. In this study, six commonly used methods (Shariatmadari et al., 2008; Benali et al., 2013; Karimpour-Fard et al., 2013; Shooshpasha et al., 2013) were examined (Table 5).

It is important to note that SPT methods do not consider the excessive pore water pressure generated during the test; therefore, the results may not be reliable in low-permeable soils such as silt and clay. In addition, in all SPT methods the pile base bearing capacity and pile shaft resistance are determined by calculating the arithmetic average of N values around the pile base and along the pile body. The energy ratio of N values was not specified in the methods proposed by Briaud and Tucker (1988) and Poulos (1989). However, it is important to note that this index is directly linked to the pile bearing capacity and has a significant impact on the obtained results.

The SPT methods used for the analysis do not have an upper limit for ultimate end bearing resistance. In dense subsoils, absence of the upper limit can significantly affect the results. For all SPT methods except for the Briaud and Tucker (1988) method, a limit value of 15 MPa was applied to the ultimate end bearing resistance. The failure criteria for pile bearing capacity except the Poulos (1989)

method are given in Table 5. Also, Table 5 shows the zone of influence of all methods around the pile base (Publication 1).

Table 5. Current SPT direct methods for the prediction of pile bearing capacity (modified after Publication 1).

Method/reference	Design formulas	
	Pile unit shaft resistance (q_s)	**Pile end bearing resistance (q_b)**
Aoki and De`Alencer (1975) Failure criteria: Van der Veen method Energy ratio for N: 70%	$q_s = \left(\dfrac{ak}{3.5}\right) N_s$ For sand: $a = 14$ and $k = 1$ For clay: $a = 60$ and $k = 0.2$	$q_b = \left(\dfrac{k}{1.75}\right) N_b$ N_b: average of three values of SPT blows around pile base
Meyerhof (1976) Failure criteria: minimum slope of load-movement curve Energy ratio for N: 55%	$q_s = n_s N_s$ Bored piles (low disp.): $n_s = 1$ Driven piles (high disp.): $n_s = 2$	$q_b = 0.4 N_1 C_1 C_2$ N_1: N value at the base level $C_1 = ((d + 0.5)/2d)^n$: $n = 1, 2$ and 3, respectively, for loose, medium and dens soil when pile diameter (d) > 0.5 m, otherwise $C_1 = 1$ $C_2 = D/10d$ when penetration in dense layer (D) > $10d$, otherwise $C_2 = 1$
Briaud and Tucker (1988) Failure criteria: penetration of pile head equal 10% of pile diameter	$q_s = \dfrac{0.1}{\dfrac{1}{k_s} + \dfrac{0.1}{r_{s.max} + r_{s.res}}} - r_{s.res}$	$q_b = \dfrac{0.1}{\dfrac{1}{k_t} + \dfrac{0.1}{r_{t.max} + r_{t.res}}} + r_{t.res}$
Decourt (1995) Failure criteria: Van der Veen method Energy ratio for N: 60%	$q_s = \alpha\, (2.8\, N_s + 10)$ Driven piles and bored piles in clay: $\alpha = 1$ Bored piles in granular soils: $\alpha = 0.5-0.6$	$q_b = k_b N_b$ Driven and bored piles in sand: $k_b = 0.325$ N_b is average N value around the pile base

Shariatmadari et al. (2008) Failure criteria: Plunging Energy ratio for N: 60% (only for sandy soils)	$q_s = 3.65\,N_{gs}$ N_{gs}: geometrical average of N values along the pile	$q_b = 0.385\,N_{gb}$ N_{gb}: geometrical average of N values between 8d above and 4d below pile base

N_s is the average value of N around pile embedment depth; $k_t = 1868400 \cdot (N_b)^{0.0065}$, where N_b is the average of SPT blow-count between 4d above and 4d under the pile base (d is pile diameter); $k_s = 20000 \cdot (N_s)^{0.27}$; $r_{t,max} = 1975 \cdot (N_b)^{0.36}$; $r_{s,max} = 22.4 \cdot (N_s)^{0.29}$; $r_{t,res} = 557 \cdot L \cdot ((k_s \cdot p)/(A_t \cdot E_p))^{0.5}$, where L: length of pile, p: perimeter of pile, A_t: cross-section area of pile, and E_p: elastic modulus of pile; $r_{s,res} = r_{t,res}\,(A_t/A_s)$, where A_s: surface area of pile.

3. Settlement analysis for screw piles based on SCPTu data

3.1 Use of SCPTu data to predict the load-displacement capacity of a pile

The analysis of pile bearing capacity can be best achieved by utilizing calculation methods that rely on the outcomes of in situ tests (Eslami et al., 1996; Cai et al., 2012; Moshfeghi et al., 2016). A crucial aspect in the analysis is to take into account the load–settlement (Q–w) relationship, which enhances comprehension of the piles' load bearing capability and facilitates the assessment of differential settlements. The accurate prediction of pile settlements forms the base for developing a cost-effective pile foundation. Figure 7 illustrates the comprehensive range of methods employed by Niazi (2014) to analyse pile Q–w relationships. A simplified analytical method is applied in this study.

It is essential to consider various factors when selecting an appropriate category of analysis and design procedure. Poulos (1989) highlighted the significance and scale of the problem, the budget allocated for foundation design, the availability of geotechnical data and the complexity of the geotechnical profile and design loading conditions as key considerations. By taking these factors into account, engineers can make informed decisions and ensure the effectiveness and efficiency of their analysis and design approach (Publication 3).
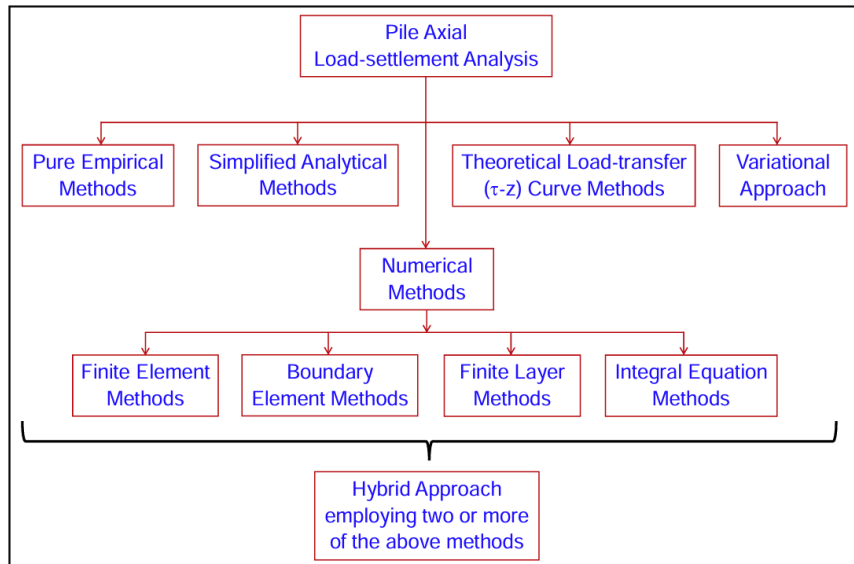
Figure 7. A chart illustrating the categorization of analysis methods used to predict the settlements of piles subjected to axial loading (Niazi, 2014).

Extensive research has been conducted on the use of analytical stress–strain–strength soil models in combination with the findings from in situ tests to determine the Q–w relationship for various piles in different soil conditions (Berardi and Bovolenta, 2005; Mayne and Niazi, 2009; Niazi and Mayne, 2015). An effective method is to use the approximate analytical elastic solution proposed by Randolph and Wroth (1978; 1979) for pile–soil interaction. The settlement of the pile top (w_t) for a compressive pile that is embedded in a linear elastic two-layered soil (see Figure 8) can be determined by employing Formula 2.

Figure 8. Elastic continuum model for axial pile displacement analysis in linear elastic two layered soil model after Randolph and Wroth (1978, 1979).

$$w_t = \frac{Q_t\left[1+\frac{4\eta\,\tanh(\mu L)L}{\pi\lambda(1-v_s)\xi(\mu L)r_0}\right]}{G_L\,r_0\left[\frac{4\eta}{(1-v_s)\xi}+\frac{2\pi\rho E\,\tanh(\mu L)L}{\zeta(\mu L)\,r_0}\right]} \tag{2}$$

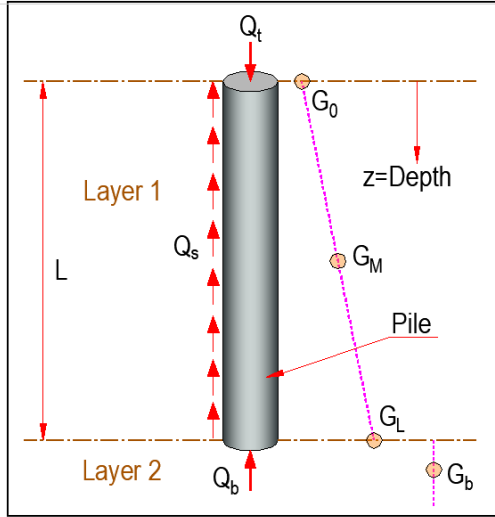where w_t represents the settlement at the pile top; Q_t is the load applied at the pile top; G_L is the operative soil shear modulus at the pile base; η is the factor for underreamed piles that take greater loads at the pile base, calculated as $\eta = r_b / r_o$; L is the pile length; r_o is the radius of the pile shaft; r_b is the pile base radius for underreamed piles; μL is the measure of pile compressibility, calculated as $\mu L = 2\cdot[2 / (\zeta\lambda)]^{0.5}\cdot(L / d_s)$; ζ is the measure of influence radius, calculated as $\zeta = \ln(r_m/r_o)$; r_m is the maximum radius of influence, calculated as $r_m = L\cdot\{0.25 + \xi\cdot[2.5\rho_E\cdot(1 - v_s) - 0.25]\}$; λ is the pile–soil stiffness ratio, calculated as E_p/G_L; E_p is the pile modulus; ξ is the factor for end bearing piles resting on a stiffer stratum ($G_b \gg G_L$), calculated as G_L/G_b; G_b is the soil shear modulus below the pile base; ρ_E is the modulus variation factor, calculated as G_M/G_L; G_M is the operative soil shear modulus at the midpoint of the pile embedment depth, calculated as $G_M = (G_o + G_L)/2$; G_o is the operative shear modulus at the pile top ($Z = 0$) and v_s is the Poisson ratio of soil (Publication 3).

Figure 9 illustrates the profile of operative shear stiffness (G) as a function of depth along the pile shaft, represented by qualitative shear stress (τ) vs. shear strain (γ) plots. It can be observed that the reduction of operative shear stiffness (G) varies inversely with depth (z) below the ground surface. As the depth increases, the load transmitted to the pile shaft decreases, resulting in a decrease in shearing stresses, influence radii, axial displacements and corresponding

reduction in the shear stiffness. The shape of the r_m profile can be attributed to the horizontal and vertical variations in shearing stresses, which can be explained by two factors. Firstly, it is hypothesized that the soil stiffness increases with depth, leading to greater resistance to shear deformations in deeper layers. Secondly, the load applied from the pile top decreases with depth, resulting in smaller shear stresses as the soil around the pile shaft is stiffer.
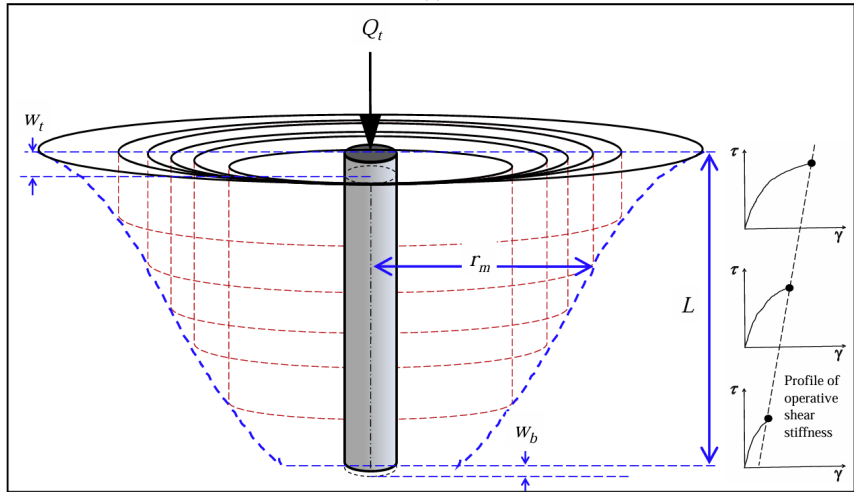

Figure 9. Displacement field model and profile of the maximum influence radius after Randolph and Wroth (1978, 1979) adopted from Niazi (2014).

The proposed solution is suitable for addressing soil conditions characterized by either constant or linearly increasing stiffness with depth, as per the Gibson-type model. It encompasses the inclusion of both end-bearing and floating-type piles. Nevertheless, it does not directly incorporate the distinctions in pile types and installation methods when evaluating the axial load response. To achieve accurate analysis of diverse pile types and their load-displacement relationships, it is essential to calibrate the solution using static pile load test data.

One of the most favourable choices for determining the value of G is to implement SCPTu. This test is used to determine penetrometer readings including in situ shear waves (S). Based on S, V_s can be measured. The determination of G_{max} or G_o relies on the V_s measurement. The conventional approach involves the assessment of shear waves at regular one-metre intervals within the borehole using downhole SCPTu. Consequently, both the V_s readings and G_o values provide an average representation of the 1-metre interval.

The initial value of soil stiffness (G_{max} or G_o) gradually decreases to G as the strains increase. To depict the decrease in modulus, a modified hyperbola is employed. In their research, Fahey and Carter (1993) proposed a modified hyperbola formula to describe the behaviour of normally consolidated sands under monotonic torsional shearing (3):

$$\frac{G}{G_{max}} = 1 - f\left(\frac{\tau}{\tau_{max}}\right)^g \tag{3}$$

where f and g are fitting parameters and G is shear modulus calculated as $G = E / [2(1+v)]$, where $v` = 0.2$ (drained case) is the approximate value of the Poisson ratio of geomaterials at small strains. The ratio τ/τ_{max} can be considered as the reciprocal of the factor of safety (FS) or $1/FS$. As a result, it can also be perceived as an indication of the mobilized load level, Q/Q_{ult}. The material exhibits a fnite stiffness at small strains, which can be quantified by the low-strain shear modulus as (4):

$$G_{max} = G_o = \rho V_s^2 \tag{4}$$

where ρ indicates the total mass density of the material. In both drained and undrained conditions, Formula 3 is applicable as the strains of G_o are too small to induce excessive porewater pressure (Mayne, 2000). Moreover, an extensive study conducted by Jamiolkowski et al. (1994) and Tatsouka et al. (1997) demonstrated that the value of G_o remains unchanged irrespective of whether the loading conditions are static (monotonic) or dynamic.

The initial assessment of $f = 1$ and $g = 0.3$ provides reasonably accurate approximations, which have been verified through laboratory tests involving torsional, triaxial and simple shear loading on unaged and uncemented quartzitic sands, as well as insensitive and unsaturated clays (Burland, 1989; Tatsuoka and Shibuya, 1992; LoPrest et al., 1993; Mayne, 1995; Burns and Mayne, 1996). The parameter g, with an approximate value of 0.3 ± 0.1, is suitable for a wide range of uncemented and nonstructured soils (Mayne, 2005, 2007) (Publication 3).

For determining the value of G_o (MPa), it is crucial to know the ρ (t/m³) values. The total mass density of the soils can be determined in the laboratory. However, the process of collecting soil samples from deep layers beneath the water table is time-consuming and complex. Consequently, the formula incorporating all three CPTu readings (f_s, q_c and u_2) was included to aid in the calculation of the soil unit weight (Mayne et al., 2010). The mass density, ρ, can be obtained from the unit weight using Formula 5. Formula 6 is established based on a diverse range of sands, clays and silts (Publication 3).

$$\rho = \gamma_t / 9.8 \tag{5}$$

$$\gamma_t [\text{kN/m}^3] = 11.46 + 0.33 \cdot \log(z) + 3.1 \cdot \log(f_s) + 0.7 \cdot \log(q_t) \tag{6}$$

4. Probabilistic and deterministic analyses of the bearing capacity of screw piles in silty soils

4.1 Reliability-based design (RBD)

The application of the reliability-based design (RBD) method in analysing the load-bearing capacity of piles has gained significance due to the growing importance of design reliability and economic considerations, which are closely tied to the latest generation of design codes worldwide.

Direct methods typically assume that the pile is situated within soil layers with uniform properties. The presence of irregularities, referred to as 'peaks and troughs', in the sounding data can be minimized by employing average values (Eslami et al., 1997). However, when the in-situ variability of the soil is significant, deterministic analysis relying solely on mean values may prove to be ineffective. To address this issue, a potential approach is to incorporate statistical distributions of soil properties into a deterministic analysis by using simulations.

Monte Carlo simulation (MCS) is a widely applied technique in reliability analysis. It involves a repetitive simulation process that generates a set of values based on random variables with known probability distributions. The accuracy of the MCS outcome improves with an increase in the number of simulations. However, excessively large numbers of simulations can slow down the analysis without significantly impacting the results. Typically, the chosen number of simulations is $N = 10^4$ or 10^5 (Orr et al., 2008). Each independent variable is assigned a probability distribution, such as normal, lognormal or beta. The outcome of the analysis can be presented in the form of a histogram or by highlighting the average value. Additionally, the RBD is used to determine the probability of failure or the reliability index.

The analysis included four piles on the Soodi site, which were evaluated using CPTu and SDT sounding data. Out of these four piles, two were Bauer full displacement piles (FDP) and the other two were displacement piles (DSP). A decision was made to use direct methods that enable the determination of the

load-bearing capacity of the pile based on both CPTu and SDT sounding data. However, the German method, which relies on tabulated values, could not be employed. Similarly, the Eurocode method was excluded due to its complexity: it requires three different q_c values for calculating the bearing capacity of the pile base. Consequently, only the LCPC method was used for the reliability-based design (RBD) simulations.

In the current investigation, the soil was partitioned into four distinct layers. The analysis focused on three of these soil layers surrounding the piles, while the fourth layer was established based on the influence zone for the pile base. According to this method, the influence zone extends 1.5 times the diameter (d) both below and above the pile base. The variable considered was the q_c value. Each layer was assigned a mean value and standard deviation. Three out of the four layers followed a normal distribution for this variable. However, for the layer predominantly composed of clayey soils, a lognormal distribution was employed. Figure 10 illustrates a representative normal distribution of the q_c value in one soil layer, while Figure 11 depicts the lognormal distribution. To generate 10,000 pile capacity values for each pile, the RiskAMP and MCS software were utilized. The average value of the results obtained for each pile was then employed for further analysis (Publication 2).
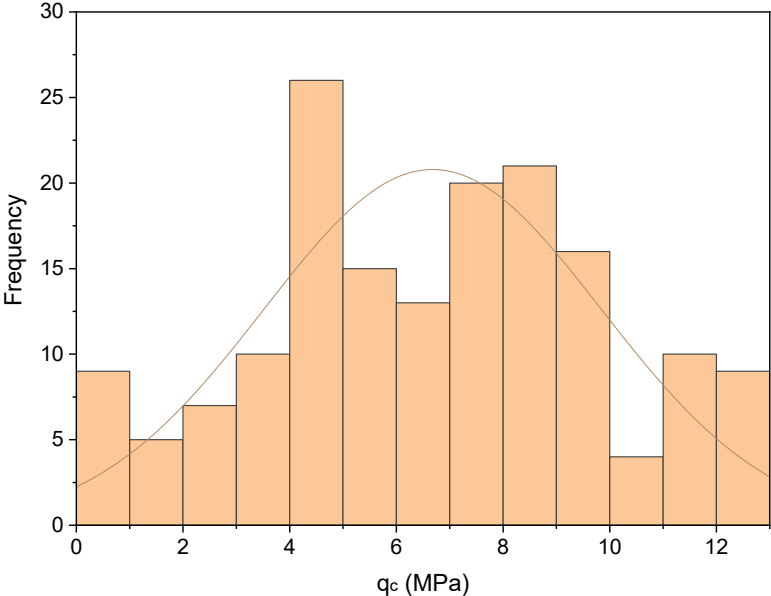
Figure 10. Normal distribution of variable q_c.
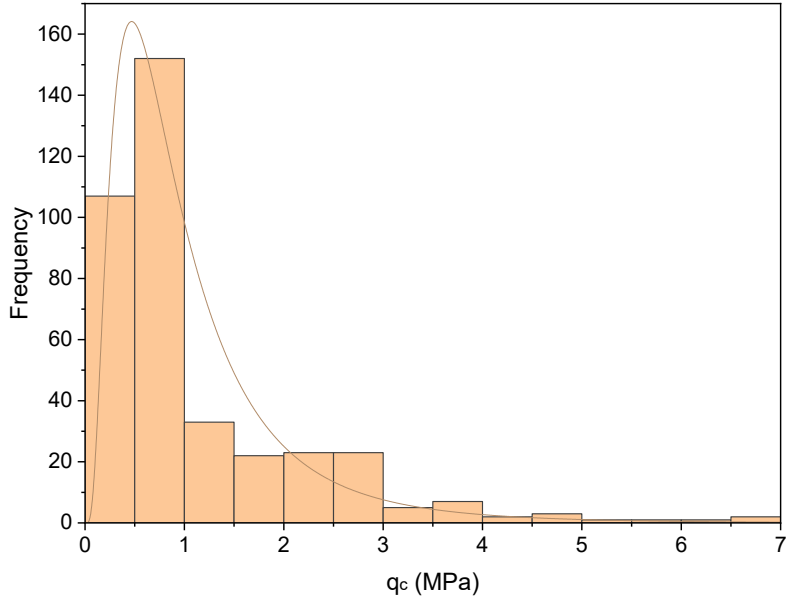
Figure 11. Lognormal distribution of variable q_c.

4.2 Pile bearing capacity analyses based on statistical determination of sounding data

Furthermore, the impact of characteristic values of soil properties, as determined by Eurocode 7 (EN 1997-2:2007), on the outcomes of the direct method were examined. The data from the Soodi test site and the LCPC method were utilized to incorporate the 95% and 5% fractiles of the soil characteristic values' distribution. In the case of uniform soil with no discernible pattern in the ground, the parameter's characteristic value X_k, serving as a reliable mean value at a 95% confidence level, can be derived from a collection of individual values following the approach proposed by Frank et al. (2005):

$$X_k = X_{mean}(1 - k_n V_x) \tag{7}$$

where X_{mean} is the arithmetical mean value of the individual sample parameter value;
V_x is the coefficient of variation of the parameter X;
k_n is a statistical coefficient.

$$V_x = \frac{s_x}{X_{mean}} \tag{8}$$

s_x is the standard deviation of the n sample test results.

The formula for determining the coefficient $k_{n,mean}$, which represents the value used to assess a characteristic value as a 95% reliable mean value, is given by the following expression:

$$k_n = 1.645\sqrt{\frac{1}{n}} \qquad (9)$$

The formula for determining the value of the coefficient $k_{n,low}$, which is used to assess a characteristic value as a 5% fractile value, can be expressed as follows:

$$k_n = 1.645\sqrt{\frac{1}{n} + 1} \qquad (10)$$

n is the number of sounding measurements.

5. Shear wave velocity and CPT–V_s correlations

The shear wave velocity (V_s) serves as a fundamental property for a range of civil engineering materials, including soil, rock, concrete and steel. Estimating V_s is particularly significant in geotechnical problems as it helps in defining the maximum soil stiffness at small strains. This is especially crucial due to the highly nonlinear stress—strain—strength response exhibited by soils (Jardine et al., 1986; Burland, 1989). The measurement of stiffness is commonly expressed through the low-amplitude shear modulus, G_{max}. At very small shear strains (γ_s < 10^{-3} %), G_{max} becomes a significant parameter that influences both the static and the cyclic loading behaviour of soils (Tatsuoka and Shibuya, 1992; Lo Presti et al., 1993).

It is important to highlight that V_s and q_c, which serve as indicators of soil behaviour, represent two distinct and opposing points along the nonlinear stress—strain—strength relationship: V_s reflects the true elastic response of the soil, corresponding to small strains typically on the order of γ_s < 10^{-5} (decimal) while q_c is associated with the undrained shear strength (s_u) or the peak shear stress at failure strains. The variation of shear modulus with strain level and its relevance to geotechnical tests are effectively demonstrated in Figure 12. Despite this apparent contradiction, both parameters exhibit a functional dependence on similar factors, including minerology, aging, the effective confining stress level and K_o stress state (Mayne and Schneider, 2001).
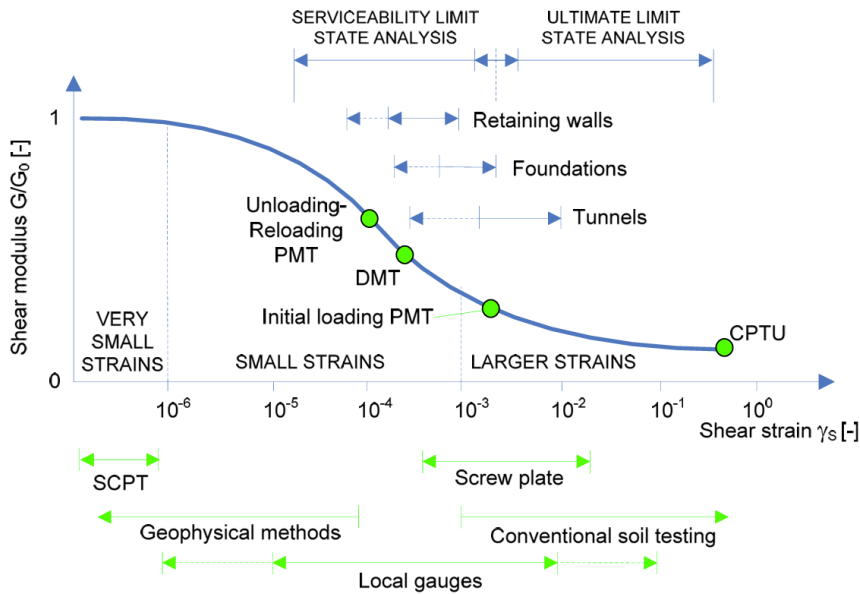
Figure 12. The variation in stiffness as a function of shear strain amplitudes is commonly depicted in a typical representation. This representation allows for a comprehensive comparison between the stiffness ranges observed in typical geotechnical problems and those obtained from a variety of geotechnical tests (Obrzud, 2010); SCPT – seismic cone penetration test; PMT – pressuremeter test; DMT – Marchetti's dilatometer test; CPTU – piezocone penetration test.

The popularity of the SCPTu test has increased globally due to its ability to optimize data collection through the combination of downhole shear wave velocity profiles and conventional penetration measurements. However, obtaining direct measurements of V_s requires special equipment and technical expertise to ensure accurate data acquisition and evaluation. As a result, for low-risk projects or initial design stages, conducting in situ seismic measurements may not be cost-effective. In such cases, empirical correlations between V_s and CPT or CPTu data can be potentially useful for obtaining an initial estimate of the small-strain stiffness of soils. Additionally, the extensive collection of CPT/CPTu data on various soil types worldwide offers the opportunity to derive reliable seismic properties of soils from conventional cone penetration readings, providing a cost-efficient approach to optimize existing measurements and calibrate local correlations on different soils.

The current research included four empirical correlations that established connections between CPTu readings and V_s (m/s). The first correlation, as described by Hegazy and Mayne (1995), utilizes a comprehensive database encompassing sand, silt, clay and mixed soils. This correlation incorporates both cone resistance (q_c) and shaft resistance (f_s) measurements. On the other hand, the second correlation formula relies on f_s readings and draws values for V_s from a database specifically designed for saturated clay, silt and sand obtained from

well-documented experimental sites (Mayne, 2006). For soils predominantly composed of sandy silt, two additional correlations have been proposed. Trevor et al. (2010) introduced a correlation tailored for sandy silt soils, using corrected cone resistance (q_t) and f_s values. Conversely, the correlation proposed by Holmsgaard et al. (2016) employs the value of q_t and is specifically suitable for sandy silt soils with clay stripes. Furthermore, this paper puts forth four correlations specifically designed for silty soils. Table 6 presents the four correlations derived from previous studies (Publication 3).

Table 6. Summary of correlations between shear wave velocity V_s and CPTu output for silty soils from this and other studies (modified after Publication 3).

Reference	Correlation	Soil type
Hegazy and Mayne (1995)	$V_s = [10.1 \cdot \log q_c - 11.4]^{1.67} [f_s/q_c \cdot 100]^{0.3}$ (q_c and f_s in kPa)	For all soils
Mayne (2006)	$V_s = 118.8 \log (f_s) + 18.5$ (f_s in kPa)	Saturated clays, silts, sands
Trevor et al. (2010)	$V_s = 12.02 \cdot q_t^{0.319} \cdot f_s^{-0.0466}$ (q_t and f_s in kPa)	Sandy silt soils
Holmsgaard et al. (2016)	$V_s = 99.45 q_t^{0.428}$ (q_t in MPa)	Sandy silt with clay stripes

6. Test data and data analysis

6.1 Tested piles

In the field of geotechnical engineering, there exists a broad range of pile types that can be used. The behaviour of these piles under loading conditions varies significantly depending on the specific installation or construction methods employed. On one end of the spectrum, we have non-displacement piles, such as bored piles or drilled shafts, while on the opposite end, we find full-displacement piles, such as closed-ended pipe piles or precast reinforced concrete piles.

Three types of piles were studied in the research: Fundex pile, Bauer full displacement pile (FDP) and displacement pile (DSP). Fundex piles can be classified as augured cast in situ concrete displacement piles (Van Baars, 2018). Certainly, the FDP and DSP piles can also be grouped together under the same classification. In Europe, these piles are commonly known as 'screw piles' (Basu et al., 2010), and they belong to the auger pile type. In the market a wide range of auger piling equipment is available, each of which is linked to a specific level of soil displacement during the installation process. Figure 13 illustrates the commonly employed terminologies for auger piles in North America and Europe.

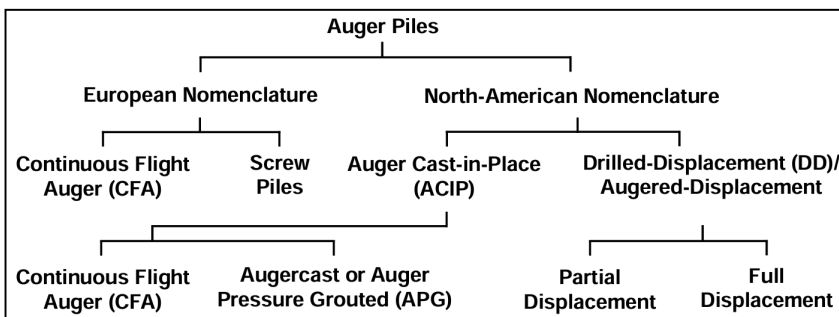**Figure 13.** Nomenclature used for auger piles in Europe and North America (after Basu et al., 2010).

In the installation process of a Fundex pile (Figure 14), a casing or tube equipped with a conical auger tip at its end is used. This casing is rotated in a clockwise direction and pushed downwards into the soil. To ensure a watertight seal, the joint between the casing and the conical tip is carefully connected. As

44

the casing penetrates the ground, the surrounding soil is displacing laterally. In situations where the soil is dense or hard, drilling can be combined with grout injection or water jetting through the conical tip to facilitate the process. Once the desired depth is achieved, the sacrificial conical tip, which forms an enlarged base for the pile, is released. Subsequently, a reinforcement cage is inserted into the casing, and concrete is then poured. During the concrete placement, the casing is extracted in an oscillating motion, moving both upward and downward, with alternating 180° clockwise and counterclockwise rotations. This withdrawal technique, involving rotations in both directions, results in a shaft that is nearly smooth in appearance.

Two numerical values are employed to specify the diameter of Fundex piles. The first value denotes the diameter of the shaft, and the second the diameter of the pile base. The study examined Fundex piles of two different base diameters: 0.45 and 0.56 metres. Of these, the former has the pile shaft diameter of 0.35 m, and the latter 0.45 m.

During the installation process of FDP piles (Figure 15), a displacement tool is used to create a cavity in the ground. This displacement tool is designed with a widening shape and is inserted into the ground by applying both pushing and rotating forces. The tool consists of a starter auger, which initially loosens the soil, and a widening displacement tool, which pushes the loosened soil laterally into the surrounding area. Once the desired depth is reached, the displacement tool is extracted, and simultaneously, the resulting cavity is filled with concrete through an opening located at the end of the drill stem. Following this, a reinforcement casing is inserted into the wet concrete. At the specific test site, the diameter of both the FDP pile base and the shaft measured 0.44 metres.

The installation of DSP piles (Figure 16), like that of Fundex piles, involves the utilization of 'Lost bit' technology. However, the DSP pile drill head has a different shape compared to Fundex pile (see Figures 17 and 19). The DSP piling method entails the drilling of a jacket pipe with a closed end into the desired depth by means of rotation and pushing. Subsequently, the drill head is unscrewed and left in the ground to serve as the pile base. As the jacket pipe is lifted, concrete is poured into the pile cavity. Two key numbers are used to specify this pile type. The DSP piles studied in the research had a shaft diameter of 0.406 m and a pile base diameter of 0.52 m.

It is essential to take into account that piles such as Fundex and DSP feature a pile base which is wider than the shaft. Consequently, during the pile installation process, the soil in the shaft area begins to loosen (Kemfert et al., 2010). In contrast, the screw-shaped pile shaft improves its load-bearing capacity when compared to a smooth pile shaft (Basu et al., 2010). Therefore, the accuracy of the actual load-bearing capacity of screw piles may not always meet the desired level of accuracy (Kemfert et al., 2010). Another aspect to consider is that Formula (1) assumes that the base and shaft resistances do not influence each other.

In reality, the relationship between these two resistances is interconnected and the interconnection is influenced by the prevailing soil conditions.

In addition, significant alterations in the void ratio and stress state of the in-situ soil occur during the installation of full-displacement piles. This is primarily due to the lateral displacement of the soil surrounding the pile shaft and the preloading of the soil beneath the pile base. As a result of these alterations, the load-displacement response of displacement piles is noticeably stiffer compared to that of replacement piles. This disparity is particularly pronounced in sandy soils, as they experience enhanced strength through the process of densification (Basu et al., 2010).

The EA-Pfähle (2014) provides tabular values for various types of piles, including driven precast piles, simplex piles, Atlas piles, Fundex piles and bored piles, in both sandy and clayey soils. Among these pile types, the DSP pile closely resembles the Fundex pile, as they both have an extended pile base, meaning that the diameter of the pile base is larger than the diameter of the pile shaft. Additionally, the pile head remains in the ground after installation for both types of piles. The German method does not include any tables for the computation of the FDP pile. Driven precast piles and Simplex piles are both categorized as driven piles. On the other hand, when installing the Atlas pile, the screw-shape shaft remains intact. It is important to note that bored piles are not considered displacement piles. Therefore, the German method of Fundex pile tables was also used for the analysis of FDP piles.

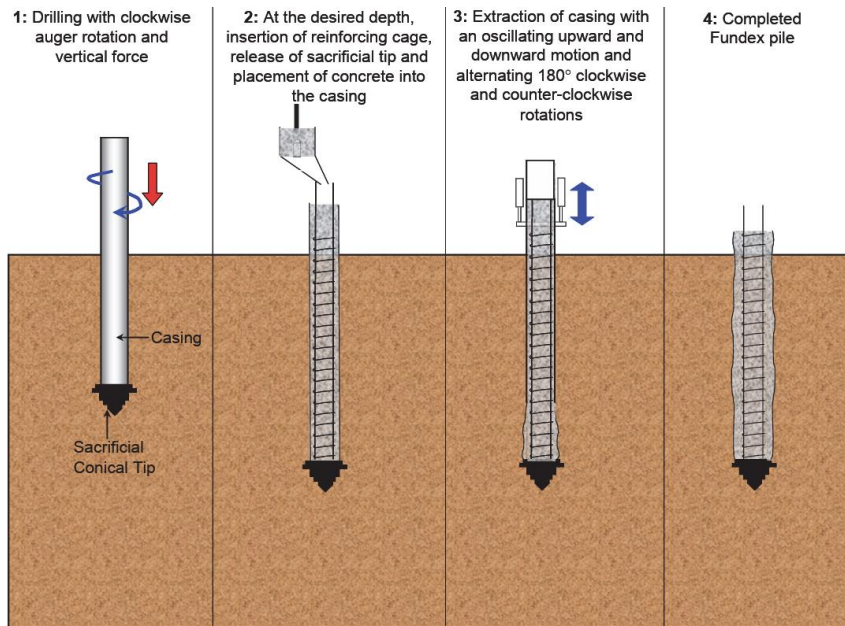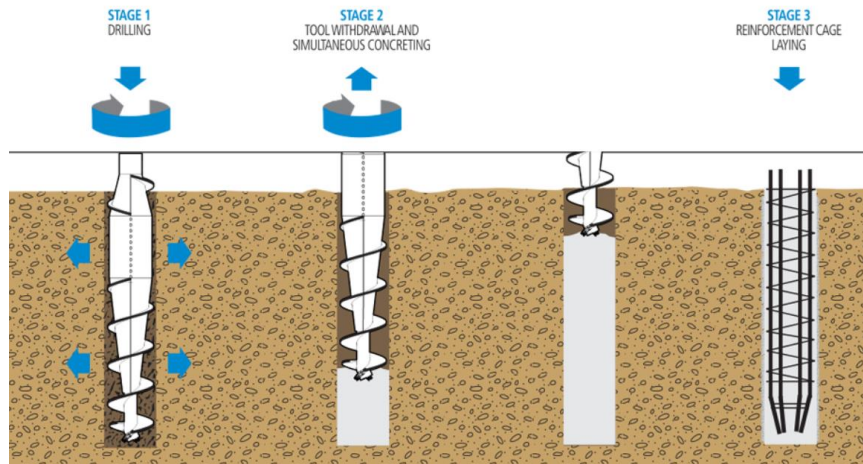**Figure 14.** The principle of installing a Fundex pile (Basu et al., 2010).

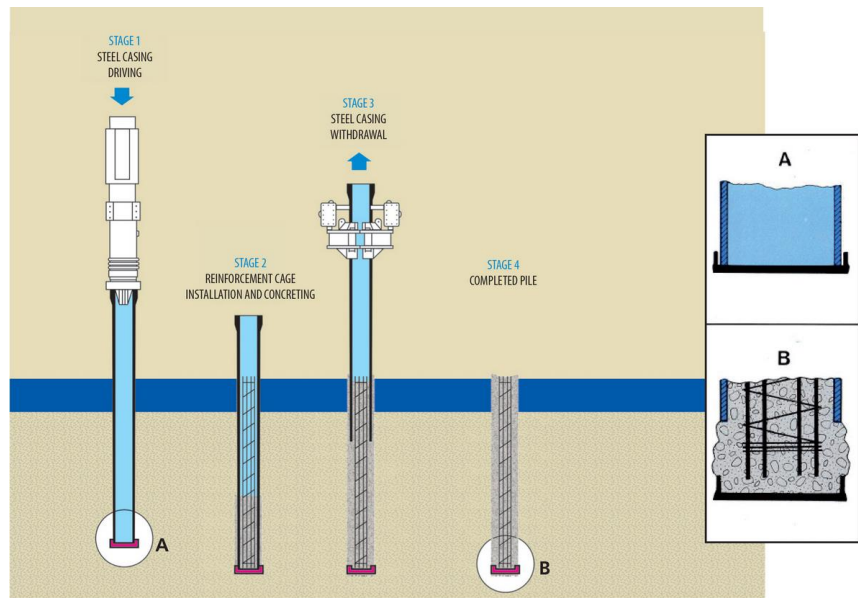**Figure 15.** The principle of installing an FDP pile https://www.trevispa.com/en/Technologies).

Figure 16. The principle of installing a DSP pile (https://www.trevispa.com/en/Technologies).

6.2 Axial static pile load test

The piles were tested in accordance with EVS-EN 1997-1:2006 (based on EN 1997-1:2004) before the other parts of the pile field were constructed. The duration of the load level for the pile was one hour, and the loading step did not exceed 1/8 of the expected bearing capacity of the pile. Two or four hydraulic jacks with a force development of 200 tonnes each were used to load the piles, along with an oil pump and a pressure gauge with a precision class of 40 kPa and a measurement range of 25 000 kPa. The force applied to the pile was determined based on the oil pressure measured by the pressure gauge, using calibration tables for the jacks. The reaction force of 8 tonnes was obtained for the jack from a steel frame, on which a maximum of 390 tonnes of metal or concrete weights were placed. The settlement of the pile was measured using three Maksimov-type wire settlement gauges (wire diameter 0.3 mm, measurement accuracy 0.1 mm). The scheme of the static pile load test is presented in Figures 17 and 18.

The test piles were loaded after a period of two to four weeks after installation. At the test sites, the groundwater level was found to be positioned roughly one metre below the ground level. The presence of high groundwater levels, especially in cohesive soils containing fine-grained particles, has a notable influence on both the sounding outcomes and the duration required for the pile to attain its load-bearing capacity. The duration for the pile to attain its load-bearing capacity is influenced by various factors, including the type and length of the pile. Additionally, it is crucial to differentiate whether the clayey soil layers are present around the base of the pile or solely above it. In cases where approximately 50% of the pile shaft is surrounded by clayey soils, the load-bearing capacity of the pile shaft may continue to increase for a period of up to 100 days following the completion of pile construction (Togliani et al., 2014).

In Estonia, it is customary to wait for three weeks (21 days) before subjecting the piles to load. Mets (1997) suggested that a two-week waiting period is sufficient for soft silts. However, in clayey soils, the shaft resistance of the pile continues to increase even after four weeks. This is advantageous for the pile capacity, providing additional safety margin. Since the test sites predominantly consisted of silty soils, a similar increase in capacity was not expected. Therefore, it was estimated that the adhesion did not significantly impact the overall load-bearing capacity of the piles.
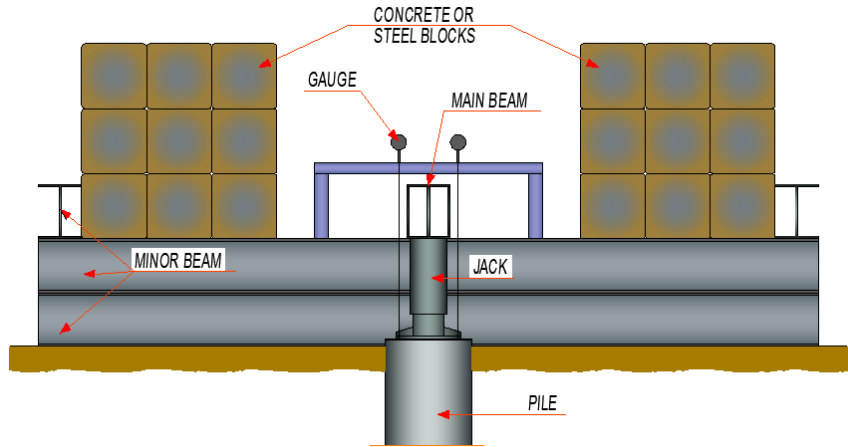
Figure 17. Scheme of a static pile load test.

Figure 18. Scheme of a static pile load test.

During the loading test, the axial displacements are carefully measured in relation to the incremental axial load. This data is then used to generate a comprehensive load-displacement (Q–w) curve. The main challenge lies in determining the capacity value along this curve, as there exist a multitude of definitions for axial pile capacity, with as many as 45 different definitions identified by various researchers (Hirany and Kulhawy, 1988; Dećourt, 1999; Niazi, 2014). Unfortunately, the lack of consensus among these definitions leads to significantly divergent results, as illustrated in Figure 19.

sin
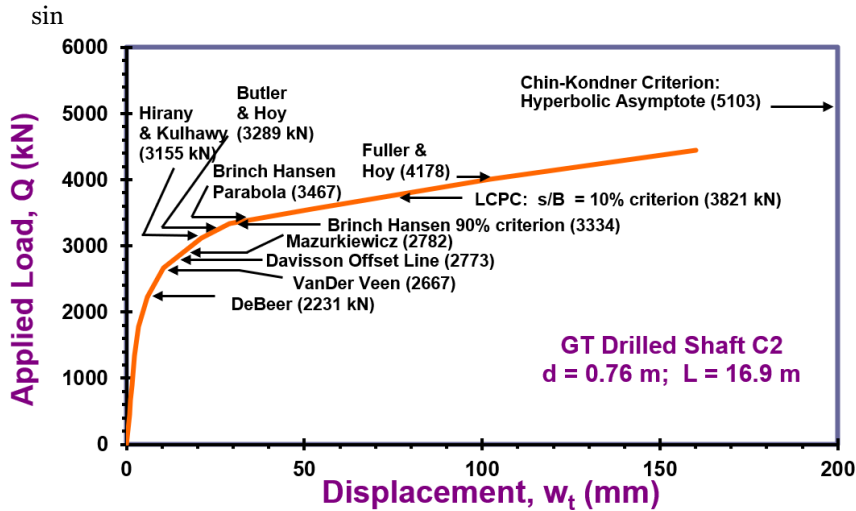
Figure 19. Comparison of capacity interpretation criteria from axial pile load tests (Niazi, 2014).

One of the earliest definitions of pile-bearing capacity refers to the point at which the movement of the pile exceeds 10% of its diameter. This particular criterion is commonly referred to as the French criterion, as documented by Vesić in 1977, and is used in the Eurocode. However, since the piles were not subjected to loading until reaching their ultimate capacity based on the French criterion, an alternative approach was employed.

The Chin extrapolation method (1970) along with load–settlement curves, was used to estimate the ultimate capacity of the piles. The assumption made by Chin is that the load–settlement relationship can be characterized as hyperbolic. To examine this hypothesis, the settlement values are divided by their corresponding load values. Subsequently, these ratios are graphed against the settlement measurements. Notably, the plotted data points exhibit a close alignment with a straight line. The inverse of the slope of this line serves as an indicator for the Chin–Kondner extrapolation limits.

The practical implementation of Chin's extrapolation method, as established by Kondner (1963), is well known and widely practiced (Al-Homoud et al., 2003; Basu et al., 2010; Elsamee, 2012; Niazi, 2014; Camacho et al., 2018). This method, in accordance with the 10% criterion, allows for the determination of the ultimate resistance of the pile, even if the settlement of the pile head does not reach 10% of the pile base diameter (Holeyman et al., 1997; Borel et al., 2004; De Cock, 2009; Basu et al., 2010). Table 7 presents the measurements of the statically tested piles, along with their maximum testing loads and corresponding settlement values. The piles at the Ahtri site are denoted by the letter 'A', the piles at the Paldiski mnt site by the letter 'P' and the letter 'S' is used to indicate the piles at the Soodi site.

Table 7. Summary of static pile load test data for all tested piles

Pile name	A-1	A-2	A-3	A-4	P-1	P-2	P-3	S-1	S-2	S-3	S-4
Pile type	Fundex 450/560	Fundex 450/560	Fundex 450/560	Fundex 450/560	Fundex 350/450	Fundex 350/450	Fundex 350/450	DSP 406/560	DSP 406/560	FDP 440	FDP440
Pile length (m)	27.0	26.0	23.2	23.5	15.5	15.5	15.0	12.7	11.3	12.4	12.5
Measured max load from pile load test (t)	360	324	360	216	120	120	120	187	170	187	187
Max settlement from pile load test (mm)	4.9	6.2	22.0	50.7	6.3	6.5	15.0	35.3	22.8	17.0	22.7

The CPT sounding conducted at the Ahtri site failed to reach the bottom depth of the pile base. Concurrently, the DPSH-A test demonstrated consistent or greater depth penetration in three test locations, with the exception close to pile A-1. However, the drilling resistance data presented in Table 8 indicate that the soil beneath both piles A-1 and A-2 exhibited comparable strength in the pile base zone during installation. This suggests that the soil beneath pile A-1 possesses similar strength characteristics to those beneath pile A-2. Furthermore, previous research conducted in the surrounding area by Saks et al. (1985) confirms that the soil strength increases up to a maximum depth of 75 m.

Table 8. Drilling resistance near the pile base on piles A-1 and A-2 to depths of 27 m and 26 m, respectively (modified after Publication 1).

Pile A-1		Pile A-2	
Depth (m)	Resistance (bar)	Depth (m)	Resistance (bar)
22.50	70–110	21.50	70–100
23.00	70–110	22.00	70–100

23.50	70–110		22.50	180–200
24.00	160–180		23.00	180–200
24.50	160–180		23.50	180–200
25.00	220–240		24.00	180–200
25.50	220–240		24.50	220–240
26.00	220–240		25.00	220–240
26.50	220–240		25.50	220–250
27.00	240–260		26.00	220–250

In addition, the reliability of the Chin method was assessed by examining the existing literature on similar soils and Fundex piles. Two Fundex 380/450 piles located in Belgium were selected for the comparison. These piles were subjected to testing until a settlement equal to or greater than 10% of the pile diameter was achieved. The first pile, A1bis, was tested in Limelette according to Maertens et al. (2003), while the second pile, designated as P3, was tested in Ghent as reported by Holeyman (2001). By comparing the extrapolated results obtained using the Chin method ($Qu_{,\text{Chin10\%}}$) with the measured values ($Qu_{,\text{SLT}}$), an assessment of the accuracy of the Chin method for different pile settlements can be made. The results for the two piles at four different settlements are presented in Table 9.

The findings indicate that the extrapolation results for the A1bis pile exhibit a high level of reliability, even at very small settlements. On the other hand, the results for pile P3 highlight the need to consider the accuracy of the extrapolation results, particularly for smaller settlements, where an accuracy of around 20% should be taken into account. Based on the findings of Publication 1, it is suggested that the Chin method can be utilized to determine the French criterion for screw piles in silty soils.

Table 9. Accuracy of determining the settlement of piles A1bis and P3 by the Chin method on the basis of four different settlements; accuracy within 10% is marked in green and accuracy above 10% is marked in red (modified after Publication 1).

Pile ID	s/B (%)	$Qu_{,\text{Chin 10\%}}/Qu_{,\text{SLT}}$	Accuracy (±%)
A1bis	1.1	0.90	10.0
A1bis	1.4	0.94	6.2
A1bis	3.5	1.03	2.7
A1bis	6.0	1.03	2.6
P3	1.2	1.09	9.3
P3	1.5	1.24	23.9
P3	2.8	1.13	13.3
P3	6.0	0.99	0.7

6.3   Sounding methods

6.3.1   CPTu soundings

The Cone Penetration Test (CPT) has been extensively utilized, studied and advanced worldwide over the past century (Massarsch, 2014). This method offers a rapid and cost-effective approach. Typically, the probe used in the CPT has a base area of 1,000 mm^2 and a sleeve surface area of 15 000 mm^2. The drive rod shares the same diameter as the probe, measuring 35.7 mm. Throughout the test, the probe is steadily pushed at a speed of 20 mm/s until it reaches the desired depth or until the compressive force is exhausted. By obtaining readings of the cone tip resistance (q_c) and sleeve friction (f_s) at short depth intervals (ranging from 10 to 20 mm), a nearly continuous representation of the soil layers can be established. In cases where the CPTu is employed, pore pressure (u_2) data are also collected. These three independent parameters can be applied for soil identification and classification as well as for the evaluation of various soil properties, including strength and deformation characteristics.

A lightweight truck (Figure 20) was used along with ground anchors. The length of the anchor in the soil was approximately three metres. In certain locations, predrilling was conducted due to the presence of impenetrable fill in the upper layer. The truck in Figure 20 is equipped with a pre-drilling nozzle. A Nova cone produced by Geotech AB with a capacity of 50 MPa was used (Figure 21). The CPT Geotech Nova system meets the standards EN ISO22476-1 and ASTM D-5778 (2000). With a 60° apex angle, the instrumented probe features a conical tip. The tip has a cross-sectional area (A_c) of 1000 mm^2, while the sleeve area (A_s) measures 15 000 mm^2. The procedures of the testing concurred with Lunne et al. (1997).

Figure 20. Lightweight truck equipped with a pre-drilling nozzle.
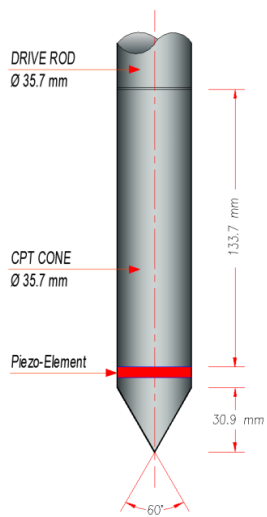
Figure 21. Piezocone penetrometer cone.

The pore water pressure measuring filter can be positioned in three different locations: u_1, u_2 and u_3 (Figure 22). The ISSMFE Reference Test Procedures specify that the preferred filter location is right behind the cone (u_2) (Lunne et al., 1997). In soft fine-grained saturated soils, where the pore pressure can be relatively high compared to the cone resistance, it is crucial to correct the pore water pressure (Jamiolkowsky et al., 1985; Robertson and Campanella, 1988; Lunne et al., 1997). The corrected cone tip stress, denoted as q_t, is determined as follows:

$$q_t = q_c + u_2(1\text{-}a) \qquad (11)$$

In this context, the net cone area ratio (a) represents the relationship between the cross-sectional area of the load cell or shaft (A_n) and the projected area of the cone (A_c), as illustrated in Figure 23. Typically, cone manufacturers determine this parameter through geometric analysis and a calibration process, and the value is generally between 0.70 and 0.85. The cone area factor a=0.859 was provided by the manufacturer.
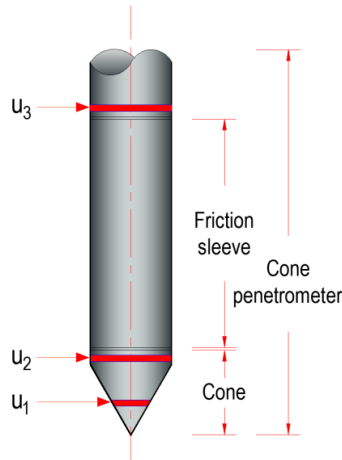
Figure 22. Pore pressure filter locations of piezocone penetrometer cone.
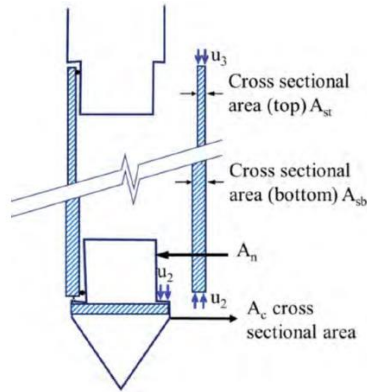
Figure 23. Unequal end area effects on cone tip and friction sleeve (Lunne et al., 1997).

Figure 24 displays the typical profiles of q_t, f_s, R_f and u_2 for the Ahtri site. The friction ratio can be calculated as $R_f = f_s/q_t \times 100\%$. On the left side, the chart illustrates the types of soil layers determined through CPTu and the soil behaviour type (SBT) according to Robertson (2010). The water table is represented as u_o (hydrostatic pressure is marked in green). The soil profiles of all three sites predominantly consist of silty soils, with a limited presence of clayey soils. An increase in the pore water pressure serves as an excellent indicator of clayey layers.
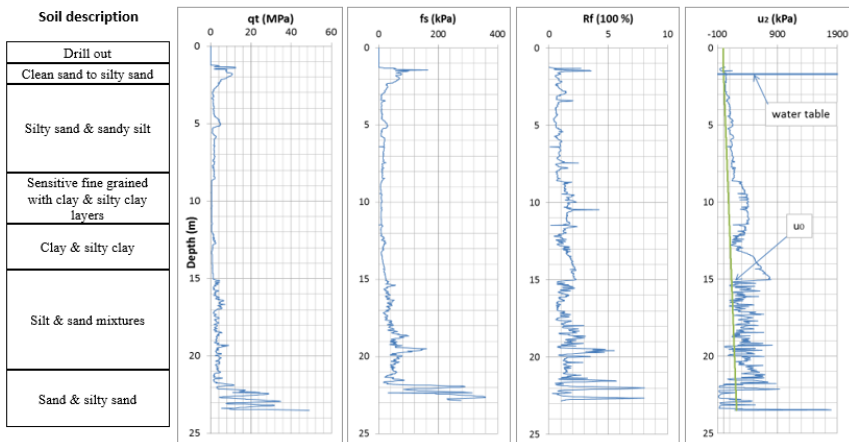
Figure 24. Results of the piezocone test at the Ahtri site. q_t, cone resistance corrected for the pore pressure effects; f_s, sleeve friction; R_f, friction ratio; u_2, pore pressure (Publication 1).

Previous CPTu soundings

Additionally, the assessment encompassed earlier soundings performed at the Ahtri site by utilizing CPT tests in addition to the CPTu soundings conducted as part of the research. The HYSON device, equipped with a 200-kN counterweight, was used to carry out the piezo-cone tests. The PAGANI CPTu penetration cone, featuring a base area of 1,000 mm^2 and a sleeve surface area of 15,000 mm^2, was employed in the testing process. This cone facilitated the determination of base and side resistance, pore water pressure and cone inclination.

6.3.2   DCPT soundings

The Dynamic Cone Penetration Test (DCPT) is an economical and straightforward technique for investigating soil properties. It involves driving a penetrometer into the ground and recording the number of blows required to reach the desired depth. Initially, dynamic cone penetrometers were developed to collect both quantitative and qualitative information on soil resistance to penetration. Their primary purpose was to assess the compactness of cohesionless soils, which often pose difficulties in sampling.

Four types of probes, namely Dynamic Probing Light (DPL), Dynamic Probing Medium (DPM), Dynamic Probing Heavy (DPH) and Dynamic Probing Super Heavy (DPSH), can be differentiated based on the size of the cone, the weight of the hammer, and the height of the drop. A selection of dynamic penetrometer nozzles are shown in Figure 25. Additionally, as per EN ISO 22476-2 (2005), DPSH is further classified into two subcategories: DPSH-A and DPSH-B. In the case of DPSH-A, the hammer is dropped from a height of 0.5 metres, while in DPSH-B, it is dropped from a height of 0.75 meters. In Estonia, the first variant, DPSH-A, has been extensively used in recent decades. It is worth noting that when the diameters of the piezocone probe and rod are equal, the external diameter (d) of the DCPT probe is larger than the outer diameter (d_t) of the rod, as depicted in Figure 26.

In the present study the DPSH-A test with a GEOTECH 504 geomachine was employed. The hammer used in the tests had a weight of 63.5 kg, while the rods weighed 6 kg/m with a diameter of 32 mm. The hammer was released from a drop height of 0.5 m. The cone tip area was 1600 mm^2. The tests involved measuring the number of blows per 200 mm.

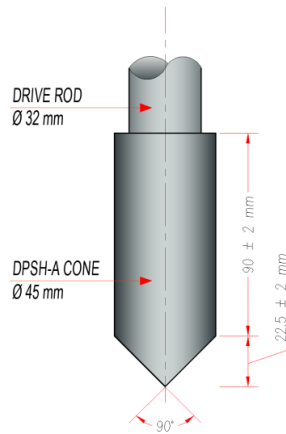**Figure 25.** A selection of dynamic probing cones.

Figure 26. Disposable DPSH-A cone.

Figure 27. SDT penetrometer cone.

58

6.3.3 Static dynamic testing

The static dynamic testing (SDT) method was originally developed in Finland during the early 1980s, with a particular focus on research conducted within the Department of Geotechnics in the City of Helsinki. This method has been extensively studied and used for several years (Melander, 1989; Rantala and Halkola, 1997). The SDT method combines both static and dynamic penetration tests to assess soil properties. Initially, the test begins as a static penetration test, where the drill rods with the cone are pressed and rotated simultaneously. The equipment used typically has a maximum compressive force of 30 kN. Once the maximum compressive force is reached, the device transitions into the dynamic penetration phase, involving hammering. If the number of blows (N_{20}) within a 0.4 m interval is less than or equal to five, the dynamic phase switches back to static penetration. Throughout the test, various parameters such as compressive force, torque, number of strokes, sounding depth and rotation speed are measured at intervals of 20 mm to 40 mm (Finnish Geotechnical Society, 2001).

The SDT method employs a loosely fitted cone that typically remains in the ground when the rods are extracted. The cone has a diameter of 45±0.2 mm and a length of 90±2 mm. It possesses an apex angle of 90°. The cross-sectional area of the cone's tip measures 1600 mm², while the area of its side surface is 12700 mm². The diameter of the drive rod is 32 mm, which is smaller than the cone's diameter of 45 mm (Figures 27 and 28). The dimensions of the SDT cone and rods are the same as those of the DPSH-A cone. Throughout the compression stage, the rods are compressed at a consistent velocity of 20±5 mm/s. For dynamic penetration, a hammer weighing 63.5±0.5 kg is utilized, along with a lowering height of 0.5 m (Finnish Geotechnical Society, 2001).
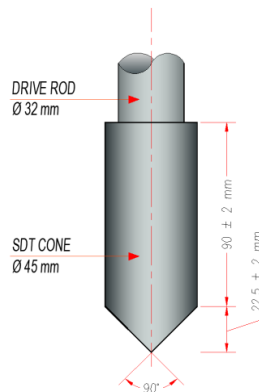

Figure 28. SDT penetrometer cone (the same as DPSH-A penetrometer cone).

SDT penetrometer coneThe determination of geotechnical parameters using the SDT method relies on calculation formulas specifically developed from CPTu sounding. Unlike the CPTu, the SDT cone has a larger diameter than the driving

rod. Consequently, it is crucial to understand the relationship between the SDT and CPT test results. Through laboratory experiments, Rantala and Halkola (1997) discovered that the cone tip resistance ($q_{c,CPT}$) of the CPTu can be derived from the SDT results of static pressure penetration using Formula 12. According to the Sounding guidelines 6-2001 by the Finnish Geotechnical Society (2001), the net resistance of the static pressure penetration in the SDT test can be calculated based on the values of total torque (M_{tot}) and total compressive force (Q_{tot}) using Formula 13. Additionally, Formula 14 can be employed to convert the blow numbers obtained from the dynamic penetration of the SDT test into the cone tip resistance ($q_{c,CPT}$) of the CPTu. The net stroke rate N_n is defined by Formula 15, which utilizes the total stroke rate (N_{20}) and total torque (M_{tot}) (Finnish Geotechnical Society, 2001).

$$q_{c,CPT} = 1.07 \cdot q_{n,SDT} \tag{12}$$

$$q_{n,SDT} = \frac{Q_{tot}}{1000 \cdot A_c} - k_p \cdot (M_{tot} - \mu_1 \cdot Q_{tot}) \tag{13}$$

$$q_{c,CPT} = 0.83 [\frac{\text{MPa}}{\frac{l}{0.2\text{m}}}] \cdot N_n \tag{14}$$

$$N_n = N_{20} - 0.04 \cdot M_{tot} \tag{15}$$

$q_{c,CPT}$ is the cone tip resistance of the CPT;

$q_{n,SDT}$ is the net resistance to the static pressure penetration [MPa] of the SDT;

Q_{tot} is the total compressive force [kN] of the SDT;

k_p is a standard ($k_p = 1/(A_c \cdot r \cdot 10^6) = 0.039$ (1/m³));

M_{tot} is the total torque value [Nm] of the SDT;

μ_1 is a device-specific constant (e.g. for GM4000 $\mu_1 = 1$ Nm/kN) to estimate the effect of axial loading of the compression phase on the friction of the transmission thrust bearing;

N_n is the net stroke rate [l/0.2 m] of the SDT;

N_{20} is the total stroke rate [l/0.2 m] of the SDT.

6.3.4   SCPTu soundings

The seismic piezocone test (SCPTu) has found extensive use in determining the small strain shear modulus (G_o) through the measurement of shear wave velocity (V_s). The modulus G_o is a significant dynamic characteristic of soil that finds applications in various fields of geotechnical and earthquake engineering. It is employed in diverse applications such as seismic site response analysis, foundation design for vibrating equipment, soil–structure interaction and the analysis of dynamic behaviour of offshore structures subjected to wave loading.

The determination of shear wave velocity V_s was accomplished by conducting an SCPTu downhole test, wherein the energy source was situated on the ground and the receiver was positioned within the cone. For the calculation of V_s

Formula 16 is used (Campanella and Steward, 1992; Sully and Campanella, 1995; Howie and Amini, 2005):

$$V_s = \frac{L_2 - L_1}{t_2 - t_1} = \frac{\Delta L}{\Delta t} \tag{16}$$

The slant distances between the source beam and the cone sensor for the first and second depths are denoted as L_1 and L_2, respectively, with a depth interval of 1 m. The time intervals for the first and second depths are represented by t_1 and t_2, respectively. An electronic trigger, which is connected to the metal plate, enables the acquisition of the exact timing of the strike. The calculation of the time interval ($\Delta t = t_2 - t_1$) can be performed using different methodologies. In this research, the well-established reverse polarity (or cross-over) method has been employed to compute the time interval and, consequently, ascertain the shear wave velocity.

When both a left and a right steel plate are utilized, the impact of hammer blows on these plates generates reversed shear wave signals. These signals exhibit a reversed amplitude pattern, facilitating the identification of the first cross-over point as the point where the main shear waves arrive and change signs. The first clear cross-over point of the two shear waves corresponds to the arrival time of the shear wave. The time interval is determined by subtracting the arrival time for the first depth from that of the second depth (Robertson et al., 1986; Campanella et al., 1989; Campanella and Steward, 1992; Areias and Impe, 2004; Liao and Mayne, 2006).

The SCPTu soundings were carried out using a Geotech AB Nova cone with a seismic module (Fig. 29, 30), which was installed on a lightweight truck. The description of the truck with anchors has already been presented in section 6.3.1. A friction-reducing module for rods was installed behind the seismic module (refer to Figure 30). The shockwaves known as S-waves were initiated by the collision between a sledgehammer (Figs 29 and 31) and a steel plate situated at the surface. The connection between the sledgehammer and the steel plate, facilitated by a triggering cable and crocodile clamps, was further enhanced by the inclusion of a SCPT signal conditioning unit. To generate a polarized shear wave, two steel plates were positioned and aligned on each side of the sounding hole. These plates, having an "L" shape, were equipped with transverse teeth to ensure optimal contact with the ground. Within the sounding hole, a SCPT adapter (accelerometer) was connected to the cone. When the hammer struck one of the steel plates, a polarized shear wave was triggered, and the time taken for this wave to travel a known distance to the sounding hole was measured.
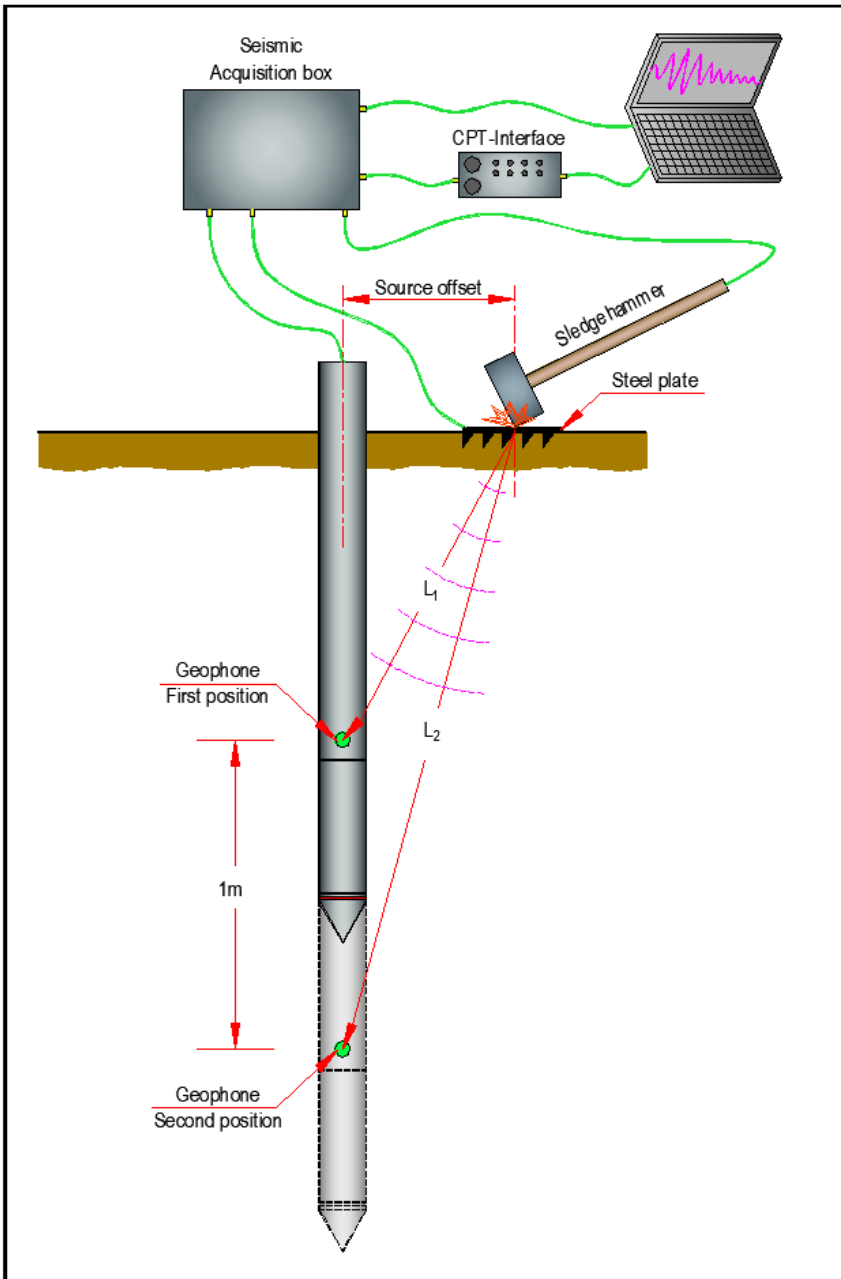
Figure 29. Shematic design of the seismic cone penetration test.

Figure 30. On top of the sounding rods is a CPTu probe connected to the seismic module and cable.

Figure 31. Sledgehammer connected to cable.

Seismic tests were carried out at regular intervals of one metre along the bore-hole, resulting in consistent V_s values. The obtained minimum and maximum V_s values from all six soundings, ranging from 37 to 352 m/s, are presented in Table 10. Furthermore, the table provides the difference between the maximum and minimum V_s values, denoted as ΔV_s. In terms of q_t and f_s values,

measurements were taken every 20 mm, and the average values of one-metre-thick layers were utilized for the analysis. Table 10 also presents the minimum and maximum q_t and f_s values for all six SCPTu soundings.

The database quality was enhanced by analysing the measured V_s values and eliminating outliers using statistical methods. The identification of outliers was done using the '2σ' statistical criteria, where σ represents the standard deviation of the variable V_s. As a result, a 95% confidence interval criterion was established for the data. In total, two V_s values (37 and 352 m/s) were identified as outliers and subsequently excluded from the analysis, leaving a database of 108 values for further examination.

Table 10. Summary of V_s values alongside the minimum and maximum results of average q_t and f_s values for 1-m-thick layers (Publication 3).

	$V_{s\text{-}min}$ m/s	$V_{s\text{-}max}$ m/s	ΔV_s m/s	$q_{t\text{-}min}$ MPa	$q_{t\text{-}max}$ MPa	Δq_t MPa	$f_{s\text{-}min}$ kPa	$f_{s\text{-}max}$ kPa	Δf_s kPa
SCPTu-A1	46	259	213	0.5	4.3	3.7	7.9	76.9	69.0
SCPTu-A3	44	203	159	0.5	8.0	7.5	3.4	107.5	104.1
SCPTu-A4	58	352	294	0.6	4.8	4.2	2.3	91.1	88.8
SCPTu-P1	37	233	196	0.4	17.7	17.3	0.6	157.3	156.6
SCPTu-P2	57	270	213	0.3	25.6	25.3	2.8	144.4	141.5
SCPTu-S1	76	248	172	0.4	18.5	18.1	0.5	137.1	136.6

7. Test sites

7.1 Ahtri test site

The Ahtri test site, situated in the northern region of Estonia, is located in the northern side of Tallinn, as depicted in Figure 32 (Map applications of the Estonian Land Board, 2024). This r site is positioned above Quaternary sediments that conceal old valleys. The various deposits within the Ahtri site include marine, lacustrine and alluvial deposits, which consist of clay, silty sands, sandy silts and sand. The hard stratum at the Ahtri test site extends to a considerable depth of dozens of metres, as shown in Figure 33. Figure 33 provides a visual representation of a rigid stratum with consistent height lines, along with the precise location of the designated test site (Map applications of the Estonian Land Board, 2024). Additionally, the map highlights an obscured ancient valley region, marked by a pink fiddle-shaped symbol. A total of the in-situ tests carried out on the Ahtri test site is shown in Table 11.

Table 11. Summary of in-situ tests carried out on the Ahtri test site.

Test name	Number
Static axial pile load test with Fundex 450/560 pile	4
DCPT (DPSH-A)	3
CPT	3
CPTu	4
SCPTu	3

Within the soil profile, there is a layer of fill that spans a range of 0.6−3.2 metres in thickness. Beneath this fill layer, one can find silty sand and sandy silt soils, extending downwards to a depth of up to 9 metres. Situated beneath these soils is a sensitive fine-grained soil layer, measuring approximately 2−3 metres in thickness. Below this layer, clay and silty clay soils are present, forming layers that are a few metres thick. At a depth of 19 metres, a combination of silt and sand mixtures occurs beneath the clayey layers. At a depth of 19−29.2 metres, sporadic thin layers of silty clay and clayey silt can be observed atop a dense sandy deposit. These layers serve as a trap for silty soils, which possess a natural water content ranging from 24.75% to 38.49%. The water table in this area lies 1.2−1.8 meters below the ground surface. In the year 2016, the construction of

a facility building involved the installation of numerous Fundex-type piles. However, the construction was halted, leading to the filling of the upper ends of these piles.

Figure 34 illustrates the site plan of 3 Ahtri Street, showcasing the presence of existing piles, tested piles (SLT) and sounding points. Furthermore, it provides the shortest distance in metres from the nearest pile for the SCPTu-A1 to SCPTu-A4 sounding points.

Figure 32. The location of the research point in Tallinn (Map applications of the Estonian Land Board, 2024). The red mark indicates the location of 3 Ahtri Street.

Figure 33. Hard stratum relief around the survey site (Map applications of the Estonian Land Board, 2024). The red mark indicates the location of 3 Ahtri Street.
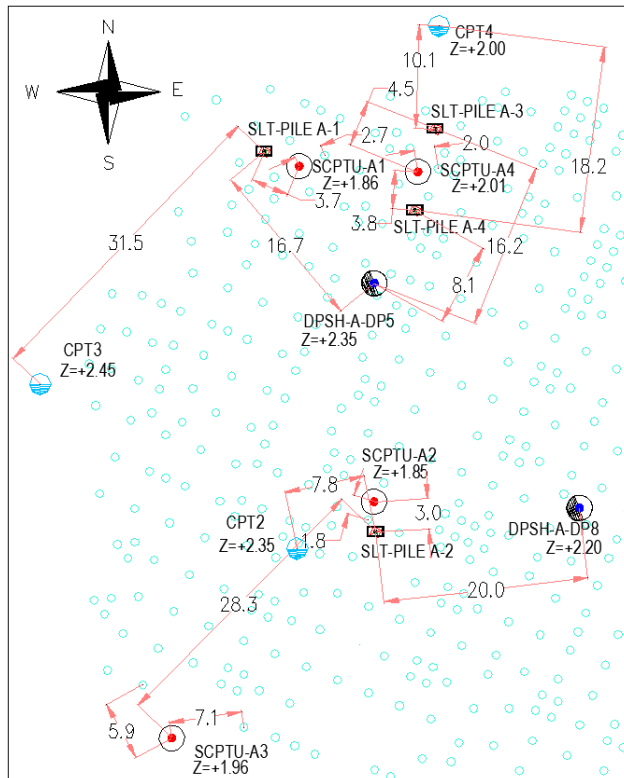
Figure 34. Site plan of 3 Ahtri Street with existing piles (light blue circles), tested piles (SLT) and sounding points. DPSH-A-DP points indicate dynamic probing positions. SCPTU-A1 to SCPTU-A4 indicate seismic CPTu soundings. Distances are shown in metres (modified after Publication 1).

7.1.1 Static pile load test data

In 2006, a static pile load test was performed on four Fundex 450/560 piles. A load of up to 3600kN was applied in the tests. The settlements of the pile head ranged from 4.9 to 50.7 mm. The testing of the piles at this site was conducted two to four weeks after their installation. It is important to note that the piles were tested prior to the completion of the entire pile field. To determine the ultimate capacity of the piles, Chin's (1970) extrapolation method and load-settlement curve were used. The analysis incorporated pile loads, resulting in a settlement of 10% of the pile base diameter. The extrapolation results for all four piles are summarized in Figure 35. The test plot of pile A-4 differs significantly from the plot of the other three pile tests (Figure 35). This refers to a possible breakage in the pile A-4 during the test and the results of this pile must be treated with caution.
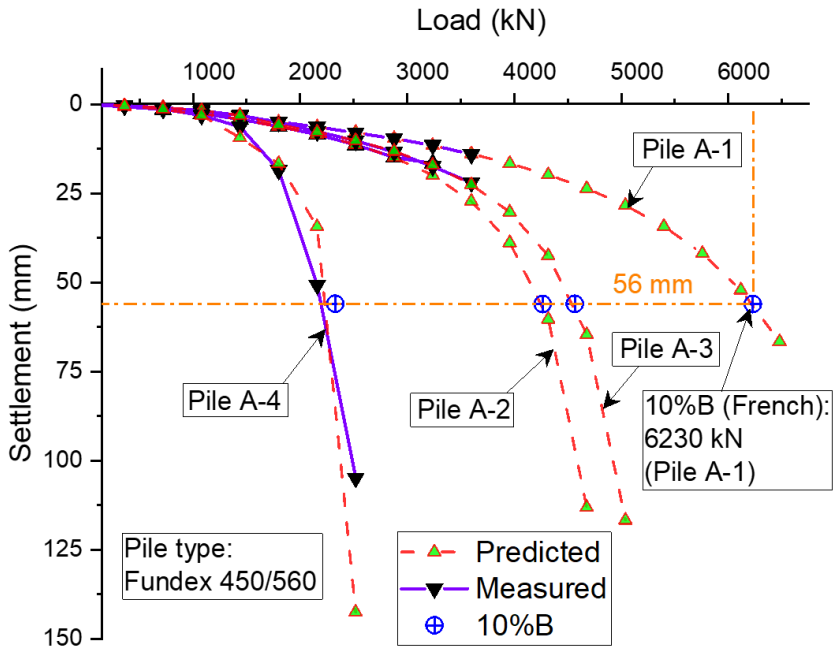
Figure 35. Load-displacement curve of the pile load test and the extrapolation results for the four piles at the Ahtri site.

Table 12 presents a summary of load tests of four piles at the Ahtri site. Table 12 is including the values of the maximum sounding readings and the depths of the soundings. Table 12 shows the soundings that are closest to the test piles.

Table 12. Pile case records summary with the pile load test data at the Ahtri site (modified after Publication 1).

Pile name	A-1	A-2	A-3	A-4
Pile type	Fundex 450/560	Fundex 450/560	Fundex 450/560	Fundex 450/560
Pile length (m)	27.0	26.0	23.2	23.5
Max load from pile load test (kN)	3600	3240	3600	2160
Max settlement from pile load test (mm)	4.9	6.2	22.0	50.7
s/B (%)	0.9	1.1	3.9	9.1
Max depth of CPT sounding (m)	20.7	20.33	22.67	22.67
Max depth of CPTu sounding (m)	23.5	20.94	22.98	22.98
Max depth of DPSH-A sounding (m)	23.6	26.0	23.6	23.6
Max q_c reading from CPT (MPa)	15.5	18.5	9.5	9.5
Max q_c reading from CPTu (MPa)	48.9	33.5	22.6	22.6
Max N_{20} reading from DPSH-A	285	467	285	285

The data presented in Table 12 show clearly that CPTu's soundings with a light-anchored machine penetrated to a greater depth than CPT soundings carried out with a heavy truck. Additionally, it is evident that the q_c values for all CPTu soundings exceed those recorded for CPT soundings. Moreover, it is evident from Table 12 that the DPSH-A soundings consistently achieved greater depths compared to the CPTu soundings (Publication 1).

7.1.2 Sounding data

DCPT tests

Thirteen DPSH-A soundings were conducted at the Ahtri site approximately one year prior to the commencement of piling work. Out of these thirteen soundings, two DCPT probings (DPSH-A-DP 5 and DPSH-A-DP 8) were included in the work, specifically carried out in close proximity to the tested piles. In order to account for the weight of the growing rods and subsequently reduce the impact energy, the number of blows required to penetrate 200 mm was adjusted. However, due to the dense subsoil, it was not possible to probe DPSH-A deeper than the pile base. The distance between the tested piles and DPSH-A soundings varied between 8.1 and 20.0 metres. The precise locations of the test points can be observed in Figure 34. The results of the two DCPT tests, together with a description of the soils, are shown in Figure 36.
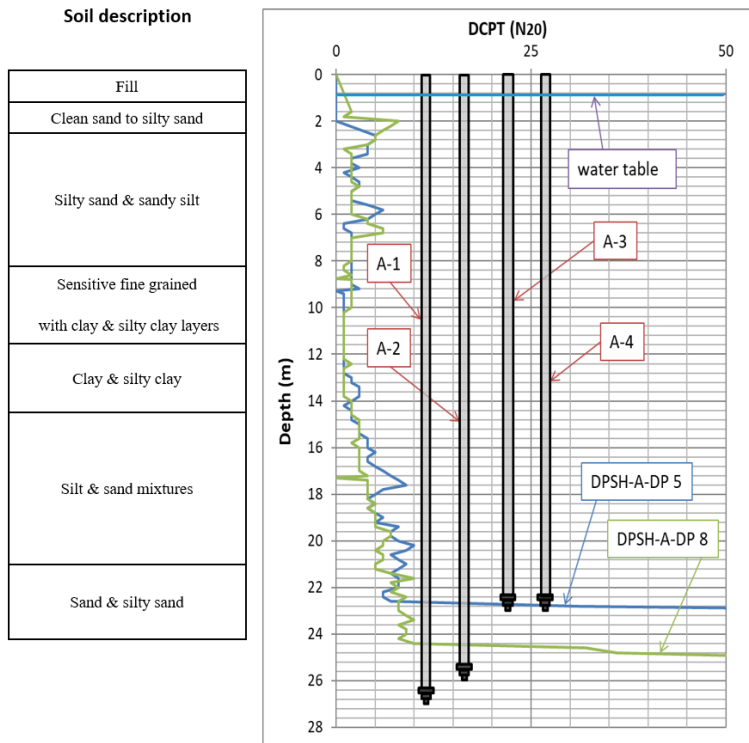
Figure 36. Soil description and the results of DPSH-A tests at the Ahtri site with tested piles. DPSH-A-DP 5 (blue) and DPSH-A-DP 8 (green). N_{20}, the number of blows per 200 mm.

CPT and CPTu tests

Ten CPTu soundings were conducted at the Ahtri site before the piles were erected. Piezocone tests were performed. The cone allowed determining the base and side resistance, pore water pressure and cone inclination. During these investigations, the measurement of pore pressure was solely conducted for the purpose of the dissipation test. A total of three sounding points (CPT2, CPT3 and CPT4) were included in the analysis. As a part of the supplementary studies conducted in 2019, four (referred to as SCPTU-A1, SCPTU-A2, SCPTU-A3 and SCPTU-A4) SCPTu soundings were performed at the Ahtri site. The machine used for sounding is described in sections 6.3.1 and 6.3.4. These soundings were specifically conducted between the piles. The minimum distance between the centre of the piles and the three SCPTu sounding points varied from 1.8 to 2.7 metres. A fourth SCPTu testing point (SCPTu-A3) was situated at a distance exceeding 5.5 metres from the piles. The purpose of sounding SCPTu-A3 was to compare the results obtained from the other three SCPTu tests and the previously conducted CPT tests, as shown in Figure 34. The profiles of q_t, f_s, R_f and u_2, which are representative of the Ahtri site soils, are illustrated in Figure 24.

At the Ahtri site, the SCPTu soundings were carried out before the piles were installed, whereas the CPTu soundings were executed between the piles five years later. This raises the question of whether there are significant variations in the CPTu sounding results between the piles compared to the previously conducted CPT data. To investigate this, the closest CPT and CPTu sounding results were examined side by side, as illustrated in Figures 37 and 38. In the comparison of CPTu readings, the designation CPTu-A1 to CPTu-A4 has been used instead of SCPTU-A1 to SCPTU-A4.

The majority of CPT and CPTu tests yield similar cone resistance values, except for CPTu-A2, which presents notable differences (see Figures 37 and 38). It is important to highlight that the sounding point for CPTu-A2 is situated closest to the previously installed piles. The installation of these piles has resulted in an increase of soil density. As a result, both cone resistance and sleeve friction values have increased. These alterations must be taken into consideration when assessing the load-bearing capacity of pile A-2 relying on the data derived from CPTu-A2 (Publication 1).
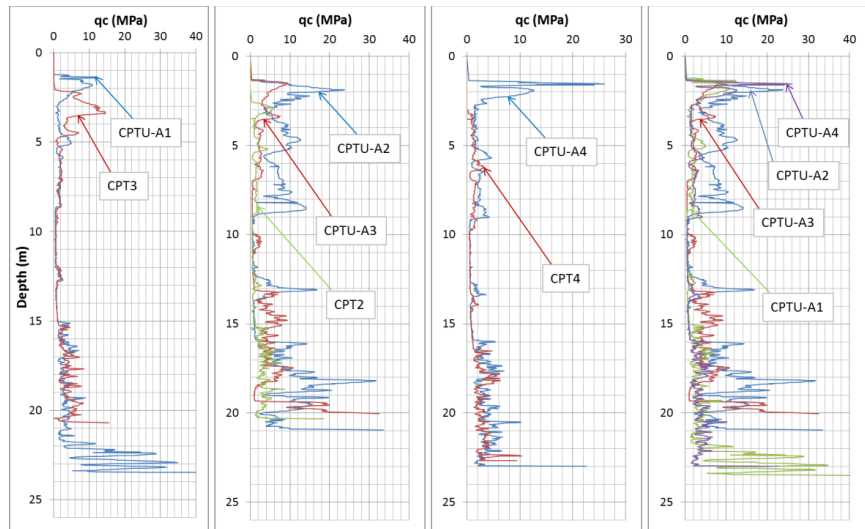
Figure 37. Values of CPT and CPTu cone resistance at the Ahtri site. q_c, cone resistance (Publication 1).
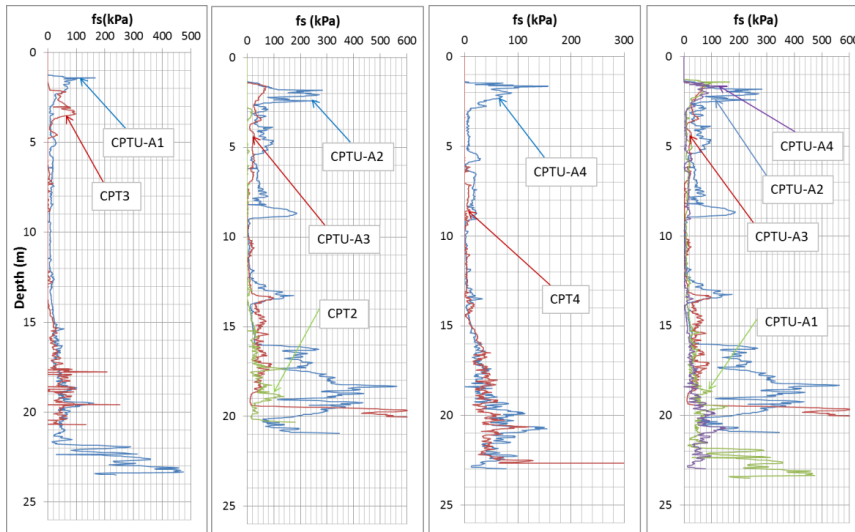
Figure 38. Values of CPT and CPTu sleeve friction at the Ahtri site. f_s, sleeve friction (Publication 1).

SCPTu tests

In 2019, a total of four SCPTu soundings were carried out at the Ahtri site, with a maximum depth of 23.5 metres. The machine used for sounding is described in section6.3.1 and 6.3.4. These soundings were conducted thirteen years after the installation of the piles. The distance between the tested piles and SCPTu soundings varied from 3 to 28 metres, as illustrated in Figure 34. It is worth noting that the readings obtained from the sounding CPTU-A2 differed significantly from those of the other CPT soundings, as illustrated in Figures 37 and 38. Consequently, the data from CPTU-A2 sounding were not included in the SCPTu figures and analyses. Furthermore, it is important to mention that the SCPTu soundings only reached the bottom plane of two piles. None of the SCPTu soundings managed to penetrate deeper than the bottom of the pile. The results of three SCPTu soundings are shown in Figure 39 (Publication 3).
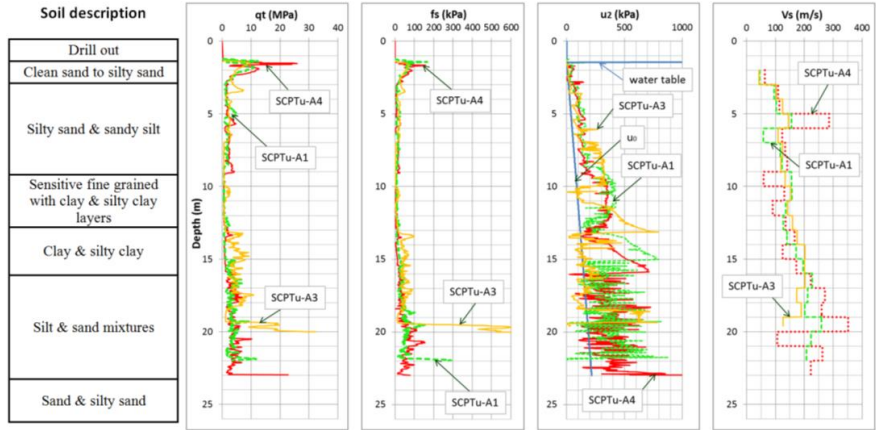
Figure 39. Results of the piezocone test at the Ahtri site. q_t, cone resistance corrected for the pore pressure effects; f_s, sleeve friction; u_2, pore pressure; V_s shear wave velocity (Publication 3).

7.2 Paldiski mnt test site

The Paldiski mnt test site, situated in the northern region of Estonia, is located on the western side of Tallinn, as indicated in Figure 40 (Map applications of the Estonian Land Board, 2024). This site is positioned above Quaternary sediments that conceal old valleys. Within the Paldiski mnt site, there are various deposits including marine, lacustrine and alluvial deposits, consisting of clay, silty clay, sand and silty sand. The test site's hard stratum extends to a considerable depth of several dozens of metres (Figure 41). Figure 41 provides a depiction of a rigid stratum with consistent height lines, along with the precise location of the designated test site (Map applications of the Estonian Land Board, 2024). Additionally, the map showcases an obscured ancient valley region, represented by a pink fiddle-shaped symbol. A total of the in-situ tests carried out on the Paldiski mnt test site is shown in Table 13.

Table 13. Summary of in situ-tests carried out on the Paldiski mnt test site.

Test name	Number
Static axial pile load test with Fundex 350/450 pile	3
DCPT (DPSH-A)	2
SCPTu	2

The Paldiski mnt site is positioned on the slope of the buried Kopli valley. At this site, the presence of alternating strata consisting of clay and silty soils can be observed. These layers are of varying thickness, ranging from 6.4 to 7.0 metres. Below these layers, there exists a deposit of clayey silt, measuring 6.2 to 11.0 metres in thickness, followed by a dense silty fine sand layer with a thickness of 2.6 to 6.8 metres. The natural water content of the clayey silt falls within

the range of 24.3% to 29.5%. The silty sand contains weak interlayers. Starting from a depth of 19.2 to 22.6 metres, a layer of fine sand is present. The water table is situated 1.0 to 1.7 metres below the ground surface.

Figure 42 presents the plan of the Paldiski mnt site, highlighting the presence of tested piles (SLT) and sounding points. It is important to mention that the SCPTu soundings were conducted after the completion of the building, leading to their location being situated 17 to 47 metres away from the test piles.

Figure 40. The location of the research point in Tallinn (Map applications of the Estonian Land Board, 2024). The red mark indicates the location of 81 Paldiski mnt.
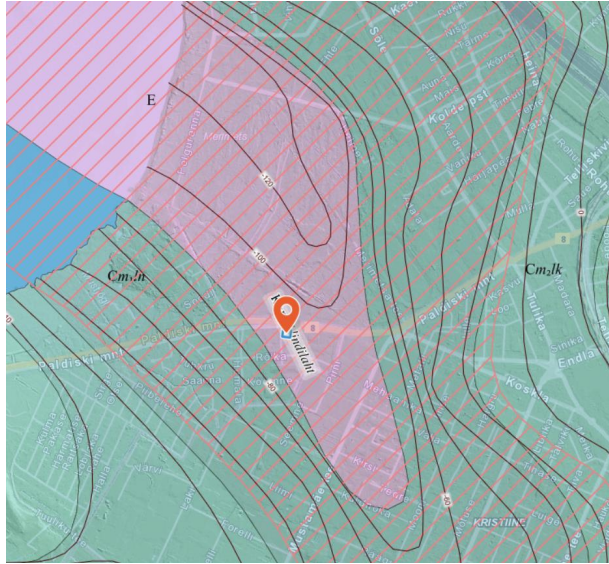
Figure 41. Hard stratum relief around the survey site. (Map applications of the Estonian Land Board, 2024). The red mark indicates the location of 81 Paldiski mnt.
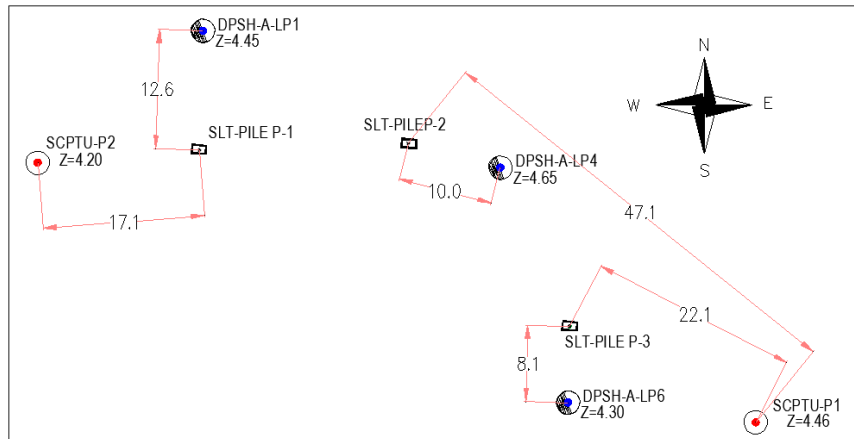
Figure 42. Site plan of 81 Paldiski mnt with tested piles (SLT) and sounding points. DPSH-A-LP points indicate dynamic probing positions. SCPTU-P1 and SCPTU-P2 indicate seismic CPTu soundings. Distances are shown in metres (modified after Publication 2).

7.2.1 Static pile load test data

In 2015 the Fundex 350/450 test pile at the Paldiski mnt test site experienced the highest load of 1200 kN. The settlement of the pile head ranged from 6.3 to 15 mm. The test piles at the site were subjected to testing two to three weeks after their installation, before the entire pile field was constructed. To determine

the ultimate capacity of the piles, Chin's (1970) extrapolation method and load-settlement curve were employed. Pile loads were taken into account during the analysis, leading to a settlement equal to 10% of the diameter of the pile base. The extrapolation results for all three piles can be found in Figure 43.
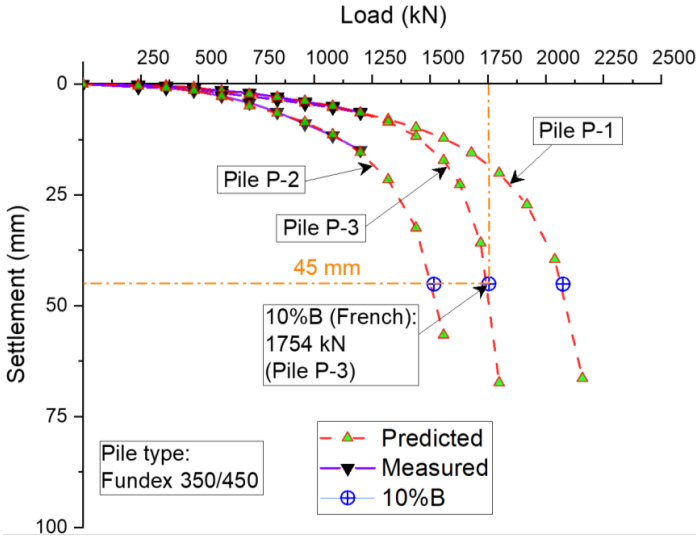
Figure 43. Load-displacement curve of the pile load test and the extrapolation results for the piles at the Paldiski mnt site.

Table 14 presents a comprehensive comparison of the lengths of the tested piles, their maximum loads, settlement, maximum sounding readings and depths of the soundings. Also, the sounding data that closely correspond to each pile are presented below it (Publication 1).

Table 14. Summary of pile case records with the pile load test data at the Paldiski mnt site (modified after Publication 1).

Pile name	P-1	P-2	P-3
Pile type	Fundex 350/450	Fundex 350/450	Fundex 350/450
Pile length (m)	15.5	15.5	15.0
Max load from pile load test (kN)	1200	1200	1200
Max settlement from pile load test (mm)	6.3	6.5	15.0
s/B (%)	1.4	1.4	3.3
Max depth of CPTu sounding (m)	18.98	19.82	19.82
Max depth of DPSH-A sounding (m)	24.41	23.6	22.4
Max q_c reading from CPTu (MPa)	37.4	33.2	33.2
Max N_{20} reading from DPSH-A	123	111	165

76

7.2.2 Sounding data

DCPT tests

Six DPSH-A soundings were executed two weeks prior to the installation of the testing piles. Three DCPT probings were included in the work out of the six carried out near the tested piles. The depth of the soundings exceeded the diameter of the pile base at minimum of 15 times. The distance between the tested piles and DPSH-A soundings ranged from 5.8 to 13.0 metres. The exact positioning of the test points is depicted in Figure 42. The description of the soils is complemented by the inclusion of DSPT sounding graphs (Figure 44).
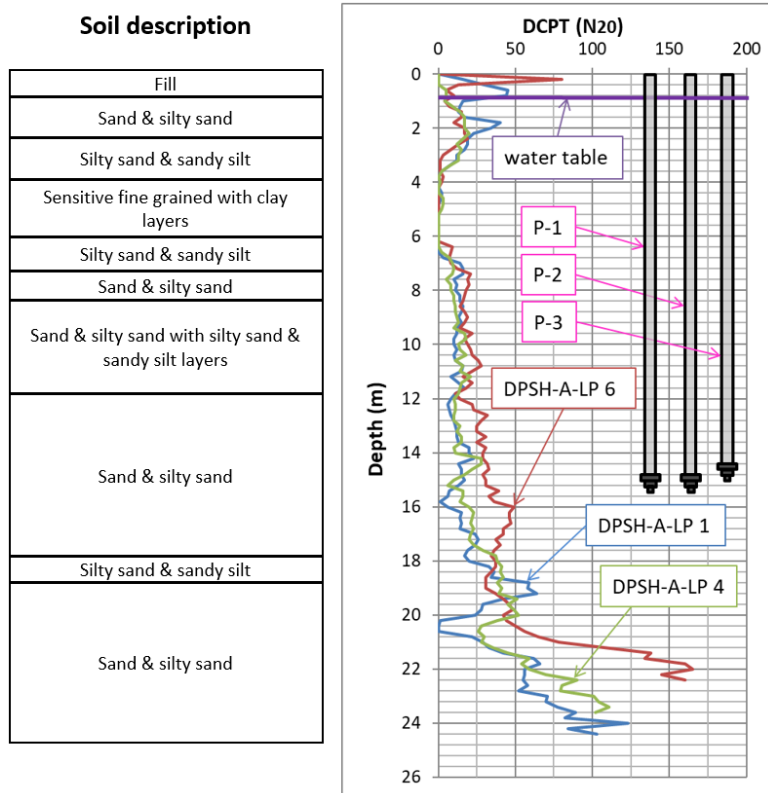
Figure 44. Soil description and the results of DPSH-A tests at the Paldiski mnt site with tested piles. DPSH-A-LP 1 (blue), DPSH-A-LP 4 (green) and DPSH-A-LP 6 (red). N_{20}, the number of blows per 200 mm.

SCPTu tests

Two SCPTu soundings were executed near the two opposite sides of the finished building in 2019. These soundings took place after a period of four and a half years following the installation of the piles. The distance between the tested

piles and SCPTu soundings ranged from 17 to 47 metres, as indicated in Figure 42. It is important to highlight that the soundings reached at least 3 metres below the pile base. The results of the two SCPTu soundings are shown in Figure 45 (Publication 3).
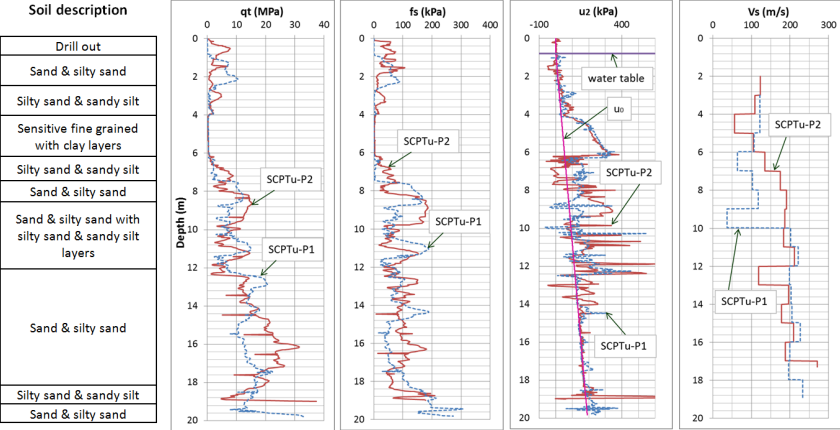
Figure 45. Soil description and the results of SCPTu tests P1 (blue figures) and P2 (red figures) at the Paldiski mnt site. q_t, cone resistance corrected for the pore pressure effects; f_s, sleeve friction; u_2, pore pressure; V_s shear wave velocity (Publication 3).

7.3   Soodi test site

Located in the northern region of Estonia, the Soodi test site is positioned on the western side of Tallinn (Map applications of the Estonian Land Board, 2024), as illustrated in Figure 46. This site is situated above a buried ancient valley that is concealed beneath Quaternary sediments. The sedimentary deposits found in this area consist of marine, lacustrine and alluvial formations, which are composed of varying layers of clay, silty clay, sand and silty sand. The first 4.1 metres of the deposits primarily comprise alternating layers of silty sand and sandy silt. At a depth of 11.7–11.9 metres, sand and silty sand deposits reemerge. Throughout the site, the layers of soft clayey and silty soil alternate. A hard stratum consisting of gravel/moraine is encountered at a depth of nearly 30 metres. The groundwater table at this location varies between 0.05 and 0.65 metres below the ground surface. The depiction in Figure 47 reveals the presence of a rigid stratum exhibiting consistent height lines, accompanied by the precise placement of the designated test site (Map applications of the Estonian Land Board, 2024). The map showcases an obscured ancient valley region, denoted by a pink fiddle-shaped symbol. This specific area encompasses the Kopli klint bay. All the in-situ tests carried out at the Soodi test site are shown in Table 15.

Table 15. Summary of in situ tests carried out on the Soodi test site.

Test name	Number
Static axial pile load test with DSP pile	2
Static axial pile load test with FTP pile	2
CPTu	2
SCPTu	1
SDT	2

For a visual representation of the sounding points and tested piles, refer to Figure 48. Prior to the installation of the test piles, the SDT soundings SLP9 and SLP10 were performed. In contrast, the CPTu soundings were assembled after the building was constructed, resulting in their location being more than 46 metres away from the test piles.
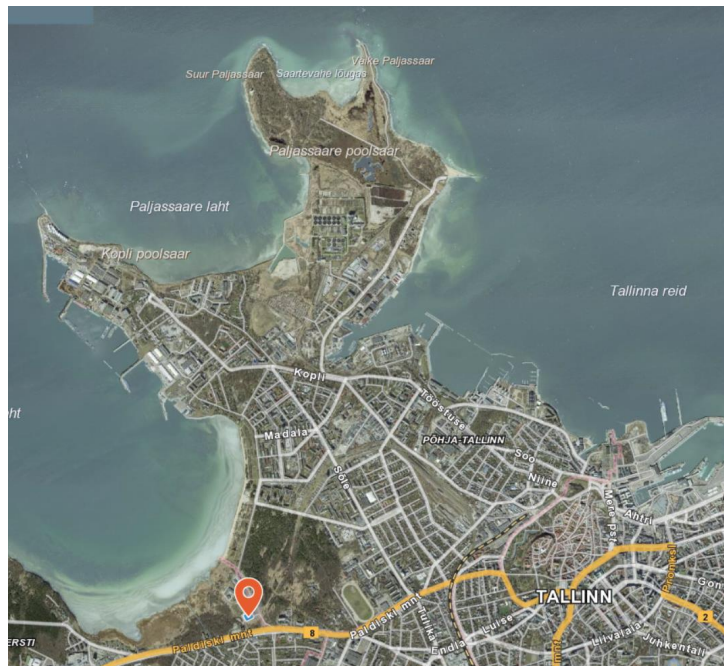
Figure 46. The location of the research point in Tallinn (Map applications of the Estonian Land Board, 2024). The red mark indicates the location of 4 Soodi Street.

Figure 47. Hard stratum relief around the survey site (Map applications of the Estonian Land Board, 2024). The red mark indicates the location of Soodi street 4.

Figure 48. Site map with the tested piles and sounding points. CPTU-S1 and CPTU-S2 indicate CPTu soundings and SCPTU-S3 indicates seismic CPTu sounding. SLP9 and SLP10 indicate SDT soundings. The pile symbols are S-1 to S-4, and the type of pile is shown next to the name of the tested piles. The dimensions given in the map are in metres (modified after Publication 2).

7.3.1 Static pile load test data

Four static pile load tests were carried out in 2016. The tested piles ranged in length from 11.34 to 12.69 metres. The two pile types that were subjected to testing were the Bauer full displacement pile (FDP) and displacement pile (DSP). Both types of test piles were subjected to a maximum load of 1870 kN, which represents 83.7–98.8% of their ultimate capacity. The settlement of the pile head ranged from 17.0 to 35.3 mm. The testing of the piles took place two to three weeks after their installation. To determine the ultimate pile capacity, Chin's (1970) extrapolation method and load-settlement curve were utilized, considering that the piles were loaded with a settlement equal to 10% of their nominal diameter. The extrapolation results for all four piles are summarized in Figure 49.
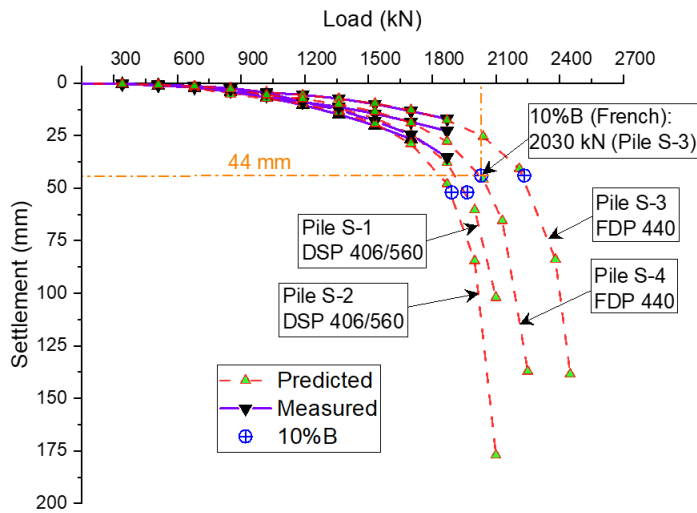
Figure 49. Load-displacement curve of the pile load test and the extrapolation results for the four piles at the Soodi site (modified after Publication 2).

The presentation in Table 16 provides a comprehensive overview of the tested piles, including their lengths, maximum loads and settlement. Additionally, it includes the values of the maximum sounding readings and the depths of the soundings. The sounding data that closely correspond to each pile are presented below it (Publication 2).

Table 16. Pile case records summary with the pile load test data at the Soodi site (modified after Publication 2).

Pile name	S-1	S-2	S-3	S-4
Pile type	DSP 406/520	DSP 406/520	FDP 440	FDP 440
Pile length (m)	12.69	11.34	12.39	12.5

Max load from pile load test (kN)	1870	1700	1870	1870
Max settlement from pile load test (mm)	35.3	22.8	17.0	22.7
s/B (%)	6.8	4.4	3.9	5.2
Max depth of CPTu sounding (m)	25.18	25.18	25.18	25.18
Max depth of SDT sounding (m)	21.49	21.13	21.3	21.3
Max q_c reading from CPTu (MPa)	21.7	21.7	21.7	21.7
Max q_c reading from SDT (MPa)	11.1	14.5	14.5	14.5
Max N_{20} reading from SDT	15	26	26	26

7.3.2 Sounding data

CPTu tests

In the year 2019, two CPTu soundings were conducted. The machine used for sounding is described in Sections 6.3.1 and 6.3.4. The locations of the study points can be observed in Figure 48. The distance between the CPTu sounding points and test piles varied between 45 and 75 metres. Figure 50 illustrates the profiles of the corrected cone resistance (q_t), unit sleeve friction resistance (f_s), friction ratio (R_f) and pore pressure measured behind the cone (u_2). To the left of the sounding results descriptions of the soils are presented. Sounding S1, which reached a depth of 25.2 metres, is represented in blue. Sounding S2, which reached a depth of 20.4 metres, is marked in red. The soils predominantly consist of various mixtures of silt. The pore water pressure image encompasses the water table and the in-situ pore pressure (u_o) profile (Publication 2).
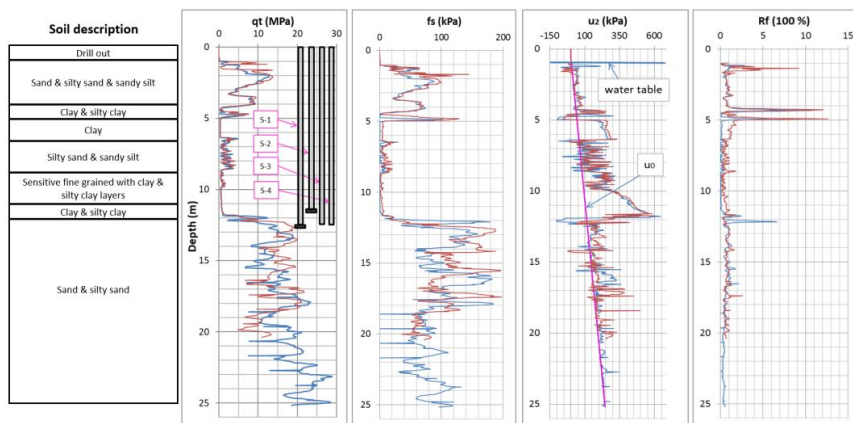

Figure 50. Soil description and the results of CPTu tests S1 (blue) and S2 (red) at the Soodi site. q_t, cone resistance corrected for the pore pressure effects with tested piles; f_s, sleeve friction; R_f, friction ratio; u_2, pore pressure (Publication 2).

SDT tests

In spring 2015, SDT soundings were carried out using the GM 65 GTT unit, following the instructions provided by Melander (1989). A total of 10 soundings were conducted, and the results from the two soundings (SLP9 and SLP10) that were closest to the tested piles were utilized. The distance between the piles and the nearest sounding point ranged from 2.9 to 8.8 metres, as depicted in Figure 48. The depths of the SDT soundings SLP9 and SLP10 were recorded as 21.13 and 21.49 meters, respectively. The findings from the soundings, along with the description of the soils, can be observed in Figure 51.

The left figure illustrates the outcomes obtained from SLP9, showcasing the clear distinction between static penetration (q_c-SDT) and dynamic penetration (N_{20}-SDT) in the SDT test. The middle figure presents the combined results of SLP9 and SLP10 tests (q_c-SDT + N_{20}-SDT), along with the q_c values obtained from these tests (q_c-SDT-CPT) after the application of Formulas 12 to 15. The rightmost figure compares the q_c values derived from the results of SLP9 and SLP10 (q_c-SDT-CPT) with the CPTu tip resistance values of S1 and S2 (q_c-CPTU) (Publication 2).
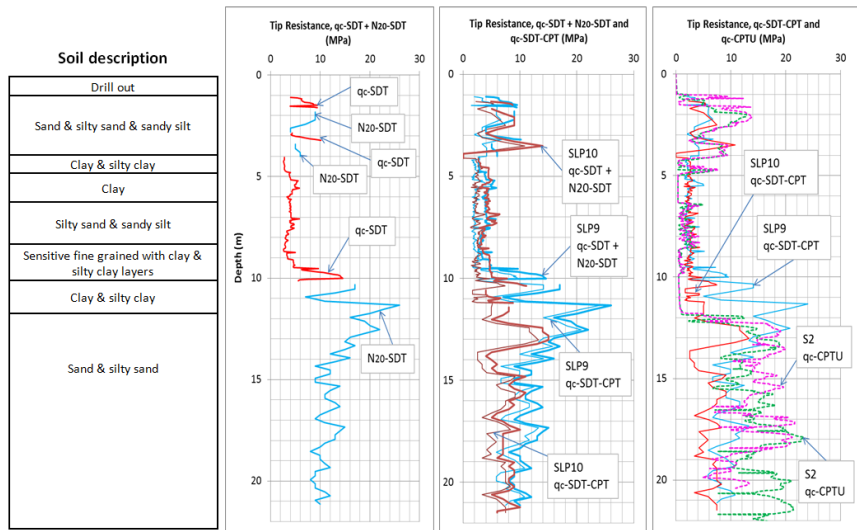
Figure 51. SLP9 sounding results in the figure on the left. The results of SLP9 and SLP10 (qc-SDT + N20-SDT) converted to the q_c value of CPT (qc-SDT-CPT) in the middle. The results of SDT test compared with the CPTu test at the Soodi site on the right. q_c-SDT, cone resistance from static readings of SDT; N_{20}-SDT, cone resistance from dynamic readings of SDT; q_c-SDT-CPT, measured and derived q_c values from SDT q_c and N_{20} values; q_c-CPTu, cone resistance from CPT (Publication 2).

SCPTu tests

In 2019, one SCPTu sounding was conducted at the Soodi site using the Geotech AB Nova cone.The distance between the tested piles and SCPTu sounding ranged from 45 to 75 metres, as shown in Figure 48. The sounding penetrated

to the depth of at least 7 metres below the pile base. The results of V_s, along with the soil description and CPTu readings, are presented in Figure 52 (Publication 3).
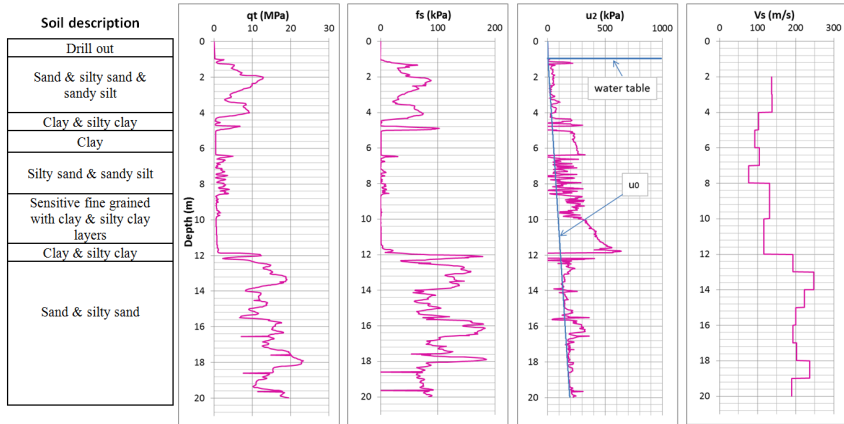
Figure 52. Results of piezocone tests at the Soodi site. q_t, cone resistance corrected for the pore pressure effects; f_s, sleeve friction; u_2, pore pressure; V_s shear wave velocity (Publication 3).

8. Comparison of axial capacity of the piles based on CPT and SPT direct methods

8.1 Results of Ahtri site

The calculations for pile A-2 were derived from the analysis of data collected from two CPTu points. The main objective of this analysis was to ascertain whether the results obtained from the probing conducted between the piles could be utilized as a foundation for determining the load-bearing capacity of the pile. Test CPTu-A2 was carried out between the piles, with the closest distance to the adjacent pile being 1.8 metres. Notably, this distance represented the shortest measurement between the survey points and the piles. Conversely, investigation point CPTu-A3 was positioned at a minimum distance of 5.5 metres from the adjoining pile and 27.7 metres from the test pile A-2.

The analysis of the data collected at the two research points reveals a remarkable similarity in the outcomes. However, the most notable difference arises when employing the Eurocode 7 method (EN 1997-2:2007). This discrepancy, amounting to 12%, is clearly depicted in Figure 53. Additionally, Figure 53 provides a clear visual representation that if the result obtained through the direct method falls within a 20% range, it consistently remains within this threshold for both CPTu-A2 and CPTu-A3, with only a slight variation observed for the LCPC method. Consequently, the results obtained from the CPTu tests conducted on the existing piles can be effectively used in the ongoing study.

The findings presented in Tables 17 to 20 and Figure 54 highlight the wide-ranging variations observed in the results obtained from the CPTu and CPT tests. These discrepancies can be attributed to the limitations inherent in the cone penetrometers used in the study. It is worth noting that the LCPC method exhibits the greatest level of variability, with a range of 96% when considering the results based on CPT data. The smallest degree of variability can be observed when employing the Nottingham and Schmertmann (1975, 1978) method and the Eurocode 7 (EN 1997-2:2007) method, both yielding results within a range of 64%.

Table 18 and Figure 55 present the calculation outcomes for pile A-2 when the probing methods CPTU-A2 and CPTU-A3 were used. Figure 55 demonstrates

that the load capacity of pile A-2, determined using the Eurocode method and data from CPTU-A3, yields favourable results.

Considerable variations can be observed in the results obtained from the calculations conducted using DPSH-A, particularly in terms of the minimum and maximum values. It is worth noting that the variability across all methods, except for the results obtained from pile A-4 (Table 20), remains within 37%. Upon evaluating the data from three different piles (Tables 17 to 19 and Fig. 54), it becomes evident that the Briaud and Tucker (1988) method consistently provides results that are within 20% of the measured capacity. Additionally, all SPT methods employed in the study exhibit a satisfactory fit within the ±20% range at the Ahtri site (Publication 1).

Table 17. Comparison between the static load test results and bearing capacity prediction for the test pile A-1.

Method	R_b (kN)	R_s (kN)	R_c (kN)	R_{cm}/R_{cp}	Absolute Difference (%)	Basis	Sounding ID
Static Loading Test (s/B=10%)			6230	1.00	0	Measured	
Nottingham and Schmertmann	3690	1610	5193	1.20	-20	CPT	CPTU-A1
de Ruiter and Beringen (Dutch)	3690	898	4481	1.39	-39	CPT	CPTU-A1
LCPC (Bustamante)	3690	1670	5253	1.19	-19	CPT	CPTU-A1
EUROCODE 7	3690	1825	5408	1.15	-15	CPT	CPTU-A1
German method	2251	2148	4291	1.45	-45	CPT	CPTU-A1
Unicone method	3690	1495	5078	1.23	-23	CPTU	CPTU-A1
Nottingham and Schmertmann	3690	1557	5140	1.21	-21	CPT	CPT3
de Ruiter and Beringen (Dutch)	3690	926	4508	1.38	-38	CPT	CPT3
LCPC (Bustamante)	1718	1785	3396	1.83	-83	CPT	CPT3
EUROCODE 7	3054	2144	5091	1.22	-22	CPT	CPT3
German method	1983	2030	3905	1.60	-60	CPT	CPT3
Aoki & De`Alencer	3690	1163	4745	1.31	-31	DPSH-A	DP5
Meyerhof	3690	950	4533	1.37	-37	DPSH-A	DP5
Briaud & Tucker	3690	2631	6214	1.00	0	DPSH-A	DP5
Poulos, Martin, Decourt	3690	1022	4605	1.35	-35	DPSH-A	DP5
Decourt	3690	1327	4910	1.27	-27	DPSH-A	DP5
Shariatmadari	3690	1107	4690	1.33	-33	DPSH-A	DP5

Table 18. Comparison between the static load test results and bearing capacity prediction for the test pile A-2.

Method	R_b (kN)	R_s (kN)	R_c (kN)	R_{cm}/R_{cp}	Absolute Difference (%)	Basis	Sounding ID
Static Loading Test (s/B=10%)			4266	1.00	0	Measured	
Nottingham and Schmertmann	3690	2626	6213	0.69	31	CPT	CPTU-A2

Method	R_b (kN)	R_s (kN)	R_c (kN)	R_{cm}/R_{cp}	Absolute Difference (%)	Basis	Sounding ID
de Ruiter and Beringen (Dutch)	3690	1164	4751	0.90	10	CPT	CPTU-A2
LCPC (Bustamante)	3296	2424	5617	0.76	24	CPT	CPTU-A2
EUROCODE 7	3690	3255	6842	0.62	38	CPT	CPTU-A2
German method	2251	2366	4514	0.95	5	CPT	CPTU-A2
Unicone method	2690	1813	5400	0.79	21	CPTU	CPTU-A2
Nottingham and Schmertmann	3690	1865	5451	0.78	22	CPT	CPTU-A3
de Ruiter and Beringen (Dutch)	3690	1152	4738	0.90	10	CPT	CPTU-A3
LCPC (Bustamante)	3195	1727	4818	0.89	11	CPT	CPTU-A3
EUROCODE 7	3690	2173	5759	0.74	26	CPT	CPTU-A3
German method	2250	2281	4429	0.96	4	CPT	CPTU-A3
Unicone method	3690	2010	5597	0.76	24	CPTU	CPTU-A3
Nottingham and Schmertmann	3690	1303	4890	0.87	13	CPT	CPT2
de Ruiter and Beringen (Dutch)	3690	833	4419	0.97	3	CPT	CPT2
LCPC (Bustamante)	2045	1543	3484	1.22	-22	CPT	CPT2
EUROCODE 7	3635	1651	5183	0.82	18	CPT	CPT2
German method	2050	1953	3899	1.09	-9	CPT	CPT2
Aoki & De`Alencer	3690	739	4326	0.99	1	DPSH-A	DP8
Meyerhof	3690	497	4084	1.04	-4	DPSH-A	DP8
Briaud & Tucker	3616	1761	5274	0.81	19	DPSH-A	DP8
Poulos, Martin, Decourt	3690	607	4194	1.02	-2	DPSH-A	DP8
Decourt	3690	929	4516	0.94	6	DPSH-A	DP8
Shariatmadari	3690	661	4248	1.00	0	DPSH-A	DP8

Table 19. Comparison between the static load test results and bearing capacity prediction for the test pile A-3.

Method	R_b (kN)	R_s (kN)	R_c (kN)	R_{cm}/R_{cp}	Absolute Difference (%)	Basis	Sounding ID
Static Loading Test (s/B=10%)			4566	1.00	0	Measured	
Nottingham and Schmertmann	3690	885	4483	1.02	-2	CPT	CPTU-A4
de Ruiter and Beringen (Dutch)	3690	506	4104	1.11	-11	CPT	CPTU-A4
LCPC (Bustamante)	2228	1071	3206	1.42	-42	CPT	CPTU-A4
EUROCODE 7	3023	1303	4234	1.08	-8	CPT	CPTU-A4
German method	2194	1489	3592	1.27	-27	CPT	CPTU-A4
Unicone method	2075	1048	3031	1.51	-51	CPTU	CPTU-A4
Nottingham and Schmertmann	3148	697	3753	1.22	-22	CPT	CPT4
de Ruiter and Beringen (Dutch)	3148	436	3492	1.31	-31	CPT	CPT4
LCPC (Bustamante)	1945	757	2610	1.75	-75	CPT	CPT4
EUROCODE 7	2519	932	3359	1.36	-36	CPT	CPT4
German method	1471	1373	2752	1.66	-66	CPT	CPT4
Aoki & De`Alencer	3690	688	4286	1.07	-7	DPSH-A	DP5
Meyerhof	3690	475	4073	1.12	-12	DPSH-A	DP5
Briaud & Tucker	3690	1722	5322	0.86	14	DPSH-A	DP5
Poulos, Martin, Decourt	3690	547	4145	1.10	-10	DPSH-A	DP5

Method	Rb	Rs	Rc	Rcm/Rcp	Absolute Difference	Basis	Sounding ID
Decourt	3690	852	4450	1.03	-3	DPSH-A	DP5
Shariatmadari	3690	632	4230	1.08	-8	DPSH-A	DP5

Table 20. Comparison between the static load test results and bearing capacity prediction for the test pile A-4.

| Method	R_b	R_s	R_c	R_{cm}/R_{cp}	Absolute Difference (%)	Basis	Sounding ID
	(kN)	(kN)	(kN)				
Static Loading Test (s/B=10%)			2329	1.00	0	Measured	
Nottingham and Schmertmann	3690	885	4482	0.52	48	CPT	CPTU-A4
de Ruiter and Beringen (Dutch)	3690	560	4156	0.56	44	CPT	CPTU-A4
LCPC (Bustamante)	2227	1156	3290	0.71	29	CPT	CPTU-A4
EUROCODE 7	3259	1387	4554	0.51	49	CPT	CPTU-A4
German method	1649	1577	3133	0.74	26	CPT	CPTU-A4
Unicone method	2179	1109	3194	0.73	27	CPTU	CPTU-A4
Nottingham and Schmertmann	3372	795	4074	0.57	43	CPT	CPT4
de Ruiter and Beringen (Dutch)	3372	484	3763	0.62	38	CPT	CPT4
LCPC (Bustamante)	1945	822	2674	0.87	13	CPT	CPT4
EUROCODE 7	2698	1031	3635	0.64	36	CPT	CPT4
German method	1471	1465	2843	0.82	18	CPT	CPT4
Aoki & De`Alencer	3690	754	4352	0.54	46	DPSH-A	DP5
Meyerhof	3690	543	4140	0.56	44	DPSH-A	DP5
Briaud & Tucker	3690	1860	5456	0.43	57	DPSH-A	DP5
Poulos, Martin, Decourt	3690	615	4212	0.55	45	DPSH-A	DP5
Decourt	3690	920	4517	0.52	48	DPSH-A	DP5
Shariatmadari	3690	700	4297	0.54	46	DPSH-A	DP5
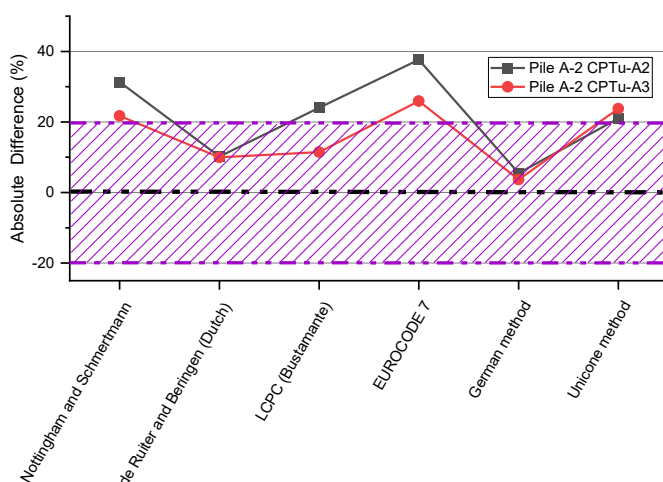
Figure 53. Comparison of the absolute difference between the measured and the predicted capacity for pile A-2 based on CPTu soundings A2 and A3 at the Ahtri site (Publication 1).
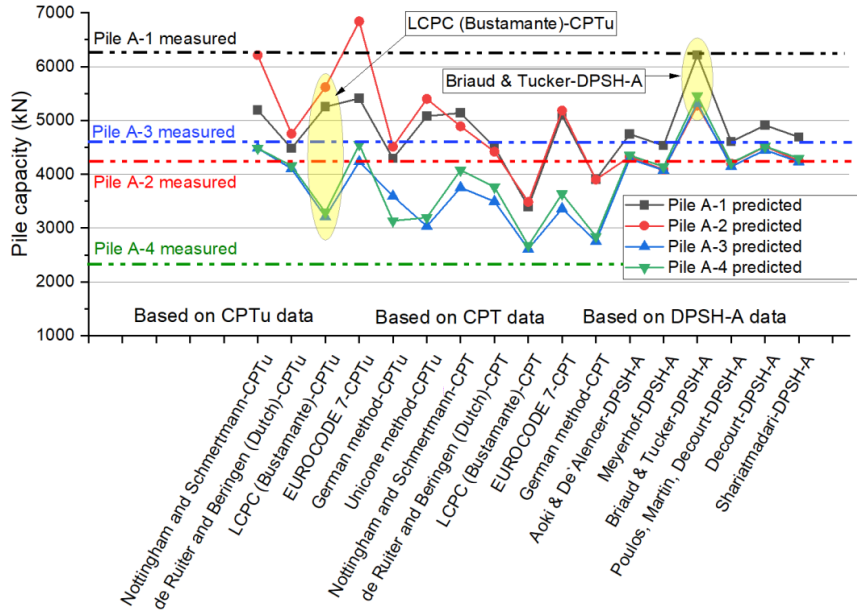
Figure 54. Comparison of the measured and the predicted capacity for piles at the Ahtri site (Publication 1).
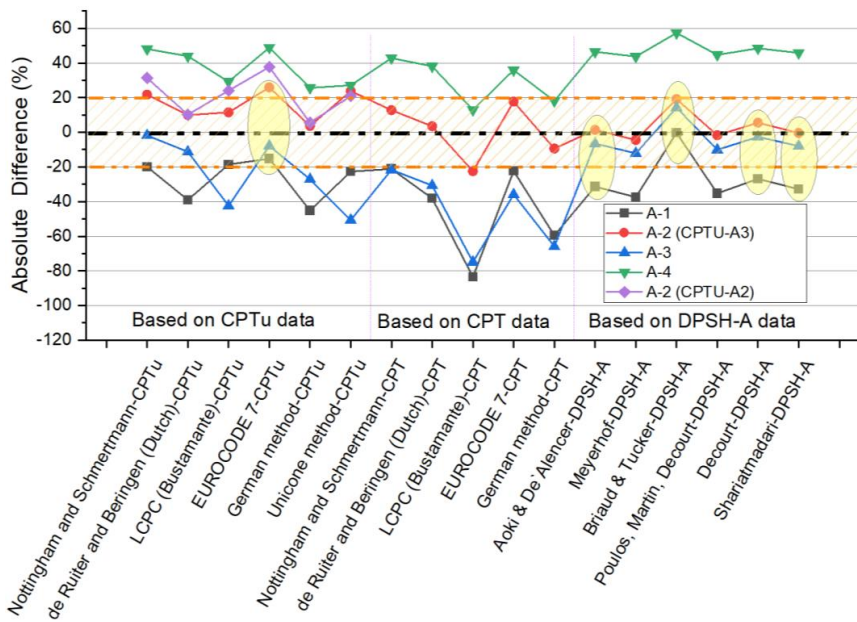

Figure 55. Comparison of the absolute difference between the measured and the predicted capacity for piles at the Ahtri site; +, overestimates; −, underestimates (modified after Publication 1).

8.2 Results from the Paldiski mnt site

The Paldiski mnt site exhibited a significantly smaller variability among different piles in results based on CPT methods compared to the Ahtri site. This is evident from the data presented in Tables 21 to 23 and Figures 56 and 57. The load-bearing capacity of the pile was clearly overestimated by both the Nottingham and Schmertmann (1975, 1978) method and the Eurocode 7 (EN 1997-2:2007) method, with none of the calculated values falling within the 20% range. Similarly, the de Ruiter and Beringen (1979) method and the Unicone (1997) method tended to overestimate the capacity of the piles. However, the LCPC method yielded results that were closest to the measured values, with all the results falling within 20% of the measured capacity. Additionally, the German (2013) method produced outcomes that were quite similar to the results obtained from the pile load test.

The direct SPT methods yielded more varied results compared to the CPT methods. Among the SPT methods, the Shariatmadar (2008) method exhibited the highest variability, with none of its values falling within the 20% range. On the other hand, the Meyerhof (1976) method produced outcomes with the least variability, although none of its results fell within the 20% range and tended to overestimate the pile capacity. In terms of accuracy, the Briaud and Tucker (1988) method provided the closest results to the pile load test outcomes. The calculations for piles P-1 and P-2 with applying the Briaud and Tucker (1988) and Aoki and De'Alencer (1975) methods were considerably accurate. However, both methods resulted in calculations for pile P-3 that were outside the 20% range, with the Aoki and De'Alencer (1975) method also tending to overestimate the pile capacity. Only the Poulos, Martin and Decourt (1989, 1987, 1982) method and the Decourt (1995) method predicted that pile P-3 would fall within the 20% range. Additionally, Figure 56 illustrates that the Poulos, Martin and Decourt (1989, 1987, 1982) method tended to underestimate the pile capacity. At the Paldiski mnt site, three CPT, one CPTu and two SPT methods produced results that fit within the 20% ± 20% range (Publication 1).

Table 21. Comparison between the static load test results and bearing capacity prediction for the test pile P-1.

Method	R_b (kN)	R_s (kN)	R_c (kN)	R_{cm}/R_{cp}	Absolute Difference (%)	Basis	Sounding ID
Static Loading Test (s/B=10%)			1754	1.00	0	Measured	
Nottingham and Schmertmann	2385	967	3315	0.53	47	CPT	CPTU-P2
de Ruiter and Beringen (Dutch)	2385	429	2777	0.63	37	CPT	CPTU-P2
LCPC (Bustamante)	1073	936	1972	0.89	11	CPT	CPTU-P2
EUROCODE 7	1880	1288	3131	0.56	44	CPT	CPTU-P2
German method	1434	975	2372	0.74	26	CPT	CPTU-P2
Unicone method	2156	531	2650	0.66	34	CPTU	CPTU-P2

Method	R_b (kN)	R_s (kN)	R_c (kN)	R_{cm}/R_{cp}	Absolute Difference (%)	Basis	Sounding ID
Aoki & De`Alencer	1333	693	1989	0.88	12	DPSH-A	LP1
Meyerhof	847	345	1155	1.52	-52	DPSH-A	LP1
Briaud & Tucker	1110	751	1824	0.96	4	DPSH-A	LP1
Poulos, Martin, Decourt	816	417	1196	1.47	-47	DPSH-A	LP1
Decourt	758	647	1368	1.28	-28	DPSH-A	LP1
Shariatmadari	705	588	1256	1.40	-40	DPSH-A	LP1

Table 22. Comparison between the static load test results and bearing capacity prediction for the test pile P-2.

Method	R_b (kN)	R_s (kN)	R_c (kN)	R_{cm}/R_{cp}	Absolute Difference (%)	Basis	Sounding ID
Static Loading Test (s/B=10%)			2075	1.00	0	Measured	
Nottingham and Schmertmann	2006	850	2819	0.74	26	CPT	CPTU-P1
de Ruiter and Beringen (Dutch)	2006	380	2349	0.88	12	CPT	CPTU-P1
LCPC (Bustamante)	903	998	1864	1.11	-11	CPT	CPTU-P1
EUROCODE 7	1549	1304	2816	0.74	26	CPT	CPTU-P1
German method	1046	924	1933	1.07	-7	CPT	CPTU-P1
Unicone method	1550	641	2154	0.96	4	CPTU	CPTU-P1
Aoki & De`Alencer	1658	676	2297	0.90	10	DPSH-A	LP4
Meyerhof	1035	336	1334	1.56	-56	DPSH-A	LP4
Briaud & Tucker	1166	746	1875	1.11	-11	DPSH-A	LP4
Poulos, Martin, Decourt	1016	407	1386	1.50	-50	DPSH-A	LP4
Decourt	943	635	1541	1.35	-35	DPSH-A	LP4
Shariatmadari	932	577	1472	1.41	-41	DPSH-A	LP4

Table 23. Comparison between the static load test results and bearing capacity prediction for the test pile P-3.

| Method	R_b (kN)	R_s (kN)	R_c (kN)	R_{cm}/R_{cp}	Absolute Difference (%)	Basis	Sounding ID
Static Loading Test (s/B=10%)			1517	1.00	0	Measured	
Nottingham and Schmertmann	1886	835	2685	0.56	44	CPT	CPTU-P1
de Ruiter and Beringen (Dutch)	1886	410	2260	0.67	33	CPT	CPTU-P1
LCPC (Bustamante)	921	959	1844	0.82	18	CPT	CPTU-P1
EUROCODE 7	1228	1262	2454	0.62	38	CPT	CPTU-P1
German method	1069	904	1937	0.78	22	CPT	CPTU-P1
Unicone method	1443	571	1978	0.77	23	CPTU	CPTU-P1
Aoki & De`Alencer	2385	923	3272	0.46	54	DPSH-A	LP6
Meyerhof	2135	460	2559	0.59	41	DPSH-A	LP6
Briaud & Tucker	1391	800	2155	0.70	30	DPSH-A	LP6
Poulos, Martin, Decourt	1577	481	2022	0.75	25	DPSH-A	LP6
Decourt	943	801	1708	0.89	11	DPSH-A	LP6
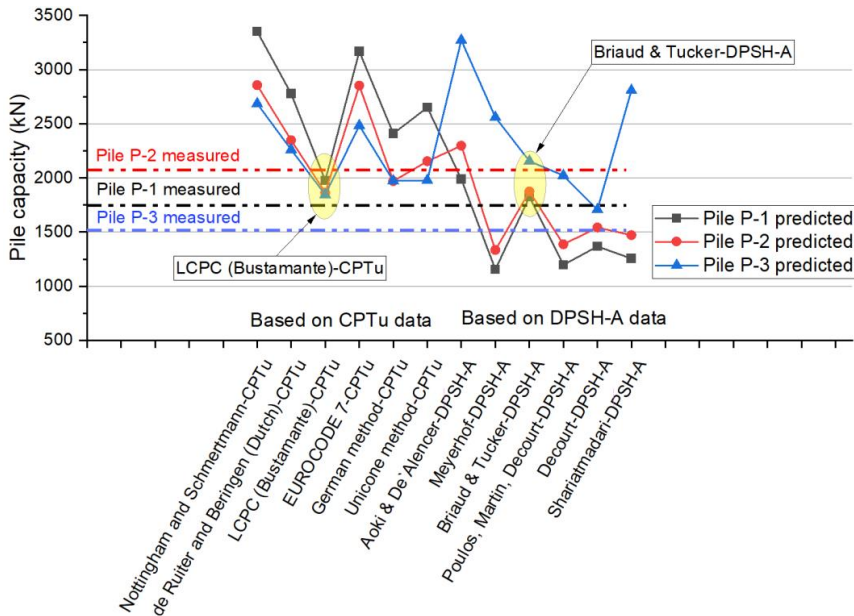
Figure 56. Comparison of the measured and predicted capacity for piles at the Paldiski mnt site (Publication 1).
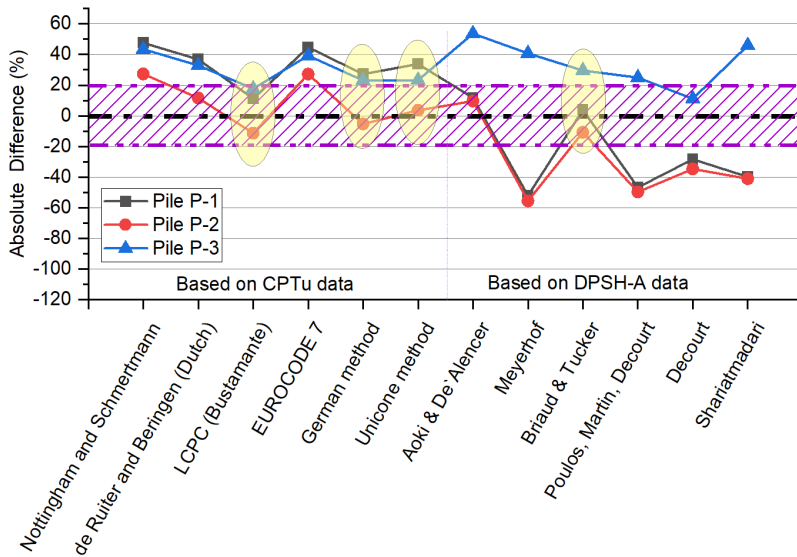

Figure 57. Comparison of the absolute difference between the measured and predicted capacity for the piles at the Paldiski mnt site; +, overestimates; −, underestimates (modified after Publication 1).

8.3 Results from the Soodi site

The load-bearing capacities of the piles were initially assessed individually using the data obtained from both CPTu soundings positioned close to each other with a gap of 8.8 metres (Figure 48). Subsequently, an evaluation of the load-bearing capacity of the piles was conducted by considering the average values derived from the CPTU-S1 (S1) and CPTU-S2 (S2) data. In this analysis, the thicknesses of the soil layers were determined based on the information obtained from the S2 data. The average values of the SLP9 and SLP10 data were also considered, and the thickness of each layer was determined based on the SLP9 probing data.

The findings of the four piles in terms of the absolute differences in bearing capacity, as determined by CPTu soundings S1 and S2 individually, are consolidated in Figure 58. The calculation techniques, based on the type of sounding test employed, are depicted on the horizontal axis in Figure 58. On the vertical axis, the absolute percentage difference between the projected and computed capacities is illustrated. The capacities determined from soundings S1 and S2 are presented side by side in pairs, allowing for a comprehensive analysis of their variations.

The hatching in Figure 58 serves as a visual representation of the ±10% and ±20% regions. The method's effectiveness is determined by the number of results falling within these regions. Figure 58 illustrates the outcomes of soundings S1 and S2 for pile S-3 performed employing the Nottingham and Schmertman method (1975, 1978). The same principle was applied to calculate the differences in the results of all four piles, as presented in Table 24. The bottom row of the table clearly indicates that the disparities range from 14.2% to 19.9% based on the results of the two CPTu soundings. The minimum difference observed is 5.2%, while the maximum difference amounts to 33.1%.

In the subsequent analysis of the load-bearing capacity of the piles, the average values of S1 and S2 were employed. Additionally, also the average values of SLP9 and SLP10 were used for this purpose.
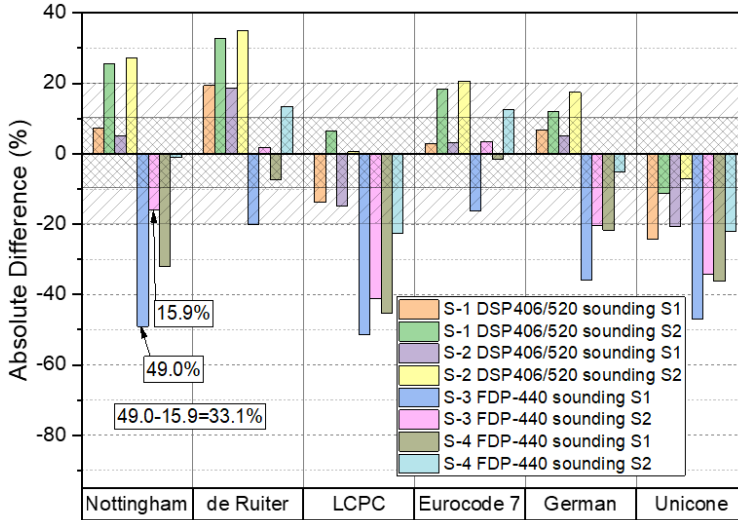
Figure 58. Comparison of the measured and predicted capacity for the piles at the Soodi site based on CPTU-S1 and CPTU-S2; + overestimates, - underestimates (Publication 2).

Table 24. Absolute percentage difference in the load-bearing capacities of four piles as the distinction between the results based on the CPTU-S1 and CPTU-S2 soundings (modified after Publication 2).

Method	S-1 DSP406/520 (%)	S-2 DSP406/520 (%)	S-3 FDP-440 (%)	S-4 FDP-440 (%)
Nottingham and Schmertmann (1975, 1978)	18.2	22.0	33.1	31.0
de Ruiter and Beringen (Dutch, 1979)	13.3	16.5	21.9	20.8
LCPC (1982; 1997)	20.2	15.6	10.2	22.8
EUROCODE 7 (EN 1997-2:2007)	15.5	17.6	19.6	13.9
German method (EA-Pfähle, 2014)	5.2	12.4	15.6	16.4
Unicone method (1997)	13.1	13.7	12.6	14.2
Average	14.2	16.3	18.9	19.9

The load-bearing capacity of the four piles determined applying all the employed techniques is illustrated in, Tables 25 to 28 and Figures 59 to 61 based on the average sounding outcomes e. These results were compared to the measured outcomes obtained from four static pile load tests. Moreover, the noteworthy findings are indicated by a yellow circle in Figure 59. Figures 60 and 61 present the identical results in terms of the absolute percentage difference between

94

the projected and computed capacities based on CPTu and SDT data, respectively.

The Eurocode 7 (EN 1997-2:2007) method demonstrates the highest level of agreement with the obtained results. Additionally, this method proved to be highly consistent when sounding data obtained by both the CPT and the SDT were used. The majority of the results obtained through the Eurocode 7 (EN 1997-2:2007) method fall within or near the ±10% range. The largest absolute difference recorded was 13%.

The two types of piles yielded significantly dissimilar results when analysed using different methods. Specifically, the results obtained from the DSP piles tended to overestimate the measured capacity. On the other hand, the calculated capacities of most FDP piles underestimated the measured values. Among the different methods used, the de Ruiter and Beringen (1979) method showed the highest overestimation for the DSP piles, with a margin of 28%. However, all other methods provided results within the range of ±20% for the DSP pile. In contrast, the LCPC method and the Unicone (1997) method exhibited the highest underestimation of the load-bearing capacity for the FDP piles, with absolute differences of 59% and 66%, respectively.

Moreover, both the LCPC method and Unicone (1997) method consistently underestimated the load-bearing capacity of all four piles when compared to the actual measured capacity. Figures 59 to 61 provide evidence that the LCPC method, along with the Eurocode method and the German method, yielded highly comparable results when the CPT and SDT sounding data were employed. The load-bearing capacity of the FDP piles exhibited a variation within a ±10% range when the de Ruiter and Beringen (1979) method and the Eurocode 7 (EN 1997-2:2007) method were used. The variability in the load-bearing capacity ranged from −7% to 5% and −5% to 6%, respectively (Publication 2).

Table 25. Comparison between the static load test results and bearing capacity prediction for the test pile S-1 (DSP406/520).

Method	R_b (kN)	R_s (kN)	R_c (kN)	R_{cm}/R_{cp}	Absolute Difference (%)	Basis
Static Loading Test (s/B=10%)			1965	1.00	Measured	
Nottingham and Schmertmann	2012	366	2377	0.83	17	CPT
de Ruiter and Beringen (Dutch)	2012	702	2673	0.74	26	CPT
LCPC (Bustamante)	1275	664	1898	1.04	-4	CPT
EUROCODE 7	1436	770	2206	0.89	11	CPT
German method	1619	675	2295	0.86	14	CPT
Unicone method	1042	668	1669	1.18	-18	CPTu
LCPC (Bustamante)	1087	682	1728	1.14	-14	SDT
EUROCODE 7	1234	1039	2232	0.88	12	SDT
German method	1395	746	2100	0.94	6	SDT

Table 26. Comparison between the static load test results and bearing capacity prediction for the test pile S-2 (DSP406/520).

Method	R_b (kN)	R_s (kN)	R_c (kN)	R_{cm}/R_{cp}	Absolute Difference (%)	Basis
Static Loading Test (s/B=10%)			1892	1.00	Measured	
Nottingham and Schmertmann	1963	347	2309	0.82	18	CPT
de Ruiter and Beringen (Dutch)	1963	702	2624	0.72	28	CPT
LCPC (Bustamante)	1124	646	1729	1.09	-9	CPT
EUROCODE 7	1421	742	2163	0.87	13	CPT
German method	1503	646	2149	0.88	12	CPT
Unicone method	1048	659	1667	1.13	-13	CPTu
LCPC (Bustamante)	1165	661	1789	1.06	-6	SDT
EUROCODE 7	1056	1010	2029	0.93	7	SDT
German method	1309	727	1999	0.95	5	SDT

Table 27. Comparison between the static load test results and bearing capacity prediction for the test pile S-3 (FDP440).

Method	R_b (kN)	R_s (kN)	R_c (kN)	R_{cm}/R_{cp}	Absolute Difference (%)	Basis
Static Loading Test (s/B=10%)			2234	1.00	Measured	
Nottingham and Schmertmann	1358	365	1723	1.30	-30	CPT
de Ruiter and Beringen (Dutch)	1358	776	2087	1.07	-7	CPT
LCPC (Bustamante)	761	689	1403	1.59	-59	CPT
EUROCODE 7	1331	788	2118	1.05	-5	CPT
German method	1058	695	1753	1.27	-27	CPT
Unicone method	910	482	1345	1.66	-66	CPTu
LCPC (Bustamante)	796	704	1453	1.54	-54	SDT
EUROCODE 7	1018	1076	2047	1.09	-9	SDT
German method	972	776	1702	1.31	-31	SDT

Table 28. Comparison between the static load test results and bearing capacity prediction for the test pile S-4 (FDP440).

Method	R_b (kN)	R_s (kN)	R_c (kN)	R_{cm}/R_{cp}	Absolute Difference (%)	Basis
Static Loading Test (s/B=10%)			2030	1.00	Measured	
Nottingham and Schmertmann	1413	376	1788	1.14	-14	CPT
de Ruiter and Beringen (Dutch)	1413	761	2126	0.95	5	CPT
LCPC (Bustamante)	815	700	1467	1.38	-38	CPT
EUROCODE 7	1352	805	2156	0.94	6	CPT
German method	1096	700	1797	1.13	-13	CPT
Unicone method	908	714	1575	1.29	-29	CPTu

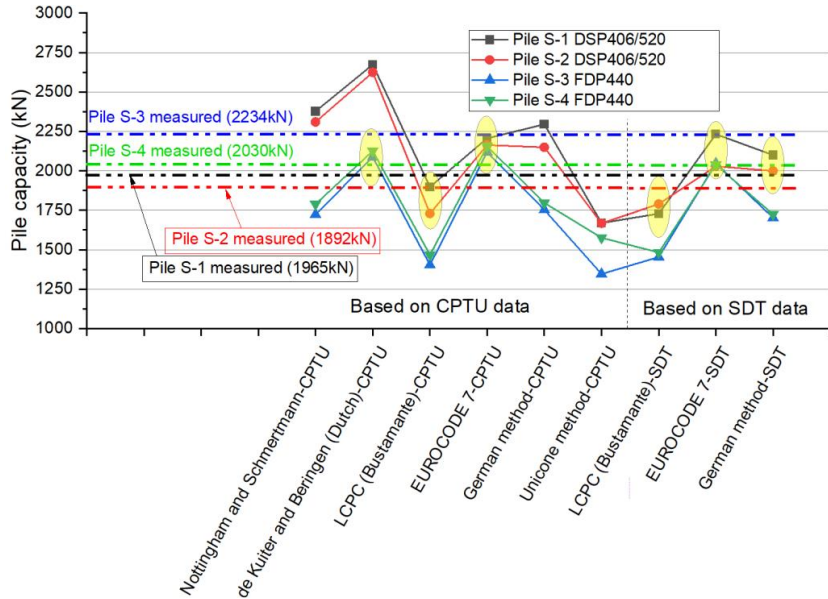| LCPC (Bustamante) | 813 | 717 | 1482 | 1.43 | -43 | SDT |
| EUROCODE 7 | 992 | 1095 | 2039 | 1.04 | -4 | SDT |
| German method | 983 | 788 | 1724 | 1.23 | -23 | SDT |

Figure 59. Comparison of the measured and the predicted capacity for the piles at the Soodi site based on CPTU-S1 and CPTU-S2 average results (modified after Publication 1).
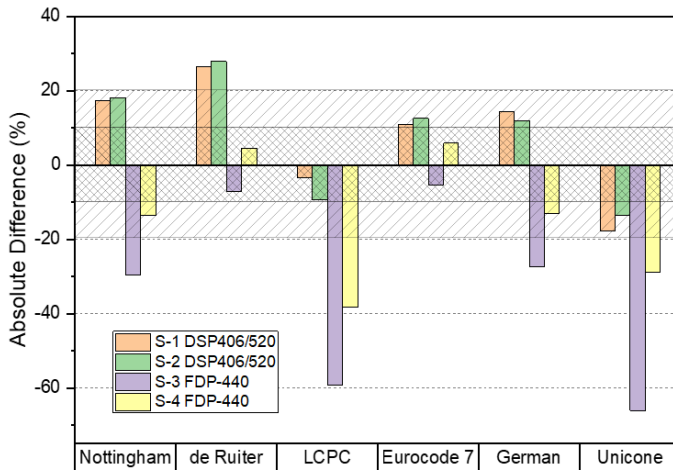

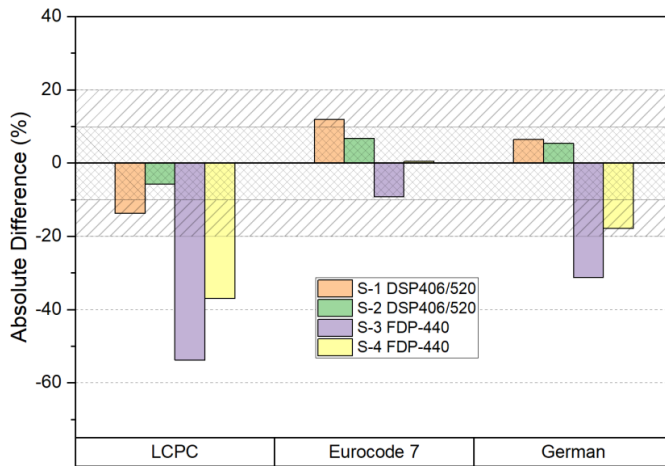**Figure 60.** Based on a comparison of CPTU-S1 and CPTU-S2 average results between pile types; + overestimates, - underestimates (Publication 2).

Figure 61. Based on a comparison of SLP9 and SLP10 average results between pile types; + overestimates, - underestimates (Publication 2).

The evaluation of the pile shaft resistance involved analysis of the average findings from S1 and S2, as well as the SLP9 and SLP10 soundings. In terms of the five CPT methods and one CPTu method, the pile shaft resistance contributed up to 30% of the overall bearing capacity for DSP piles and 37% for FDP piles. By considering the average results from the two SDT soundings, the average values of the three CPT methods were determined to be 41% and 49% for DSP and FDP piles, respectively. The greater proportion of the bearing capacity at the base of the DSP piles can be explained by the larger diameter of the pile base in comparison to the pile shaft (Publication 2).

8.3.1 Probabilistic and statistical capacity of the piles

Figures 62 and 63 present a comparison between the average and MCS outcomes, in relation to the 95% reliable estimate of the mean value and the 5% fractile measured and calculated pile bearing capacity absolute difference results obtained through the LCPC method. The data displayed in Figure 62 are derived from the CPTu soundings S1 and S2, while the results in Figure 63 are based on the SDT soundings SLP9 and SLP10. The analysis and evaluation of the results are conducted by considering the absolute differences between the various parameters.

In contrast to the absolute difference, the MCS and characteristic values derived from the S1 and S2 soundings exhibited a comparable pattern across all four piles. Notably, the largest disparity observed was 3%. When considering the S1 and S2 soundings obtained using average values, the outcomes were consistently 3-8% lower than the MCS and characteristic values. Furthermore, the

Low 5 values obtained from these soundings were significantly lower, ranging from 43% to 132% below the RBD and characteristic values.

The results derived from the SDT soundings SLP9 and SLP10 indicate a close similarity between the average values and the RBD values. Nevertheless, a slight discrepancy ranging from 1% to 3% is observed. Conversely, the characteristic values consistently exhibit a lower magnitude, approximately 5–11% lower than both the average and RBD values. It is worth noting that the lower 5% values display a significant reduction, ranging from 47% to 96%, when compared to the average and MCS values (Publication 2).
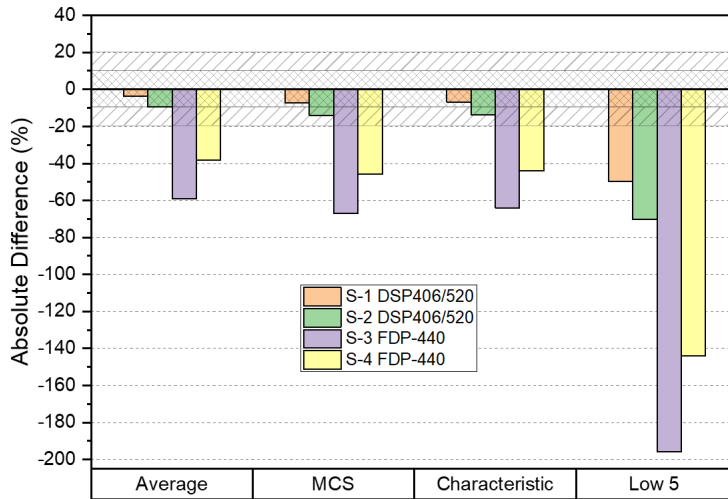

Figure 62. Comparison of average (Average), Monte Carlo simulation (MCS), 95% reliable estimate of the mean value (characteristic) and 5% fractile (Low 5) measured and calculated pile bearing capacity absolute difference values based on LCPC method based on CPTU-S1 or CPTU-S2 results comparison between pile types; + overestimates, - underestimates (Publication 2).
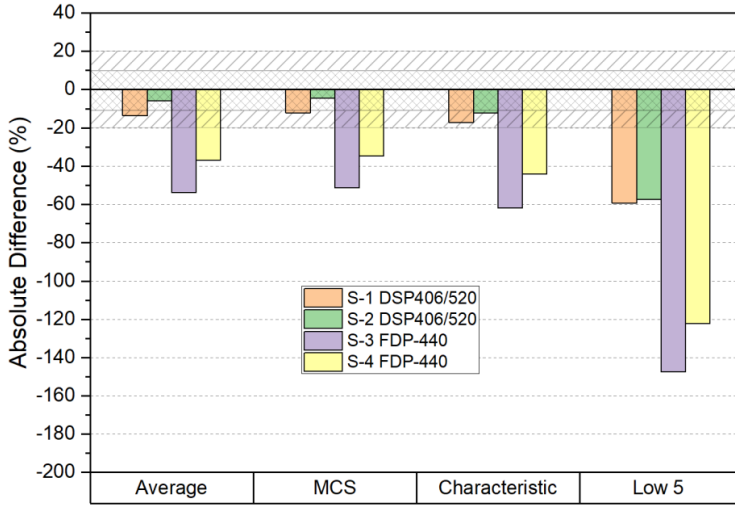
Figure 63. Comparison of average (Average), Monte Carlo simulation (MCS), 95% reliable estimate of the mean value (characteristic) and 5% fractile (Low 5) measured and calculated pile bearing capacity absolute difference values based on LCPC method based on SLP9 and SLP10 results comparison between pile types; + overestimates, - underestimates (Publication 2).

9. Axial elastic response of single screw pile in silty soils based on SCPTu data

9.1 Estimated versus measured load-displacement capacity of the screw pile

The G_{max} values were determined using the V_s values obtained from the soundings SCPTu-A4, SCPTu-S1, SCP-Tu-P1 and SCPTu-P2. Formula 4 was utilized to calculate the G_{max} values both along the pile and beneath the pile base. To ascertain the mass density of the soil, CPTu readings were employed in accordance with Formula 6. It is important to note that the soil layers adjacent to the pile were considered as a single soil layer, wherein the increase in the G_{max} value is dependent on the depth (Niazi and Mayne, 2015).

The depth–G_{max} data were compiled from all four soundings, and a best-fit line was determined (Figures 64 to 67). The soil surrounding the pile base was treated as a separate soil layer. The values of G_{max} were determined based on the V_s values measured at the depth of the pile base.
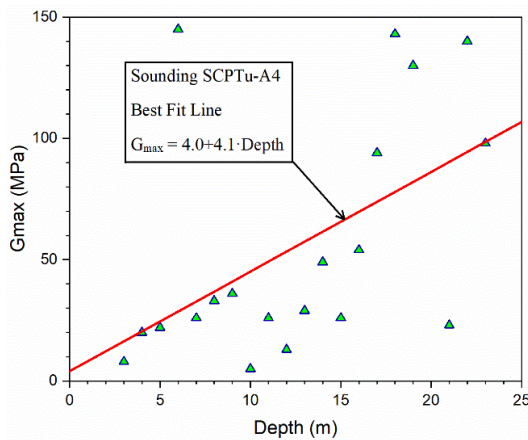

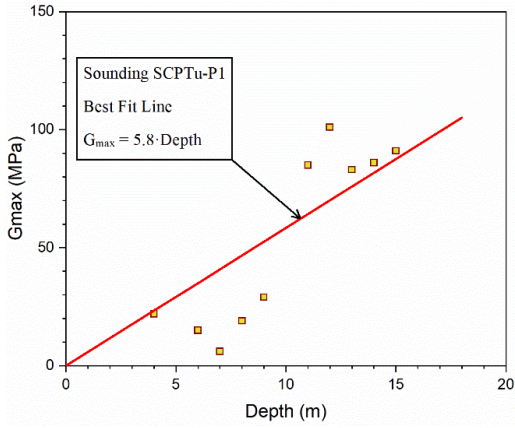**Figure 64.** Depth–G_{max} figures for SCPTu-A4 sounding with best-fit lines (Publication 3).

Figure 65. Depth–G_{max} figures for SCPTu-P1 sounding with best-fit lines (Publication 3).
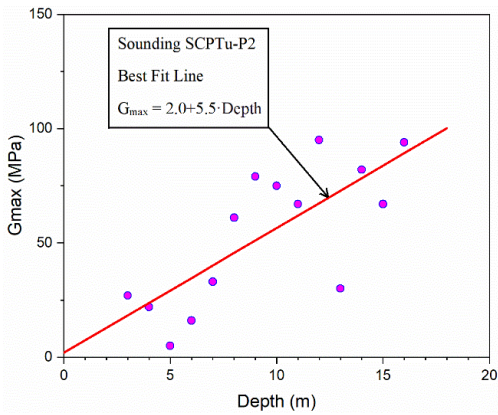

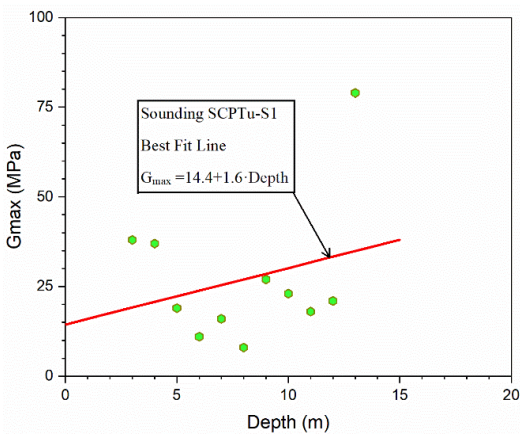**Figure 66.** Depth–G_{max} figures for SCPTu-P2 sounding with best-fit lines (Publication 3).

Figure 67. Depth–-G_{max} figures for SCPTu-S1 sounding with best-fit lines (Publication 3).

The determination of the Q–w relationship for seven screw piles in silty soils was carried out using Formula 2. To conduct this analysis, different values were assigned to the variables f and g. The value of f was consistently set to 1, while the values of g varied and were selected as 0.2, 0.3 and 0.4.

The Q–w curves for all seven piles are displayed in Figure 68, as static pile load tests were not conducted until pile failure. To extend these curves, Chin's (1970) extrapolation method was employed. At the Soodi site the last one to two Q–w values of piles were extrapolated. In the case of pile A-3, the extrapolation was applied to the last third of the Q–w curve values. Piles P-1 and P-3 had to be extrapolated with nearly half of the Q–w values (Figure 68).

The extrapolated results that were closest to the measured values for most analysed piles were obtained at a value of g = 0.4. This value provided a satisfactory alignment with the measured values for the DSP piles (S-1 and S-2). However, for the FDP piles (S-3 and S-4), the use of g = 0.4 tended to underestimate the bearing capacity of the pile. On two out of three Fundex piles (A-3, P-1 and P-3), the Q–w curves showed a suitable alignment with the g = 0.4 line. Therefore, it is justifiable to utilize g = 0.4 to derive the Q–w curve for Fundex piles in silty soils (Publication 3).
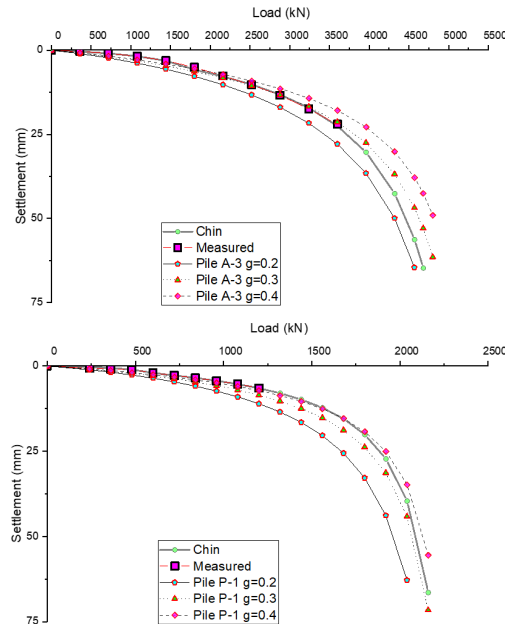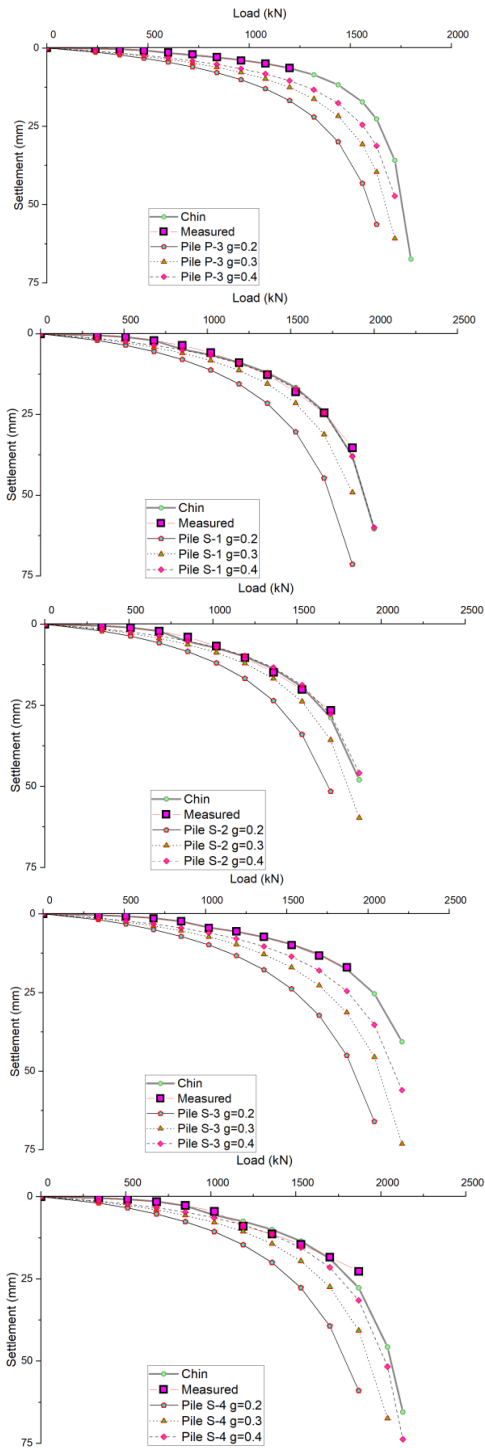
Figure 68. Estimated pile Q–w relationships found by Formulas 2 and 3 with g = 0.2, 0.3 and 0.4 for all seven piles. The results are side-by-side with those of the static pile load test curves. The last parts of the pile load test curves were extrapolated using Chin's method (Publication 3).

9.2 Back-analysis of shear modulus from load tests

The findings from the seven static pile load tests were utilized to conduct back-calculations, which yielded a correlation (17) between the normalized operative shear stiffness (G/G_{max}) and the normalized pseudo-strain ($\gamma_p/\gamma_{p\text{-}ref}$). The current study conducted an analysis of a specific form of correlation, as previously presented by Niazi and Mayne (2015). This analysis involved the examination of 299 pile load tests at 61 different sites. In their research, Niazi and Mayne (2015) introduced a modified hyperbola, which was based on the curves developed by Vardanega and Bolton (2013). The proposed correlation (18) by Niazi and Mayne (2015) was established by considering the stiffness reduction observed in the 299 pile load tests, which were obtained through a process of back-analysis. The correlation involved the utilization of two parameters, namely coefficient α_1 and exponent β_1, which were used to identify the pile typology and installation methods. These parameters were further detailed in Table 29, where piles were categorized into four groups: driven, jacked, auger and bored cast in situ. The values of α_1 and β_1, obtained from the current study, were presented in the final line of Table 29. This correlation exhibited a coefficient of determination of R^2 = 0.97, based on a dataset comprising 101 data points. The graphical representation of these results can be observed in Figure 69.

The values presented in this study show a notable contrast to those proposed by Niazi and Mayne (2015). Figure 69 clearly demonstrates that the correlations established by Niazi and Mayne (2015) for different categories of piles significantly deviate from the correlation suggested in this research for screw piles in silty soils. Specifically, screw piles exhibit a gradual decrease in shear stiffness within the initial range of $\gamma_p/\gamma_{p\text{-}ref}$ <0.3, but this decrease becomes steeper for higher values. Moreover, Figure 69 also highlights that screw piles possess a superior load-bearing capacity compared to the other types of piles mentioned, especially at small strains. These findings emphasize the necessity of incorporating a wider range of pile types in different soil conditions when developing similar correlations (Publication 3).

Extrapolation can have a significant impact on the outcomes observed in the region of higher strains, specifically in the lower right quadrant of the diagram. Nevertheless, it is worth noting that the data obtained from various piles in this particular section of the graph exhibit minimal dispersion, as illustrated in Figure 69. Consequently, the correlations presented in this study yield favourable results and warrant careful consideration.
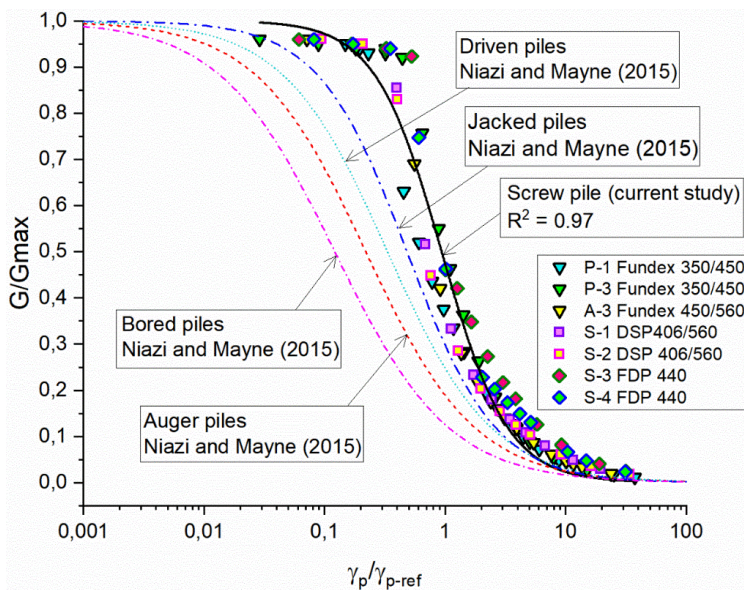
Figure 69. Correlation between normalized operative shear stiffness (G / G_{max}) and normalized pseudo-strain ($\gamma_p / \gamma_{p\text{-ref}}$), where $\gamma_p = w_t / d$ and $\gamma_{p\text{-ref}} = 0.01$ (Publication 3).

Current study

$$\frac{G}{G_{max}} = \frac{1}{\left[1+1.108\left(\dfrac{\gamma_p}{\gamma_{p-ref}}\right)^{1.58}\right]}. \tag{17}$$

Niazi and Mayne (2015)

$$\frac{G}{G_{max}} = \frac{1}{\left[1+3.634\alpha1\left(\dfrac{\gamma_p}{\gamma_{p-ref}}\right)^{0.942\beta1}\right]}. \tag{18}$$

Table 29. Coefficients and exponents for (G / G_{max}) vs. normalized pseudo-strain ($\gamma_p / \gamma_{p\text{-ref}}$) formulation (Formula 18) (modified after Publication 3).

Pile classification (type/installation method)	α1	β1
Driven	0.837	1.068
Jacked	0.648	1.247
Auger	1.176	1.013
Bored cast in situ	1.912	0.971
Screw in-situ displacement (current study)	0.305	1.680

10. Empirical correlation results between V_s and CPTu in silty soils

In conjunction with the measured V_s results presented in Table 10, the calculated values are derived from four empirical regression formulas sourced from the literature. These formulas are applied to all six SCPTu soundings and are visually depicted in Figures 70 and 71. The specific details of these correlations can be found in Table 6. However, due to the lack of strong agreement between the existing correlations and the dataset utilized in this study, three new correlations have been introduced. The first relationship (19) proposed in this study applies f_s values, while the second relationship (20) incorporates q_c and u_2 values. Both these correlations can be used simultaneously to compare the calculated V_s values. Additionally, a third correlation (21) is proposed which simultaneously utilizes both q_t and f_s values. The calculated V_s values obtained from Formulas 19 to 21 are also included in Figures 70 and 71. It is important to note that the V_s values obtained from these correlations are calculated based on CPTu readings taken at intervals of 20 mm and rounded to 1-metre-thick layers. The rounded layer interval aligns with the V_s measurements.

$$V_s = 95.7 \cdot f_s^{0.155} \quad (f_s \text{ in kPa}) \tag{19}$$

$$V_s = 128.4 \cdot q_t^{0.169} \quad (qt \text{ in MPa}) \tag{20}$$

$$V_s = 103.9 \cdot q_t^{0.058} \cdot f_s^{0.107} \quad (q_t \text{ in MPa and } f_s \text{ in kPa}) \tag{21}$$
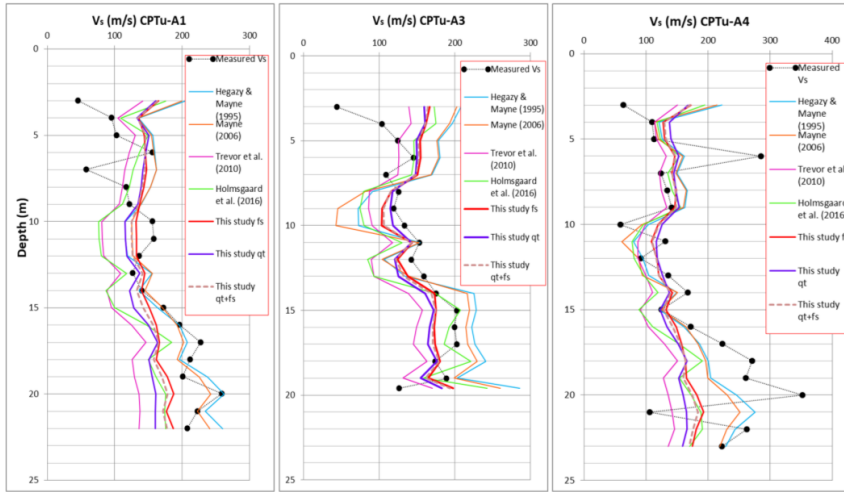
Figure 70. Comparison of V_s as predicted from CPT-Vs correlations and as measured by SCPTu at the Ahtri site (Publication 3).
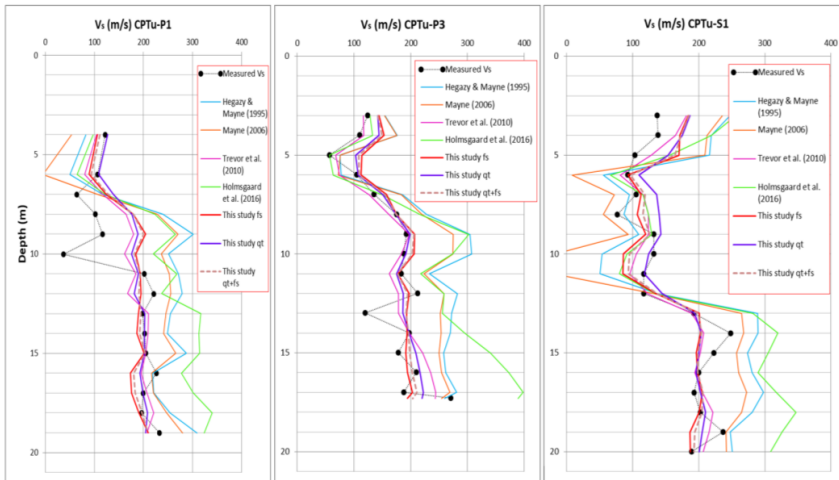
Figure 71. Comparison of V_s as predicted from CPT-Vs correlations and as measured by SCPTu at the Paldiski and Soodi sites (Publication 3).

Figures 72 to 78 display the plotted values of computed V_s against measured V_s, serving as a means to assess the performance of both existing and newly derived functions. To determine the most accurate representation of the computed/measured ratios of V_s, regression analyses were conducted on each set of results. These analyses aimed to establish the best-fit line, which indicates the

108

level of correlation between the computed and measured values. By obtaining the linear regression function and the corresponding coefficient of determination (R^2) and coefficient of variation (COV), the quality of the correlation function can be evaluated. A higher R^2 value signifies a closer alignment between the best-fit line and the ideal-fit line, indicating a stronger correlation. A low COV indicates that the data points are tightly clustered around the mean, leading to reduced variability. The R^2 values obtained from these analyses are presented in Table 30 and in Figures 72 to 78. The COV values obtained from the analyses are depicted in Figures 72 to 78.

Due to the lowest correlation observed in the Ahtri site's results, its data was subjected to separate analysis, whereas the data from the Paldiski and Soodi sites were analysed collectively. The Paldiski and Soodi sites yielded the most favourable results among all seven correlations. Among the available functions, the correlation proposed by Trevor et al. (2010) demonstrated the most promising outcomes when considering the data from the Paldiski and Soodi sites, as indicated by the R^2 value and the best-fit line. This correlation yielded an R^2 value of 0.70.

The correlations presented in this study demonstrate consistent findings for the Paldiski and Soodi sites, as indicated by the R^2 and best-fit lines. Specifically, function (19) exhibits an R^2 value of 0.55, function (20) has an R^2 value of 0.69, and function (21) shows an R^2 value of 0.61. However, when considering the results from all three sites, it is evident that all three correlations proposed in this paper yield the most favourable outcomes. Notably, functions (19) and (21) exhibit the highest R^2 value of 0.33 for the data collected from all three sites. Additionally, functions (20) and (21) demonstrate the lowest COV value of 0.28 for the data obtained from all three sites. Conversely, the Ahtri site displays the weakest correlation, with R^2 values ranging from 0.10 to 0.17 across all seven correlations examined in this study.

Table 30. Coefficient of determination (R^2) for all seven correlations (modified after Publication 3).

Name of test sites and number of data points	Hegazy and Mayne (1995)	Mayne (2006)	Trevor et al. (2016)	Holm-sgaard et al. (2016)	Current study based on f_s (19)	Current study based on q_t (20)	Current study based on q_t+f_s (21)
Ahtri+Paldiski+ Soodi (n=106)	0.32	0.31	0.29	0.30	0.33	0.31	0.33
Paldiski+Soodi (n=48)	0.55	0.51	0.70	0.71	0.55	0.69	0.61
Ahtri (n=58)	0.16	0.17	0.10	0.11	0.17	0.11	0.16

The results obtained from this study demonstrate a wide range of variability. Nevertheless, the correlation suggested yields similar outcomes when compared to the measured V_s values at all three sites, as illustrated in Figures 70 and 71. Notably, a significant discrepancy was observed exclusively in the CPTu-A1, CPTu-A3, and CPTu-A4 soundings that exceeded a depth of 14 metres at the

Ahtri site. The correlations proposed by Hegazy and Mayne (1995) and Mayne (2006) exhibited substantial fluctuations at these three specific investigation points. However, in the remaining third of the study points, these correlations did not exhibit a satisfactory level of consistency. The correlation suggested by Holmsgaard et al. (2016) indicated a substantial overlap within a small subset of study points.
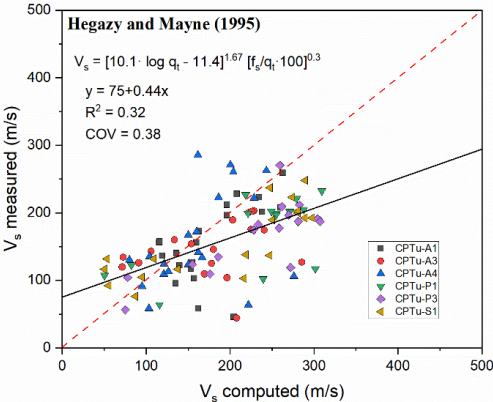

Figure 72. Evaluation of correlation by Hegazy and Mayne (1995) between computed and measured shear wave velocity V_s for silty soils (Publication 3).

Figure 73. Evaluation of correlation by Mayne (2006) between computed and measured shear wave velocity V_s for silty soils (Publication 3).
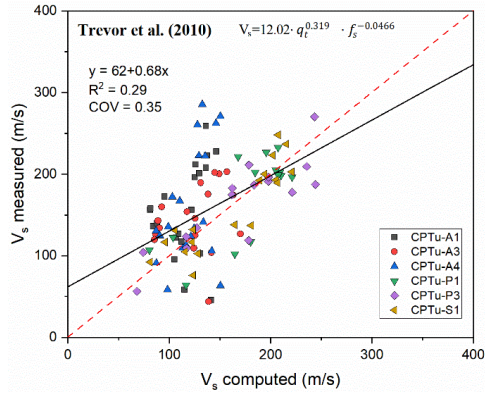
Figure 74. Evaluation of correlation by Trevor et al. (2010) between computed and measured shear wave velocity V_s for silty soils (Publication 3).
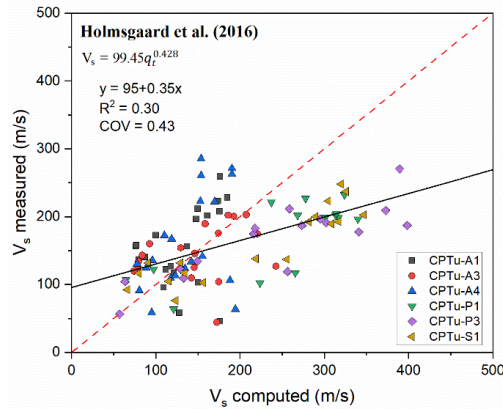
Figure 75. Evaluation of correlation by Holmsgaard et al. (2016) between computed and measured shear wave velocity V_s for silty soils (Publication 3).
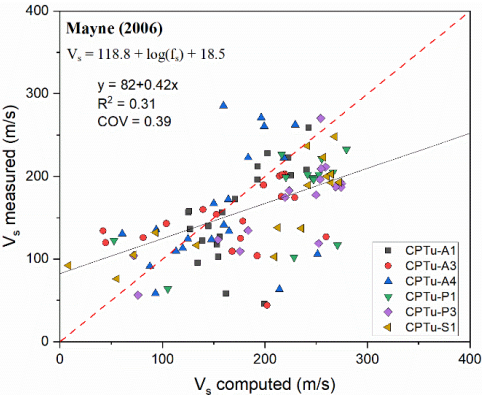

Figure 76. Evaluation of correlation by Leetsaar et al. (2024) between computed and measured shear wave velocity V_s based on f_s data for silty soils (Publication 3).

Figure 77. Evaluation of correlation by Leetsaar et al. (2024) between computed and measured shear wave velocity V_s based on q_t data for silty soils (Publication 3).

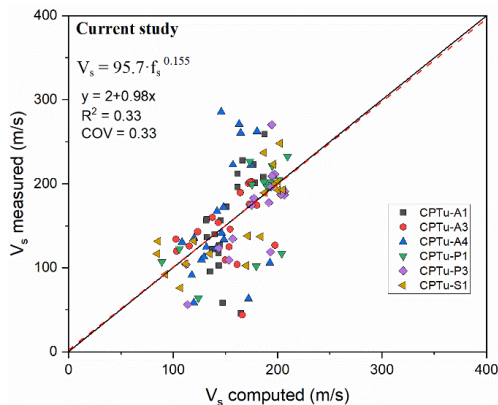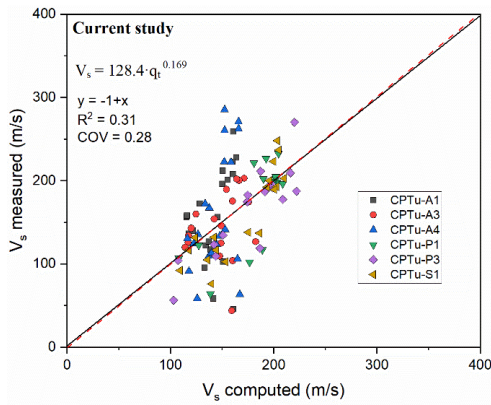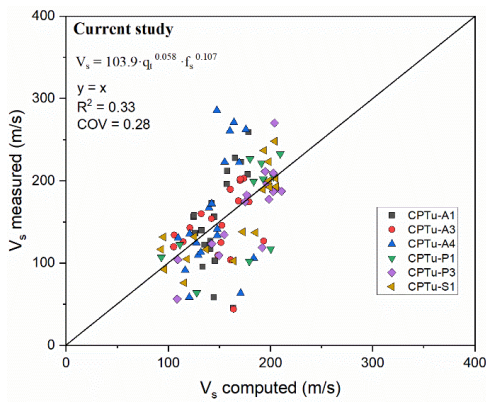**Figure 78.** Evaluation of correlation by Leetsaar et al. (2024) between computed and measured shear wave velocity V_s based on q_t and f_s data for silty soils (Publication 3).

11.   Discussion

In-situ tests

Conducting static pile load tests in parallel with sounding enables to calculate the bearing capacity of a pile solely based on the results of the penetration test. This approach also allows for future estimations of the pile's bearing capacity under similar conditions, using only the sounding data. To define soil type and its properties for estimating pile capacity, the CPT and CPTu sounding methods are widely recognized as fast and reliable. Previous studies (Briaud et al., 1988; Eslami et al., 1995; Eslami et al., 1997; Rollins et al., 1999; Abu-Farsakh et al., 2004; Cai et al., 2009; Mayne et al., 2009; Niazi et al., 2010; Pardoski, 2010; Reuter, 2010; Titi et al., 2010; Cai et al., 2011; Eslami et al., 2011; Hu et al., 2012; Flynn et al., 2014; Moshfeghi et al.,2016; Amirmojahedi et al., 2019) have provided clear evidence that direct methods based on CPT or CPTu data yield reliable results across different soil types and piles (Publications 1 and 2).

   Nevertheless, in the case of denser soils, it is essential for the penetrometer to possess a capacity of up to 500 kN (Eslami and Fellenius, 1997). In this study, a portable lightweight truck (see Figure 20) was utilized to investigate the CPTu. The truck was secured into the soil with a pair of anchors approximately 3 metres in length. In addition, prior to that, CPT soundings with a 200 kN counter-reaction heavy vehicle were conducted at the Ahtri site. Friction reducers were employed for the rods situated behind the CPTu probe during the sounding process. The use of friction reducers during CPT soundings has not been documented. The data presented in Table 12 indicate that using a light machine that is anchored allowed for deeper sounding compared to using a heavy machine. The movement of the anchors of a light machine within the soil during sounding will have a consequential influence on the sounding results. The examination of Figures 37 and 38 reveals that the anchored light machine produced CPTu results that closely resemble the CPT sounding data acquired from a heavy machine, as evidenced by the comparison of q_c and f_s values. Nevertheless, Table 12 indicates that at the Ahtri test site, no CPT or CPTu soundings were conducted deeper than the base level of the tested piles. Only one CPTu sounding reached the base plane of the tested pile. DPSH-A probing yielded slightly improved outcomes, with soundings reaching the base plane of three out of the four piles in the vicinity. However, the DPSH-A device was unable to probe significantly deeper than the bottom of the pile near any of the tested piles. This

refers to the presence of very dense subsoils at the Ahtri test site. In the future, when encountering comparable soil conditions, it is rational to execute DPSH-A soundings as an additional measure to CPT soundings. SDT probing stands as another viable choice for comparable soil conditions. The penetration of SDT in the soil is akin to that of the DPSH-A device. However, a notable advantage of SDT lies in its ability to offer higher reading accuracy, particularly when dealing with weaker soil layers. Furthermore, the SDT readings exhibited a strong correlation with the CPT q_c values as indicated by research carried out at the Soodi test site (Publications 1 and 2).

The Ahtri site exhibits notable discrepancies in the load-bearing capacities of the four piles, as evidenced by Figures 54 and 55. Nevertheless, when the outcome of pile A-4 is disregarded, all SPT methods demonstrate relatively consistent results with minimal variability ranging from 19% to 33%. In contrast, the CPT and CPTu methods exhibit significantly larger variations compared to the SPT methods. This discrepancy can be primarily attributed to the fact that the CPT soundings did not penetrate the level of the pile base. The load-bearing capacities of piles at the Paldiksi mnt site were found to be quite similar, as indicated in Figures 56 and 57. Upon comparing the measured load-bearing capacities with the calculated values using various methods, it was evident that the LCPC and Briaud and Tucker (1988) methods exhibited notable accuracy. These two methods displayed significantly less variability compared to the other methods considered in the study. The Eurocode 7 method demonstrated superior performance for DSP and FDP piles at the Soodi site, as evidenced by the analysis of both CPT and SDT soundings, as well as Figures 59 and 60. The majority of results obtained using this method were within or close to the ±10% range, with the largest absolute difference being 13%. Conversely, other direct methods tended to overestimate the load-bearing capacity of DSP piles and underestimate the load-bearing capacity of FDP piles. In terms of determining the load-bearing capacity of the DSP pile, all methods, except for the de Ruiter and Beringen (1979) method, yielded satisfactory results. The LCPC method, in particular, underestimated the load-bearing capacities of both DSP piles by less than 10%, as depicted in Figure 60. It is important to highlight that within the three direct methods, namely LCPC, Eurocode 7 and Briaud and Tucker (1988), the failure criterion for pile is defined as s/B=10%. The comparable outcomes observed in these three methods in relation to the pile test results may also be influenced by this factor. In addition, separate attention deserves the fact that the application of the SDT sounding outcome in the CPT direct methods provided comparable results to the application of the CPTs sounding data. This supports claims about the correlation of SDT and CPT q_c values by Rantala & Halkola (1997) (Publications 1 and 2).

Screw piles and direct methods in silty soils

It is crucial to conduct a comparison of the results obtained from the analysis of the three different types of screw piles discussed in this study. The Fundex and DSP piles exhibit a striking similarity in terms of their pile shape, while they differ significantly from the FDP pile. Figure 60 illustrates that, in four out of the six methods employed, the direct methods tended to overestimate the bearing capacity of the DSP piles. However, the LCPC and Unicone methods only underestimated the load-bearing capacity of the piles. This observation can be attributed to the fact that the DSP piles possess a pile base with a larger diameter and their installation technique resembles that of a Fundex pile. Consequently, it is expected that the behaviour of DSP piles would be similar to that of Fundex piles. Kemfert et al. (2010) highlighted that an increase in the diameter of a pile base can cause the ground in the shaft area to become less compact, leading to a decrease in shaft resistance. Conversely, Basu et al. (2010) pointed out that the screw-shaped shaft of a pile enhances its load-bearing capacity compared to a smooth shaft pile. As a result, the accuracy of load-bearing capacity calculations for screw-shaped piles may not always be achieved using conventional methods, as noted by Kempfert et al. (2010). The comparison between the results obtained from the two DSP piles investigated in this study at the Soodi site and the three Fundex piles at the Paldiski mnt site (Publication 1) is presented in Table 31. The data in Table 31 reveal that most of the methods exhibit a similar trend in their results. Notably, both the de Ruiter and Beringen method and the German method yield identical outcomes for both sites. However, the Unicone method demonstrates a significant level of variability. This particular method consistently underestimates the load-bearing capacity of the pile by an average of 16% at the Soodi site, while overestimating it at the Paldiski mnt site. It is worth noting that the potential overestimation of the load-bearing capacity of the pile by direct methods may be attributed to the timing of the pile testing after its completion. In this study, the piles were subjected to loading within two to three weeks after their construction. However, Togliani et al. (2014) highlighted that the load-bearing capacity of the pile may continue to increase even after 100 days from the pile's construction, particularly in cases where approximately 50% of the pile is surrounded by clayey soils (Publications 1 and 2).

Table 31. Absolute percentage difference in load-bearing capacity of two DSP piles at the Soodi site and three Fundex piles at the Paldiski mnt site; + overestimates, - underestimates (Publication 2).

Method	Soodi site Absolute Difference (%)	Paldiski mnt site Absolute Difference (%)
Nottingham and Schmertmann (1975, 1978)	18	39
de Ruiter and Beringen (Dutch, 1979)	27	27

LCPC (1982; 1997)	-7	6
EUROCODE 7 (EN 1997-2:2007)	12	36
German method (EA-Pfähle, 2014)	13	14
Unicone method (1997)	-16	20

Additionally, the results of the LCPC (LCPC-A, LCPC-P, DSP-LCPC-S and FDP-LCPC-S) and the Briaud & Tucker method (B&T) (B&T-A and B&T-P) are statistically compared in Table 32 with the results of the pile load test (SLT-A, SLT-P, DSP-SLT-S and FDP-SLT-S). The letter A indicates the Ahtri site, the letter P indicates the Paldiski mnt site and the letter S stands for the Soodi test site. The results of the pile types DSP and FDP have also been separated at the Soodi site. The abbreviation SLT refers to a static pile load test. The mean value ($\bar{x}$), standard deviation (SDx), and coefficient of variation (COVx) were computed for the data set. It is important to note that the results obtained from pile A-4 were excluded from the statistical analysis. The percentage accuracy was determined by comparing the pile load test results with the calculated mean value. A negative percentage value signifies an underestimation of the measured result by the calculation, while a positive percentage value indicates an overestimation of the measured values. Table 32 presents the findings indicating that the Ahtri site exhibits a coefficient of variation ranging from 0.09 to 0.28, while the Paldiski mnt site demonstrates a coefficient of variation ranging from 0.04 to 0.16. On the other hand, the Soodi site displays a coefficient of variation within the range of 0.03 to 0.07. It is worth noting that the accuracy of the calculated values, excluding the values of FDP piles, falls between 6.0% and 10.4%. This evidence supports the notion that LCPC yields equally satisfactory outcomes for screw piles with an expanded pile bottom in silty soils, including Fundex and DSP piles. However, it is imperative to conduct a more comprehensive analysis of the load-bearing capacity of the DSP pile in conjunction with a Fundex pile.

Table 32. Determination of pile bearing capacity accuracy based on LCPC and Briaud and Tucker (1988) methods (modified after Publication 1).

Variable	$\bar{x}$ (kN)	SDx (kN)	COVx	Measured $\bar{x}$/predicted $\bar{x}$	Accuracy (±%)
SLT-A	5021	1058	0.21	1	0
LCPC-A	4692	1300	0.28	1.070	-7.0
B&T-A	5603	529	0.09	0.896	10.4
SLT-P	1782	280	0.16	1	0
LCPC-P	1895	72	0.04	0.940	6.0
B&T-P	1951	178	0.09	0.913	8.7
DSP-SLT-S	1929	52	0.03	1	0
DSP-LCPC-S	1814	120	0.07	1.063	-6.3

FDP-SLT-S	2132	144	0.07	1	0
FDP-LCPC-S	1435	45	0.03	1.486	-48.6

The underestimation of the load-bearing capacity of FDP piles by most direct methods may suggest that these methods do not fully account for the actual behaviour of this type of pile in the soil. Bush et al. (2013) determined that the installation of FDP piles in soils containing silt and sand leads to a notable rise in cone resistance. This increase was observed to persist up to the depth of the displacement body, as indicated by their findings. Furthermore, slight decreases in cone resistance below the displacement body did not have any adverse impact on the pile's bearing capacity. This implies that the load-bearing capacity of FDP piles remains unaffected even after the displacement body. The density of the soil surrounding the pile exhibited minimal alterations, as indicated by their calculations, while the primary changes were observed in the horizontal stresses. Measuring the horizontal stress state and void ratio in situ proves to be a challenging task. Consequently, it becomes imperative to conduct a comprehensive examination of this particular type of pile through static load tests, in conjunction with CPT and SDT soundings. Pile tests should be conducted in a manner that enables the distinction between the load-bearing capacity of the pile base and shaft, and the overall load-bearing capacity of the pile. By utilizing the results obtained from the load test and soundings, more accurate calibration of direct methods can be achieved (Publications 1 and 2).

Figure 79 displays the ratio between the capacities of the pile base and shaft, as determined by LCPC methods, for all eleven piles. The vertical axis of the figure also represents the depth at which the piles were installed. However, as the DPSH-A probings were conducted only at the Ahtri and Paldiski mnt sites, the Briaud and Tucker (1988) method could be applied just to the seven piles within these two sites. Figure 80 illustrates the proportion of load capacities between the end and side of the pile, as determined by the Briaud and Tucker (1988) method. The piles installed at the Ahtri site were embedded in a denser and deeper subsoil compared to the Paldiski mnt and Soodi sites. In terms of load-bearing capacity, both the LCPC and Briaud and Tucker (1988) methods indicate a striking similarity between the pile base and the overall pile capacity at the Ahtri site. The LCPC method yields values ranging from 58% to 69%, while the Briaud and Tucker (1988) method provides values within the range of 58% to 68%. On the other hand, at the Paldiski mnt site, the Briaud and Tucker (1988) method indicates a higher load-bearing capacity of the pile base compared to the LCPC method. Specifically, the Briaud and Tucker (1988) method yields values ranging from 60% to 61%, whereas the LCPC method indicates values within the range of 48% to 53%. Based on the LCPC method, the load-bearing capacity of the bottom of the DSP piles on the Soodi site was found to resemble that of the Fundex piles at the Ahtri site. This similarity is observed within a range of 64%66%. Conversely, the LCPC method reveals that the FDP

piles have lower carrying capacities at the bottom, ranging from 52% to-54% at the Soodi site (Publications 1 and 2).
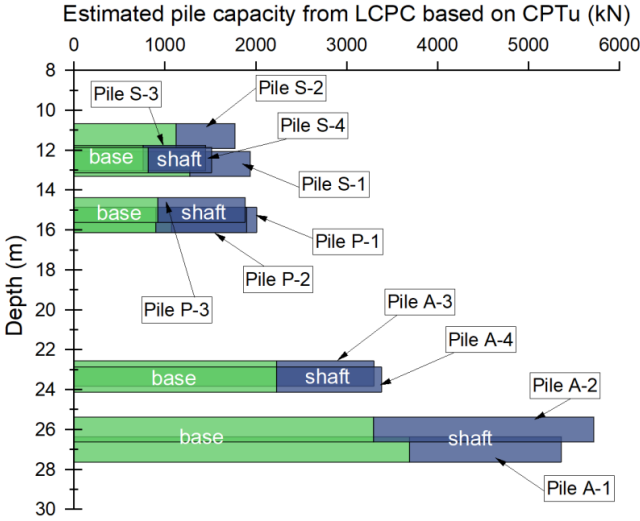

Figure 79. Comparison of the proportion of base and shaft resistance based on the LCPC method for all piles (modified after Publication 1).
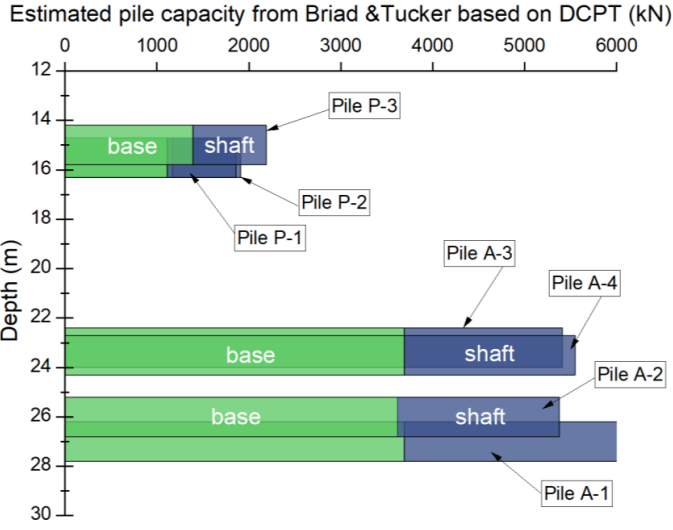

Figure 80. Comparison of the proportion of pile base and shaft resistance based on the Briaud and Tucker (1988) method for seven Fundex piles (modified after Publication 1).

Probabilistic and statistical capacity of the piles

Based on average, MCS and characteristic values, the results differed by up to 11% based on SDT data and up to 8% based on CPT data. Although both RBD and statistical determination yielded similar outcomes when analysing CPT and SDT data, the emphasis of the results analysis lies exclusively on the examination of CPT data. It is important to acknowledge that the process of deriving CPT data from SDT probing readings inherently introduces inaccuracies due to correlation. The pile capacity obtained from MCS and characteristic values was found to be 3%–8% lower than the average values. However, it is important to consider that the q_c values of only one out of the four soil layers did not follow a normal distribution. If the q_c values of most soil layers deviate from the normal distribution, using average values may lead to significantly inaccurate pile load-bearing results. In comparison to analytical methods, RBD takes into account the variability of parameters, provides more comprehensive information and offers a reliable assessment of the probability of failure or actual safety. The Low 5% fractile results exhibited variations of up to 132% in comparison to the average values. According to Eurocode 7 (Frank et al., 2005), it is advised to utilize the Low 5% fractile in cases where the soil volume affected by a specific condition is significantly smaller than the extent of soil property fluctuation. In the soils under investigation, the Low 5% values indicated a substantial safety margin for the pile's load-bearing capacity (Publication 2).

The soil stiffness values (G_{max} or G_o) were determined using the V_s values obtained from the soundings. The analytical elastic solution proposed by Randolph and Wroth (1978, 1979) for analysing the interaction between piles and soil incorporates the G_{max} value. This solution considers the presence of piles in soils with Gibson-type characteristics, where the soil stiffness increases linearly with depth. Furthermore, it also accounts for piles in homogenous two-layered soils, where the soil stiffness remains constant throughout the depth. With applying Randolph and Wroth's (1978, 1979) solution, the Q–w relation of 11 screw piles in silty soils was determined. According to the results obtained from this study, the parameter g=0.4 is identified as the most appropriate value for Formula 3 when dealing with screw piles in silty soils. Moreover, two correlations (17 and 18) have been established between the normalized operative shear stiffness (G/G_{max}) and the normalized pseudo-strain ($\gamma_p/\gamma_{p\text{-}ref}$) with an R² value of 0.97. These correlations were developed based on the back-calculations of the static pile load test results, which consisted of 101 data points. The parameters $\alpha 1$ and $\beta 1$, presented in Table 29, are used to identify the pile type and installation methods. The piles are categorized into four groups: driven, jacked, auger and bored cast in situ. The values of $\alpha 1$ and $\beta 1$ obtained are provided in the last line of Table 29. The results, as shown in Figure 69, clearly demonstrate that the correlations (18) suggested by Niazi and Mayne (2015) for different categories of piles deviate significantly from the correlation (17 and 18) established in this study specifically for screw piles in silty soils. The screw piles exhibited a gradual

decrease in shear stiffness within the initial range of γ_p/γ_{p-reo} <0.3, but this decrease will become steeper for higher values. Additionally, Figure 69 reveals that screw piles have a higher load-bearing capacity compared to other types of piles, especially at small strains. This highlights the importance of including a wider range of pile types in different soil conditions when developing similar correlations (Publication 3).

V_s soundings and correlations

The results presented in Figures 39, 45 and 52 show that V_s values of approximately 100 m/s, and as low as 37 m/s, were measured in sensitive fine-grained, silty sand and sandy silt layers that were not deeper than 10 metres. In deeper layers, the measured V_s values ranging from 150 to 250 m/s aligned, with minor deviation, with the range proposed by Holmsgaard et al. (2016). Furthermore, these measured values fell within the range presented by Hussien and Karray (2016) and Poulos (2022). In the current study, most of the measured V_s values at depths greater than 10 metres were approximately 200 m/s (Publication 3).

The analysis of CPTu and V_s correlations involved treating the results obtained at the Ahtri site separately. It was observed that the soil layers below a depth of 14−16 metres at the Ahtri site had a higher silt content compared to the other two sites. This observation is clearly depicted in Figure 70, where the correlations proposed in this study show a clear interlacing pattern at depths of 14−16 metres for all three study sites. Other correlations that were investigated also showed satisfactory results within the range of 14−16 metre depths. However, in the deeper layers, only the correlations from Hegazy and Mayne (1995) and Mayne (2006) provided an approximate fit. The Ahtri site had complex silt and sand mixtures in the deeper layers, and the transition from silt to sand mixtures was well-defined in the u_2 profile (Figure 39) between 13 and 16 metres, where a sharp drop in pore water pressure occurred. For these types of soils, all the correlations reviewed in this study significantly underestimated the V_s values, except for the correlations provided by Hegazy and Mayne (1995) and Mayne (2006). The best fit for the Paldiski and Soodi sites was achieved through the utilization of Formulas 19, 20 and 21 as proposed correlations (Figure 71). Also a correlation presented by Trevor et al. (2010) yielded excellent outcomes. However, the remaining three correlations exhibited a significant overestimation of the V_s value in most soil layers at study points SCPTu-P1 and SCPTu-P3 at the Paldiski site. Similarly, at study point SCPTu-S1, these three correlations displayed a substantial overestimation of the V_s value in several layers, simultaneously underestimating it in other layers. This clearly demonstrates the complexity of developing CPTu and V_s correlations for mixed soils. Universal correlations may not be sufficient in obtaining accurate results for mixed soils, thus emphasizing the necessity for correlations based on specific soil types. Consequently, further investigation is required to better understand the behaviour of mixed soils in the future. Furthermore, it can be observed from Figures 70 and

71 that the V_s values obtained from the correlations proposed by Hegazy and Mayne (1995) and Mayne (2006) closely resemble each other at all the points examined in the study. The correlation developed by Hegazy and Mayne (1995) incorporate all the readings obtained from CPTu, while the correlation presented by Mayne (2006) uses only f_s values. Moreover, Formula 21 did not yield superior outcomes compared to Formulas 19 and 20. Hence, it can be inferred that correlations based on a single input parameter can yield satisfactory results. This serves as compelling evidence that correlations relying on either q_t or f_s values should be employed independently. Consequently, this approach enables a meaningful comparison of correlation findings derived from separate analyses of the same CPTu soundings (Publication 3).

Limitations

Limitations of this study:

- The static pile load test was employed to ascertain the ultimate capacity of the pile through the utilization of extrapolation. The prevalent approaches for this determination are the offset limit- or extrapolation-based methods. Nevertheless, it is important to acknowledge that the choice of the method for evaluating the ultimate pile capacity can have an impact on the obtained results.
- Pile shaft and base resistance affect each other, but they have been treated separately in calculations.
- At the Ahtri test site, the soundings were unable to penetrate significantly deeper than the plane of the base of the test piles. Several soundings failed to even reach the level of the pile base.
- At each of the three test sites, the groundwater levels were observed to be remarkably high, with a depth of approximately one metr below the ground level. This substantial elevation in groundwater has the potential to introduce uncertainties in the sounding results and may also prolong the assessment of the pile bearing capacity.
- The accuracy of these results may vary when applied to different pile and soil types.

12.   Conclusions and recommendations for future work

The research focused on comparing different direct methods that utilize CPT and SPT data to assess the load-bearing capacity of screw piles in silty soils. By investigating the applicability of DPSH-A readings in SPT-based methods, the study aimed to enhance the accuracy of predictions regarding pile bearing capacity. Moreover, the utilization of SDT data in CPT-based direct methods for evaluating the load-bearing capacity of a screw pile in silty soil was explored. With the growing emphasis on reliability and economic constraints in design, the reliability-based design (RBD) method has been utilized to assess he load-bearing capacity of piles based on the LCPC method. A Monte Carlo simulation (MCS) involving 10,000 simulations was executed for this analysis. The distribution of soil characteristic values, following the LCPC method, incorporated the 95% and 5% fractiles.

Understanding the potential of using SCPTu data for pile analysis is essential. This research employed analytical elastic continuum solutions to gain a more profound insight into the correlations within the test data. The study examined four established empirical correlations between V_s and CPTu, while also introducing three novel correlations specifically for silty soils. By applying an elastic solution proposed by Randolph and Wroth (1978, 1979), the Q–w relationship of piles was determined following Niazi and Mayne's (2015) methodology. Furthermore, the analysis included an evaluation of the exponent parameter g for screw piles in silty soils and the development of correlations between G/G_{max} and $\gamma_p/\gamma_{p\text{-}ref}$ based on back-calculations from static pile load test results. The key outcomes and recommendations for future studies are detailed as follows:

Conclusions of Publication 1
- The research conclusively indicated that when the soundings did not penetrate to the required depth of the base, the resulting calculation frequently led to an underestimation of the pile capacity.

- The variability of the calculated results was considerably smaller when the CPTu or DPSH-A test was conducted at a depth exceeding several metres below the pile tip.
- As to the CPT-based direct methods, it was found that the LCPC method yielded the most satisfactory results for Fundex piles.
- Among the various SPT methods available, the Briaud and Tucker (1988) method stands out as particularly noteworthy due to its exceptional performance in predicting outcomes for Fundex piles.

Conclusions of Publication 2
- It was found that the use of the SDT sounding outcome in the CPT direct methods produced results that were comparable to those obtained from using the CPT sounding data.
- Analysis of the arithmetic average values obtained from the CPT and SDT soundings for DSP and FDP piles revealed that the Eurocode 7 method exhibited the most favourable performance.
- Other direct methods that were included in the study tended to overestimate the load-bearing capacity of DSP piles and underestimate the load-bearing capacity of FDP piles.
- The pile-bearing capacities, as determined by the CPT and SDT soundings, showed a fluctuation of 11% in the absolute difference between the average, RBD and characteristic values.

Conclusions of Publication 3
- The optimal fit for the specified CPT–V_s correlations across all three locations were identified using the correlation established by Trevor et al. (2010).
- The paper presented three site-specific CPT–V_s correlations, and it was found that there was a significant overlap in the V_s values for most soil layers among these correlations.
- It is advisable to prioritize correlations that rely on q_t or f_s values when assessing correlation findings from distinct readings of a CPTu sounding.
- The sensitive fine-grained layers, along with the silty sand and sandy silt layers, exhibited minimum V_s values and values close to 100 m/s. These measurements were observed up to a depth of 10 metres. Below this depth, the dominant V_s values were approximately 200 m/s.
- The results of this study suggest that a value of $g = 0.4$ (Formula 3) is the most appropriate option for screw piles specifically designed for silty soil conditions.
- The relationship between normalized operative shear stiffness (G/G_{max}) and normalized pseudo-strain (γ_p/γ_{p-ref}) was thoroughly

examined (N=101), resulting in a highly significant correlation (R^2=0.97).

- The load-bearing capacity of screw piles in silty soils surpasses that of other pile types, especially under conditions of low strain.

Common conclusions of Publications 1 and 2

- In these publications, the s/B=10% failure criterion was utilized for the assessment of the piles and the identification of the best direct methods. These studies indicate that all three direct methods (Briaud and Tucker (1988) method, LCPC method, and Eurocode 7 method), which demonstrated satisfactory outcomes, incorporate the s/B=10% failure criterion also.

Recommendations for future work

- Further exploration is warranted in assessing the pile capacity calculation utilizing DPSH-A data through direct methods based on SPT data, particularly when considering various types of piles in different soil conditions.
- In the future, it is imperative to conduct additional research on the outcomes of static pile load tests in conjunction with DPSH-A, SDT and SCPTu tests using various piles across diverse soil types.
- Further research is needed to explore the utilization of RBD in assessing the load-bearing capability of piles through direct methods.
- It is imperative to conduct further research on mixed soils in order to establish appropriate V_s–CPTu correlations.
- It is essential to establish additional correlations between the normalized operative shear stiffness (G/G_{max}) and the normalized pseudo-strain (γ_p/γ_{p-ref}) for a wider range of pile types in diverse soil conditions.

References

Abu-Farsakh, M. Y. and Titi, H. H. (2004). "Assessment of direct cone penetration test methods for predicting the ultimate capacity of friction driven piles." *Journal of Geotechnical and Geoenvironmental Engineering*, 130(9), 935–944.

Alboom, G. V. and Whenham, V. (2003). "Soil investigation campaign at Limelette (Belgium)." *Proceedings of the Second Symposium on Screw Piles – Belgian Screw Pile Technology – Design and Recent Developments*. Brussels, Balkema, Rotterdam; ISBN: 90 5809 578 9, 21–70.

Al-Homoud, A.S., Fouad, T. and Mokhtar, A. (2003). "Comparison between measured and predicted values of axial end bearing and skin capacity of piles bored in cohesionless soils in the Arabian Gulf Region." *Geotechnical and Geological Engineering,* 21, 47–62.

American Society for Testing & Materials, (2000). *ASTM Book of Standards*, vol. 4, Section 08 and 09. Construction Materials. Soils Rocks, Philadelphia, PA.

Amirmojahedi, M. and Abu-Farsakh, M. (2019). "Evaluation of direct pile-CPT methods for estimating the ultimate capacity of driven piles." *Proceedings of the 8th international conference on case histories in geotechnical engineering*, March 24-27, 2019, Philadelphia, Pennsylvania, 167–177.

Aoki, N. and De Alencar, D. (1975). "An Approximate Method to Estimate the Bearing Capacity of Piles." *Proceedings of the 5th Pan-American Conference of Soil Mechanics and Foundation Engineering*, Buenos Aires, 1, 367–376.

Arbeiter, R. (1962). "Tallinna ehitusgeoloogilise rajoniseerimise visand." *Eesti ehitusgeoloogiline kogumik I*, Tallinn, 23–34.

Areias, L., and Impe, W. V. (2004) "Interpretation of SCPT data using cross-over and cross correlation methods." *Engineering geology for infrastructure planning in Europe: A European perspective*. Springer, Berlin, Heidelberg, 110–116.

Bandini, P. and Salgado, R. (1998). "Methods of pile design based on CPT and SPT results." *Geotechnical site characterization conference*, Balkema, Rotterdam, 936–942.

Basu, P., Prezzi, M. and Basu, D. (2010). "Drilled displacement piles – current practice and design." *The Journal of the Deep Foundations Institute*, 4(1), 3–20.

Benali, A., Nechnech, A. and Bouafia, A. (2013). "Bored pile capacity by direct SPT methods applied to 40 case histories." Special issue for international congress on material & structural stability, Rabat, Morocco. *Civil and environmental research*, 5, 118–122.

Berardi, R. and Bovolenta, R. (2005). "Pile-settlement evaluation using field stiffness non-linearity." *Proceedings* of the *Institution of Civil Engineers, Geotechnical Engineering*, 158, 35–44.

Bergdahl, U. and Ottosson, E. (1988). "Soil Characteristics from Penetration test results: A Comparison between various investigation methods in non cohesive soils." *Proceedings, First international symposium on penetration testing*, Orlando, Florida, 1, 399–405.

Borel, S., Bustamante, M. and Gianeselli, L. (2004). "An appraisal of the Chin method based on 50 instrumented pile tests." *Ground Engineering*, 37(1), 22–26.

Briaud, J. L. and Tucker, L. M. (1988). "Measured and predicted axial response of 98 piles." *Journal of Geotechnical Engineering*, 114(9), 984–1001.

Burns, S. E. and Mayne, P. W. (1996). "Small- and high-strain soil properties using the seismic piezocone." *Transportation Research Record* 1548, Washington, D.C., 81–88.

Burland, J. B. (1989). "Small is beautiful: The stiffness of soils at small strains." *Canadian Geotechnical Journal*, 26(4), 499–516.

Bush, P., Grabe, J. and Gerressen, F. W. (2013). "Influence of the installation process of full displacement bored piles on the subsoil." *Baltic Piling* – Mets & Raudsepp (Eds), Taylor & Frances Group, London, ISBN 978-0-415-64334-4, 157–163.

Bustamante, M. and Frank, R. (1997). "Design of axially loaded piles – French practice." *Design of axially loaded piles. European practice, proceeding of the ERTC3 seminar*, Brussels, Belgium, Balkema, Rotterdam, The Netherlands, 161–175.

Bustamante, M. and Gianeselli, L. (1982). "Pile bearing capacity predictions by means of static penetrometer CPT." *Proceedings of 2nd European symposium on penetration testing*, Amsterdam, 493–500.

Cai, G., Liu, S. and Puppala, A. J. (2011) "Evaluation of Pile Bearing Capacity from Piezocone Penetration Test Data in Soft Jiangsu Quaternary Clay Deposits." *Marine Georesources & Geotechnology*, 29(3), 177–201.

Cai, G., Liu, S. and Puppala, A. J. (2012). "Reliability assessment of CPTu-based pile capacity predictions in soft clay deposits." *Engineering Geology*, 141, 84–91.

Cai, G., Liu, S., Tong, L. and Du, G. (2009). "Assessment of direct CPT and CPTu methods for predicting the ultimate bearing capacity of single piles." *Engineering Geology*, 104, 211–222.

Camacho, M. A., Meija, J., Camacho, C. B., Heredia, W. and Salinas, L. M. (2018). "Ultimate capacity of drilled shaft from CPTu test and static load test." *Proceedings of the 4th International Symposium on Cone Penetration Testing (CPT'18)*, 21-22 June 2018, Delft, The Netherlands. Cone Penetration Testing 2018, 193–198.

Campanella, R. G., Baziw, E. J. and Sully, J. P. (1989). "Interpretation of seismic cone data using digital filtering techniques." *Proceedings of 12th International Conference on Soil Mechanics and Foundation Engineering*, Rio de Janeiro, Brazil, 1, 195–199.

Campanella, R. G., and Steward, W. P. (1992). "Seismic cone analysis using digital signal processing for site characterization." *Canadian Geotechnical Journal*, 29(3), 477–486.

Chin, F. K. (1970). "Estimation of the ultimate load of piles from test not carried to failure." *Proceedings of the Second Southeast Asia Conference on Soil Engineering,* Singapore, 81–90.

Cooke, R. W., Price, G. and Tarr, K. (1979). "Jacked piles in London Clay: a study of load transfer and settlement under working conditions." *Géotechnique*, 29(2), 113–147.

De Cock, F. A. (2009). "Sense and sensitivity of pile load-deformation behavior." *Deep foundation on bored and auger piles*, Van Impe, W. F and Van Impe P.O. (eds), Taylor & Frances Group, London, 23–44.

Decourt, L. (1982). "Prediction of the bearing capacity of piles based exclusively on N values of the SPT." *Proceeding of the 2nd European Symposium on Penetration Testing, Amsterdam,* 29–34.

Decourt, L. (1995). "Prediction of load-settlement relationships for foundations on the basis of the SPT-T." *Ciclo de Conferencias Internationale*, Leonardo Zeevaert, UNAM, Mexico, 85–104.

Decourt, L. (1999). "Behavior of foundations under working load conditions." *Proceedings of the 11th Pan-American Conference on Soil Mechanics and Geotechnical Engineering*, Foz Do Iguassu, Brazil, 4, 453–488.

De Ruiter, J. and Beringen, F. L. (1979)." Pile foundation for large North Sea structures." *Marine Geotechnol*ogy, 3(3), 267–314.

De Cock, F. A. (2009). "Sense and sensitivity of pile load-deformation behavior." *Deep foundation on bored and auger piles*, Van Impe, W.F. and Van Impe, P.O, (eds), Taylor & Frances Group, London, 23–44.

Duan, W., Cai, G., Yuan, J. and Liu, S. (2018). "Evaluation of the Variation of Deformation Parameters Before and After Pile Driving Using SCPTU Data." *Proceedings of China-Europe Conference on Geotechnical Engineering*. Springer Series in *Geomechanics and Geoengineering*. Springer, Cham.

EA-Pfähle. (2014). "Recommendations on piling (EA-Pfähle)." Ed by *German Geotechnical Society*, DGGT. Ernst & Sohn, Berlin.

Fahey, M. and Carter, J. (1993). "A finite element study of the pressuremeter using a nonlinear elastic plastic model." *Canadian Geotechnical Journal*, 30(2), 348–362.

Elsamee, W. (2012). "Evaluation of the Ultimate Capacity of Friction Piles." *Engineering*, 4, 778–789.

EN 1997-1:2004. Eurocode 7: Geotechnical Design - Part 1: General Rules, Brussels, Belgium, 2004.

EN 1997-2:2007. Eurocode 7 Geotechnical Design - Part 2: Ground Investigation and Testing, Brussels, Belgium, 2007.

Eslami, A. (1996). "Bearing capacity of piles from cone penetrometer test data." *Ph. D. Thesis*, University of Ottawa, Department of Civil Engineering.

Eslami, A., Aflaki, E. and Hosseini, B. (2011). "Evaluating CPT and CPTu Based pile bearing capacity estimation methods using Urumiyeh lake causeway piling records." *Scientia Iranica*, 18, 1009–1019.

Eslami, A. and Fellenius, B. H. (1995). "Toe bearing capacity of piles from cone penetration test (CPT) data." *Proceedings of the International Symposium on Cone Penetration Testing*, CPT'95, Linkoping, Sweden, October 4 - 5, Swedish Geotechnical Institute, SGI, Report 3:95, 2, 453–460.

Eslami, A. and Fellenius, B. H. (1996). "Pile shaft capacity determined by piezocone data." *Proceedings of the 49th Canadian Geotechnical Conference*, St. John`s, Newfoundland, September 23 – 25, 2, 859–867.

Eslami, A. and Fellenius, B. H. (1997), "Pile capacity by direct CPT and CPTu methods applied to 102 case histories." *Canadian Geotechnical Journal*, 34(6), 880–898.

Fahey, M. and Carter, J. (1993). "A finite element study of the pressuremeter using a nonlinear elastic plastic model." *Canadian Geotechnical Journal*, 30(2), 348-362.

Fellenius, B. H. (2020). Excerpt from Chapter 7 of the red book electronic edition: direct methods for estimating pile capacity, in Background to UniCone, http://www.fellenius.net. Accessed 13.01.2020.

Fellenius, B. H. and Eslami, A. (2000). "Soil profile interpreted from CPTu data." *Proceedings Of Year 2000 Geotechnics Conference,* Southeast Asian Geotechnical Society, Asian Institute of Technology, Bangkok, Thailand, November 27-30, 2000, Editors Balasubramaniam, A.S., Bergado, D.T., Der Gyey, L., Seah, T.H., Miura, K., Phien wej, N. and Nutalaya, P., 1, 163–171.

Finnish Geotechnical Society. (2001). Sounding guidelines 6 – 2001 CPTu / cone penetration testing and static dynamic testing. Nummela: Nummelan Kopiopalvelu Oy.

Flynn, K. N., McCabe, B. A. and Egan, D. (2014). "Driven cast-in-situ piles in granular soil: applicability of CPT methods for pile capacity." *Proceedings of the 3rd International Symposium on Cone Penetration Testing (CPT'14)*, 12-14 May 2014, Las Vegas, USA, 1–8.

Frank, R., Bauduin, C., Driscoll, R., Kavvadas, M., Krebs Ovesen, N., Schuppener, T. Orr, B. and Gulvanessian, H. (2005). Designers' Guide to EN 1997-1 Eurocode 7: Geotechnical Design – General Rules. ICE Publishing, ISBN: 9780727731548.

Gadeikis S., Žaržojus G. and Urbaitis D. (2010). "Comparing CPT and DPSH in Lithuanian soils." *Proceedings of the 2nd* International *Symposium on Cone Penetration Testing*, Huntington Beach, CA, USA. Volume 2&3: Technical Papers, Session 3: Applications, 3–22.

Hegazy, Y. A. and Mayne, P. W. (1995). "Statistical Correlations Between *Vs* and CPT Data for Different Soil Types." *Proceedings of the Symposium on Cone Penetration Testing*, Vol. 2, Swedish Geotechnical Society, Linköping, Sweden, 173–178.

Hirany, A. and Kulhawy, F.H. (1989). "Interpretation of load tests on drilled shafts: axial compression." *Foundation Engineering: Current Principles and Practices*, Vol. 2, ASCE, Reston, Virginia, 1132–1149.

Holeyman, A. E. (2001). "Screw piles – installation and design in stiff clay." Swets & Zeitlinger, Lisse, ISBN 90 5809 192 9.

Holmsgaard, R., Ibsen, L. B. and Nielsen, B. N. (2016). "Interpretation of Seismic Cone Penetration Testing in Silty Soil." *Electronic Journal of Geotechnical Engineering*, 21(15), 4759–4779.

Howie, J. A. and Amini, A. (2005). "Numerical simulation of seismic cone signals." *Canadian Geotechnical Journal*, 42(2), 574–586.

Hu, Z., McVay, M., Bloomquist, D., Horhota, D. and Lai, P. (2012). "New ultimate pile capacity prediction method based on cone penetration test (CPT)." *Canadian Geotechnical Journal*, 49(8), 961–967.

Hussien, M. N., and Mourad, K. (2016). "Shear wave velocity as a geotechnical parameter: an overview." *Canadian Geotechnical Journal*, 53(2), 252–272.

Huybrechts, N. and Whenham, V. (2003). "Pile testing campaign on the Limelette test site and installation techniques of screw piles." *Proceedings of the 2nd Symposium on Screw Piles – Belgian Screw Pile Technology – Design and Recent Developments*. Brussels, Balkema, ISBN: 90 5809 578 9, 71–130.

Jamiolkowski, M., Ladd, C. C., Germaine, J. T. and Lancellotta, R. (1985). "New developments in field and laboratory testing of soils." *Proceedings of the 11th International Conference on Soil Mechanics and Foundation Engineering*, San Francisco, 1, 57–153.

Jamiolkowski, M., Lancellotta, R., Lo Presti, D. C. F. and Pallara, O. (1994). "Stiffness of Toyoura sand at small and intermediate strain." *Proceedings* of the *13th International Conference on Soil Mechanics and Foundation Engineering* (1), New Delhi, 169–172.

Jardine, R. J., Potts, D. M., Fourie, A. B. and Burland, J. B. (1986). "Studies of the influence of nonlinear stress-strain characteristics in soil-structure interaction." *Géotechnique*, 36(3), 377–396.

Jardine, R. J., Zhu, B. T., Foray, P. and Yang, Z. X. (2013). "Measurement of stresses around closed-ended displacement piles in sand." *Géotechnique,* 63(1), 1–17.

Karimpour-Fard, M. and Eslami, A. (2013). "Estimation of vertical bearing capacity of piles using the results CPT and SPT tests." *Geotechnical and Geophysical Site Characterization* vol 4, ed Coutinho and Mayne (London: Taylor & Francis Group), 1055–1059.

Kempfert, H.-G. and Becker, P. (2010). "Axial pile resistance of different pile types based on empirical values." *Proceeding of Geo-Shanghai 2010 deep foundation and geotechnical in situ testing*, ASCE, Reston, VA, 2010, 149–154.

Kondner, R. L. (1963). "Hyperbolic stress-strain response: cohesive soils." *Journal of the Soil Mechanics and Foundation Division*, ASCE, 89(4), 241–242.

Leetsaar, L., Korkiala-Tanttu, L. and Kurnitski, J. (2022). "CPT, CPTu and DCPT Methods for Predicting the Ultimate Bearing Capacity of Cast In Situ Displacement Piles in Silty Soils." *Geotechnical and Geological Engineering*, 41, 631–652.

Leetsaar, L. and Korkiala-Tanttu, L. (2023). "Deterministic and probabilistic analyses of the bearing capacity of screw cast in situ displacement piles in silty soils as measured by CPT and SDT." *The Baltic Journal of Road and Bridge Engineering*, 18(2), 99–127.

Leetsaar, L. and Korkiala-Tanttu, L. (2024). "Advantages of using a seismic piezocone penetration test for analysis of a single screw in situ displacement pile in silty soils." *Indian Geotechnical Engineering*.

Liao, T., and Mayne, P.W. (2006) "Automated post-processing of shear wave signals." *Proceedings of the 8th U.S. National Conference on Earthquake Engineering*, San Francisco, CA, USA, 18-22 April 2006, paper no. 460.

Lo Presti, D. C. F., Pallara, O., Lancellotta, R., Armandi, M. and Maniscalco, R. (1993). "Monotonic and cyclic loading behavior of two sands at small strains." *ASTM Geotechnical Testing Journal*, 16(4), 409–424.

Lunne, T., Robertson, P. K. and Powell, J. J. M. (1997). *Cone Penetration Testing in Geotechnical Practice*. Blackie Academic, EF Spon/Routledge Publishers, New York, p. 312.

Map applications of the Estonian Land Board, 202017.04.

Massarsch, K. R. (2014). "Cone penetration testing - A historic perspective." *Proceedings of the CPT'14*. Las Vegas, May 12-14, 2014, 97–134.

Maertens, J. and Huybrechts, N. (2003). "Results of the static pile load tests at the Limelette test site." *Proceedings of the 2nd Symposium on Screw Piles – Belgian Screw Pile Technology – Design and Recent Developments*, Brussels, Balkema, ISBN: 9058095789, 167–214.

Martin, R. E., Seli, J. J., Powell, G. W. and Bertoulin, M. (1987). "Concrete pile design in Tidewater, Virginia." *Journal of Geotechnical Engineering,* 113(6), 568–585.

Mayne, P. W. (1995). "Application of G/G_{max} modulus degradation to foundation settlement analyses." *Proceedings* of the *U.S.-Taiwan Workshop on Geotechnical Collaboration, National Science Foundation*, Washington D.C. and National Science Council, Taipei, 136–148.

Mayne, P. W. (2000). "Enhanced geotechnical site characterization by seismic piezocone penetration tests." *Invited Lecture, Fourth International Geotechnical Conference*, Cairo University, January 2000, 95–120.

Mayne, P. W. (2005). "Integrated ground behavior: In-situ and laboratory tests." *Deformation Characteristics of Geomaterials* (2), Taylor & Francis, UK, 155–177.

Mayne, P. W. (2006). "The 2nd James K. Mitchell Lecture: Undisturbed Sand Strength from Seismic Cone Tests." *Geomechanics and Geoengineering*, 1(4), 239–247.

Mayne, P. W. (2007). "In-Situ Test Calibrations for Evaluating Soil Parameters." *Characterization & Engineering Properties of Natural Soils*, Vol. 3, Taylor & Francis Group, London, 1602–1652.

Mayne, P.W. and Niazi, F.S. (2009). "Evaluating axial elastic pile response from cone penetration tests." (2009 Michael O'Neill Lecture), *The Journal of Deep Foundation Institute*, 3(1), 3–12.

Mayne, P. W and Schneider, J. A. (2001). "Evaluating axial drilled shaft response by seismic cone." *Foundation and Ground Improvement. Geotechnical Special Publication* No. 113, ASCE, Reston, VA, 655–669.

Melander, K. (1989). "Static-dynamic sounding method." The publication 48 by the department of geotechnics of city of Helsinki. Helsingin kaupungin kiinteistövirasto, *Geotekninen osasto* 1989.

Mets, M. and Leppik, V. (2016). "Pile foundations in Estonia." *Design of Piles in Europe – How did Eurocode 7 change daily practice?* International Symposium 28 and 29 April 2016 Leuven, Belgium, 101–116.

Meyerhof, G. G. (1956). "Penetration tests and bearing capacity of cohesionless soils." *Journal of Geotechnical Engineering*, ASCE, 82, 1–12.

Meyerhof, G. G. (1976). "Bearing capacity and settlement of pile foundations." *Journal of Geotechnical Engineering*, ASCE, 102, 195–228.

Molina-Gómez, F., Viana da Fonseca, A., Ferreira, C., Sousa, F. and Bulla-Cruz, L. (2021). "Defining the soil stratigraphy from seismic piezocone data: a clustering approach." *Engineering Geology*, 287, 106–111.

Moshfeghi, S. and Eslami, A. (2016). "Study on pile ultimate capacity criteria and CPT-based direct methods." *International Journals of Geotechnical Engineering*, 12(1), 28–39.

Niazi, F.S. (2014). "Static axial pile foundation response using seismic piezocone data." *PhD Thesis*, School of Civil & Environmental Engineering., Georgia Institute of Technology, Atlanta, GA.

Niazi, F.S. and Mayne, P. W. (2013). "Cone penetration test based direct methods for evaluating static axial capacity of single piles: a state-of-the-art review." *Geotechnical and Geological Engineering*, 31(4), 979–1009.

Niazi, F. S. and Mayne, P. W. (2015). "Operational Soil Stiffness from Back-Analysis of Pile Load Tests within Elastic Continuum Framework." *Geotechnical Engineering Journal of the SEAGS & AGSSEA,* 46, 1–19.

Niazi, F. S. and Mayne, P. W. (2016). "CPTu-based enhanced UniCone method for pile capacity." *Engineering Geology*, 212, 21–34.

Nottingham, L. C. (1975). "Use of quasi-static friction cone penetrometer data to predict load capacity of displacement piles." *PhD Thesis*, University of Florida.

Obrzud, R. F. (2010). "On the use of the Hardening Soil Small Strain model in geotechnical practice." *Numerics in Geotechnics and Structures*, Elmepress International, Lausanne, 15–32.

Orr, T. L. L. and Denys, B. (2008). Eurocode 7 and reliability-based design. Reliability-based design in geotechnical engineering. Edited by K.-K. Phoon. Taylor and Francis, Oxon, UK, 298–343.

Poulos, H. G. (1989). "Pile behaviour-theory and application." *Géotechnique*, 39(3), 365–415.

Poulos, H. G. (2022). "Use of Shear Wave Velocity for Foundation Design." *Geotechnical and Geological Engineering,* 40, 1921–1938.

Randolph, M. F. and Wroth, C.P. (1978). "Analysis of deformation of vertically loaded piles." ASCE *Journal of the Geotechnical and Geoenvironmental Engineering*, 104, 1465–1488.

Randolph, M. F. and Wroth, C.P. (1979). "A simple approach to pile design and the evaluation of pile tests." *Behavior of Deep Foundations*, STP 670, ASTM, West Conshohocken, 484–499.

Rantala, K. and Halkola, H. (1997). "The definition of the bearing capacity of a pile with static-dynamic sounding." The publication 74/1997 by the department of geotechnics of city of Helsinki. Helsingin kaupungin kiinteistövirasto, *Geotekninen* osasto 1997.

Reinders, K., van Seters, A. and Korff, M. (2016), "Design of piles according to Eurocode 7 – Dutch practice." *Design of Piles in Europe – How did Eurocode 7 change daily practice?* International Symposium 28 and 29 April 2016 Leuven, Belgium, 75–100.

Robertson, P. K. (2010). "Soil behaviour type from the CPT: an update." *Proceedings of the 2nd International Symposium on Cone Penetration Testing*, CPT'10, Huntington Beach, CA, USA.

Robertson, P. K. and Cabal, K. L. (2015). "Guide to cone penetration testing for geotechnical engineering." 6th edition, Gregg Drilling & Testing Inc, Signal Hill, CA, USA.

Robertson, P. K. and Campanella, R. G. (1988). "Guidelines for geotechnical design using CPT and CPTU." University of British Columbia, Vancouver, Department of Civil Engineering, *Soil Mechanics Series*.

Robertson, P. K., Campanella, R. G., Gillespie, D. and Rice, A. (1986). "Seismic CPT to measure in-situ shear wave velocity." *Journal of Geotechnical Engineering*, 112(8), 791–803.

Rollins, K. M., Miller, N. P. and Hemenway, D. (1999). "Evaluation of Pile Capacity Prediction Methods Based on Cone Penetration Testing Using Results from I-15 Load Tests." *Transportation Research Record*, 1675(1), 40–50.

Saks, M. and Smirnov, L. (1985). "Tallinna kiirtramm." *Eesti Ehitusgeoloogia Fond*, 2452X/2952E.

Schmertmann, J. H. (1978). "Guidelines for cone penetration test, performance and design." *U.S. Department of Transportation*, Washington, DC, Report No. FHW A-TS-78-209.

Shariatmadari, N., Eslami, A. and Karimpour-Fard, M. (2008). "Bearing capacity of driven piles in sands from SPT–applied to 60 case histories." *Iranian Journal of Science & Technology*, 2008, 32, 125–140.

Shooshpasha, I., Hasanzadeh, A. and Taghavi, A. (2013). "Prediction of the axial bearing capacity of piles by SPT-based and numerical design methods." *International Journal of GEOMATE*, 4(2), 560–564.

Sully, J. P., and Campanella, R. G. (1995). "Evaluation of in situ anisotropy from crosshole and downhole shear wave velocity measurements." *Géotechnique*, 45(2), 267–282.

Žaržojus, G. (2010). Summary of Doctoral Thesis_ Analysis of the results and it influence factors of dynamic probing test and interrelation with cone penetration test data in Lithuanian soils. Vilnius.

Tatsuoka, F. and Shibuya, S. (1992). "Deformation characteristics of soils and rocks from field and laboratory tests." *Report of the Institute of Industrial Science*, 37(1), Serial No. 235, The University of Tokyo.

Tatsuoka, F., Jardine, R.J., Lo Presti, D. C. F., Di Benedetto, H. and Kodaka, T. (1997). Theme Lecture: Characterizing the pre-failure deformation properties of geomaterials.

Proceedings of the 14th International Conf. on Soil Mechanics & Foundation Engineering, Vol. 4, Hamburg.

Titi, H. and Murad, A. F. (1999). "Evaluation of Bearing Capacity of Piles from Cone Penetration Test Data." LTRC Project No. 98-3Gt, State Project No. 736-99-0533, Louisiana Transportation Research Center, LA.

Togliani, G. and Reuter, G. R. (2014). "CPT/CPTu Pile Capacity Prediction Methods: Question Time." *Proceedings of the CPT'14*. Las Vegas, May 12-14, 2014, 993–1002.

Tonni, L. and Simonini, P. (2013). "Shear wave velocity as function of cone penetration test measurements in sand and silt mixture." *Engineering Geology*, 163, 55–67.

Trevor, F. A., Paisley, J. M. and Mayne, P. W. (2010). "Cone penetration tests at active earthquake sites." *Proceedings of the 2nd International Symposium on Cone Penetration Testing*, (CPT'10), Huntington Beach, CA, USA, 9-11 May, 519–526.

Van Baars, S., Rica, S., De Nijs, G. A., De Nijs, G. J. J. and Riemens, H. J. (2018). "Dutch field tests validating the bearing capacity of Fundex piles." *Proceedings of CPT`18 – International Symposium on Cone penetration testing*, CRC Press, Leiden, 101–107.

Vardanega, P. J. and Bolton, M. D. (2013). "Stiffness of clays and silts: normalizing shear modulus and shear strain." *Journal of Geotechnical and Geoenvironmental Engineering*, 139(9), 1575–1589.

Vesić, A. S. (1977). "Design of pile foundations." *NCHRP Synthesis of Highway Practice 42*, Transportation Research Board, National Research Council, Washington, D.C.

Wrana, B. (2015). "Pile Load Capacity—Calculation Methods." *Studia Geotechnica et Mechanica* 37, 83–93.

Zhang, X., Liu, X., An, R. and Li, X. (2023). "Site observations of weathered granitic soils subjected to cementation and partial drainage using SCPTU." *Journal of Rock Mechanics and Geotechnical Engineering*, 15(4), 984–996.

Publication 1

Leetsaar, Lehar; Korkiala-Tanttu, Leena; Kurnitski, Jarek. CPT, CPTu and DCPT Methods for Predicting the Ultimate Bearing Capacity of Cast In Situ Displacement Piles in Silty Soils. Springer. *Geotechnical and Geological Engineering,* **2022; 10.1007/s10706-022-02292-6.**

ORIGINAL PAPER

CPT, CPTu and DCPT Methods for Predicting the Ultimate Bearing Capacity of Cast In Situ Displacement Piles in Silty Soils

L. Leetsaar [ID] · **L. Korkiala-Tanttu** · **J. Kurnitski**

Abstract Determining the load-bearing capacity of piles using the results of in situ tests is one of the most widely used methods. The objective of this study is to examine suitable cone penetration test (CPT)-based methods for predicting the load-bearing capacity of piles in silty soils. In addition, it is analysed whether standard penetration test (SPT)-based methods can be used with dynamic probing super heavy (DPSH-A) test data to evaluate pile capacity. Five CPTs and one piezocone penetration test (CPTu) based on direct methods were applied to determine the load-bearing capacity of piles. In addition, six SPT direct methods were used based on DPSH-A test data to estimate the load-bearing capacity of the investigated piles. The capacity of the pile obtained by various direct methods was compared with the outcome of the pile load test. Of the direct CPT methods, the LCPC (also known as French method) method and the German method demonstrated decent results when CPT probing reached deeper than the pile. The use of SPT-based direct methods with DPSH-A test data for displacement piles in silty soils seems to be promising. Specifically, the Briaud and Tuckers` method provided excellent results for most of the piles studied.

1 Introduction

Geological conditions in Tallinn vary substantially. There are areas where limestone's hard stratum is, on average, 1 m deep. Furthermore, there are areas where rock is cut by a complex system of several ancient valleys buried by dense fluvioglacial sands and soft limnoglacial and marine clayey sediments, often tens of metres thick (Arbeiter 1962; Estonian Land Board 2020). The use of pile foundations for buildings in such places is unavoidable. Boring piles, displacement piles and continuous flight auger (CFA) piles are the most frequently used pile types in Estonia (Mets et al. 2016). For safe and economic foundations, it is essential to determine the bearing capacity of the piles as precisely as possible. Due to the large variety of soil types and pile installation procedures, it is generally complicated to predict the axial bearing capacity of the pile. The capacity of the single

L. Leetsaar (✉) · L. Korkiala-Tanttu
Department of Civil Engineering, Aalto University, Espoo, Finland
e-mail: lehar.leetsaar@taltech.ee

L. Leetsaar
Tallinn University of Technology Tartu College, Tartu, Estonia

L. Leetsaar · J. Kurnitski
Department of Civil Engineering and Architecture, Tallinn University of Technology, Tallinn, Estonia

compressed pile (R_c) is calculated as the sum of the base capacity (R_b) and shaft friction capacity (R_s) using the following formula EN 1997–1 (2004):

$$R_c = R_b + R_s = q_b \cdot A_b + \sum_{i=1}^{n} q_{s,i} \cdot A_{s,i} \qquad (1)$$

The weight of the pile must be deducted from the defined R_c value. The end bearing capacity (R_b) is determined by multiplying the end bearing resistance (q_b) by the pile tip area (A_b). The shaft friction capacity (R_s) is calculated as the sum of the product of the unit shaft friction ($q_{s,i}$) and the outer pile shaft area ($A_{s,i}$) for different soil layers.

The most accurate method to define pile capacity is the static pile load test, which results in a load-settlement relation. Because of its high cost, the static loading test is usually not used in the early stages of construction planning. One possibility is to collect disturbed or undisturbed samples from the construction site and test them in the laboratory, after which the results can be used in theoretical pile bearing capacity calculation methods. There are many inaccuracies in the taking and testing of specimens, especially when the sampling depth increases. Furthermore, many such design methods have several inherent drawbacks (Niazi et al. 2013). Adopting calculation methods based on the results of 'in situ' tests is the most informative and useful method nowadays (Eslami and Fellenius 1997; Cai et al. 2012; Moshfeghi and Eslami 2016).

In Estonia, site investigations are usually carried out using a dynamic probing super heavy (DPSH-A) test. On certain occasions, investigations are performed using the cone penetration test (CPT). Although DPSH is fast and inexpensive and penetrates thicker soil layers with ease, it is primarily intended for use in cohesionless soils. Soundings in fine-grained soils or below groundwater level may lead to erroneous results (Gadeikis et al. 2010; Žaržojus 2010; Czado et al. 2012). CPT offers continuous, reliable and repeatable data; however, in some cases, anchoring or larger reaction mass to reach deeper layers is needed. In addition, the cone penetrometer can be considered a mini-pile foundation (Bandini and Salgado 1998; Mayne 2007; Jardine et al. 2013). As indicated by Eslami and Fellenius (1997) and Ardalan et al. (2009), the

mean effective stress, compressibility and rigidity of the surrounding soil medium affect the pile and the cone in a similar manner. Therefore, CPT data enables the evaluation of pile capacity without the need to supplement the field data with laboratory testing. This approach has led to the evolution of a significant number of CPT-based design methods (Nottingham 1975; Schmertmann 1978; De Ruiter and Beringen 1979; Bustamante and Gianeselli 1982; Eslami and Fellenius 1997; Kempfert and Becker 2010). The CPT-based methods can be divided into two groups (Eslami and Fellenius 1997, Mayne 2007; Ardalan et al. 2009): direct and indirect (rational) approaches. Many studies have compared the pile test results of various pile types in allogeneous soils with different CPT methods all over the world (i.e. Briaud et al. 1988; Eslami and Fellenius 1995; Eslami and Fellenius 1997; Rollins et al. 1999; Abu-Farsakh et al. 2004; Cai et al. 2009; Mayne et al. 2009; Niazi et al. 2010; Pardoski 2010; Reuter 2010; Titi et al. 2010; Cai et al. 2011; Eslami et al. 2011; Hu et al. 2012; Flynn et al. 2014; Moshfeghi and Eslami 2016; Amirmojahedi et al. 2019). Most of the studies rely on a large number of testing sites with different soils. The studies clearly demonstrate the universality of various CPT methods. However, only a few of these studies offer an opportunity to estimate the bearing capacity of piles in silty soils (Cai et al. 2009). This study focuses primarily on defining the pile capacity in silty soils with the help of CPT test results. Five CPTs and one CPTu based on direct methods were implemented and compared to evaluate the eligibility for the use of these methods in this area. In addition, pile bearing capacities were determined from DPSH-A data. Since there are no DPSH-A-based direct methods, six commonly used methods based on the standard penetration test (SPT) were used. The outcomes were compared to static pile load tests with a French criterion of $s/B = 10\%$, where B denotes the diameter of the pile tip and s denotes the settlement of the pile head. For that purpose, a database of seven Fundex piles in silty soils with adjacent CPT, CPTu, DPSH-A and static pile load test data at two sites was analysed. This analysis included the analytical calculations. Further analysis and verification of the results will continue with, for example, numerical and more detailed statistical methods. Those results will be recorded in future publications.

2 Use of Sounding Test Methods for the Prediction of Axial Pile Bearing Capacity

2.1 CPT, CPTu and DCPT Methods

Finding the accurate values of the base and shaft resistances (q_b and f_{pi}) is one of the keys for calculating the capacity of the pile foundations. Without a doubt, penetration tests are one of the best solutions for this purpose. Penetration testing has become very popular during the past four decades and continues to provide an abundance of research topics for scientists around the world. Whereas SPT dominates outside Europe, various types of dynamic and static penetrometers are used in Europe (Massarsch 2014).

The CPT is recognized as one of the most effective in situ options for the characterization of soil. During the test, the probe is pushed into the soil at a constant speed to the desired depth or as long as the counterweight is sufficient. The CPT is a decent, quick, simple, economic and robust test providing continuous readings of subsurface soil, while the electrical CPT probe (piezocone) allows the measurement of the cone base resistance (q_c) and sleeve friction (f_s). The piezocone (CPTu) also provides the measurement of pore water pressure (u_2). These are three independent parameters that can be used for soil identification and classification and the evaluation of different soil properties, such as strength and deformation characteristics. In soft fine-grained saturated soils, in which pore pressure can be relatively large compared to cone resistance, pore water pressure correction is especially crucial.

The dynamic cone penetration test (DCPT) is a simple and inexpensive soil investigation method with a solid penetrometer driven into the ground. The number of blows to drive the cone to the desired depth is recorded. Originally, dynamic cone penetrometers were designed to gather quantitative and qualitative data on the soil resistance to penetration and mainly to determine the compactness of the cohesionless soils, which are frequently challenging to samples. Depending on the size of the cone, the weight of the hammer and the height of the drop, four types of probes can be differentiated: dynamic probing light (DPL), dynamic probing medium (DPM), dynamic probing heavy (DPH) and dynamic probing super heavy (DPSH). According to EN ISO 22476-2 (2005), DPSH is further divided into two categories: DPSH-A and DPSH-B. In the first case, the drop height of the hammer is 0.5 m and in the second case 0.75 m. The shapes of the cone and drive rod also differ. In Estonia, the first variant has been widely used in recent decades.

2.2 Direct Approaches to Define Pile Capacity

2.2.1 Direct Approaches for CPT and CPTu Soundings

Direct cone penetration methods for CPT apply cone sleeve friction for unit shaft resistance and cone bearing for end bearing resistance of the pile by the analogy of the cone penetrometer as a model pile.

To determine the axial bearing capacity of piles, more than 30 different CPT- and CPTu-based methods have been developed. New methods are being elaborated, and the existing ones are being refined based on larger databases of pile load tests. Niazi and Mayne (2013) have reviewed existing methods and have developed new ones (Niazi and Mayne 2016). Six methods were examined in this study: five most appropriate direct CPT methods and the Unicone method based on CPTu results (Table 1).

The Eurocode 7 method has no upper limits for pile unit shaft friction. In the present work, the Eurocode 7 method has been modified, and a limit value of 120 kPa has been used for the pile unit shaft friction.

2.2.2 Direct Approaches for DCPT Based on SPT Methods

The DCPT device DPSH-A complies with Swedish standard EVN 1997-3; 1995 for HfA. HfA is reported in the literature (Bergdahl and Ottosson 1988), saying that the number of blows N20 received by the device is equal to the number of shots N30 recorded by the SPT device. This allows the correlation of soil properties developed for SPT to be used for evaluation. Site investigations in Estonia often refer to this correlation. Unfortunately, no corresponding local tests have been carried out to verify the validity of the correlation. Six commonly used methods (Shariatmadari et al. 2008; Benali et al. 2013; Karimpour-Fard et al. 2013; Shooshpasha et al. 2013) were examined in this study (Table 2). Before using SPT methods, it must be kept in mind that they do not take into account the excessive pore water pressure generated during the

Table 1 Summary of direct CPT-based pile design methods

Method/reference	Design equations	
	Pile unit shaft friction (q_s)	Pile end bearing resistance (q_b)
Nottingham (1975) and Schmertmann (1978) (for driven concrete, steel and timber piles, and drilled shafts in all soil types)	In clay: $q_s = K_f \cdot f_s \leq 120$ kPa, $K_f = 0.2$–1.25; K_f is a function of the sleeve resistance. In sand: $q_s = c_s \cdot q_c$ or $f_p = k \cdot f_s$; $c_s = 0.8$–1.8%, $k = 0.8$–2.5	$q_b = C \cdot q_{ca} \leq 15$ MPa (in sands) and 10 MPa (in very silty sands); $C = 0.5$–1.0 depending on overconsolidation rate (OCR); $q_{ca} = (q_{c1} + q_{c2})/2$
Dutch method (de Ruiter and Beringen 1979) (for offshore piles in all soil types)	In clay: $q_s = \alpha \cdot s_u \leq 120$ kPa; $\alpha = 1$ for NC clay and 0.5 for OC clay; $s_u = q_{cd}/N_{kt}$; $N_{kt} = 15$–20. In sand: $q_s = \min[f_s, q_c/300$ for compression, $q_c/400$ for tension, 120 kPa]	In clay: $q_b = N_c \cdot s_u \leq 15$ MPa, $s_u = q_{cd}/N_{kt}$, $N_c = 9$; $N_{kt} = 15$–20; $q_{ca} = (q_{c1} + q_{c2})/2$. In sand: similar to Nottingham (1975) and Schmertmann (1978) method
LCPC or French method (Bustamante and Gianeselli 1982; Bustamante and Frank 1997) (for all pile types in all soil types)	$q_s = q_{side}/k_s \leq f_{p(max)}$; $k_s = 30$–150 depending on soil type, pile type and installation procedure	$q_b = k_b \cdot q_{eq}$ depending on soil types: $k_b = 0.15$–0.375 for non-displacement piles; $k_b = 0.375$–0.60 for displacement piles
EUROCODE 7 (EN 1997-2: 2007) (for all pile types in all soil types)	$q_s = \alpha_s \cdot q_{c,z}$; $\alpha_s = 0.005$–0.030 depending on soil type or pile type and installation procedure	$q_b = 0.5 \cdot \alpha_p \cdot \beta \cdot s \left\{ \dfrac{q_{c,Imean} + q_{c,IImean}}{2} + q_{c,IIImean} \right\}$ $q_{b,max} \leq 15$ MPa; $\alpha_p = 0.6$–1.0 depending on soil type, pile type and installation procedure; β factor that takes into account the shape of the pile tip; s factor that takes into account the shape of the bottom of the pile
German method (EA-Pfähle 2014) (for piles in sandy soils)	Provides upper and lower bound estimates of q_s (kPa) based on q_c (measured in MPa)	Provides upper and lower bound estimates of q_b (MPa) based on q_c (measured in MPa)
Unicone method (Eslami and Fellenius 1995, 1996, 1997; Fellenius and Eslami 2000; Eslami 1996; Fellenius 2020)	$q_s = C_{se} \cdot q_E$; $q_E = q_t - u_2$; $C_{se} = 0.8$–8% (see Fig. 4 for C_{se}); $q_s = C_{se} \cdot q_E$	$q_b = C_{te} \cdot q_{Eg}$; q_{Eg} is the geometric average of q_c; C_{te} is generally taken as 1; for pile diameter $d > 0.4$ m $C_{te} = 1/(3d)$; $q_b = C_{te} \cdot q_{Eg}$; q_{Eg} is the geometric average of q_c

Table 2 Current SPT direct methods for prediction of pile bearing capacity

Method/reference	Design equations	
	Pile unit shaft resistance (q_s)	Pile end bearing resistance (q_b)
Aoki and De`Alencer (1975)	$q_s = \left(\frac{ak}{3.5}\right)N_s$	$q_b = \left(\frac{k}{1.75}\right)N_b$
Failure criteria: Van der Veen method		
Energy ratio for N: 70%	For sand: $a = 14$ and $k = 1$ For clay: $a = 60$ and $k = 0.2$	N_b: average of three values of SPT blows around pile base
Meyerhof (1976) Failure criterion: minimum slope of load-movement curve Energy ratio for N: 55%	$q_s = n_s N_s$ Bored piles (low disp.): $n_s = 1$ Driven piles (high disp.): $n_s = 2$	$q_b = 0.4 N_1 C_1 C_2$ N_1: N_b value at the base level $C_1 = ((B+0.5)/2B)^n$: $n = 1$, 2 and 3, respectively, for loose, medium and dens soil when pile diameter (B) > 0.5 m, otherwise $C_1 = 1$ $C_2 = D/10B$ when penetration in dense layer (D) > $10B$, otherwise $C_2 = 1$
Briaud and Tucker (1988)	$q_s = \dfrac{0.1}{\dfrac{1}{k_s} + \dfrac{0.1}{r_{s.max} + r_{s.res}}} - r_{s.res}$	$q_b = \dfrac{0.1}{\dfrac{1}{k_t} + \dfrac{0.1}{r_{t.max} + r_{t.res}}} + r_{t.res}$
Failure criteria: penetration of pile head equal 10% of pile diameter		
Poulos (1989) Martin (1987) Meyerhof (1956) Decourt (1982)	$q_s = \alpha + \beta N_s$ For cohesionless soil: $\alpha = 0$, $\beta = 2.0$ For cohesionless and cohesive soil: $\alpha = 10$, $\beta = 3.3$ $q_s = \alpha + \beta N_s$	$q_b = K N_b$ For silt and sandy silt: $K = 0.35$ For sand: $K = 0.4$–0.45
(for driven displacement piles)		
Decourt (1995)	$q_s = \alpha (2.8 N_s + 10)$ Driven piles and bored piles in clay: $\alpha = 1$ Bored piles in granular soils: $\alpha = 0.5$–0.6	$q_b = k_b N_b$ Driven and bored piles in sand: $k_b = 0.325$
Shariatmadari et al. (2008)	$q_s = 3.65 N_{gs}$ N_{gs}: geometrical average of N values along the pile	$q_b = 0.385 N_g$ N_{gb}: geometrical average of N values between 8D above and 4D below pile base

N_s is the average value of N around pile embedment depth; $k_t = 1{,}868{,}400 \cdot (N_b)^{0.0065}$, where N_b is the average of SPT blow-count between 4B above and 4B under the pile base; $k_s = 20{,}000 \cdot (N_s)^{0.27}$; $r_{t.max} = 1975 \cdot (N_b)^{0.36}$; $r_{s.max} = 22.4 \cdot (N_s)^{0.29}$; $r_{t.res} = 557 \cdot L \cdot ((k_s \cdot p)/(A_t \cdot E_p))^{0.5}$, where L: length of pile, p: perimeter of pile, A_t: cross-section area of pile, and E_p: elastic modulus of pile; $r_{s.res} = r_{t.res} (A_t/A_s)$, where A_s: surface area of pile

test. Therefore, the results may not be reliable in low-permeable soils such as silt and clay.

The SPT methods used for the analysis do not have an upper limit for ultimate end bearing resistance. In dense subsoils, it can significantly affect the results. For all SPT methods except for the Briaud and Tucker (1988) method, a limit value of 15 MPa was applied to the ultimate end bearing resistance.

3 Test Sites

Both test sites of this study are located in Tallinn (see Fig. 1), northern Estonia. They are both over old valleys buried in Quaternary sediments. Marine, lacustrine and alluvial deposits incorporate clay, silty sands, sandy silts, and sand at the Ahtri site and clay, silty clay, sand, and silty sand at the Paldiski mnt site. The hard stratum of both sites is tens of metres deep (see Fig. 1). Soil behaviour type (SBT) was selected for soil classification because the chart is global in nature and in the studied cases presents the alternation of thin layers of soil well. Soil was classified according to a non-normalized CPT SBT chart (Robertson 2010). This was done using the CpeT-IT 3.0 program.

The Ahtri test site is located by the Baltic Sea in the centre of Tallinn. The soil profile consists of 0.6–3.2 m fill. At a depth of 19–29.2 m, sporadic thin layers of
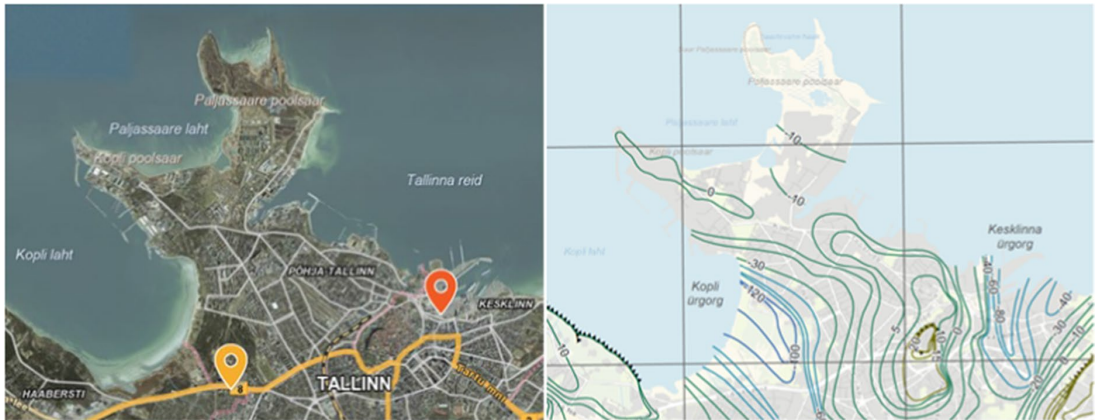
Fig. 1 On the left location of research points in Tallinn (Map applications of the Estonian Land Board 2020). Yellow indicates the location of Paldiski mnt 81 and red indicates the location of Ahtri street 3. On the right hard stratum relief around survey sites (Map applications of the Estonian Land Board 2020)

silty clay and clayey silt lie on the dense sandy deposit. Silty soils with natural water content ranging from 24.75 to 38.49% are trapped there. The water table is 1.2–1.8 m below the ground surface. In 2016, hundreds of Fundex-type piles were erected to the facility building. The construction stopped, and the upper ends of the piles were filled with fillings.

The Paldiski mnt site is located on the slope of the buried Kopli valley. Up to 6.4–7.0 m layers of clay and silty soils alternate. Beneath them, there is a 6.2–11.0-m-thick deposit of clayey silt and then there is a 2.6–6.8-m-thick dense silty fine sand layer. The natural water content of the clayey silt is between 24.3 and 29.5%. The silty sand contains weak interlayers. From the depth of 19.2–22.6 m, a layer of fine sand begins. The water table is 1.0–1.7 m below the ground surface.

The site plan of Ahtri st 3 with the existing piles, tested piles (SLT) and sounding points is presented in Fig. 2. In addition, the shortest distance in metres from the nearest pile is given for CPTu survey points. Figure 3 shows the Paldiski mnt site with tested piles (SLT) and sounding points.

4 Pile Tests and Analyses

4.1 Characteristics of the Investigated Piles

Data from static pile load test reports were collected and analysed. On both sites, static loading tests were carried out with Fundex piles. The pile tip diameters were 0.45 and 0.56 m. The length of the piles was between 15.0 and 27.5 m. Fundex piles can be arranged as cast in situ concrete displacement piles (Van Baars 2018). In Europe, these piles are commonly known as 'screw piles' (Basu et al. 2010). The number, diameter and depth of piles tested are given in Table 3. The diameter of the Fundex piles is given with two numbers. The first value designates the shaft diameter, and the second value indicates the diameter of the pile tip. As Fundex pile has a pile tip with overlap, it leads to a loosening of the ground in the shaft area. In succession, it leads to the reduction of shaft resistance (Kempfert et al. 2010). Table 4 summarizes the main case records, including the pile embedment depth, measured bearing capacity and settlement from the pile load tests. In addition, the maximum depths of soundings are given with the maximum q_c and N_{20} values. The pile head settlement is s; pile tip diameter B ratio (s/B) is given as a percentage. The letter 'A' indicates the piles of the Ahtri site and the letter 'P' the piles of the Paldiski mnt site. Table 4 shows clearly that the dynamic penetration soundings reached the deepest layers in all investigation points. Furthermore, all the CPTu soundings carried out with an anchored lightweight machine at the Ahtri site penetrated deeper than the previous CPT soundings with a heavy truck. However, no CPT probing reached the depth of the pile tip at the Ahtri site. In three cases, DPSH-A test reached the same

Fig. 2 Site plan of Ahtri st 3 with existing piles, tested piles (SLT) and sounding points
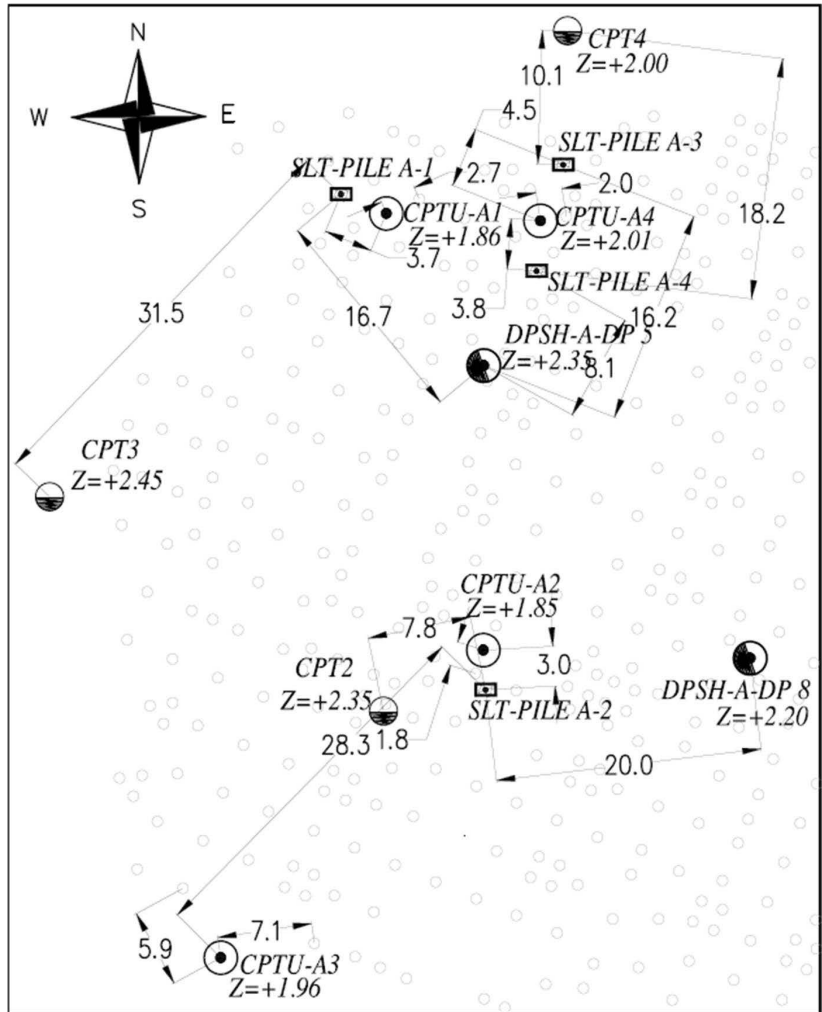
or deeper depth with a pile tip at the Ahtri site. Only pile A-1 did not reach by any sounding. Nevertheless, Table 5 shows the pile drilling resistance in the zone of pile tip when installing piles A-1 and A-2. It is clear that the soil under pile A-1 has soil with similar strength as that under pile A-2. In addition, previous studies (Saks et al. 1985) in the vicinity have proven that to a maximum depth of 75 m, the soil strength is increasing.

4.2 Static Axial Pile Load Tests

The piles were tested in accordance with EVS-EN 1997-1:2006 based on EN 1997-1 (2004). The largest load on the test pile was 3600 kN on the Ahtri site and 1200 kN on the Paldiski mnt site. The pile head settlement was between 4.9 and 50.7 mm. The piles were tested 2–4 weeks after installation at the Ahtri site and 2–3 weeks after installation at the Pald-iski mnt site. More exact time is not available. The test piles were tested before the entire pile field was constructed.

There are different techniques to determine the ultimate capacity of a pile from the results of a static load test (Hirany and Kulhawy 1989). These methods for evaluating ultimate pile capacity can be divided into two: offset limit and extrapolation. On the basis of the offset limit method, many researchers have
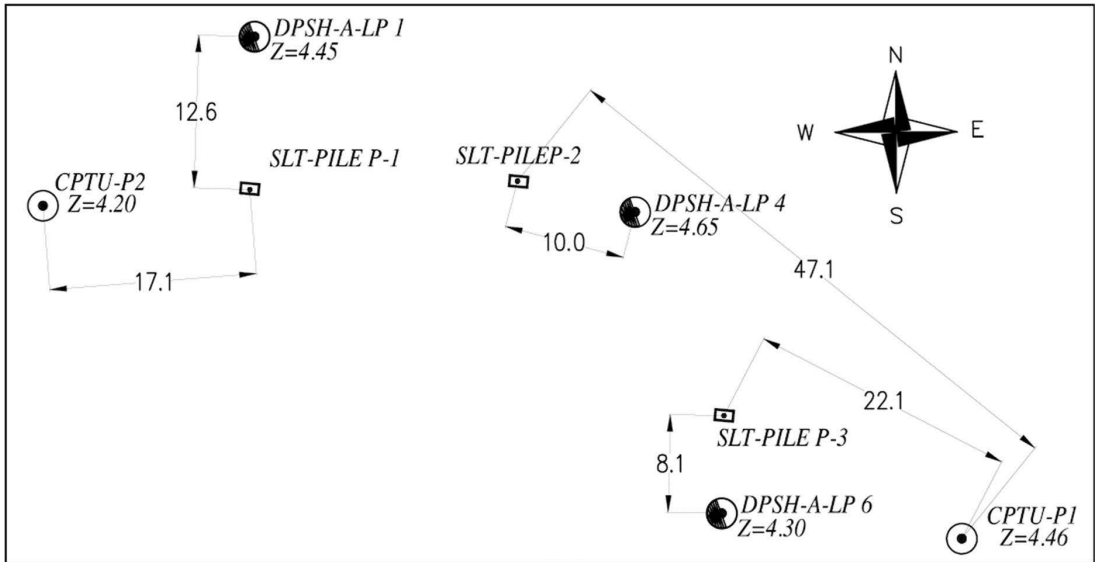
Fig. 3 Site plan of Paldiski mnt 81 with sounding points

Table 3 Statically tested piles

Site	Pile type	Diameter of piles	Number of tested piles	Depth of piles (m)
Ahtri	Fundex	450/560	4	23.2–27.0
Paldiski mnt	Fundex	350/450	3	15.0–15.5

Table 4 Pile case records summary with the measured bearing capacity and maximum settlement from the pile load tests

Pile name	A-1	A-2	A-3	A-4	P-1	P-2	P-3
Pile length (m)	27.0	26.0	23.2	23.5	15.5	15.5	15.0
Max load from pile load test (kN)	3600	3240	3600	2160	1200	1200	1200
Max settlement from pile load test (mm)	4.9	6.2	22.0	50.7	6.3	6.5	15.0
s/B (%)	0.9	1.1	3.9	9.1	1.4	1.4	3.3
Max depth of CPT sounding (m)	20.7	20.33	22.67	22.67	–	–	–
Max depth of CPTu sounding (m)	23.5	20.94	22.98	22.98	18.98	19.82	19.82
Max depth of DPSH-A sounding (m)	23.6	26.0	23.6	23.6	24.41	23.6	22.4
Max q_c reading from CPT (MPa)	15.5	18.5	9.5	9.5	–	–	–
Max q_c reading from CPTu (MPa)	48.9	33.5	22.6	22.6	37.4	33.2	33.2
Max N_{20} reading from DPSH-A	285	467	285	285	123	111	165

suggested that the pile ultimate resistance should take a load corresponding to a settlement that equals 10% of the pile diameter. Eurocode also sets the failure criterion, as the pile shows a settlement equal to 10% of its nominal diameter. This principle is also known as the French criterion, introduced by Vesić (1977).

Since the piles were not loaded to the ultimate capacity, the Chin (Chin 1970) extrapolation method and load-settlement curve were used to estimate the ultimate pile capacity. Based on Kondner's (1963) work, the Chin extrapolation method is well known and widely used in practice (Al-Homoud et al. 2003;

Table 5 Drilling resistance near the pile tip on piles A-1 and A-2

Pile A-1		Pile A-2	
Depth (m)	Resistance (bar)	Depth (m)	Resistance (bar)
22.50	70–110	21.50	70–100
23.00	70–110	22.00	70–100
23.50	70–110	22.50	180–200
24.00	160–180	23.00	180–200
24.50	160–180	23.50	180–200
25.00	220–240	24.00	180–200
25.50	220–240	24.50	220–240
26.00	220–240	25.00	220–240
26.50	220–240	25.50	220–250
27.00	240–260	26.00	220–250

Table 6 Accuracy of determining the settlement of piles A1bis and P3 by the Chin method on the basis of four different settlements

Pile ID	s/B (%)	$Q_{u,\text{Chin }10\%}/Q_{u,\text{SLT}}$	Accuracy ($\pm$%)
A1bis	1.1	0.90	10.0
A1bis	1.4	0.94	6.2
A1bis	3.5	1.03	2.7
A1bis	6.0	1.03	2.6
P3	1.2	1.09	9.3
P3	1.5	1.24	23.9
P3	2.8	1.13	13.3
P3	6.0	0.99	0.7

Basu et al. 2010; Elsamee 2012; Niazi 2014; Camacho et al. 2018). Concurrently, this method allows predicting the ultimate resistance, according to the 10% criteria, even if the pile head settlement does not reach 10% of the pile diameter (Holeyman et al. 1997; Maertens et al. 2003; Borel et al. 2004; De Cock 2009; Basu et al. 2010).

As the maximum settlement of most of the tested piles was less than 10% of the pile diameter, the reliability of the Chin method was examined on the basis of the literature for similar soils and Fundex piles. Two Fundex 380/450 piles in Belgium were analysed. Both piles were tested to at least a settlement equal to 10% of the pile diameter. The first A1bis was tested in Limelette (Maertens et al. 2003). Another, designated P3, was tested in Ghent (Holeyman 2001). The soils of the Ahtri site are more similar to those of the Limelette test site and the soils of the Paldiski mnt to those of the Ghent test site. Thus, the results of pile A1bis should be compared with piles A-1 to A-4 and the results of P3 with piles P-1 to P-3. Comparison of the results extrapolated by the Chin method ($Q_{u,\text{Chin}10\%}$) with the measured values ($Q_{u,\text{SLT}}$) should give an idea of the accuracy of the Chin method for different pile settlements. The accuracy results of the two piles for the four different settlements are given in Table 6. The results show that the reliability of the extrapolation results of the A1bis pile is high even at very small settlement. The results of pile P3 demonstrate that for smaller settlements, the accuracy of the extrapolation results must be taken into account

around 20%. The s/B values in Table 4 show that the most accurate results should be for piles A-3 and P-3. Pile A-4 has the most sizeable settlement at the lowest load compared to piles A-1 to A-3. The results of the A-4 pile should be treated with caution.

In this research, the extrapolation of the Chin method was used to determine the pile load at a settlement equal to 10% of the pile diameter. The results were compared with the pile capacities calculated by different direct methods. In Fig. 4, the load–displacement curve from the pile load test and the hyperbolic curves as a result of the extrapolation of the compressed pile are presented.
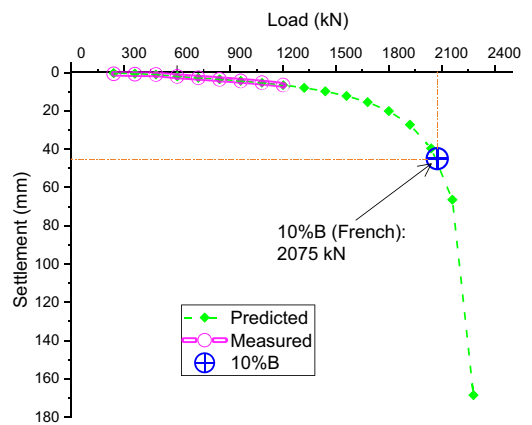

Fig. 4 Load–displacement curve of the pile load test and the extrapolation results for one pile

4.3 CPTu Testing

A total of six CPTu soundings were made at two sites. At the Ahtri site, four CPTu soundings were conducted between the piles in the framework of the supplementary studies in 2019. The minimum distance between the three CPTu sounding points and the centre of piles varied from 1.8 to 2.7 m. The fourth CPTu testing point (CPTu-A3) located more than 5.5 m from the piles was made to compare the other three CPTu tests and previously made CPT tests (see Fig. 2).

At the Paldiski mnt site, two CPTu soundings were conducted near the two opposite sides of the completed building. It was four and a half years after the piles were installed. The distance between the tested piles and CPTu soundings varied between 18 and 20 m at the Paldiski mnt site (Fig. 3). The soundings were at least 3 m deeper from the pile tip.

For CPTu soundings, a lightweight truck with ground anchors was used. In some places, predrilling was carried out because of impenetrable fill in the upper layer. A Nova cone produced by Geotech AB was used. CPT Geotech Nova system meets the standards EN ISO22476-1 and ASTM D-5778 (2000). The probe had a 10 cm^2 base area and 150 cm^2 sleeve surface area. The procedures of the testing concurred with Lunne et al. (1997).

The typical sounding profiles of q_t, f_s, R_f and u_2 for both sites are shown in Figs. 5 and 6. R_f is defined as $f_s/q_t \times 100\%$. The types of soil layers defined via CPTu SBT (Robertson 2010) are shown on the left. The water table was indicated with u_0 (hydrostatic pressure) and u_2 profiles. The soil profile of both objects shows that silty soils predominate. There is a limited amount of clayey soils at both sites. An increase in pore water pressure is an excellent indicator of clay layers. This helps to highlight the presence of thin clay layers, which can be clearly seen from the pore water graph of the Ahtri site at depths lower than 16 m. The thicknesses and location of the layers vary within a few metres between the probing points on the Ahtri site. The variability at the Paldiski mnt site is not significant.

4.4 Previous Soundings

In addition to the CPTu soundings conducted during the research, previous soundings (at the Ahtri site CPT and DPSH-A tests and at the Paldiski mnt site DPSH-A tests) were also included in the analysis. Piezocone tests were performed on a HYSON
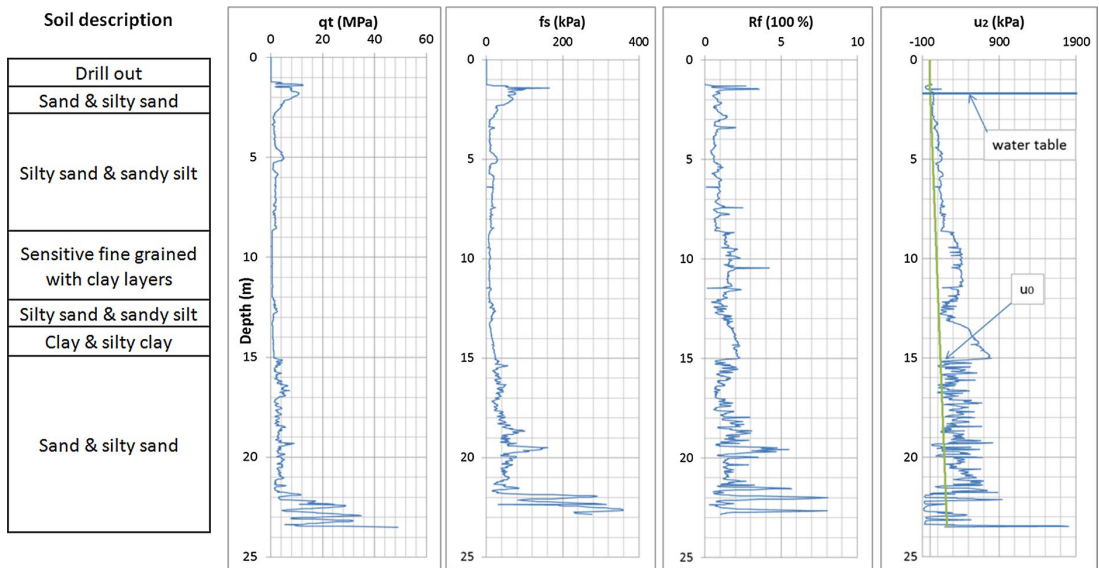

Fig. 5 Results of the piezocone test at the Ahtri site. q_t, cone resistance corrected for the pore pressure effects; f_s, sleeve friction; R_f, friction ratio; u_2, pore pressure
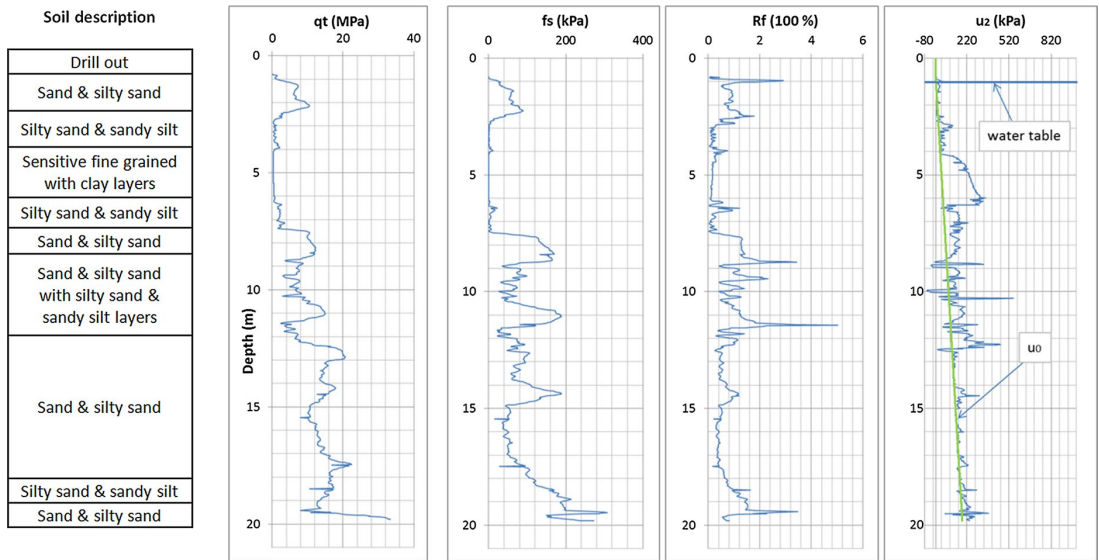
Fig. 6 Results of the piezocone test at the Paldiski mnt site. q_t, cone resistance corrected for pore pressure effects; f_s, sleeve friction; R_f, friction ratio; u_2, pore pressure

device with a 200-kN counterweight. The PAGANI CPTu penetration cone with a 10-cm^2 base area was used. The cone allowed determining the base and side resistance, pore water pressure and cone inclination. Dynamic penetration tests (DPSH-A) were carried out with GEOTECH 504. The weight of the hammer was 63.5 kg, and the weight of the rods was 6 kg. The hammer was lowered from 0.5 m drop height. The cone tip area was 1600 mm^2. The number of blows per 200 mm was measured.

At the Ahtri site, 10 CPT and 13 DPSH-A soundings were conducted nearly 1 year before the piling work. For CPT soundings, CPTu probes were used. The pore pressure was measured only for the dissipation test. Due to the dense subsoil, neither CPT nor DPSH-A could be probed deeper than the pile tip. Beside some piles, the probes did not even reach the depth of the pile tip because of the lack of pushing force. The distance between the tested piles and CPT soundings varied between 3.0 and 4.5 m. At the Paldiski mnt site, six DPSH-A soundings were made 2 weeks before the installation of the testing piles. The soundings were at least 15 times deeper than the pile tip diameter. The distance between the tested piles and DPSH-A soundings varied between 5.8 and 13.0 m. At the Ahtri site, the number of blows

recorded to pass 200 mm was corrected for growing rods weight and thereby diminishing impact energy.

The CPT soundings at the Ahtri site were carried out before the piles were installed, and the CPTu soundings were executed between the piles 5 years later. This raises the question of whether CPTu sounding results between piles differ significantly from CPT data. For this purpose, the closest CPT and CPTu sounding results have been considered side by side, as shown in Figs. 7 and 8.

Most CPT and CPTu cone resistance values are akin. Only the results of CPTu-A2 are significantly different. This sounding point is also closest to the previously installed piles. The installation of the pile has increased the density of the soil. Therefore, the values of cone resistance and sleeve friction have also increased. This must be taken into account in the analysis of the load-bearing capacity of pile A-2 based on CPTu-A2 data.

5 Estimated Versus Measured Ultimate Pile Capacity

The test piles were loaded 2–4 weeks after the installation of the piles. Togliani et al. (2014) mentioned
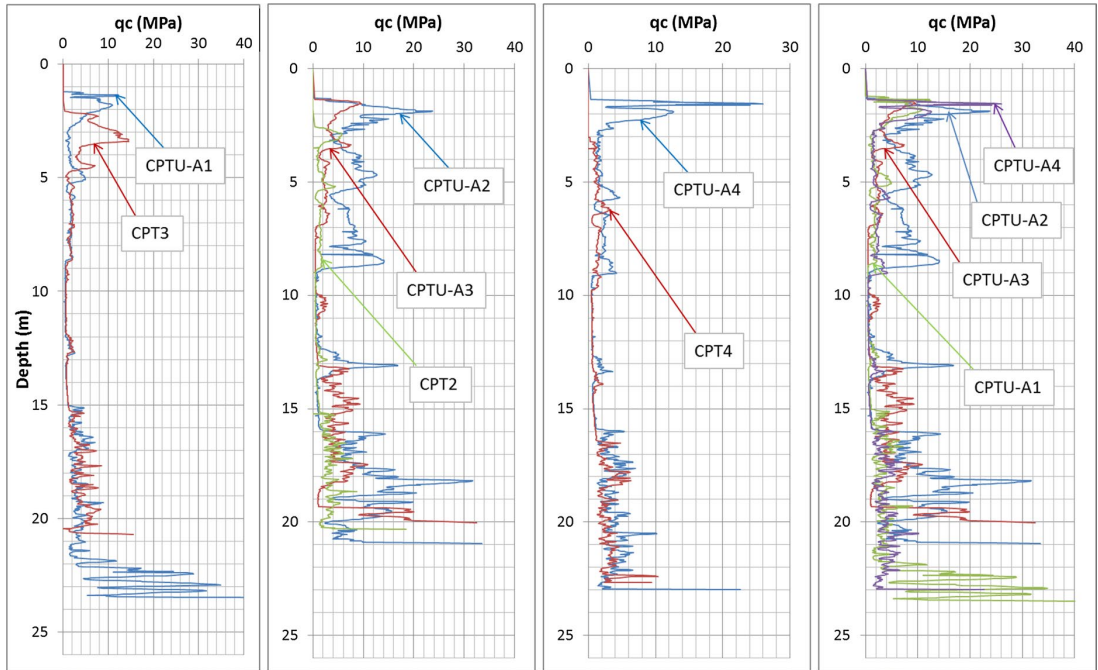
Fig. 7 Results of CPT and CPTu cone resistance values side by side at the Ahtri site. q_c, cone resistance

that piles installed in partly clayey and partly sandy soils would increase their bearing capacity for at least 100 days after the pile had been deployed. In practice, the waiting time used in Estonia is 3 weeks (21 days). Mets (1997) claimed that for soft silts, a 2-week waiting period would be sufficient. In clayey soils, shaft friction increases even after 4 weeks. For pile capacity, this is in favour of the reserve. As the test sites were predominantly silty soils, a similar kind of capacity increase was not expected; therefore, it was estimated that the increase did not significantly affect the pile total load-bearing capacity.

For each of the tested piles, the closest sounding was used to calculate the axial bearing capacity. Five CPT methods, one CPTu method, and six SPT methods were used for the analyses. If the pile calculation method did not provide a maximum value for the pile bottom and lateral friction, a limiting ultimate unit shaft friction of 120 kPa (Poulos 2016) and limiting ultimate end bearing resistance of 15 MPa were used. The Eurocode method results based on CPT data and SPT methods except for the Briaud and Tucker (1988) method at the Ahtri site were most affected. Without

restrictions, these methods would significantly overestimate the pile bearing capacity in the occurrence of very dense subsoils.

If the probing did not reach the depth of the pile tip, the last reading of the probing was used in the analysis. This assumption has a major impact on the analysis based on the CPT result and tends to underestimate the load-bearing capacity of the pile. The analysis based on DPSH-A results is not affected.

The results are summarized in Figs. 9, 10 and 11. The calculation methods with reference to the type of probing test used are shown on the horizontal axis; only the calculation method is presented on the horizontal axis. The vertical axis shows the absolute percentage difference between the predicted and calculated capacities. In addition, the hatched area in the figures indicates 20% variability around the 0 value. The 20% limit is used to assess the accuracy of the different methods. The more the results within ± 20%, the better the method.

The calculations for pile A-2 are based on data from two CPTu points. The aim was to determine whether the results of the probing made between the
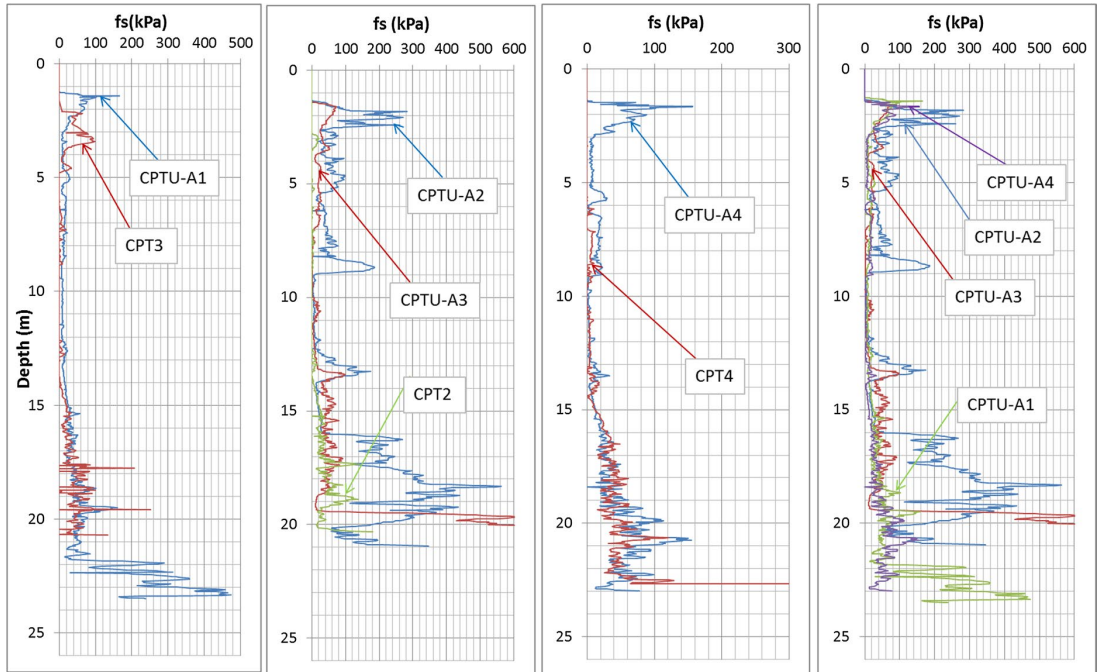
Fig. 8 The results of CPT and CPTu sleeve friction values side by side at the Ahtri site. f_s, sleeve friction

Fig. 9 Comparison of the absolute difference between the measured and predicted capacity for piles at the Ahtri site; +, overestimates; −, underestimates
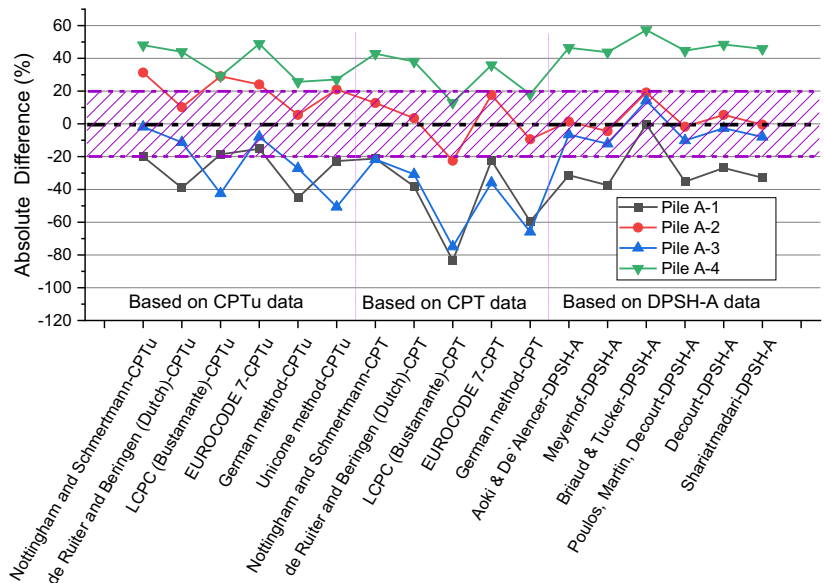
Fig. 10 Comparison of the absolute difference between the measured and predicted capacity for pile A-2 based on CPTu sounding A2 and A3 at the Ahtri site
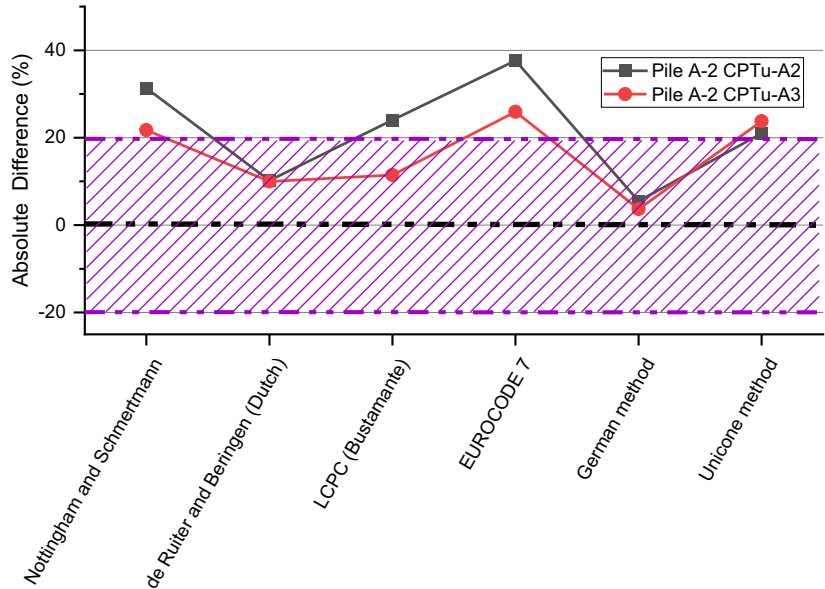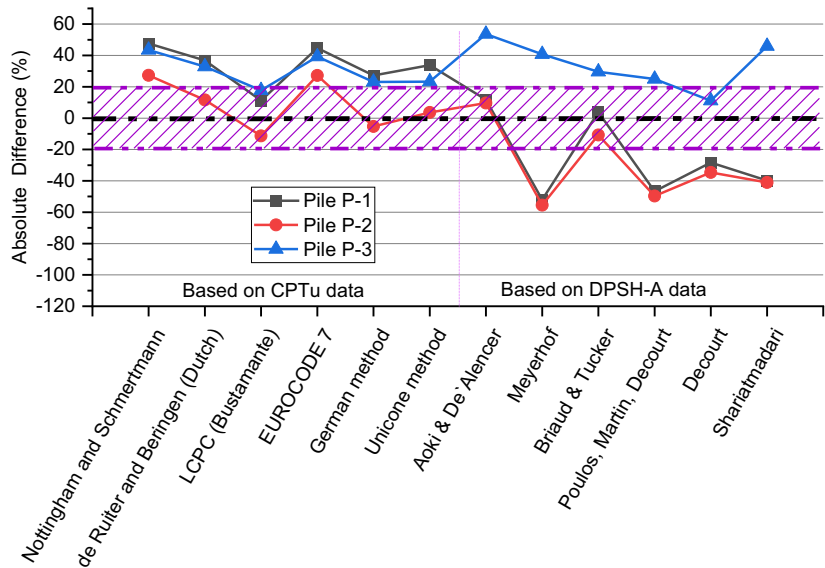

Fig. 11 Comparison of the absolute difference between the measured and predicted capacity for the piles at the Paldiski mnt site; +, overestimates; −, underestimates

piles could be used as a basis for calculating the load-bearing capacity of the pile. Test CPTu-A2 was made between the piles, and the minimum distance from the adjacent pile was 1.8 m. It was also the shortest distance between the survey points and the piles. The investigation point CPTu-A3 was at least 5.5 m from the adjoining pile and 27.7 m from the test pile A-2.

The calculations performed with the five CPT and one CPTu method are compared in Fig. 10. The results based on the data from the two study points are similar. The biggest difference was observed using the Eurocode 7 method (EN 1997–2:2007). Figure 10 shows that this difference is 12%. In addition, it can be clearly seen from Fig. 10 that if the

result of the direct method remained within 20% of the area, it remained there according to both CPTu-A2 and CPTu-A3, with a small difference for the LCPC method. Hereby, the results of the CPTu tests between the existing piles can be used in the study.

Figure 9 shows that the results found on the basis of the CPTu and CPT vary widely between the piles. This can be attributed to the limiting capacity of the cone penetrometers. The greatest variability between the results calculated by the LCPC method is based on CPT data, and it is in the range of 96%. The smallest variability is calculated on the basis of two methods, the Nottingham and Schmertmann (1975, 1978) method and the Eurocode 7 (EN 1997-2: 2007) method, both being within 64%. The minimum and maximum values of the calculations performed with DPSH-A results also vary considerably. Excluding the pile A-4 results, the variability for all methods is within 37%. Based on three piles, the Briaud and Tucker (1988) method gives results within 20% of the measured capacity. Furthermore, the results of all SPT methods fit within the ± 20% range at the Ahtri site.

At the Paldiski mnt site, the variability of CPT-based methods between different piles was significantly smaller than at the Ahtri site, as shown in Fig. 11. The Nottingham and Schmertmann (1975, 1978) method and Eurocode 7 (EN 1997-2: 2007) method clearly overestimated the load-bearing capacity of the pile. Furthermore, none of the calculated values fell within the 20% range. The De Ruiter and Beringen (1979) method and the Unicone method tended to overestimate capacity. The closest results to the measured ones were received by the LCPC method; all the results were also within 20% of the measured capacity. The German (EA-Pfähle 2014) method also gave quite similar results to the outcomes obtained from the pile load test.

The results from the direct SPT methods varied more than the results attained by the CPT methods. The results achieved by the Shariatmadar (2008) method varied the most, and no value fell within the 20% range. The outcomes with the least variability were obtained by the Meyerhof (1976) method. Nevertheless, no result fell within the 20% range, and outcomes overestimated the capacity of the pile. The Briaud and Tucker (1988) method provided the closest results compared to the outcomes of the pile load test. The calculation results of piles P-1 and

P-2 by the Briaud and Tucker (1988) and Aoki and De`Alencer (1975) methods were of considerable accuracy. However, the calculation results of pile P-3 were outside the 20% range by both methods. The method by Aoki and De`Alencer (1975) also tended to overestimate the pile capacity. Both the (Poulos 1989; Martin 1987; Decourt; 1982) method and the Decourt (1995) method predicted that only pile P-3 would be within the 20% range. Furthermore, it can be seen from Fig. 11 that the (Poulos 1989; Martin 1987; Decourt; 1982) method tended to underestimate the capacity of the pile. The results of three CPT, one CPTu, and two SPT methods fit within the 20% ± 20% range at the Paldiski mnt site.

Based on the results of the Ahtri site, it is obvious that if the probing did not even reach the depth of the pile tip, the use of direct methods was restricted. The results of the pile capacity calculations were also of questionable value. At the Ahtri site, dynamic penetration was achieved in deeper layers related to CPTu and CPT soundings. This was reflected in the smaller variability of the results. One possibility in such circumstances would be to investigate further the calculation of the shaft friction capacity from CPTu data. At the same time, DPSH-A data could be utilized to calculate the end bearing capacity of the pile.

Measuring pore water pressure is a useful value in determining the correct shaft friction capacity of the pile. It also provides the possibility to determine the SBT and the interlayer of soils. At the Ahtri site, soft interlayers of clay appeared. If the pile tip remained above such a weak layer, the pile capacity was reduced remarkably.

At the Paldiski mnt site, where the probing reached at least 3.48 m deeper than the pile tip, the calculation results had significantly less variability than at the Ahtri site, excluding piles A-2 and A-3 based on SPT methods. The best results were obtained by the LCPC method. The German method also provided similar pile capacities. Many researchers (Rollins et al. 1999; Abu-Farsakh et al. 2004; Cai et al. 2009; Titi et al. 2010; Pardoski 2010; Hu et al. 2012; Amirmojahedi et al. 2019) have also concluded that the LCPC method shows acceptable performance among CPT-based methods. One reason for this could be the influence zone for the pile utilized in the LCPC method, which is 1.5D below and above the pile tip. The pile zone of influence in silty soils estimated by Yang (2006) covers a reasonably balanced range between

those used in the LCPC method. Moshfeghi and Eslami (2016) highlighted the promising performance of the German method for different piles in different soils. The achievement of the German method in the present work could be explained by the fact that this method offers an empirical relation solely for Fundex piles. Nevertheless, all CPT-based methods outlined in the paper should be used for pile capacity analysis under similar conditions in the future. Mayne and Niazi (2009) find it prudent to use a number of different CPT methods and see how they compare or disagree with each other. They suggest that averaging the methods seems to be warranted in such cases. Determining the local correlation factors helps to increase the accuracy of the direct methods as well. In addition, it would help to understand when to use the upper and lower limits of the unit shaft and toe capacity, for example, utilizing the German method.

Of the SPT methods, the Briaud and Tucker (1988) method is worth highlighting. It proposed remarkably good results at both sites. It was also the only SPT method used that referred to the $s/B = 10\%$ failure criterion. Notable results at both sites are a clear indication that DPSH-A data can be used with SPT-based direct methods under similar conditions. In the future, a comparative analysis of the piles, together with the results of the pile load tests, should also be performed adopting SPT direct methods.

6 Summary

The static pile load test is the most accurate method for determining the static load-bearing capacity of a pile. Due to their high cost, such tests are rarely performed in Estonia. On certain occasions when such tests are carried out, the piles are loaded no more than 3 weeks after the installation of the test piles. The piles are not tested for failure but only up to 120% of the expected design load. In practice, soundings are needed to design how many piles are needed and what their size and depth would be. Static loading tests are used after piling to check how reliable the design has been. A large number of static pile load tests in parallel with probing allow the calculation of the bearing capacity of a pile based only on the results of the penetration test. The probing data alone can be used to find the pile bearing capacity in the future under similar conditions. CPT and CPTu sounding are fast and

reliable methods to define soil type and its properties for pile capacity estimations. Several previous studies (Briaud et al. 1988; Eslami et al. 1995; Eslami and Fellenius 1997; Rollins et al. 1999; Abu-Farsakh et al. 2004; Cai et al. 2009; Mayne et al. 2009; Niazi et al. 2010; Pardoski 2010; Reuter 2010; Titi et al. 2010; Cai et al. 2011; Eslami et al. 2011; Hu et al. 2012; Flynn et al. 2014; Moshfeghi and Eslami 2016; Amir-mojahedi et al. 2019) have clearly demonstrated that direct methods based on CPT or CPTu data provide reliable results in different soils on different piles. However, in denser soils, the penetrometer must have a sufficient capacity of up to 500 kN (Eslami and Fellenius 1997). As CPTs with such a high capacity are seldom available, one alternative could be to apply the DPSH-A system. DPSH-A penetration is fast and inexpensive, which also penetrates denser soil layers. One possible approach to using the results of the DPSH-A test to identify the load-bearing capacity of a pile is to use SPT-based direct methods. When using the results received with this device, it must be kept in mind that the pore pressure and cohesion of the soil can significantly affect the results.

The load-bearing capacities of the four piles differ significantly at the Ahtri site, as shown in Fig. 12. However, if the result of pile A-4 is excluded, all SPT methods show results with relatively little variability (19–33%). The variability of the CPT and CPTu methods is significantly larger than that of the SPT methods. The main reason for this is the fact that CPT soundings did not penetrate the pile tip level. At the Paldiksi mnt site, the measured load-bearing capacities of piles are similar (see Fig. 13). Comparing the measured and calculated load-bearing capacities of the piles in Fig. 13, the LCPC and Briuad and Tucker (1988) methods stand out clearly. The variability of these two methods is considerably less than that of the other methods.

The results of the LCPC (LCPC-A and LCPC-P) and B&T (B&T-A and B&T-P) methods have been statistically compared in Table 7 with the results of the pile load test results (SLT-A and SLT-P). B&T is an abbreviation of the Briaud & Tucker method. The letter A indicates the Ahtri site, and the letter P indicates the Paldiski mnt site. The mean value ($\bar{x}$), standard deviation (SDx) and coefficient of variation (COVx) were calculated. The results of pile A-4 were not included in the analysis. The percentage accuracy was defined between the pile load test

Fig. 12 Comparison of the measured and predicted capacity for piles at the Ahtri site
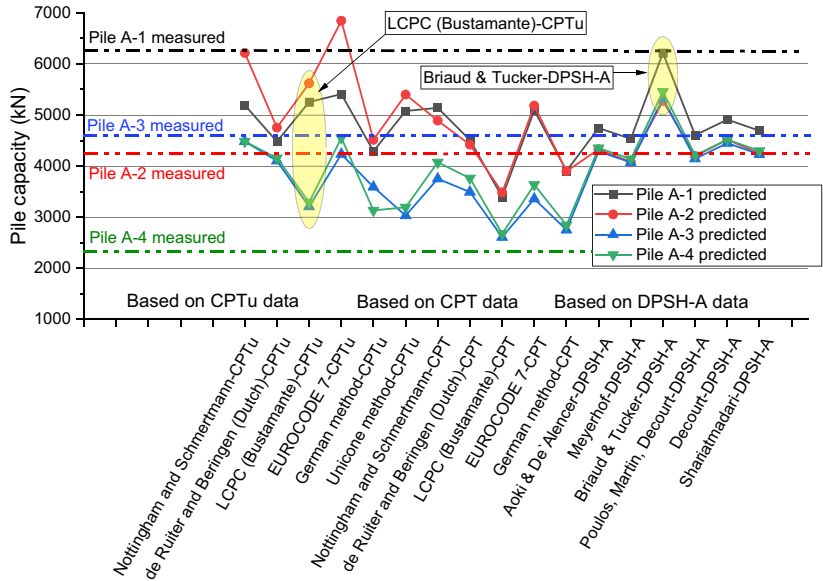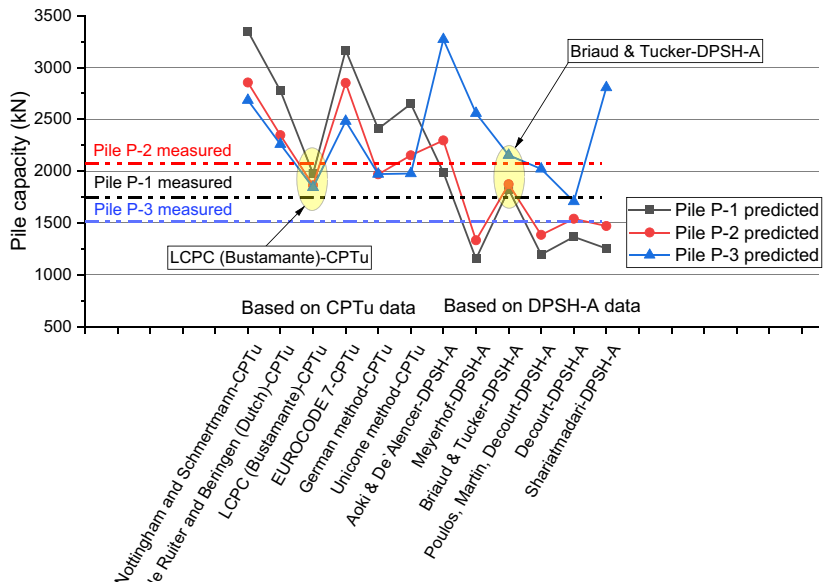

Fig. 13 Comparison of the measured and predicted capacity for piles at the Padiski mnt site

and the calculated mean value. A minus percentage value indicates that the calculation underestimates the measured result. On the contrary, a plus sign indicates that the calculations overestimate the measured values.

Table 7 shows that the coefficient of variation is in the range 0.09–0.28% in the Ahtri site and in the range 0.04–0.16% in the Paldiski mnt site. The accuracy of the calculated values is in the range of 6.0–10.4%. The LCPC method underestimates the load-bearing capacity of a pile at the Ahtri site by 7.0%. In all other cases, the calculation overestimates the load-bearing capacity of the pile.

Table 7 Determination of pile bearing capacity accuracy based on LCPC and Briaud and Tucker (1988) methods

Variable	$\bar{x}$(kN)	SDx (kN)	COVx	Measured $\bar{x}$/predicted $\bar{x}$	Accuracy ($\pm\%$)
SLT-A	5021	1058	0.21	1	0
LCPC-A	4692	1300	0.28	1.070	-7.0
B&T-A	5603	529	0.09	0.896	10.4
SLT-P	1782	280	0.16	1	0
LCPC-P	1895	72	0.04	0.940	6.0
B&T-P	1951	178	0.09	0.913	8.7

The pile tip and shaft capacities derived by LCPC and Briaud and Tucker (1988) methods for all seven piles are shown in Fig. 14. The vertical axis of the figure also shows the installation depth of the piles. The piles at the Ahtri site were installed in a deeper and stronger subsoil than at the Paldiski mnt site. The load-bearing capacity of the pile base compared to the whole pile capacity at the Ahtri site is very similar by both LCPC and Briaud and Tucker (1988) methods. The values found by the LCPC method are in the range of 58–69% and by the Briaud and Tucker (1988) method in the range of 58–68%. At the Paldiski mnt site, the load-bearing capacity of the pile base compared to the whole pile capacity is higher by the Briaud and Tucker (1988) method than by the LCPC method. It is in the range of 60–61% for the

Briaud and Tucker (1988) method and 48–53% for the LCPC method.

This study focused on Fundex-type piles. It must be borne in mind that such piles have a pile tip with overlap. As a result, when installing the pile, the soil starts loosening in the shaft area (Kemfert et al. 2010). In contrast, the screw-shaped shaft of the pile increases the load-bearing capacity of the pile compared to the smooth pile shaft (Basu et al. 2010). Therefore, pile calculation methods do not always estimate the actual load-bearing capacity of such piles with the desired accuracy (Kemfert et al. 2010). Another issue is that Eq. (1) includes the idea that base and shaft resistance do not affect each other and the superposition principle is valid. In reality, these two resistances depend on each other; how much there is a correlation depends on soil conditions.

7 Limitations of this Study

- Extrapolation was used to determine the ultimate pile capacity from the static pile load test. Offset limit- or extrapolation-based methods are most common. However, the method for evaluating ultimate pile capacity can affect the results.
- The piles studied in the research are 15–26 m long, and the resistance of the shaft is a significant part of the load-bearing capacity of the pile.
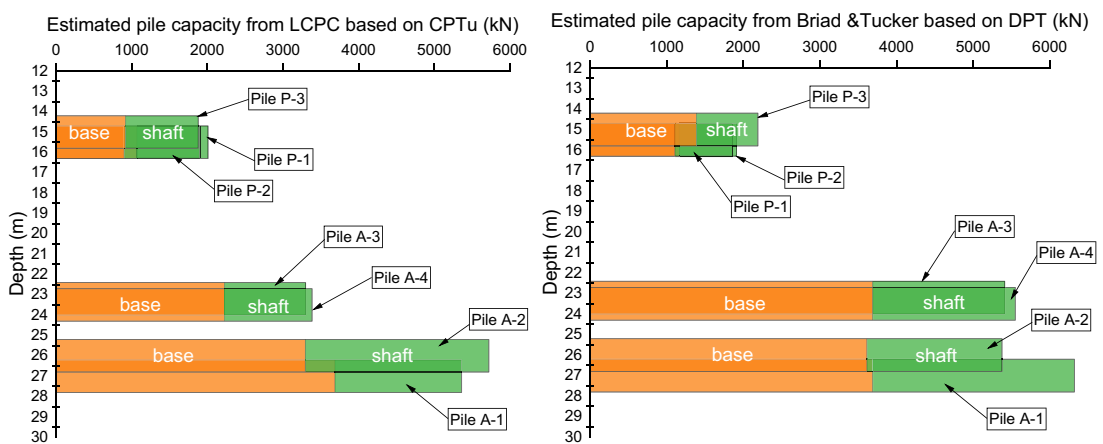

Fig. 14 Comparison of the pile tip and shaft resistance proportions based on LCPC and Briaud and Tucker (1988) methods for all piles

- Both test sites had very high groundwater levels, approximately 1 m below the ground level. It could affect sounding results and the time of the pile bearing capacity.
- These results may be inaccurate for other pile and soil types.

8 Conclusion

The study compared the outcome of five CPT, one CPTu and six SPT-based direct methods with the results of seven pile load tests from two sites. A pile failure criterion of $s/B = 10\%$ was used by extrapolating the pile load test results. To compare the methods, the absolute percentage difference between the results calculated by direct methods and those obtained as a result of the pile load test was determined.

One of the main objectives of this work was to identify suitable CPT-based methods to predict the load-bearing capacity of piles in silty soils. In addition, the possibility of applying DPSH-A readings in SPT-based methods appraising pile bearing capacity was investigated. Data with two different densities of subsoil were used as a basis for analysis. Limits of 20% were used to identify the best method. Statistically, the percentage of accuracy was found for the LCPC and Briaud and Tucker (1988) methods.

The research clearly showed that if the soundings did not reach at least the depth of the pile tip, the calculation outcome often underestimated the pile capacity. The calculated load-bearing capacity results of the piles varied up to 96%. The reason is that the soundings have ended into stiff layers, which tend to get stiffer by depth, increasing the pile capacity. When the CPTu or DPSH-A test reached several metres deeper than the pile tip, the variability of the calculated results was significantly reduced. Of the CPT-based direct methods, the LCPC method demonstrated the best results. This method underestimated the load-bearing capacity of the piles on average at the Ahtri site by 7.0% and overestimated at the Paldiski mnt site by 6.0%. The German method also provided similar pile capacities. Nevertheless, the CPTu method used in the study should be applied comparatively in silty soils with Fundex piles in the future. Of the SPT methods, the Briaud and Tucker (1988) method deserves special attention because it provided remarkably good results on both sites studied. This method overestimated the load-bearing capacity of the piles on average at the Ahtri site by 10.4% and at the Paldiski mnt site by 8.7%. In the attendance of dense subsoil, other SPT methods demonstrated similar results. It can be clearly seen that in the presence of dense subsoils in silty soils, the results of DPT can be of considerable use in predicting the load-bearing capacity of the pile. Therefore, the calculation of the pile capacity based on DPSH-A data using SPT-based direct methods deserves further investigation with different piles for different soils.

Data availability Enquiries about data availability should be directed to the authors.

Declarations

Conflict of interest The authors have not disclosed any competing interests.

References

Abu-Farsakh MY, Titi HH (2004) Assessment of direct cone penetration test methods for predicting the ultimate capacity of friction driven piles. J Geotechn Geoenviron Eng 130(9):935–944

Al-Homoud AS, Fouad T, Mokhtar A (2003) Comparison between measured and predicted values of axial end bearing and skin capacity of piles bored in cohesionless soils in the Arabian Gulf Region. Geotech Geol Eng 21:47–62. https://doi.org/10.1023/A:1022932630538

Amirmojahedi M, Abu-Farsakh M (2019) Evaluation of direct pile-CPT methods for estimating the ultimate capacity of driven piles. In: 8th international conference on case histories in geotechnical engineering, Philadelphia, Pennsylvania, pp 167–177

Aoki N, De Alencar D (1975) An approximate method to estimate the bearing capacity of piles. Proc Fifth Pan-Am Conf Soil Mech Found Eng b. Aires 1:367–376

Arbeiter R (1962) Tallinna ehitusgeoloogilise rajoniseerimise visand. Eesti Ehitusgeoloogiline Kogumik I, Tallinn, pp 23–34

Ardalan H, Eslami A, Nariman-Zahed N (2009) Piles shaft capacity from CPT and CPTu data by polynomial neural networks and genetic algorithms. Comput Geotech 36:616–625

American Society for Testing & Materials (2000) ASTM book of standards, vol. 4, Section 08 and 09. Construction materials. Soils Rocks, Philadelphia, PA

Bandini P, Salgado R (1998) Methods of pile design based on CPT and SPT results. In: Geotechnical site characterization conference, Blekma, Rotterdam, pp 936–942

Basu P, Prezzi M, Basu D (2010) Drilled displacement piles: current practice and design. Deep Found Inst J 4(1):3–20

Benali A, Nechnech A, Bouafia A (2013) Bored pile capacity by direct SPT methods applied to 40 case histories. Special issue for international congress on material & structural stability, Rabat Morocco. Civil Environ Res 5:118–122

Bergdahl U, Ottosson E (1988) Soil characteristics from penetration test results: a comparison between variuos investigation methods in non cohesive soils. In: Proceedings, First ineternational symposium on penetration testing, ISOPT-1, Orlando, Florida, Vol 1, pp 399–405

Borel S, Bustamante M, Gianeselli L (2004) An appraisal of the Chin method based on 50 instrumented pile tests. Ground Eng 37(1):22–26

Briaud JL, Tucker LM (1988) Measured and predicted axial response of 98 piles. J Geotechn Eng 114(9):984–1001

Bustamante M, Gianeselli L (1982) Pile bearing capacity predictions by means of static penetrometer CPT. In: Proceeding of 2nd European symposium on penetration testing (ESOPT-II), Amsterdam, pp 493–500

Bustamante M, Frank R (1997) Design of axially loaded piles: French practice. In: Design of axially loaded piles—European practice, proceeding of the ERTC3 seminar, Brussels, Belguim, Balkema, Rotterdam, The Netherlands, pp 161–175

Cai G, Liu S, Tong L, Du G (2009) Assessment of direct CPT and CPTu methods for predicting the ultimate bearing capacity of single piles. Eng Geol 104(1–2):211–222

Cai G, Liu S, Puppala AJ (2011) Evaluation of pile bearing capacity from piezocone penetration test data in soft Jiangsu Quaternary clay deposits. Mar Georesour Geotechnol 29(3):177–201

Cai G, Liu S, Puppala AJ (2012) Reliability assessment of CPTu-based pile capacity predictions in soft clay deposits. Eng Geol 141–142:84–91

Camacho MA, Meija J, Camacho CB, Heredia W, Salinas (2018) Ultimate capacity of drilled shaft from CPTu test and static load test. In: Proceedings of the 4th international symposium on cone penetration testing (CPT'18), 21–22 June, 2018, Delft, The Netherlands. Cone Penetration Testing 2018, pp 193–198

Chin FK (1970) Estimation of the ultimate load of piles from test not carried to failure. In: Proceeding of the second Southeast Asia conference on soil engineering. Singapure, pp 81–90

Czado B, Pietras JS (2012) Comparison of the cone penetration resistance obtained in static and dynamic field tests. AGH J Min Geoeng 36(1):97–105

De Cock FA (2009) Sense and sensitivity of pile load-deformation behavior. In: Van Impe (ed) Deep foundation on bored and auger piles. Taylor & Frances Group, London, pp 23–44

De Ruiter J, Beringen FL (1979) Pile foundation for large North Sea structures. Mar Geotechnol 3(3):267–314

Decourt L (1982) Prediction of the bearing capacity of piles based exclusively on N values of the SPT. In: Proceedings of ESOPTZ, Amsterdam 1, pp 29–34

Decourt L (1995) Prediction of load-settlement relationships for foundations on the basis of the SPT-T. In: Ciclo de conferencias internationale, leonardo Zeevaert, UNAM, pp 85–104

EA-Pfähle (2014) Recommendations on piling (EA-Pfähle). Ed by German Geotechnical Society, DGGT. Ernst & Sohn, Berlin

Elsamee W (2012) Evaluation of the ultimate capacity of friction piles. Engineering 4(11):778–789

EN ISO 22476-3 (2005) Geotechnical investigation and testing: field testing—part 2: dynamic probing. International organization for standardization, Geneva

EN 1997-1 (2004) Eurocode 7: geotechnical design—part 1: general rules, brussels, Belgium, p 171

EN 1997-2 (2007) Eurocode 7 geotechnical design: part 2—ground investigation and testing, Brussels, Belgium, p 199

Eslami A, Fellenius BH (1995) Toe bearing capacity of piles from cone penetration test (CPT) data. In: Proceedings of the international symposium on cone penetration testing, C P T'95, Linkoping, Sweden, Swedish Geotechnical Institute, SGI, Report 3:95, Vol 2, pp 453–460

Eslami A, Fellenius BH (1996) Pile shaft capacity determined by piezocone data. In: Proceeding of the 49th Canadian geotechnical conference, St. John`s Newfoundland, September 23–25, Vol 2, pp 859 –867

Eslami A, Aflaki E, Hosseini B (2011) Evaluating CPT and CPTu Based pile bearing capacity estimation methods using urmiyeh lake causeway piling records. Sci Iran 18(5):1009–1019

Eslami A (1996) Bearing capacity of piles from cone penetrometer test data. Ph. D. Thesis, University of Ottawa, Deparment of Civil Engineering, p 516

Eslami A, Fellenius BH (1997) Pile capacity by direct CPT and CPTU methods applied to 102 case histories. Canadian Geotechnical J 34(6):886–904

Estonian Land Board, 202017.04. Map applications https://geoportaal.maaamet.ee/est/Kaardirakendused-p2.html

Fellenius BH, Eslami A (2000) Soil profile interpreted from CPTu data. In: Balasubramaniam AS, Bergado DT, Der Gyey L, Seah TH, Miura K, Phien Wej N, Nutalaya P (Ed) Proceedings of year 2000 geotechnics conference, Southeast Asian geotechnical society, Asian Institute of Technology, Bankok, Thailand, Vol 1, pp 163–171

Felleniu BH (2020) Excerpt from chapter 7 of the red book electronic edition: direct methods for estmating pile capacity, in Background to UniCone http://www.fellenius.net. Accessed 13 Jan 2020

Flynn KN, McCabe BA, Egan D (2014) Driven cast-in-situ piles in granular soil: applicability of CPT methods for

pile capacity. In: Proceedings of the 3rd international symposium on cone penetration testing (CPT'14), Las Vegas, pp 1–8

Gadeikis S, Žaržojus G, Urbaitis D (2010) Comparing CPT and DPSH in lithuanian soils, 2nd international symposium on cone penetration testing, Huntington Beach. Vol 2&3: Technical Papers, Session 3: Applications, pp 3–22

Hirany A, Kulhawy FH (1989) Interpretation of load tests on drilled shafts: axial compression. In: Foundation engineering: current principles and practices, Vol 2 (GSP 22), ASCE, Reston/Virginia, pp 1132–1149

Holeyman AE, Bauduin C, Bottiau M, Debacker P, De Cock F, Dupont E, Hilde JL, Legrand C, Huybrechts N, Menge PP, Miller J, Simon G (1997) Design of axially loaded piles: Belgian practice. Design of axially loaded piles European practice. pp 57–82

Holeyman AE (2001) Screw piles: installation and design in stiff clay, Swets & Zeitlinger, Lisse, ISBN 90 5809 192 9, p 117

Hu Z, McVay M, Bloomquist D, Horhota D, Lai P (2012) New ultimate pile capacity prediction method based on cone penetration test (CPT). Can Geotech J 49(8):961–967

Jardine RJ, Zhu BT, Foray P, Yang ZX (2013) Measurement of stresses around closed-ended displacement piles in sand. Géotechnique 63(1):1–17

Karimpour-Fard M, Eslami A (2013) Estimation of vertical bearing capacity of piles using the results CPT and SPT tests. In: Geotechnical and geophysical site characterization vol 4, ed Coutinho and Mayne Taylor & Francis Group, London, pp 1055–1059

Kempfert H-G, Becker P (2010) Axial pile resistance of different pile types based on empirical values. In: Proceeding of Geo-Shanghai 2010 deep foundation and geotechnical in situ testing (GSP 205), ASCE, Reston, pp 149–154

Kondner RL (1963) Hyperbolic stress-strain response: cohesive soils. J Soil Mech Found Div ASCE 89(4):241–242

Lunne T, Robertson PK, Powell JJM (1997) Cone penetration testing in geotechnical practice. Blackie Academic EF Spon/Routledge Publishers, p 312

Maertens J, Huybrechts N (2003) Belgian screw pile technology: design and recent developments. Swets & Zeitlinger, Lisse, p 191

Martin RE, Seli JJ, Powell GW, Bertoulin M (1987) Concrete pile design in Tidewater, Virginia. J Geotech Eng Am Sot Civ Eng 113(6):568–585

Massarsch KR (2014) Cone penetration testing: a historic perspective. In: Proceedings CPT'14. Las Vegas, pp 97–134

Mayne PW, Niazi FS (2009) Evaluating axial elastic pile response from cone penetration tests (The 2009 Michael O' Neill Lecture). J Deep Found Inst 3(1):3–12

Mayne PW (2007) Cone penetration testing: a synthesis of highway practice. NCHRP Synthesis 368, Transportation Research Board, Washington, p 117

Mets M, Leppik V (2016) Pile foundations in Estonia. Design of piles in Europe: how did Eurocode 7 change daily practice? International symposium 28 and 29 April 2016 Leuven, Belgium. pp 101–116

Mets M (1997) The bearing capacity of a single pile: experience in Estonia. In: Design of axially loaded piles European practice. pp 115–132

Meyerhof GG (1956) Penetration tests and bearing capacity of cohesionless soils. J Geotechn Eng ASCE 82(SM1):1–12

Meyerhof GG (1976) Bearing capacity and settlement of pile foundations. J Geotech Eng ASCE 102(GT3):195–228

Moshfeghi S, Eslami A (2016) Study on pile ultimate capacity criteria and CPT based direct methods. Int J of Geotechnical Eng 12(1):28–39

Niazi FS, Mayne PW, Woeller DJ (2010) Case history of axial pile capacity and load-settlement response by SCPTu. In: 2nd International symposium on cone penetration testing, Huntington Beach, pp 9–16

Niazi FS, Mayne PW (2013) Cone penetration test based direct methods for evaluating static axial capacity of single piles: a state-of-the-art review. Geot Geol Eng 31(4):979–1009

Niazi FS, Mayne PW (2016) CPTu-based enhanced UniCone method for pile capacity. Eng Geol 212:21–34

Niazi FS (2014) Static axial pile foundation response using seismic piezocone data. PhD Thesis, School of Civil and Environment Engineering, Georgia Institute of Technology, Atlanta

Nottingham LC (1975) Use of quasi-static friction cone penetrometer data to predict load capacity of displacement piles. PhD Thesis, University of Florida

Pardoski KV (2010) Derivation of CFA pile capacity in a silty clay soil using CPTu. In: 2nd International symposium on cone penetration testing, Huntington Beach, Vol 2&3: Technical Papers, Session 3: Applications, pp 307–314

Poulos HG (1989) Pile behaviour-theory and application. Geotechnique 39(3):365–415

Poulos HG (2016) Tall building foundations: design methods and applications. Innov Infrastruct Solut 1:10. https://doi.org/10.1007/s41062-016-0010-2

Reuter GR (2010) Pile capacity prediction in minnesota soils using direct CPT and CPTu methods. In: Proceedings of the 2nd international symposium on cone penetration testing (CPT'10). Huntington Beach, Omnipress

Robertson PK (2010) Soil behaviour type from the CPT: an update. In: 2nd international symposium on cone penetration testing, CPT'10, Huntington Beach. www.cpt10.com

Rollins KM, Miller NP, Hemenway D (1999) Evaluation of pile capacity prediction methods based on cone penetration testing using results from I-15 load tests. Transp Res Rec 1675(1):40–50. https://doi.org/10.3141/1675-06

Saks M, Smirnov L (1985) Tallinna kiirtramm, Eesti Ehitusgeoloogia Fond, 2452X/2952E

Schmertmann JH (1978) Guidlines for cone penetration test, performance and design. U.S. Department of Transportation, Washington, Report No. FHW A-TS-78-209, p 145

Shariatmadari N, Eslami A, Karimpour-Fard M (2008) Bearing capacity of driven piles in sands from SPT–applied to 60 case histories. Iran J SciTechnol 32:125–140

Shooshpasha I, Hasanzadeh A, Taghavi A (2013) Prediction of the axial bearing capacity of piles by SPT-based and numerical design methods. Int J GEOMATE 4(2):560–564

Titi H, Abu-Farsakh M (2010) Evaluation of bearing capacity of driven piles from CPT data and development of design program. the art of foundation engineering practice. Geotechn Spec Publ 198:670–686

Togliani G, Reuter GR (2014) CPT/CPTu pile capacity prediction methods: question time. In: Proceedings CPT'14. Las Vegas, pp 993–1002

Vesić AS (1977) Design of pile foundations. In: NCHRP synthesis of highway practice 42, transportation research board, National Research Council, Washington, p 68

Van Baars S, Rica S, De Nijs GA, De Nijs GJJ, Riemens HJ (2018) Dutch field tests validating the bearing capacity of fundex piles proceedings of CPT`18, In: International symposium on cone penetration testing, CRC Press, Leiden, pp 101–107

Yang J (2006) Influence zone for end bearing of piles in sand. J Geotech Geoenviron Eng 132(9):1229–1237

Žaržojus G (2010) Summary of doctoral thesis_analysis of the results and it influence factors of dynamic probing test and interrelation with cone penetration test data in Lithuanian soils. Vilnius, p 31

Publication 2

Leetsaar, Lehar; Korkiala-Tanttu, Leena. Deterministic and Probabilistic Analyses of the Bearing Capacity of Screw Cast in Situ Displacement Piles in Silty Soils as Measured by CPT and SDT. *The Baltic Journal of Road and Bridge Engineering***, 2023; 10.7250/bjrbe.2023-18.600.**

DETERMINISTIC AND PROBABILISTIC ANALYSES OF THE BEARING CAPACITY OF SCREW CAST IN SITU DISPLACEMENT PILES IN SILTY SOILS AS MEASURED BY CPT AND SDT

LEHAR LEETSAAR[1,2,3*], LEENA KORKIALA TANTTU[1]

[1]*Department of Civil and Structural Engineering,
Aalto University, Espoo, Finland*

[2]*Tallinn University of Technology Tartu College, Tartu, Estonia*

[3]*Department of Civil Engineering and Architecture,
Tallinn University of Technology, Tallinn, Estonia*

Abstract. The bearing capacity of screw cast in situ displacement piles is mostly unexplored. There is also insufficient research on piles in silty soils. Therefore, five cone penetration tests (CPT) and one piezocone penetration test (CPTu) using direct methods were utilised to determine the load-bearing capacity of four displacement piles in Estonia. In addition to the CPT sounding data, static-dynamic test (SDT) results were used to analyse the load-beating capacity of the piles. Both deterministic and probabilistic methods were used in the analysis. Characteristic values as a 95% reliable mean and 5% fractile values for sounding parameters, according to the Eurocode 7, were included. Additionally, Monte Carlo simulation was included in the reliability-based design (RBD). The bearing

* Corresponding author. E-mail: lehar.leetsaar@taltech.ee

Lehar LEETSAAR (ORCID ID 0000-0002-0621-7951)
Leena Korkiala TANTTU (ORCID ID 0000-0003-0894-7218)

capacities of screw cast in situ displacement piles in silty soils, here based on the CPT and SDT sounding data, were similar. The adaptation of SDT results for the CPT direct methods for pile load-bearing capacity analysis certainly deserves attention and further investigation. For both sounding types, the Eurocode 7 method provided the best results for all piles. The results of pile-bearing capacities in the absolute difference varied within ±11% between the average, RBD and characteristic values.

Keywords: bearing capacity of pile, cone penetration test (CPT), Monte Carlo simulation, pile, static-dynamic probing test (SDT), static load test.

Introduction

In the Tallinn area, geological conditions vary substantially. There are areas where, on average, limestone hard stratum is at a depth of 1 m. On the other hand, there are areas where the hard stratum is cut by a complex system of several ancient valleys that are buried by dense fluvioglacial sands and soft limnologlacial and marine clayey sediments, which are often tens of meters thick (Arbeiter, 1962; Map applications of the Estonian Land Board, 2020). The use of piles under buildings in these conditions is often required. Bored piles and displacement piles are the most frequently used pile types in Estonia (Mets & Leppik, 2016). As a result of the diversity of soil types and pile installation methods, it is generally complicated to anticipate the vertical bearing capacity of the pile. The static axial compression resistance of a single pile (R_c) is calculated as the sum of the pile base resistance (R_b) and shaft resistance (R_s); this is done by implementing the following formula (EN 1997-2:2007, 2007):

$$R_c = R_b + R_s = q_b \cdot A_b + \sum_{i=1}^{n} q_{s,i} \cdot A_{s,i}. \tag{1}$$

The pile base capacity (R_b) is found by multiplying the unit end bearing or base resistance (q_b) by the pile toe area (A_b). The shaft friction capacity (R_s) is calculated as the sum of the product of the unit shaft friction ($q_{s,i}$) and the outer pile shaft area ($A_{s,i}$) for each soil layer. The static pile load test is the most accurate method for defining pile capacity after installation, which results in a load–settlement relation. Because of its high cost, the static loading test is often not used in the early phases of construction planning or in small piling sites.

Soil properties are often defined from the in situ sounding resistance. Simultaneously, pile-bearing capacity calculation methods based on the results of in situ tests, which are informative and useful method, are applied more regularly nowadays (Eslami & Fellenius, 1997; Cai et al., 2012; Moshfeghi & Eslami, 2016). The cone penetrometer test (CPT) is

Lehar Leetsaar,
Leena Korkiala Tanttu

Deterministic
and Probabilistic
Analyses
of the Bearing
Capacity of Screw
Cast in Situ
Displacement
Piles in Silty Soils
as Measured by CPT
and SDT

one of the most generally implemented methods for pile-bearing capacity analysis (Niazi & Mayne, 2013). In addition, there are methods that utilise all readings of piezocone test (CPTu) (Eslami & Fellenius, 1997).

In Estonia, the most popular sounding type is the dynamic probing– super heavy test (DPSH-A). Some investigation companies have also actively adopted the static-dynamic probing test (SDT). Various variants of this method are widely used in the Nordic countries. In fine-grained soils or below groundwater level, DPSH-A may lead to erroneous results (Gadeikis et al., 2010; Žaržojus, 2010). CPT has been used in Estonia in a small number of investigations. CPT provides continuous, repeatable and reliable data. However, in some cases, anchoring or a larger reaction mass is needed to reach deeper layers when using CPT. Comparatively, the SDT method pushes the probe until upper anchoring resistance is reached. After that, the denser layers penetrate with dynamic blows. If there is a weaker layer under the denser layer and the anchoring is sufficient, probing can be continued by pushing the probe. This could be a good alternative in fine-grained soils, in which the CPT method cannot penetrate to the required depth. Passing through deep soils is essential for calculating the base bearing capacity of piles.

Because the cone penetrometer can be considered a mini-pile foundation (Bandini & Salgado, 1998; Mayne, 2007; Jardine et al., 2013), this has led to the evolution of a significant number of CPT-based pile-bearing capacity calculation methods (e.g., Nottingham, 1975; Schmertmann, 1978; de Kuiter & Beringen, 1979; Bustamante & Gianeselli, 1982; Eslami & Fellenius, 1997; Kempfert & Becker, 2010). In the present research, direct methods were used to find the load-bearing capacity of piles. As the SDT method does not have direct methods for defining the load-bearing capacity of a pile, CPT-based direct methods have been adjusted for SDT by converting sounding resistance to cone tip resistance (q_c).

The current study focuses on finding the load-bearing capacity of four piles from the CPT and SDT results in silty soils for screw cast in situ displacement piles from the Soodi site in Tallinn. One CPTu-based and five CPT-based calculation methods were used and analysed. The results were compared with a static pile load test with French criterion $s/B = 10\%$. In the criterion, s denotes the settlement of the pile head, while B denotes the diameter of the pile tip.

As the reliability and economic requirements of the design become increasingly important and related to the new generation of design codes around the world, the reliability-based design (RBD) method was also used in the analysis of the load-bearing capacity of the piles based on the LCPC method. Monte Carlo simulation (MCS) based on 10 000 simulations was implemented for this purpose. Based on the LCPC

method, 95% and 5% fractiles of the distribution of soil characteristic values were included.

Niazi (2014) has presented four alternatives for interpreting pile axial capacity based on in-situ geotechnical investigations (Figure 1). In the paper, three of the four possibilities were used in the analysis: correlation (empirical methods), statistics (analytical methods) and full-scale load test (experimental tests). Numerical methods should be included in the subsequent research.

1. Use of sounding methods and data for the prediction of pile-bearing capacity

1.1. CPT, CPTu and SDT soundings

The CPT is one of the most common probing methods to be widely used, studied and developed around the world for the past hundred years (Massarsch, 2014). The method is fast and economical. The probe has a 1000 mm^2 base area and 15 000 mm^2 sleeve surface area. The drive rod has the same diameter as the probe (35.7 mm). During the test, the probe is pushed at a constant speed of 20 mm/s to the required depth or until the compressive force runs out. The readings of the cone tip resistance (q_c) and sleeve friction (f_s) with short depth intervals (from 10 to 20 mm) create a nearly continuous representation of the soil layers. Additionally, pore pressure (u_2) data are collected if the CPTu is employed. These three independent parameters allow us to determine the properties of the soil, including its strength and compressibility (Massarsch, 2014).
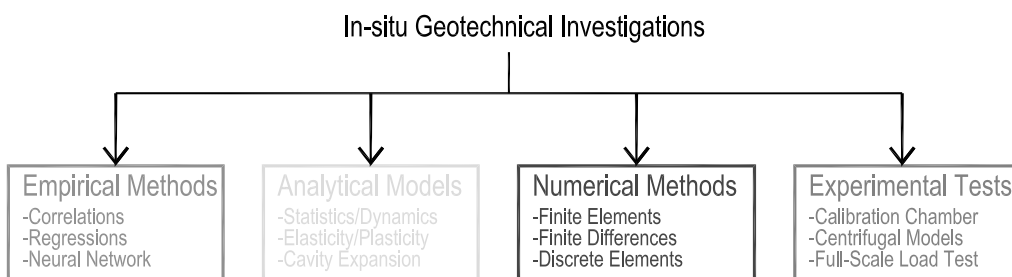

Figure 1. Alternatives to interpret axial pile response from in-situ geotechnical investigations (Niazi, 2014)

Lehar Leetsaar,
Leena Korkiala Tanttu

Deterministic
and Probabilistic
Analyses
of the Bearing
Capacity of Screw
Cast in Situ
Displacement
Piles in Silty Soils
as Measured by CPT
and SDT

The SDT method was developed in Finland in the early 1980s. Especially in the Department of Geotechnics of the City of Helsinki, the method has been studied more intensely (Melander, 1989; Rantala & Halkola, 1997) and used for years. This method combines static and dynamic penetration tests. The test started as a static penetration test in which the drill rods with the cone were pressed and rotated simultaneously. The equipment usually has a maximum compressive force of 30 kN. When the maximum compressive force is reached, the device switches to the dynamic penetration phase (hammering). The dynamic phase switches to static penetration again if the amount of the blows (N20) value is less than or equal to five within 0.4 m. During the test, compressive force, torque, number of strokes, sounding depth and speed of rotation are measured in the intervals of 20 mm to 40 mm (Finnish Geotechnical Society, 2001).

The SDT method uses a loose cone, which remains almost always on the ground when the rods are pulled out. The cone must be 45 ± 0.2 mm in diameter and 90 ± 2 mm in length. The apex angle is 90°. The cross-sectional area of the cone end is 1600 mm^2, and the area of the side surface is 12 700 mm^2. The diameter of the drive rod is 32 mm, which is smaller than the diameter of the cone (45 mm). During the compression stage, the rods are compressed at a constant speed of 20 ± 5 mm/s. A hammer weighing 63.5 ± 0.5 kg and a lowering height of 0.5 m are used for dynamic penetration (Finnish Geotechnical Society, 2001).

Determining the geotechnical parameters from the results of the SDT method is based on calculation formulas developed for CPTu sounding. Unlike the CPTu, the diameter of the SDT cone is larger than the driving rod (Figure 2). Accordingly, the relationship between the SDT and CPT test results must be known. Based on laboratory experiments, Rantala & Halkola (1997) have determined that the cone tip resistance ($q_{c,CPT}$) of the CPTu can be found from SDT results of static pressure penetration using Equation (2). According to Sounding guidelines 6-2001 (Finnish Geotechnical Society, 2001), the net resistance of the static pressure penetration of the SDT test can be calculated based on the total torque (M_{tot}) and total compressive force (Q_{tot}) values using Equation (3). Based on the results of the dynamic penetration of the SDT test, Equation (4) can be utilised to convert the blow numbers to cone tip resistance ($q_{c,CPT}$) of the CPTu. The net stroke rate N_n is defined from Equation (5) with the help of the total stroke rate (N_{20}) and total torque (M_{tot}) (Finnish Geotechnical Society, 2001).

$$q_{c,CPT} = 1.07 \cdot q_{n,SDT} \tag{2}$$

$$q_{n,SDT} = \frac{Q_{tot}}{1000 \cdot A_c} - k_p \cdot \left(M_{tot} - \mu_1 \cdot Q_{tot} \right), \tag{3}$$

$$q_{c,CPT} = 0.83 \left[\frac{MPa}{\frac{l}{0.2m}} \right] \cdot N_n, \tag{4}$$

$$N_n = N_{20} - 0.04 M_{tot}, \tag{5}$$

where

$q_{c,CPT}$ is cone tip resistance of CPT;

$q_{n,SDT}$ is the net resistance to static pressure penetration, MPa, of SDT;

Q_{tot} is the total compressive force, kN, of SDT;

k_p is a standard ($k_p = 1/(A_c \cdot r \cdot 10^6) = 0.039$ (1/m^3));

M_{tot} is the total torque value, Nm, of SDT;

μ_1 is a device-specific constant (e.g., for GM4000 $\mu_1 = 1$ Nm/kN) to estimate the effect of axial loading of the compression phase on the friction of the transmission thrust bearing;

N_n is the net stroke rate [$l/0.2$ m] of SDT;

N_{20} is the total stroke rate [$l/0.2$ m] of the SDT.

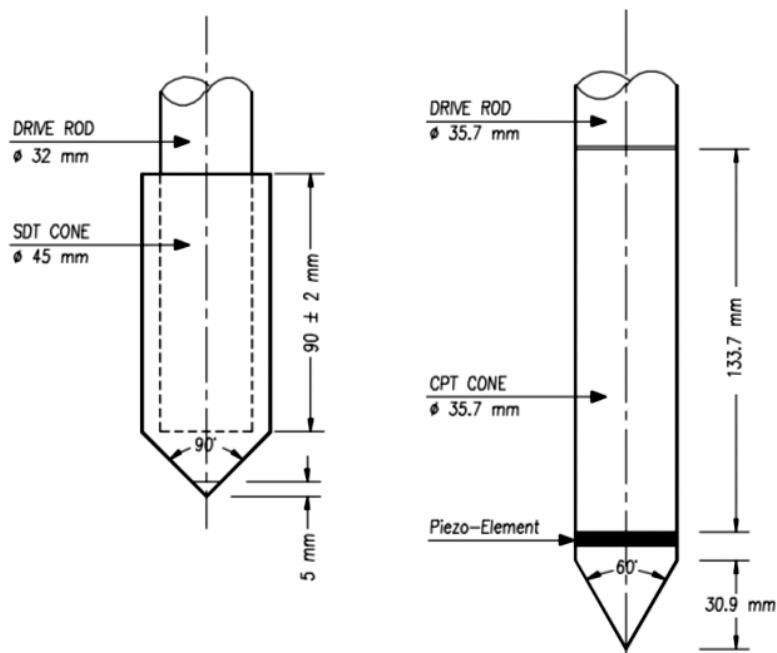**Figure 2.** SDT penetrometer cone on the left and CPTu cone on the right.

Lehar Leetsaar,
Leena Korkiala Tanttu

Deterministic
and Probabilistic
Analyses
of the Bearing
Capacity of Screw
Cast in Situ
Displacement
Piles in Silty Soils
as Measured by CPT
and SDT

1.2. Direct approaches for CPT and CPTu soundings to define pile capacity

The mean effective stress, compressibility and rigidity of the surrounding soil medium have an effect on the CPT cone and pile in a comparable manner (Eslami & Fellenius, 1997; Ardalan et al., 2009). Direct cone penetration methods for the CPT apply cone sleeve friction for unit shaft resistance and cone bearing for the unit end-bearing resistance of the pile, here by the analogy of the cone penetrometer as a model pile (Mayne, 2007). This concept has led to the development of many direct CPT methods around the world, whereby CPT readings are simply scaled up and used to evaluate the load-bearing capacity of full-scale piles (Niazi & Mayne, 2013). More than around 30 different CPT- and CPTu-based direct methods have been developed (Niazi & Mayne, 2013). Six direct methods were applied in the present study: five CPT methods and the Unicone method, which is based on CPTu results. The methods are the Nottingham (1975) and Schmertmann (1978) method, de Kuiter & Beringen (1979) method (Dutch method), LCPC method (Bustamante & Gianeselli, 1982; Bustamante & Frank, 1997), Eurocode 7 (EN 1997-2:2007, 2007) method and German method (EA-Pfähle, 2014). The Unicone (Eslami & Fellenius 1995, 1996, 1997; Fellenius & Eslami, 2000; Eslami, 1996; Fellenius, 2020) method is certainly a remarkable method because it is the first method to use all three readings of the CPTu sounding (q_t, f_s and u_2) in the pile load-bearing capacity analysis. In addition, the Unicone method developed a new soil profiling chart. The methods were chosen based on the fact that most of them were suitable for all soil types and for a wide range of piles. The only exception is the German method (EA-Pfähle, 2014), which is suitable for sandy soils. Concurrent, the German (EA-Pfähle, 2014) method offered good results in similar soils for screw cast in situ displacement piles (Leetsaar et al., 2022). The current study applies these methods to piles installed in silty soils. A summary of the methods used is presented in Table 1. Based on the SDT data, three of the six methods were used to analyse the load-bearing capacity of the piles. The Nottingham (1975) and Schmertmann (1978) method, together with the de Kuiter & Beringen method (1979), utilises the value of f_s to determine the load-bearing capacity of the pile. In addition to reading f_s, the Unicone (Eslami & Fellenius, 1997) method also exploits u_2 readings. SDT sounding does not record either of these readings.

Table 1. Summary of direct CPT-based pile design methods

Method/reference	Design equations	
	Pile unit shaft friction (q_s)	Pile end bearing resistance (q_b)
Nottingham (1975) and Schmertmann (1978) (for driven concrete, steel and timber piles, and drilled shafts in all soil types)	In clay: $q_s = K_f \cdot f_s \le 120$ kPa, $K_f = 0.2–1.25$ K_f is a function of the sleeve resistance In sand: $q_s = c_s \cdot q_c$ or $f_p = k \cdot f_s$ $c_s = 0.8–1.8\%$, $k = 0.8–2.5$	$q_b = C \cdot q_{ca} \le 15$ MPa (in sands) and 10 MPa (in very silty sands) $C = 0.5–1.0$ depending on overconsolidation rate (OCR) $q_{ca} = (q_{c1} + q_{c2})/2$
Dutch method (de Kuiter & Beringen 1979) (for offshore piles in all soil types)	In clay: $q_s = \alpha \cdot s_u \le 120$ kPa; $\alpha = 1$ for NC clay and 0.5 for OC clay; $s_u = q_{ca}/N_{kt}$; $N_{kt} = 15–20$ In sand: $q_s = \min[f_s, q_c/300$ for compression, $q_c/400$ for tension, 120 kPa]	In clay: $q_b = N_c s_u \le 15$ MPa, $s_u = q_{ca}/N_{kt}$, $N_c = 9$; $N_{kt} = 15–20$; $q_{ca} = (q_{c1} + q_{c2})/2$ In sand: similar to Nottingham (1975) and Schmertmann (1978) method
LCPC or French method (Bustamante & Gianeselli, 1982; Bustamante & Frank, 1997) (for all pile types in all soil types)	$q_s = q_{side}/k_s \le f_{p(max)}$ $k_s = 30–150$ depending on soil type, pile type and installation procedure	$q_b = k_b \cdot q_{eq}$ depending on soil types: $k_b = 0.15–0.375$ for non-displacement piles $k_b = 0.375–0.60$ for displacement piles
EUROCODE 7 (EN 1997-2:2007, 2007) (for all pile types in all soil types)	$q_s = \alpha_s \cdot q_{c,z}$ $\alpha_s = 0.005 – 0.030$ depending on soil type or pile type and installation procedure	$q_b = 0.5 \cdot \alpha_p \cdot \beta \cdot s$ $\left\{ \dfrac{q_{c,\text{I,mean}} + q_{c,\text{II,mean}}}{2} + q_{c,\text{III,mean}} \right\}$ $q_{b,max} \le 15$ MPa; $\alpha_p = 0.6–1.0$ depending on soil type, pile type and installation procedure; β factor that takes into account the shape of the pile tip; s factor that takes into account the shape of the bottom of the pile
German method (EA-Pfähle, 2014) (for piles in sandy soils)	Provides upper and lower bound estimates of q_s, kPa, based on q_c (measured in MPa)	Provides upper and lower bound estimates of q_b, MPa, based on q_c (measured in MPa)
Unicone method (Eslami & Fellenius, 1995, 1996, 1997; Fellenius & Eslami, 2000; Eslami, 1996; Fellenius, 2020) (all piles in all soils)	$q_s = C_{se} \cdot q_E$ $q_E = q_t – u_2$ $C_{se} = 0.8–8\%$	$q_b = C_{te} \cdot q_{Eg}$; q_{Eg} is the geometric average of q_c C_{te} is generally taken as 1; for pile diameter $d > 0.4$ m $C_{te} = 1/(3d)$ $q_b = C_{te} \cdot q_{Eg}$; q_{Eg} is the geometric average of q_c

Lehar Leetsaar,
Leena Korkiala Tanttu

Deterministic
and Probabilistic
Analyses
of the Bearing
Capacity of Screw
Cast in Situ
Displacement
Piles in Silty Soils
as Measured by CPT
and SDT

1.3. Statistical determination of sounding data

In the current study, the characteristic value (here as a 95% reliable mean) and 5% fractile values for the sounding parameters were included in analysis of the direct methods in the pile capacity calculations. The aim is to determine how the characteristic values of soil properties based on EC7 change the results of these direct methods. For homogeneous soil without a significant trend in the ground, the characteristic value X_k as a 95% reliable mean value of the parameter can be determined from a set of individual values according to Frank et al. (2005):

$$X_k = X_{mean}\left(1 - k_n V_x\right),\tag{6}$$

where
X_{mean} is the arithmetical mean value of the individual sample parameter value;
V_x is the coefficient of variation of the parameter X;
k_n is a statistical coefficient.

$$V_x = \frac{s_x}{X_{mean}},\tag{7}$$

where s_x is the standard deviation of the n sample test results.

The value of the coefficient $k_{n,mean}$ for the assessment of a characteristic value as a 95% reliable mean value equation is as follows:

$$k_n = 1.645\sqrt{\frac{1}{n}}.\tag{8}$$

The value of the coefficient $k_{n,low}$ for the assessment of a characteristic value as a 5% fractile value equation is as follows:

$$k_n = 1.645\sqrt{\frac{1}{n} + 1},\tag{9}$$

where n is the number of test results of the soundings.

1.4. Reliability-based design (RBD)

Direct methods usually assume that the pile is located in soil layers with homogeneous properties. Odd 'peaks and troughs' in the sounding data are reduced when using mean values (Eslami et al., 1997). In cases where in situ soil variability is considerable, deterministic analysis based on the mean values could be inefficient. One possible solution is to use statistical distributions of soil properties and implement them in a deterministic analysis with simulations.

One of the most commonly used techniques of reliability analysis is Monte Carlo Simulation (MCS), which is a repetitive simulation process that generates a set of values based on random variables with the known probability distribution. The increase in the number of simulations increases the accuracy of the MCS outcome. However, a very large number of simulations make the analysis slow and has little effect on the results. Typically $N=10^4$ or 10^5 number of simulation is chosen (Orr & Denys, 2008). The probability distribution (i.e., beta, normal, lognormal, etc.) for each independent variable is provided. The outcome can be presented in a histogram or an average value can be highlighted. In addition, the RBD determines the probability of failure or reliability index.

In the present study, the soil was divided into four layers. Three soil layers were analysed around the piles. The fourth layer was formed based on the influence zone for the pile according to the LCPC method. For the LCPC method the influence zone is 1.5 D below and above the pile base. The variable of the soil layers was the q_c value. The layers were assigned a mean value and standard deviation. Three of the four layers used a normal distribution for the variable. For the layer dominated by clayey soils, a lognormal distribution was used. Using software RiskAMP and MCS, 10 000 pile capacity values for each pile were generated. The average value of the results for each pile was used in the analysis.

A choice was made between those methods that allow the load-bearing capacity of the pile to be determined from both CPTu and SDT sounding data. The German method is based on tabulated values; therefore, it cannot be used in MC simulations. The Eurocode method was also excluded because it is too complicated, needing three different q_c values for calculating the bearing capacity of the pile base. Only the LCPC method was used for the RBD simulations.

2.   Test site and tested pile types

The test site was Soodi, which is located in Tallinn (see Figure 3), northern Estonia. It lies above an old valley buried in Quaternary sediments. Marine, lacustrine and alluvial deposits consist of varying layers of clay, silty clay, sand and silty sand. To a depth of 4.1 m, there are mainly alternating silty and sandy silt layers. At a depth of 11.7–11.9 m, the sand and silty sand deposits appear again. Between the soft clayey and silty soil, the layers alternate. The hard stratum of gravel/moraine is found at a depth of almost 30 m. The ground water table varies between 0.05 and 0.65 m below the ground surface. A map of the sounding points and tested piles is shown in Figure 4. The SDT soundings SLP9 and SLP10 were performed before the erection of the test piles. The

Lehar Leetsaar,
Leena Korkiala Tanttu

Deterministic
and Probabilistic
Analyses
of the Bearing
Capacity of Screw
Cast in Situ
Displacement
Piles in Silty Soils
as Measured by CPT
and SDT

CPTu soundings were assembled after the construction of the building and, therefore, are located more than 46 m from the test piles. A non-normalised CPT soil behaviour type (SBT) chart (Robertson, 2010) was used for soil classification. Internationally, the SBT chart is a global and favourable basis for comparing soils and test results.
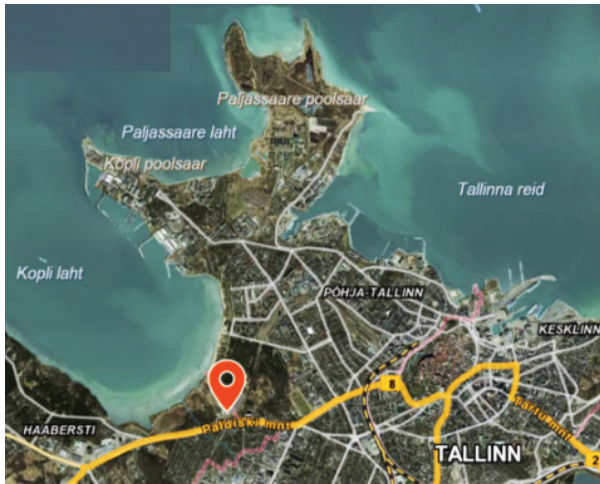

Figure 3. On the left, the location of the research point in Tallinn (Map applications of the Estonian Land Board, 2020). The red mark indicates the location of Soodi Street 4
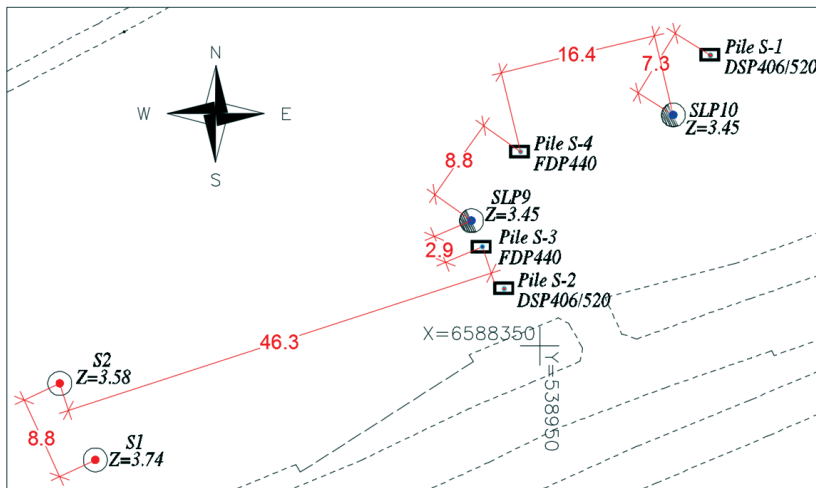

Figure 4. Site map with the tested piles and sounding points. S1 and S2 indicate CPTu soundings. SLP9 and SLP10 indicate SDT soundings. The pile symbols are S-1 to S-4, and the type of pile is shown next to the name of the tested piles. The dimensions given in the map are in metres

The two tested pile types were the Bauer full displacement pile (FDP) and displacement pile (DSP). During FDP pile installation (Figure 5 on the left), a displacement tool with a widening shape is drilled into the ground by pushing and rotating it. The displacement tool includes a starter auger, which first loosens the soil, and then, the widening displacement tool pushes it laterally into the surrounding soil. After reaching the designed depth, the displacement tool is removed and the cavity is simultaneously filled with concrete through an opening at the end of the drill stem. After this, reinforcement casing is pushed into the wet concrete. 'Lost bit' technology was used to install DSP piles (Figure 5 on the right). By rotating and pushing, the jacket pipe with a closed end is drilled into the desired depth. The drill head is unscrewed
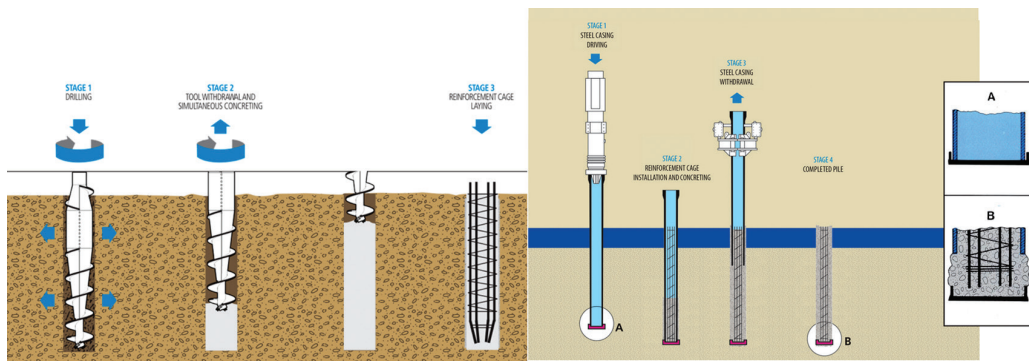

Figure 5. The principle of installing an FDP pile is shown on the left; the principle of installing a DSP pile is shown on the right (https://www.trevispa.com/en/Technologies)

Table 2. Summary of pile and sounding data

Pile name	S-1	S-2	S-3	S-4
Pile type	DSP 406/520	DSP 406/520	FDP 440	FDP 440
Pile length, m	12.69	11.34	12.39	12.5
Max load from pile load test, kN	1870	1700	1870	1870
Max settlement from pile load test, mm	35.3	22.8	17.0	22.7
Max depth of CPTu sounding, m	25.18	25.18	25.18	25.18
Max depth of SDT sounding, m	21.49	21.13	21.3	21.3
Max q_c reading from CPTu, MPa	21.7	21.7	21.7	21.7
Max q_c reading from SDT, MPa	11.1	14.5	14.5	14.5
Max N_{20} reading from SDT	15	26	26	26

Lehar Leetsaar,
Leena Korkiala Tanttu

Deterministic
and Probabilistic
Analyses
of the Bearing
Capacity of Screw
Cast in Situ
Displacement
Piles in Silty Soils
as Measured by CPT
and SDT

and left in the ground as a pile toe. While lifting the jacket pipe up, the pile cavity is filled with concrete. Both pile types can be classified as cast in situ concrete displacement piles. At the test site, the diameter of the FDP pile head and shaft was 0.44 m. The shaft diameter of the DSP pile was 0.406 m, and the pile tip was 0.52 m. The length of the piles varied between 11.34 and 12.69 m. Piles of this type are classified in Europe as 'screw piles' (Basu et al., 2010). Table 2 shows the lengths of the statically tested piles with the maximum testing loads and respective settlements. In addition, the maximum resistance values of the CPTu and SDT soundings are given.

The German method contains tabular values for driven precast piles, simplex piles, Atlas piles, Fundex piles and bored piles in sandy and clayey soils (EA-Pfähle, 2014). The DSP pile most closely resembles the Fundex pile. Both pile types have a pile tip with overlap, i.e., the diameter of the pile tip is bigger than the diameter of the pile shaft. The pile head remains in the ground after the pile installation on both types of piles. Driven precast piles and simplex piles are both driven piles. When installing the Atlas pile, the screw-shape shaft remains. Bored piles are not displacement piles. Thus, the FDP pile is also calculated on the basis of the Fundex pile tables using the German method.

3. Pile tests and soundings

3.1. Static axial pile load tests

The piles were tested in accordance with EVS-EN 1997-1:2006 (based on EN 1997-1:2004) before the other parts of the pile field were constructed. The largest load on both types of test piles was 1870 kN. This is 83.7–98.8% from the ultimate capacity. The pile head settlement was between 17.0 mm and 35.3 mm. The piles were tested two to three weeks after installation.

According to Hirany & Kulhawy (1989), there are different methods to determine the ultimate capacity of a pile from the results of a static load test. One of the oldest definitions of pile-bearing capacity is the load at which the pile movement exceeds 10% of the diameter of the pile. This principle is also known as the French criterion (Vesić, 1977) and is used in Eurocode.

As the piles were loaded into the settlement equal to 10% of its nominal diameter, Chin's (1970) extrapolation method and load-settlement curve were used to determine the ultimate pile capacity. The extrapolation results for all four piles are summarised in Figure 6. Based on Kondner's (1963) work, Chin's extrapolation method is familiar and

extensively used in practice (Al-Homoud et al., 2003; Basu et al., 2010; Elsamee, 2012; Niazi, 2014; Camacho et al., 2018). In agreement with the 10% criteria, this method allows the ultimate resistance to be defined, even if the pile head settlement does not reach 10% of the pile diameter (Holeyman et al., 1997; Borel et al., 2004; De Cock, 2009; Basu et al., 2010).

3.2. CPTu tests

Two CPTu soundings were made in 2019. CPTu soundings were performed with a Nova cone manufactured by Geotech AB and mounted on a lightweight truck. The Nova cone has a 1000 mm^2 project area and 15 000 mm^2 sleeve surface area, according to ASTM D-5778 (2000) and EN ISO22476-1 standards. The covering fill layer was penetrated by predrilling. The lightweight truck was anchored with two ground anchors to achieve a higher compression force. The tests were performed according to Lunne et al. (1997) guidelines.

The distance between CPTu sounding points and test piles varied from 44.9 to 75.3 m. The sounding profiles of the corrected cone resistance (q_t), unit sleeve friction resistance (f_s), friction ratio (R_f) and pore pressure measured behind the cone (u_2) are shown in Figure 7. Sounding S1, which reached a depth of 25.18 m, is marked in blue. Sounding S2 reached a depth of 20.42 m and is marked in red.
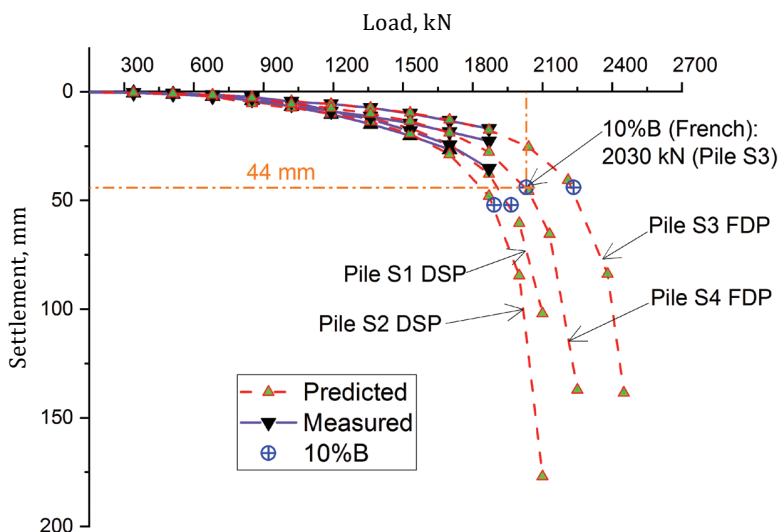

Figure 6. Load-displacement curve of the pile load test and the extrapolation results for the four piles

Lehar Leetsaar,
Leena Korkiala Tanttu

Deterministic
and Probabilistic
Analyses
of the Bearing
Capacity of Screw
Cast in Situ
Displacement
Piles in Silty Soils
as Measured by CPT
and SDT

R_f is defined as $f_s/q_t \times 100\%$. The types of soil layers defined by SBT (Robertson, 2010) are shown on the left. Different mixtures of silt predominate in soils. The pore water pressure image also includes the water table and in situ pore pressure (u_0) profile.

3.3. Static-dynamic probing tests

SDT soundings were performed in spring 2015 with the GM 65 GTT unit, here according to Melander's (1989) instructions. A total of 10 soundings were conducted. The results of the two soundings closest to the piles tested were utilised. The distance of the piles from the nearest sounding point varied between 2.9 and 8.8 m (see Figure 4). The depths of the SDT soundings SLP9 and SLP10 were 21.13 and 21.49 m, respectively. The results of the soundings are shown in Figure 8. The figure on the left shows the results of SLP9. The figure clearly demonstrates the alternation of static penetration (q_c–SDT) with dynamic penetration (N_{20}–SDT) of the SDT test. The middle figure shows the SLP9 and SLP10 test results (q_c–SDT + N_{20}–SDT) with the q_c values derived from the SLP9 and SLP10 results (q_c–SDT–CPT) after applying Equations (2) to (5). In the figure on the right, the q_c values derived from the results of SLP9 and SLP10 (q_c–SDT–CPT) are compared with the CPTu tip resistance values of S1 and S2 (q_c–CPTU).
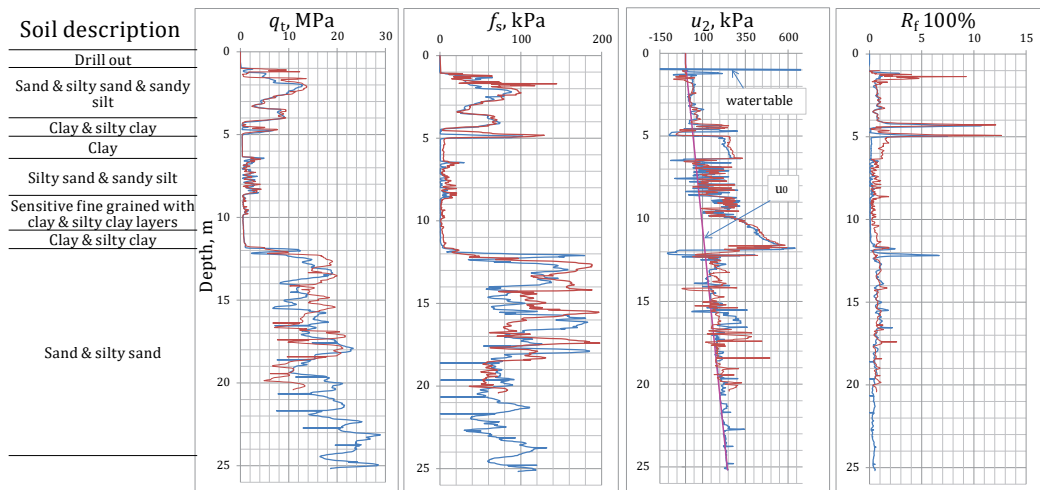

Figure 7. Soil description and the results of CPTu tests *S*1 (blue figures) and S2 (red figures) at the Soodi site. q_t, cone resistance corrected for the pore pressure effects; f_s, sleeve friction; R_f, friction ratio; u_2, pore pressure

4.   Estimated versus measured ultimate pile capacity

The current study has analysed piles ranging in length from 11.34 to 12.69 m. Settlement of the pile equalling 10% of the pile diameter should be 56 mm for the DSP pile and 44 mm for the FDP pile. The two tested DSP piles had a maximum settlement of 37% and 59% less than the required size of 10% of the pile base diameter. On the two FDP piles, the percentage was 61% and 48%, respectively. The results might be affected by extrapolation, which was done to define the ultimate pile capacity.

A high groundwater level could also affect sounding results and the time of the pile-bearing capacity, especially for fine-grained cohesive soils. The effect of time on the pile load-bearing capacity certainly depends on the type and length of the pile. It is also important to distinguish whether the clayey soil layers are around the pile base or only above it. In conditions where nearly 50% of the pile is surrounded by clayey soils, the load-bearing capacity of the pile may increase for up to 100 days after construction of the pile (Togliani & Reuter, 2014).
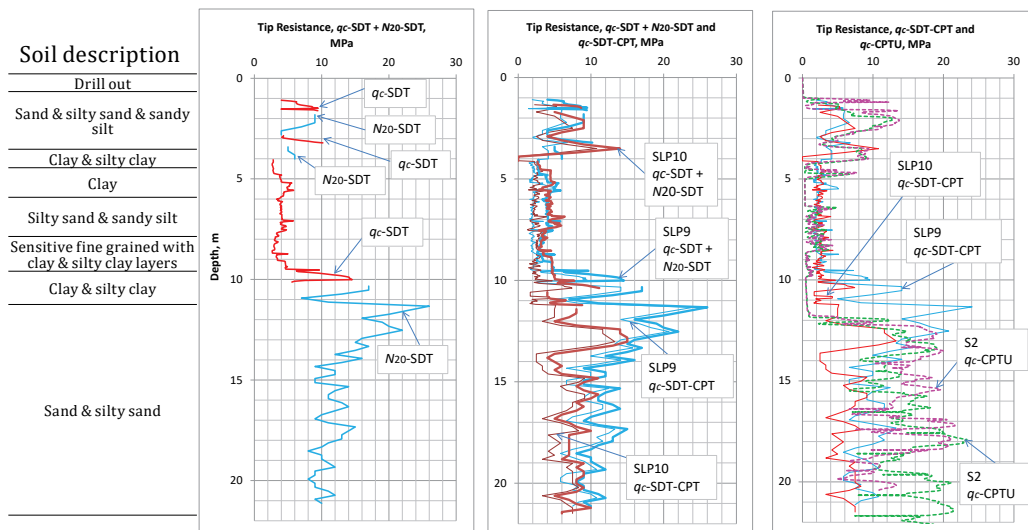

Figure 8. SLP9 sounding results in the figure on the left. The results of SLP9 and SLP10 (q_c–SDT + N_{20}–SDT) converted to the q_c value of CPT (q_c–SDT–CPT) in the middle. The results of SDT test compared with the CPTu test at the Soodi site on the right. q_c–SDT, cone resistance from static readings of SDT; N_{20}–SDT, cone resistance from dynamic readings of SDT; q_c–SDT–CPT, measured and derived q_c values from SDT q_c and N_{20} values; q_c–CPTu, cone resistance from CPT

Lehar Leetsaar,
Leena Korkiala Tanttu

Deterministic
and Probabilistic
Analyses
of the Bearing
Capacity of Screw
Cast in Situ
Displacement
Piles in Silty Soils
as Measured by CPT
and SDT

The piles included in the present study had clayey soils layers above the pile base; thus, generating adhesion on the pile shaft affected the load-bearing capacity of the pile. Therefore, it is important to know how quickly the load tests were performed after installation and how much of the total pile load-bearing capacity was the pile shaft capacity. The pile shaft resistance was analysed based on the average results of $S1$ and $S2$, as well as on the SLP9 and SLP10 soundings. As an average of the results for the five CPT methods and one CPTu method, pile shaft resistance accounted for 30% of the total bearing capacity for DSP piles and 37% for FDP piles. Using the average results of the two SDT soundings, the average values of the results of the three CPT methods were 41% and 49%, respectively. The higher proportion of the bearing capacity of the base of the DSP piles can be explained by the larger diameter of the pile base compared with the pile shaft. Because the load-bearing capacity of the pile shaft is a significant part of the total load-bearing capacity, it can be assumed that the actual load-bearing capacity of the tested piles was higher than that measured during the static load test.

The five CPT methods and one CPTu method referred to in Section 2.2 were used for analyses. The estimated pile capacities (R_{cp}) from the different sounding data were compared with the measured capacities (R_{cm}). The results for pile S-1 based on $S1$ and SLP10 soundings are shown in Table 3. In Table 3, the ratios of the measured total capacity, R_{cm}, to estimated pile capacity, R_{cp}, are given, along with the absolute percentage difference between the estimated and measured capacities. The minus sign indicates that the calculation method underestimates the load-bearing capacity of the pile. In addition to the total load-bearing capacity (R_c) of the pile, the base capacity (R_b) and shaft friction capacity (R_s) are also shown separately for different calculation methods. The sounding ID indicates which investigation point data were used to calculate pile capacity. Only the soundings made during the research after the installation of the piles carry the abbreviation CPTu in sounding ID.

As the distance between two CPTu soundings was only 8.8 m and the tested piles were more than 46 m away from the sounding points, the results of axial bearing capacity based on two CPTu soundings were first compared. The results of the four piles in bearing capacity absolute differences based on CPTu soundings $S1$ and $S2$ are summarised in Figure 9. The calculation methods with reference to the type of probing test used are shown on the horizontal axis in Figure 9. The vertical axis shows the absolute percentage difference between the predicted and calculated capacities. The values calculated from soundings CPTU-S1 ($S1$) and CPTU-S2 ($S2$) are presented side by side in pairs. In the figure, ±10% and ±20% areas are indicated by hatching. The more the results

Table 3. Comparison between the static load test results and bearing capacity prediction for the test pile S-1

| Method	R_b, kN	R_s, kN	R_c, kN	R_{cm}/R_{cp}	Absolute difference, %	Sounding ID
Static Loading Test (s/B=10%)			1965	1.0000	0	
Nottingham (1975) and Schmertmann (1978)	1797	325	2121	0.9264	7	CPTU-S1
de Kuiter and Beringen (1979)	1797	680	2436	0.8067	19	CPTU-S1
LCPC (1982; 1997)	1128	640	1727	1.1378	−14	CPTU-S1
EUROCODE 7 (EN 1997-2:2007, 2007)	1263	763	2025	0.9704	3	CPTU-S1
German method (EA-Pfähle, 2014)	1448	659	2107	0.9326	7	CPTU-S1
Unicone method (1997)	961	663	1582	1.2421	−24	CPTU-S1
LCPC (1982; 1997)	1012	629	1600	1.2281	−23	SLP10
EUROCODE 7 (EN 1997-2:2007, 2007)	1005	916	1880	1.0452	−5	SLP10
German method (EA-Pfähle, 2014)	1058	616	1632	1.2040	−20	SLP10
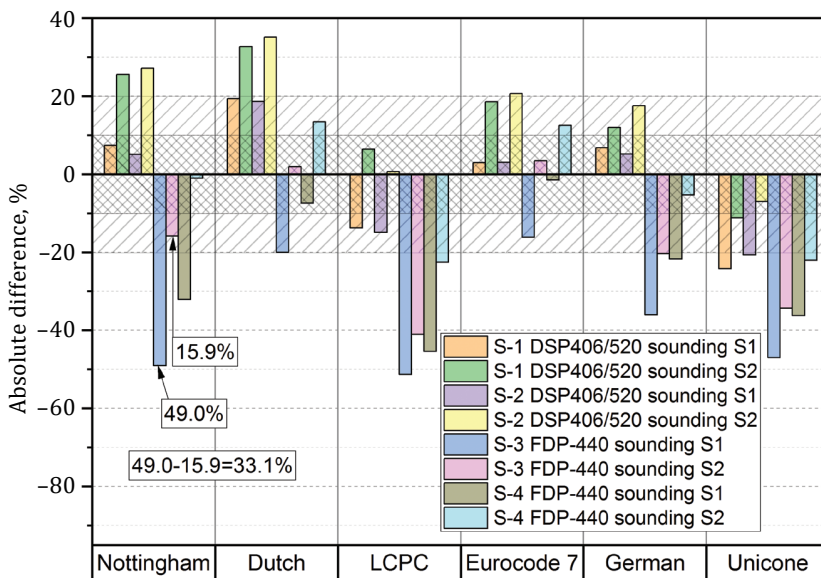
Figure 9. Comparison of the measured and predicted capacity for the piles at the Soodi site based on CPTU-S1 and CPTU-S2; + overestimates, – underestimates

Lehar Leetsaar,
Leena Korkiala Tanttu

Deterministic
and Probabilistic
Analyses
of the Bearing
Capacity of Screw
Cast in Situ
Displacement
Piles in Silty Soils
as Measured by CPT
and SDT

were within ±20% or even ±10%, the better the method. Figure 9 shows the difference between the results of soundings *S*1 and *S*2 as calculated for pile S-3, here based on the Nottingham (1975) and Schmertman (1978) method. Differences in the results of all four piles have been calculated using the same principle. The results are shown in Table 4. The average values in the bottom row clearly show that the results differ in the range of 14.2–19.9% based on the results of the two CPT soundings. The smallest difference is 5.2%, and the largest difference is 33.1%. Hereinafter, the average values of *S*1 and *S*2 were used in load-bearing capacity analysis of the piles. The average values of SLP9 and SLP10 were also used.

Based on the average sounding results, the load-bearing capacity of the four piles found by all the utilised methods is shown in Figure 10. The results were compared with the measured results of four static pile load tests. In addition, the significant results are marked with a yellow circle. In Figure 11, the same results are shown as an absolute percentage difference between the predicted and calculated capacities.

As can be clearly seen in Figures 10 and 11, when comparing the measured and calculated results of all four piles, the best agreement is with the results obtained by the Eurocode 7 (EN 1997-2:2007, 2007) method. In addition, very comparable results were achieved with this method based on both the CPT and SDT sounding data. Most results of the Eurocode 7 (EN 1997-2:2007, 2007) method are within or close to the ±10% range. The largest absolute difference was 13%.

Table 4. Absolute percentage difference in load-bearing capacity of four piles as the distinction between the results based on the CPTU-S1 and CPTU-S2 soundings

Method	S-1 DSP406/520, %	S-2 DSP406/520, %	S-3 FDP-440, %	S-4 FDP-440, %
Nottingham (1975) and Schmertmann (1978)	18.2	22.0	33.1	31.0
de Kuiter and Beringen (1979)	13.3	16.5	21.9	20.8
LCPC (1982; 1997)	20.2	15.6	10.2	22.8
EUROCODE 7 (EN 1997-2:2007, 2007)	15.5	17.6	19.6	13.9
German method (EA-Pfähle, 2014)	5.2	12.4	15.6	16.4
Unicone method (1997)	13.1	13.7	12.6	14.2
Average	14.2	16.3	18.9	19.9

Other methods gave significantly different results between the two types of piles. The results of the DSP piles tended to overestimate the measured capacity. In contrast, the calculated capacities of most FDP piles underestimated the measured values. The results of the DSP piles were most overestimated by the Dutch (de Kuiter & Beringen, 1979) method (28%). Nevertheless, all other methods offered results for the DSP pile within the ±20% range. The LCPC method and the Unicone (1997) method underestimated the load-bearing capacity of the FDP piles the most. The absolute differences were 59% and 66%, respectively. Further, the LCPC method and Unicone (1997) method underestimated the load-bearing capacity of all four piles compared to the measured capacity. Figure 11 shows that the LCPC method, together with the Eurocode method and German method, gave very comparable results based on both the CPT and SDT sounding data. The load-bearing capacity of the FDP piles varied within a ±10% range using the Dutch (de Kuiter & Beringen, 1979) method and the Eurocode 7 (EN 1997-2:2007, 2007) method. The variability ranged from −7% to 5% and −5% to 6%, respectively.
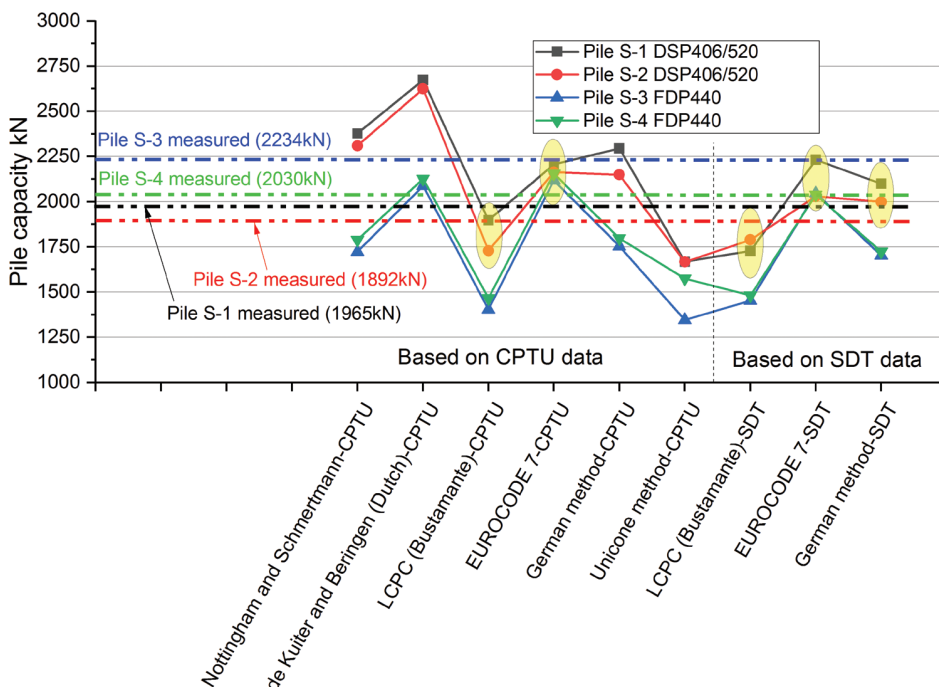

Figure 10. Comparison of the measured and predicted capacity for the piles at the Soodi site based on CPTU-S1 and CPTU-S2 average results

Lehar Leetsaar,
Leena Korkiala Tanttu

Deterministic
and Probabilistic
Analyses
of the Bearing
Capacity of Screw
Cast in Situ
Displacement
Piles in Silty Soils
as Measured by CPT
and SDT

Figure 12 compares the average (average) and MCS results against the 95% reliable estimate of the mean value (characteristic) and 5% fractile (Low 5) results obtained by the LCPC method. The results shown in Figure 12 on the left are based on CPTu soundings *S*1 and *S*2. The results in Figure 12 on the right are based on SDT soundings SLP9 and SLP10. The results are presented and compared based on the absolute differences.

Compared with the absolute difference, the MCS and characteristic values based on the *S*1 and *S*2 soundings were similar for all four piles.
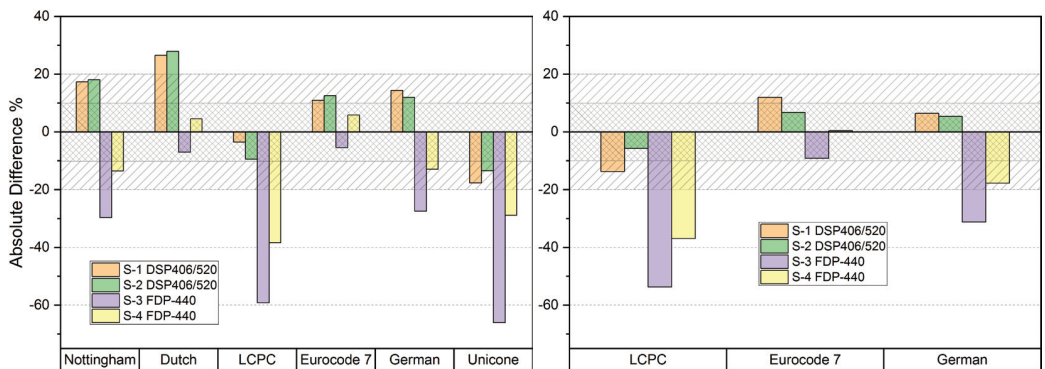

Figure 11. On the left based on a comparison of CPTU-S1 or CPTU-S2 average results between pile types; on the right based on a comparison of SLP9 and SLP10 average results between pile types; + overestimates, – underestimates
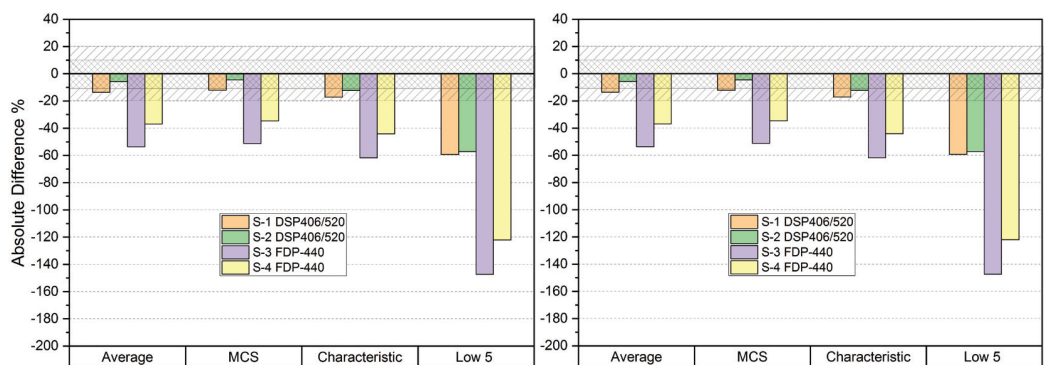

Figure 12. Comparison of average (Average), Monte Carlo simulation (MCS), 95% reliable estimate of the mean value (characteristic) and 5% fractile (Low 5) values based on LCPC method. On the left based on CPTU-S1 or CPTU-S2 result comparison between pile types; on the right based on SLP9 and SLP10 result comparison between pile types; + overestimates, – underestimates

The biggest difference was 3%. The results based on the $S1$ and $S2$ soundings obtained with the average values are 3–8% lower than the MCS and characteristic values. Low 5 values of the same soundings are 43–132% lower than the RBD and characteristic values. The average values based on the results of SDT soundings SLP9 and SLP10 are similar to the RBD values. The difference is between 1% and 3%. The characteristic values are 5–11% lower than the average and RBD values. Low 5 values are 47–96% lower than the average and MCS values.

5. Discussion

As shown in Figure 11, in four out of the six methods, the direct methods tended to overestimate the bearing capacity of the DSP piles. The load-bearing capacity of the pile was underestimated by the LCPC and Unicone methods only. As the DSP piles have a pile tip with a larger diameter and the installation technology resembles a Fundex pile, they should behave in a similar way. According to Kemfert & Becker (2010), a pile tip with a larger diameter leads to loosening of the ground in the shaft area, resulting in a reduction of shaft resistance. In contrast, the screw-shaped shaft of the pile increases the load-bearing capacity of the pile when compared with a smooth pile shaft (Basu et al., 2010). This may be the reason why pile calculation methods do not always provide the actual load-bearing capacity of such screw-shaped type piles with the desired accuracy (Kemfert & Becker, 2010). The results of the two DSP piles in the present study are compared with the results of the three Fundex piles at the Paldiski mnt site (Leetsaar et al., 2022) in Table 5. Table 5 shows that the results have the same trend for most methods.

Table 5. Absolute percentage difference in load-bearing capacity of two DSP piles at the Soodi site and three fundex piles at the Paldiski mnt Site; + Overestimates, – Underestimates

Method	Soodi site Absolute Difference, %	Paldiski mnt site Absolute Difference, %
Nottingham (1975) and Schmertmann (1978)	18	39
de Kuiter and Beringen (1979)	27	27
LCPC (1982; 1997)	–7	6
EUROCODE 7 (EN 1997-2:2007, 2007)	12	36
German method (EA-Pfähle, 2014)	13	14
Unicone method (1997)	–16	20

Lehar Leetsaar,
Leena Korkiala Tanttu

Deterministic
and Probabilistic
Analyses
of the Bearing
Capacity of Screw
Cast in Situ
Displacement
Piles in Silty Soils
as Measured by CPT
and SDT

The Dutch (de Kuiter & Beringen, 1979) method and the German method offer identical results for both sites. The Unicone method demonstrates the most significant variability. This method underestimates the load-bearing capacity of the pile by an average 16% at the Soodi site and overestimates it at the Paldiski mnt site. The reason that direct methods may overestimate the load-bearing capacity of the pile could be related to the testing time of the pile after completion of the pile. The piles in the current study were loaded two to three weeks after completion. Togliani & Reuter (2014) have stated that the load-bearing capacity of the pile may increase even after 100 days from the construction of the pile in conditions where nearly 50% of the pile is surrounded by clayey soils. Further examination of the bearing capacity of the DSP pile in parallel with a Fundex pile is necessary.

The fact that some direct methods underestimate the load-bearing capacity of the FDP pile may indicate a lack of these methods considering the actual behaviour of this pile type in the soil. Bush et al. (2013) concluded that in silty and sandy soils, the cone resistance because of FDP pile installation was increased down to the depth of the displacement body. In addition, a slight decrease below the displacement body had no negative effect on the bearing capacity of the pile. Based on the calculations, in the soil around the pile, there were only minor changes in density and primarily changes in the horizontal stresses. It is very difficult to measure the horizontal stress state and void ratio in situ. Therefore, it is necessary to investigate this type of pile by static load tests in parallel with CPT and SDT soundings. Based on the load test and sounding results, direct methods can be better calibrated.

Based on average, MCS and characteristic values, the results differed by up to 11%. Characteristic values gave the pile capacity 3–8% lower than the average values. The results for the Low 5 fractile differed up to 132% compared with the average values. Eurocode 7 (Frank et al., 2005) recommends the use of the Low 5 fractile when the soil volume involved in a limited state is very small compared with the length of the fluctuation of the soil property. In the studied soils, Low 5 values gave the capacity of the pile with a large reserve.

Conclusion

In the current study, the load-bearing capacity of four screw cast in situ displacement piles in silty soils was analysed. The outcome of the static pile load tests were compared with the results of five CPT-based methods and one CPTu-based direct method. The results of static pile load tests were extrapolated, and the $s/B = 10\%$ failure criterion was

applied to the piles. Data from both the CPT and SDT soundings were included in load-bearing capacity analysis of the piles. As there are no direct methods to apply the SDT results to pile-bearing capacity analysis, three CPT direct methods were used. The percentage of absolute difference was used to compare the methods. The percentage of absolute difference was found to be the difference between the calculated and measured load-bearing capacity from the pile load test. The comparison of the methods was based on the principle that the more the results were within ±20% or even ±10%, the better the method. In addition to deterministic methods, the probabilistic method with MCS was used for the analysis.

The results indicated that the application of the SDT sounding outcome in the CPT direct methods provided comparable results to the utilisation of the CPTs sounding data. However, a comparison of the bearing capacities calculated from the results of two close CPT soundings showed significant variations. The percentage of absolute difference varied between 5.2% and 33.1%. This is a clear indication of the need for statistical processing of sounding data prior to pile-bearing capacity analysis. As a result, the soil around the piles was divided into three layers and treated statistically. The results of the CPT two soundings were considered together. The two SDT soundings were treated in the same way. The Eurocode 7 method showed the best performance based on analysis of the arithmetic average values of both the CPT and SDT soundings. Most of the results when using this method were within or close to the ±10% range, and the largest absolute difference was 13%. Other direct methods tended to overestimate the load-bearing capacity of DSP piles and underestimate the load-bearing capacity of FDP piles. Except for the Dutch (de Kuiter & Beringen, 1979) method, all other methods offered results for the DSP pile within a ±20% range. The LCPC method and Unicone (1997) method underestimated the load-bearing capacity of all four piles when compared with the measured capacity. The biggest absolute differences were 59% and 66%, respectively.

RBD analysis of the piles was performed using the LCPC method. Density functions were accomplished on the soil layers. Pile-bearing capacity was determined by the LCPC method with MCS, here based on the arithmetic average values of soils layers and standard deviation. Here, 10 000 simulations were used in the simulation. In addition, characteristic 95% reliable estimate of the mean value and 5% fractile results were obtained based on the LCPC method. Based on CPT and SDT soundings, the outcome of pile-bearing capacities in the absolute difference varied within 11% between the average, RBD and characteristic values. Based on CPT soundings, the 5% fractile was

Lehar Leetsaar,
Leena Korkiala Tanttu

Deterministic
and Probabilistic
Analyses
of the Bearing
Capacity of Screw
Cast in Situ
Displacement
Piles in Silty Soils
as Measured by CPT
and SDT

43–132% lower than the RBD and characteristic values. Using SDT sounding data, 5% fractile results were 47–96% lower than the RBD and characteristic values.

The use of SDT sounding results in the CPT direct methods for analysing pile-bearing capacity in this case gives good results and deserves attention and further investigation. Studies should explore parallel soundings of the CPT and SDT in different soils along with different pile types tested statically. The piles must be loaded up to a s/B=10% failure criterion. Sounding data should be applied to load-bearing analysis of the pile by sounding separately and then being statistically combined. In addition to average values, characteristic values should be used in parallel. Compared with analytical methods, RBD takes account of the variability of the parameters, provides more information and gives a reliable assessment of the probability of failure or actual safety. RBD should increasingly be included in load-bearing capacity analysis of piles, including direct methods, in the future.

REFERENCES

Al-Homoud, A. S., Fouad, T., & Mokhtar, A. (2003). Comparison between measured and predicted values of axial end bearing and skin capacity of piles bored in cohesionless soils in the Arabian Gulf Region. *Geotechnical and Geological Engineering, 21*, 47–62. https://doi.org/10.1023/A:1022932630538

Arbeiter, R. (1962). Tallinna ehitusgeoloogilise rajoniseerimise visand. *Eesti ehitusgeoloogiline kogumik I*, Tallinn, 23–34.

Ardalan, H., Eslami, A., & Nariman-Zahed, N. (2009). Piles shaft capacity from CPT and CPTu data by polynomial neural networks and genetic algorithms. *Computers and Geotechnics*, *36*(4), 616–625.
https://doi.org/10.1016/j.compgeo.2008.09.003

Bandini, P., & Salgado, R. (1998). Methods of pile design based on CPT and SPT results. *Geotechnical Site Characterization Conference*, Blekma, Rotterdam, 936–942.

Basu, P., Prezzi, M., & Basu, D. (2010). Drilled displacement piles – current practice and design. *The Journal of the Deep Foundations Institute*, *4*(1), 3–20. https://doi.org/10.1179/dfi.2010.001

Borel, S., Bustamante, M., & Gianeselli, L. (2004). An appraisal of the Chin method based on 50 instrumented pile tests. *Ground Engineering*, *37*(1), 22–26. https://cdn.ca.emap.com/wp-content/uploads/sites/13/2004/01/2004-01_Pages_22-26.pdf

Bush, P., Grabe, J., & Gerressen, F. W. (2013). Influence of the installation process of full displacement bored piles on the subsoil. In M. Mets & R. Raudsepp (Eds.), *Baltic Piling* (1st ed., pp. 157–163). Taylor & Frances Group, London.

Bustamante, M., & Frank, R. (1997). Design of axially loaded piles – French practice. In: *Design of axially loaded piles – European practice, proceeding of*

the ERTC3 seminar, Brussels, Belguim, Balkema, Rotterdam, The Netherlands, pp. 161-175.

Bustamante, M., & Gianeselli, L. (1982). Pile bearing capacity predictions by means of static penetrometer CPT. *Proceeding of 2nd European Symposium on Penetration Testing (ESOPT-II)*, Amsterdam, 493–500. https://www.cpt-robertson.com/PublicationsPDF/Pile%20Bearing%20 Cap%2CCPT-LCPC%20Method-Bustamonte%20et%20al-ESOPT2-198.pdf

Cai, G., Liu, S., & Puppala, A. J. (2012). Reliability assessment of CPTu-based pile capacity predictions in soft clay deposits. *Engineering Geology*, *141–142*, 84–91. https://doi.org/10.1016/j.enggeo.2012.05.006

Cai, G., Liu, S., Tong, L., & Du, G. (2009). Assessment of direct CPT and CPTu methods for predicting the ultimate bearing capacity of single piles. *Engineering Geology*, *104*(1–2), 211–222. https://doi.org/10.1016/j.enggeo.2008.10.010

Camacho, M. A., Meija, J., Camacho, C. B., Heredia, W., & Salinas, L. M. (2018). Ultimate capacity of drilled shaft from CPTu test and static load test. In *Cone Penetration Testing 2018* (1st ed., pp. 193–198). CRC Press. https://www. taylorfrancis.com/chapters/oa-edit/10.1201/9780429505980-22/ultimate-capacity-drilled-shaft-cptu-test-static-load-test-camacho-mejia-camacho-heredia-salinas

Chin, F. K. (1970). Estimation of the ultimate load of piles from test not carried to failure. *Proceeding of the Second Southeast Asia Conference on Soil Engineering*, Singapore, 81–90.

De Cock, F. A. (2009). Sense and sensitivity of pile load-deformation behavior. In Van Impe (eds.), *Deep foundation on bored and auger piles* (pp. 23–44). Taylor & Frances Group, London.

De Kuiter, J., & Beringen, F. L. (1979). Pile foundations for large North Sea structures. Marine Geotechnology, *3*(3), 267–314. https://doi.org/10.1080/10641197909379805

EA-Pfähle. (2014). *Recommendations on piling (EA-Pfähle)*. Ed. by German Geotechnical Society, DGGT. Ernst & Sohn, Berlin. https://download.e-bookshelf.de/download/0005/0450/23/L-G-0005045023-0019229730.pdf

Elsamee, W. (2012). Evaluation of the ultimate capacity of friction piles. *Engineering*, *4*(11), 778–789. https://doi.org/10.4236/eng.2012.411100

EN 1997-1:2004. (2004). *Eurocode 7: Geotechnical Design – Part 1: General Rules*, Brussels, Belgium, p. 171.

EN 1997-2:2007. (2007). *Eurocode 7: Geotechnical Design – Part 2: Ground Investigation and Testing*, Brussels, Belgium, p. 199.

Eslami, A. (1996). *Bearing capacity of piles from cone penetrometer test data* [PhD Thesis, University of Ottawa, Deparment of Civil Engineering]. http://dx.doi.org/10.20381/ruor-8038

Eslami, A., & Fellenius, B. H. (1995). Toe bearing capacity of piles from cone penetration test (CPT) data. *Proceedings of the International Symposium on Cone Penetration Testing, C P T'95*, Linkoping, Sweden, Report 3:95, *2*, 453–460. https://www.fellenius.net/papers/180%20Toe%20 Resistance%20from%20CPT%20analysis.pdf

*Lehar Leetsaar,
Leena Korkiala Tanttu*

Deterministic
and Probabilistic
Analyses
of the Bearing
Capacity of Screw
Cast in Situ
Displacement
Piles in Silty Soils
as Measured by CPT
and SDT

Eslami, A., & Fellenius, B. H. (1996). Pile shaft capacity determined by piezocone data. *Proceeding of the 49th Canadian Geotechnical Conference*, St. John`s Newfoundland, *2*, 859–867.

Eslami, A., & Fellenius, B. H. (1997). Pile capacity by direct CPT and CPTu methods applied to 102 case histories. *Canadian Geotechnical Journal*, *34*(6), 880–898. https://doi.org/10.1139/t97-056

Fellenius, B. H. (2020). *Excerpt from Chapter 7 of the red book electronic edition: direct methods for estimating pile capacity, in Background to UniCone*. http://www.fellenius.net. Accessed 13.01.2020.

Fellenius, B. H., & Eslami, A. (2000). Soil profile interpreted from CPTu data. *Proceedings of Year 2000 Geotechnics Conference*, Bankok, Thailand. A.S. Balasubramaniam, D.T. Bergado, L. Der Gyey, T.H. Seah, K. Miura, N. Phien Wej, & P. Nutalaya (Eds.), *1*, 163–171. https://www.fellenius.net/papers/202%20Soil%20Profile%20from%20CPT.pdf

Finnish Geotechnical Society. (2001). *Sounding guidelines 6 – 2001 CPTu / cone penetration testing and static dynamic testing*. Nummela: Nummelan Kopiopalvelu Oy.

Frank, R., Bauduin, C., Driscoll, R., Kavvadas, M., Krebs Ovesen, N., Schuppener, T., Orr, B., Gulvanessian, H. (2005). Designers' Guide to EN 1997-1 Eurocode 7: Geotechnical Design – General Rules. ICE Publishing.

Gadeikis, S., Žaržojus, G., & Urbaitis, D. (2010). Comparing CPT and DPSH in Lithuanian soils, *2nd International Symposium on Cone Penetration Testing*, Huntington Beach, CA, USA, *2&3*, 3–22. https://www.geoengineer.org/storage/publication/18421/publication_file/2660/3-22Gadcca.pdf

Hirany, A., & Kulhawy, F.H. (1989). Interpretation of load tests on drilled shafts: axial compression. *Foundation Engineering: Current Principles and Practices*, *2*(GSP 22), 1132–1149.

Holeyman, A., Bauduin, C., Bottiau, M., Debacker, P., De Cock, F., Dupont, E., Hilde, J.L., Legrand, C., Huybrechts, N., Menge, P. P., Miller, J., & Simon, G. (1997). Design of axially loaded piles – Belgian practice. In F. De Cock & C. Legrand (Eds.), *Design of axially loaded piles – European practice* (pp. 57–82). https://www.fondytest.com/Alain-Holeyman-s-publications/pdf/1997-Design-Axially-Loaded-Piles-2.pdf

Jardine, R. J., Zhu, B. T., Foray, P., & Yang, Z. X. (2013). Measurement of stresses around closed-ended displacement piles in sand. *Gotechnique*, *63*(1), 1–17. https://doi.org/10.1680/geot.9.P.137

Kempfert, H.-G., & Becker, P. (2010). Axial pile resistance of different pile types based on empirical values. *Proceeding of Geo-Shanghai 2010 deep foundation and geotechnical in situ testing (GSP 205)*, Reston, VA, 149–154. https://doi.org/10.1061/41106(379)18

Kondner, R. L. (1963). Hyperbolic stress-strain response: cohesive soils. *Journal of the Soil Mechanics and Foundation Division*, *89*(4), 241–242.

Leetsaar, L., Korkiala-Tanttu, L., & Kurnitski, J. (2022). CPT, CPTu and DCPT methods for predicting the ultimate bearing capacity of cast in situ displacement piles in silty soils. *Geotechnical and Geological Engineering*, *41*, 631–652. https://doi.org/10.1007/s10706-022-02292-6

Lunne, T., Robertson, P. K., & Powell, J. J. M. (1997). *Cone penetration testing in geotechnical practice*. Blackie Academic, EF Spon/Routledge Publishers, New York.

Map applications of the Estonian Land Board. (2020, April 17). https://geoportaal.maaamet.ee/est/Kaardirakendused-p2.html

Massarsch, K. R. (2014). Cone penetration testing – A historic perspective. *Proceedings CPT'14*, Las Vegas, USA, 97–134. https://www.g-i.co.nz/wp-content/uploads/historic-overview-of-cpt-massarsch-2014.pdf

Mayne, P. W. (2007). *Cone penetration testing – a synthesis of highway practice*. NCHRP Synthesis 368, Transportation Research Board, Washington, DC. https://mcipin.com/publications/CPT/nchrp_syn_368.pdf

Melander, K. (1989). *Static-dynamic sounding method*. The publication 48 by the department of geotechnics of city of Helsinki. Helsingin kaupungin kiinteistövirasto, Geotekninen osasto 1989.

Mets, M., & Leppik, V. (2016). Pile foundations in Estonia. *Design of Piles in Europe – How did Eurocode 7 change daily practice? International Symposium*, Leuven, Belgium, 101–116.

Moshfeghi, S., & Eslami, A. (2016). Study on pile ultimate capacity criteria and CPT-based direct methods. *International Journal of Geotechnical Engineering*, *12*(1), 28–39. https://doi.org/10.1080/19386362.2016.1244150

Niazi, F. S. (2014). *Static axial pile foundation response using seismic piezocone data* [PhD Thesis, Georgia Institute of Technology, Atlanta, GA].

Niazi, F. S., & Mayne, P. W. (2013). Cone penetration test based direct methods for evaluating static axial capacity of single piles: a state-of-the-art review. *Geotechnical and Geological Engineering*, *31*(4), 979–1009. https://doi.org/10.1007/s10706-013-9662-2

Nottingham, L. C. (1975). Use of quasi-static friction cone penetrometer data to predict load capacity of displacement piles [PhD Thesis, University of Florida].

Rantala, K., & Halkola, H. (1997). *The definition of the bearing capacity of a pile with static-dynamic sounding*. The publication 74/1997 by the department of geotechnics of city of Helsinki. Helsingin kaupungin kiinteistövirasto, Geotekninen osasto 1997.

Robertson, P. K. (2010). Soil behaviour type from the CPT: an update. *2*nd *International Symposium on Cone Penetration Testing*, *CPT'10*, Huntington Beach, CA, USA. https://www.geoengineer.org/storage/publication/18399/publication_file/2638/56RobSBT.pdf

Schmertmann, J. H. (1978). *Guidelines for cone penetration test, performance and design* (Report No. FHW A-TS-78-209). U.S. Department of Transportation, Washington, DC. https://rosap.ntl.bts.gov/view/dot/958

Orr, T. L. L., & Denys, B. (2008). Eurocode 7 and reliability-based design. In K.-K. Phoon (ed.), *Reliability-based design in geotechnical engineering* (pp. 298–343), Taylor and Francis, Oxon, UK.

Žaržojus, G. (2010). *Analysis of the results and it influence factors of dynamic probing test and interrelation with cone penetration test data in Lithuanian soils* [PhD Thesis, summary]. Vilnius.

Lehar Leetsaar,
Leena Korkiala Tanttu

Deterministic
and Probabilistic
Analyses
of the Bearing
Capacity of Screw
Cast in Situ
Displacement
Piles in Silty Soils
as Measured by CPT
and SDT

Togliani, G., & Reuter, G. R. (2014). CPT/CPTu pile capacity prediction methods: Question time. *Proceedings CPT'14*, Las Vegas, 993–1002. https://www. togliani.ch/wp-content/uploads/2021/03/CPT14-Togliani-Reuter-1.pdf

Vesić, A. S. (1977). Design of pile foundations. In *NCHRP Synthesis of Highway Practice 42*, Transportation Research Board, National Research Council, Washington, D.C.

Publication 3

4. Leetsaar, Lehar; Korkiala-Tanttu, Leena. Advantages of using a seismic piezocone penetration test for analysis of a single screw in situ displacement pile in silty soils. *Indian Geotechnical Journal*, **2024; 10.1007/s40098-024-00942-5.**

Check for updates

Advantages of Using a Seismic Piezocone Penetration Test for Analysis of a Single Screw In Situ Displacement Pile in Silty Soils

Lehar Leetsaar[1,2,3] · Leena Korkiala-Tanttu[1]

Abstract The determination of pile bearing capacity using the load–settlement relationship has been widely recognised as an effective means of directly determining the bearing capacity of a pile through in situ tests. Among the various techniques available for such investigations, the seismic cone penetration test (SCPTu) stands out as one of the most reliable. One key advantage of this test is its ability to measure the shear wave velocity (V_s) during the sounding process. In this study, the range of V_s values was examined specifically in silty soils. The data for this study were obtained from six SCPTu soundings and load tests conducted on seven screw in situ displacement piles. In addition to the four known correlations between the cone penetration test (CPTu) and V_s, three new correlations were developed, showing promising results for most of the soil layers examined. Moreover, a correlation between the normalised operative shear stiffness and the normalised pseudo-strain was established based on back-calculations using the results of static pile load tests. The findings of this study highlight the complexity of the correlation between CPTu readings and V_s in silty soils, emphasising the need for further research in this area.

Keywords Seismic piezocone penetration test · Shear wave velocity · Pile load–displacement · Pile · Pile capacity · Static load test · Elastic continuum solution · Correlation

✉ Lehar Leetsaar
lehar.leetsaar@taltech.ee

1 Department of Civil Engineering, Aalto University, Espoo, Finland

2 Tallinn University of Technology Tartu College, Tartu, Estonia

3 Department of Civil Engineering and Architecture, Tallinn University of Technology, Tallinn, Estonia

Introduction

Extensive research has been conducted globally to establish correlations between the cone penetration test with pore pressure measurement (CPTu) readings and shear wave velocity (V_s) values [1–4]. The four selected correlations have been divided into two categories: two correlations suitable for various soil types, including silty soils, and two correlations specifically applicable to sandy silt soils. To assess the appropriateness of these correlations for different soil conditions, it is necessary to get measurements of the shear wave velocity. The in situ measurement of V_s using seismic non-destructive tests is primarily accomplished using a multi-channel analysis of surface waves, cross-hole seismic testing or up-and down-hole methods. The seismic cone penetration test (SCPTu) can be adopted to measure V_s values using the cross-hole or down-hole testing approach. In this study, data were gathered from down-hole tests. The dataset comprised six SCPTu soundings conducted at three sites, with a maximum depth of 23 m. The most informative, reliable and useful approach for analysing pile bearing capacity is the adoption of calculation methods based on the results of in situ tests [5–7]. One important factor to consider when assessing pile load capacity is the load–settlement (Q–w) relationship of the piles, which provides a better understanding of the load-carrying capacity of the piles and enables the evaluation of differential settlements. To determine the Q–w relationship for different piles in different soils, analytical stress–strain–strength soil models in conjunction with the results of in situ tests have been extensively studied [8–12]. In this study, the Q–w relationship of seven screw in situ displacement piles (hereafter referred to as 'screw piles') in silty soils was analysed using static pile load tests and seismic cone penetration soundings. The Q–w relationship of piles is significantly influenced by the heterogeneity of

stiffness. Cook et al. [13] demonstrated that the operative shear modulus (G) is the most critical factor in determining the Q–w performance of a loaded pile. In the pile Q–w analysis, the shear modulus (G) is preferred over the Young's modulus, E, for two reasons: (1) the shear modulus is often unaffected by whether the loading conditions are undrained or drained and (2) the primary deformation of the soil occurs in shear along the pile shaft. The small strain shear modulus (G_{max} or G_0) is generally calculated based on the measured shear wave velocity (V_s).

It is crucial to comprehend the potential presented by using SCPTu data for the analysis of a pile. This study used analytical elastic continuum solutions to achieve a deeper understanding of the correlations of the test data. Four known empirical correlations between V_s and CPTu were analysed, and three new correlations for silty soils were proposed. An elastic solution proposed by Randolph and Wroth [14, 15] was applied to determine the Q–w relationship of piles based on Niazi and Mayne's [11] methodology. The exponent parameter g [16] for the screw piles in silty soils was analysed. Correlations between the normalised operative shear stiffness (G/G_{max}) and normalised pseudo-strain ($\gamma_p/\gamma_{\text{p-ref}}$) were developed based on the back-calculations of the static pile load test results. In normalised pseudo-strain, $\gamma_p = w_t/d$ and $\gamma_{\text{p-ref}} = 0.01$, where w_t represents the settlement at the pile top and d is the pile diameter. The results of the back-calculations of the static pile load tests were compared with those obtained by Niazi and Mayne [11]. Because the piles were not loaded to their ultimate capacity during the static pile load test, extrapolation was used. Since most of the tested piles had significant settlements, potential biases resulting from these extrapolations were found to have no significant effect on the results.

CPT–V_s Correlations

Four empirical correlations that connected CPTu readings with V_s (m/s) were included in the analyses. The first correlation uses a database that includes sand, silt and clay, as well as mixed soils, as derived by Hegazy and Mayne [1]. It uses both cone (q_c) and shaft resistance (f_s). The second correlation equation derives the value of V_s only from the f_s

readings, using a database for saturated clay, silt and sand from well-documented experimental sites [3]. The following two correlations have been proposed for soils dominated by sandy silt. Trevor et al. [4] proposed a correlation for sandy silt soils using corrected cone resistance q_t and f_s values. The correlation proposed by Holmsgaard et al. [2] uses the value of q_t and is suitable for sandy silt with clay stripes. In addition, this paper proposes three correlations for silty soils. Four correlations from previous studies are presented in Table 1.

Use of SCPTu Data to Predict the Load–Displacement Capacity of a Pile

SCPTu was used to determine the penetrometer readings and in situ shear waves (S). According to shear wave theory, V_s can be measured. For this purpose, a geophone is integrated into the cone. G_{max} or G_0 is calculated based on the V_s value. Most commonly, shear waves are measured at every metre in the borehole with the down-hole SCPTu. For this reason, both V_s readings and G_0 values represent the average value of a one-metre interval.

The initial value of soil stiffness (G_{max} or G_0) gradually decreases to G as the strain increases. The decrease in the modulus can be described with a modified hyperbola. Fahey and Carter [16] proposed a modified hyperbola form for the monotonic torsional shearing of normally consolidated sands (1):

$$\frac{G}{G_{max}} = 1 - f \left(\frac{\tau}{\tau_{max}} \right)^g. \tag{1}$$

Here, f and g are fitting parameters, and G is a shear modulus calculated as $G = E/[2(1+\nu)]$, where $\nu` = 0.2$ (drained case) is the approximate value of the Poisson's ratio of geomaterials at small strains. The value of τ/τ_{max} can be treated as the reciprocal of the factor of safety (FS) or $1/FS$. Therefore, it can also be considered a level of mobilised load, Q/Q_{ult}. At small strains, the material's stiffness is finite and can be indicated by the low-strain shear modulus:

$$G_{max} = G_0 = \rho V_s^2, \tag{2}$$

Table 1 Summary of correlations between shear wave velocity V_s and CPTu output from other studies

References	Correlation	Soil type
[1]	$V_s = [10.1 \cdot \log q_c - 11.4]^{1.67} [f_s/q_c \cdot 100]^{0.3}$	For all soils
[3]	$V_s = 118.8 \log (f_s) + 18.5$ (f_s in kPa)	Saturated clays, silts, sands
[4]	$V_s = 12.02 \cdot q_t^{0.319} \cdot f_s^{-0.0466}$ (q_t in kPa)	Sandy silt soils
[2]	$V_s = 99.45 \, q_t^{0.428}$ (q_t in MPa)	Sandy silt with clay stripes

q_t, cone resistance corrected for the pore pressure effects; q_c, cone resistance; f_s, sleeve friction; and V_s, shear wave velocity

where ρ indicates the total mass density of the material. As the strains of G_0 are too small to cause excess pore water pressure, Eq. 2 applies to both drained and undrained conditions [17]. In addition, previous studies have shown that the value of G_0 is the same under both static (monotonic) and dynamic loading conditions [18, 19].

The first-order evaluation values of $f = 1$ and $g = 0.3$ provide normally reasonable approximations and have been confirmed by laboratory torsional, triaxial and simple shear tests for the monotonic loading of unaged and uncemented quartz sands and insensitive and unsaturated clays [20, 21]. The exponent parameter, $g \approx 0.3 \pm 0.1$, is suitable for many uncemented and nonstructured soils [22, 23]. In our analysis, the values of $f = 1$, $g = 0.2$, $g = 0.3$ and $g = 0.4$ were adopted in Eq. 1.

In addition to the load-bearing capacity of a pile, it is necessary to determine the Q–w relationship to design an economical foundation solution. A suitable approach is to use the approximate analytical elastic solution for pile–soil interaction, provided by Randolph and Wroth [14, 15]. This solution accounts for piles in Gibson-type soils (i.e. linearly increasing soil stiffness with depth) and in homogenous two-layered soils (i.e. constant soil stiffness with depth). The settlement of pile top (w_t) for a compressible pile can be calculated as follows [14, 15]:

$$w_t = \frac{Q_t \left[1 + \frac{4\eta \tanh(\mu L)L}{\pi \lambda (1-\nu_s)\xi(\mu L)r_0}\right]}{G_L r_0 \left[\frac{4\eta}{(1-\nu_s)\xi} + \frac{2\pi \rho E \tanh(\mu L)L}{\zeta(\mu L)r_0}\right]}, \tag{3}$$

where w_t represents the settlement at the pile top; Q_t is the load applied at the pile top; G_L is the operative soil shear modulus at the pile base; η is the factor for underreamed piles that take greater loads at the pile base, calculated as $\eta = r_b / r_o$; L is the pile length; r_o is the radius of the pile shaft; r_b is the pile base radius for underreamed piles; μL is the measure of pile compressibility, calculated as $\mu L = 2 \cdot [2/(\zeta \lambda)]^{0.5} \cdot (L/d_s)$; ζ is the measure of influence radius, calculated as $\zeta = \ln(r_m/r_o)$; r_m is the maximum radius of influence, calculated as $r_m = L\{0.25 + \xi \cdot [2.5\rho_E \cdot (1-\nu_s) - 0.25]\}$; λ is the pile–soil stiffness ratio, calculated as E_p/G_L; E_p is the pile modulus; ξ is the factor for end-bearing piles resting on a stiffer stratum ($G_b >> G_L$), calculated as G_L/G_b; G_b is the soil shear modulus below the pile base; ρ_E is the modulus variation factor, calculated as G_M/G_L; G_M is the operative soil shear modulus at the midpoint of the pile embedment depth, calculated as $G_M = (G_o + G_L)/2$; G_o is the operative shear modulus at the pile top ($Z = 0$); and ν_s is the Poisson ratio of soil.

The solution is suitable for both constant and linearly increasing soil stiffness with depth (Gibson-type model) conditions; it incorporates end-bearing and floating piles. However, the solution does not directly account for the differences in pile types and pile installation methods. For an accurate analysis of different pile types and their load–displacement relationships, the solution must first be calibrated with the static pile load test data. An important variable in this analysis is the parameter g in Eq. 1, which is assigned values of 0.2, 0.3 and 0.4 in the analysis.

To determine the value of G_0, it is essential to know the total mass density ρ values. The total mass density of the soils can be determined in the laboratory. However, collecting soil samples from deep layers below the water table is a complex and time-consuming process. Furthermore, it is practically impossible to obtain undisturbed samples from silty soils below the water table. Thus, an expression that uses all three CPTu readings (f_s, q_t and u_2) is included to determine the soil unit weight [24]. The mass density, ρ, can be obtained from the unit weight as $\rho = \gamma_t / 9.8$. Equation (4) is based on a variety of clays, silts and sands.

$$\gamma_t = 11.46 + 0.33 \cdot \log(z) + 3.1 \cdot \log(f_s) + 0.7 \cdot \log(q_t). \tag{4}$$

Test Sites and Tested Piles

All three test sites are located in Tallinn, northern Estonia, and are found in old valleys buried under quaternary sediments. Marine, lacustrine and alluvial deposits incorporate sandy silts, silty sands, clay and sand at the Ahtri site and silty sand, sandy clay, clay and sand at the Paldiski mnt site [25]. At the Soodi site, the soil deposits comprise varying layers of silty clay, silty sand, clay and sand [26].

At all three sites, static loading tests were conducted. At the Ahtri site, one Fundex pile (A3) was tested; at the Paldiski mnt site, two Fundex piles (P-1 and P-3) were tested [25] and at the Soodi site, two displacement piles (S-1 and S-2) and two Bauer full displacement piles (S-3 and S-4) were tested [26]. All piles were tested in accordance with EVS-EN 1997–1:2006 based on EN 1997–1:2004 [27]. Because the piles were not loaded to their ultimate capacity, Chin's [28] extrapolation was used to complete the Q–w curves. This method was chosen because it was also used by Maertens and Huybrecht [29] in silty soils with the same type of piles. In a previous study [25] using Fundex piles, Chin's method also demonstrated favourable results in silty soils. Therefore, it was assessed as the most reliable method. Table 2 shows the pile types and lengths, with the maximum testing loads and the respective settlements. The diameter specifications of Fundex piles in Table 2 are denoted by two numerical values. The first value corresponds to the diameter of the shaft, while the second value represents the diameter of the pile tip. This particular study focused on Fundex piles with two different diameters, where the pile tip diameters were measured at 0.45 and 0.56 m. The respective diameters of

Table 2 Summary of pile data

Pile name	A-3	P-1	P-3	S-1	S-2	S-3	S-4
Pile type	Fundex 450/560	Fundex 350/450	Fundex 350/450	DSP 406/560	DSP 406/560	FDP 440	FDP440
Pile length (m)	23.2	15.5	15.0	12.69	11.34	12.39	12.5
Measured max load from pile load test (kN)	3600	1200	1200	1870	1700	1870	1870
Max settlement from pile load test (mm)	22.0	6.3	15.0	35.3	22.8	17.0	22.7

the pile shaft were 0.35 and 0.45 m. Notably, both the FDP pile base and shaft had a consistent diameter of 0.44 m.

SCPTu Soundings

Six SCPTu soundings were conducted at all three sites. At the Ahtri site, three SCPTu soundings, with depths ranging between 20.0 and 23.5 m, were conducted (Fig. 1). At the Paldiski mnt site, two SCPTu soundings, with depths ranging between 19.0 and 19.8 m, were conducted (Fig. 2). At the Soodi site, one SCPTu sounding, with a depth of 20.0 m, was performed (Fig. 3). The corrected cone resistance (q_t) and sleeve friction (f_s) values were reported for all soundings. At all sounding points, the ground water level was at a depth of almost one metre above the ground surface. Pore water pressure was measured behind the cone (u_2) and

presented with in situ pore pressure (u_0) profiles. The types of soil layers, presented on the left of the sounding figures, were defined using CPTu and the soil behaviour type (Robertson 2010 [30]). At all three sites, silty soils predominated.

The Geotech AB Nova cone, mounted on a lightweight truck, was used to perform all soundings. To ensure a higher compression force, the truck was secured in the soil using two screw anchors. To penetrate the covering fill layers, predrilling was conducted. The Nova cone, in accordance with ASTM D-5778 [31] and EN ISO 22476–1:2012 [32], had a project area of 1000 mm^2 and a sleeve surface area of 15,000 mm^2.

The shear wave velocity was determined through an SCPTu down-hole test, where the energy source was positioned on the ground and the receiver was placed in the cone. Seismic tests were conducted at one-metre intervals throughout the borehole, resulting in consistent V_s
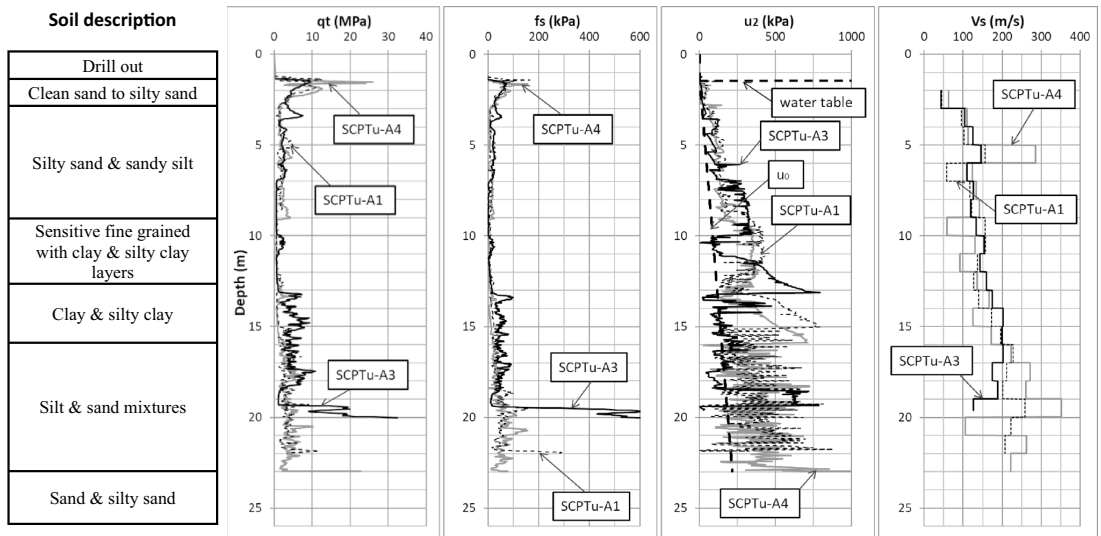

Fig. 1 Results of the piezocone test at the Ahtri site. q_t, cone resistance corrected for the pore pressure effects; f_s, sleeve friction; u_2, pore pressure; and $V_{s,}$ shear wave velocity
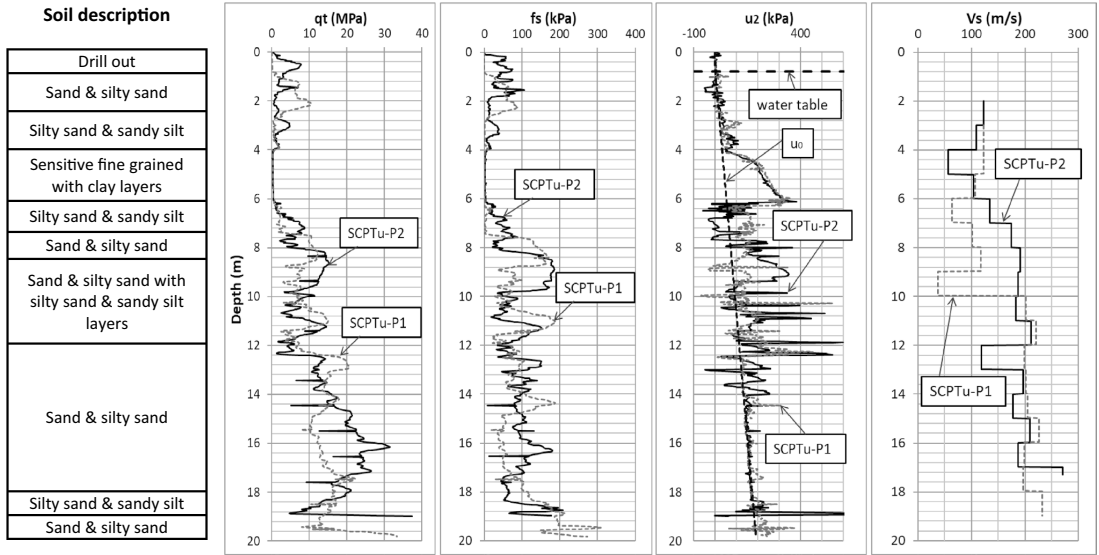
Fig. 2 Soil description and the results of SCPTu tests P1 (blue figures) and P2 (red figures) at the Paldiski mnt site. q_t, cone resistance corrected for the pore pressure effects; f_s, sleeve friction; u_2, pore pressure; and V_s, shear wave velocity
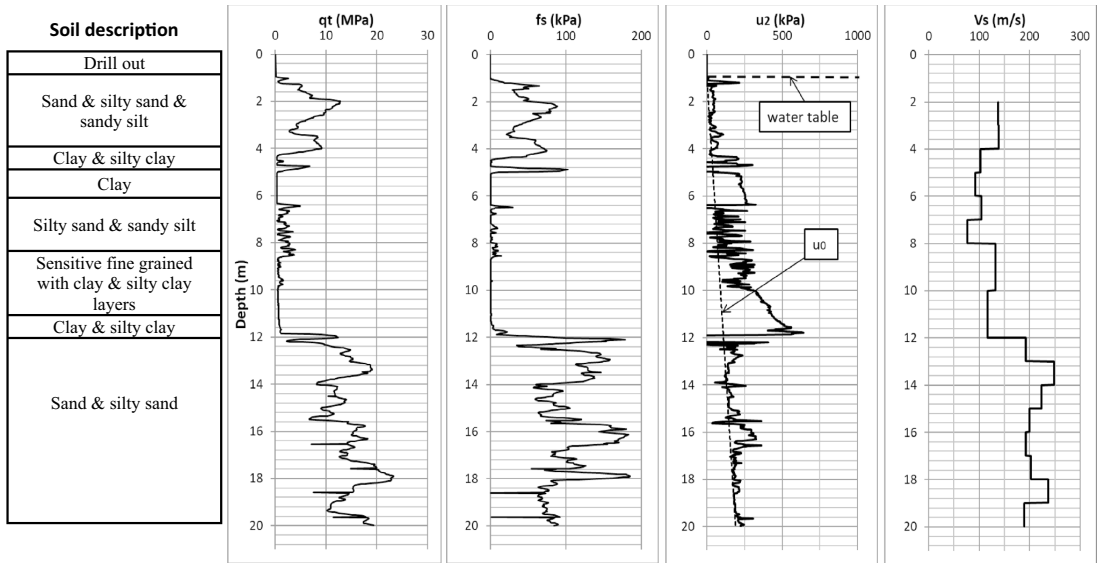

Fig. 3 Results of piezocone tests at the Soodi site. q_t, cone resistance corrected for the pore pressure effects; f_s, sleeve friction; u_2, pore pressure; and V_s, shear wave velocity

and G_{max} values (refer to Figs. 1, 2, 3). Table 3 displays the minimum and maximum V_s values obtained from all six soundings, which ranged from 37 to 352 m/s.

Additionally, the table presents the difference between the maximum and minimum V_s values (ΔV_s). As for the q_t and f_s values, measurements were taken every 20 mm, and

Table 3 Summary of V_s values alongside the minimum and maximum results of average q_t and f_s values for 1-m-thick layers

	$V_{s\text{-min}}$ m/s	$V_{s\text{-max}}$ m/s	ΔV_s m/s	$q_{t\text{-min}}$ MPa	$q_{t\text{-max}}$ MPa	Δq_t MPa	$f_{s\text{-min}}$ kPa	$f_{s\text{-max}}$ kPa	Δf_s kPa
SCPTu-A1	46	259	213	0.5	4.3	3.7	7.9	76.9	69.0
SCPTu-A3	44	203	159	0.5	8.0	7.5	3.4	107.5	104.1
SCPTu-A4	58	352	294	0.6	4.8	4.2	2.3	91.1	88.8
SCPTu-P1	37	233	196	0.4	17.7	17.3	0.6	157.3	156.6
SCPTu-P2	57	270	213	0.3	25.6	25.3	2.8	144.4	141.5
SCPTu-S1	76	248	172	0.4	18.5	18.1	0.5	137.1	136.6

the average values of one-metre-thick layers were used for the analysis. Table 3 also includes the minimum and maximum q_t and f_s values for all six soundings.

The measured V_s values were analysed to improve the database quality by removing outliers based on statistical considerations. Outliers were identified through the '2σ' statistical criteria, where σ is the standard deviation of the variable V_s. This resulted in 95% confidence interval criteria for the data. Two V_s values (37 and 352 m/s) out of 108 were removed from the entire database and not included in the analysis.

Estimated Versus Measured V_s Values

Alongside the measured V_s results, the calculated values are based on four empirical regression equations from the literature for all six SCPTu soundings, as presented in Figs. 4 and 5. The details of these correlations are presented in Table 1. Because the existing correlations did not provide overwhelming fitness to the dataset used in this study, three new correlations were introduced. The first relationship (5) proposed in this work uses f_s values, and the second (6) uses q_c and u_2 values. Both correlations can be used in parallel to compare the calculated V_s values. In addition, a correlation is proposed that exploits both q_t and f_s values simultaneously. The values of V_s calculated using Eqs. 5–7 are also included in Figs. 4 and 5. The V_s values obtained
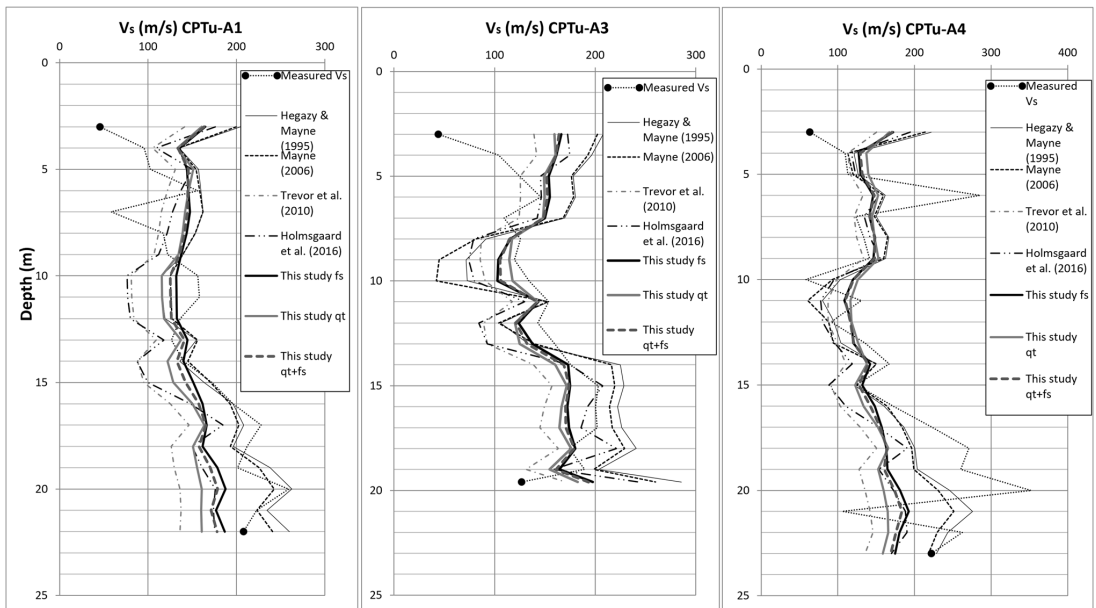

Fig. 4 Comparison of V_s as predicted from CPT–V_s correlations and as measured by SCPTu at the Ahtri site
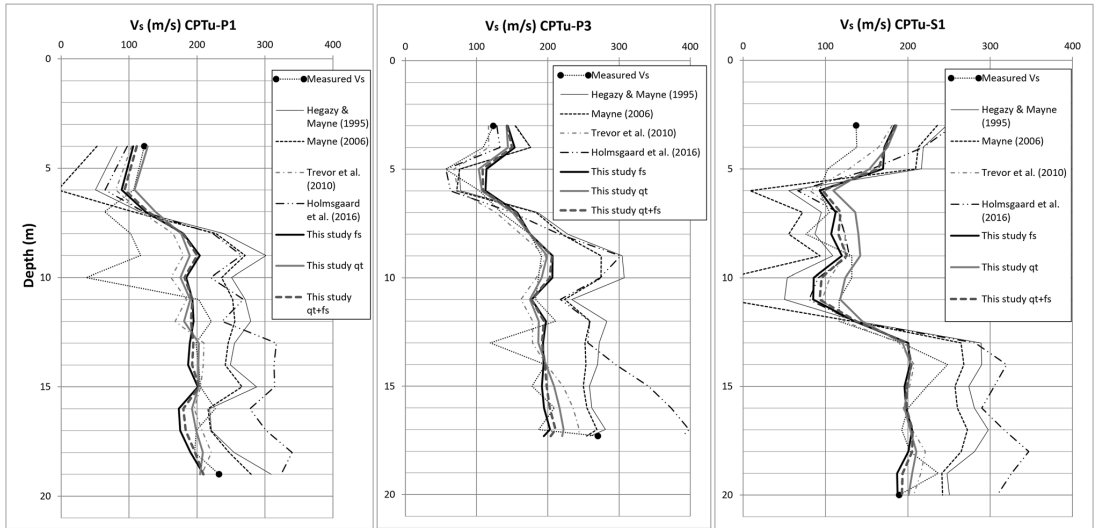
Fig. 5 Comparison of V_s as predicted from CPT–V_s correlations and measured using SCPTu at the Paldiski and Soodi sites

from the correlations are calculated from CPTu readings, measured at intervals of 20 mm and rounded to 1-m-thick layers. The rounded layer interval is the same as that in the V_s measurements.

$$V_s = 95.7 \cdot f_s^{0.155}, \tag{5}$$

$$V_s = 128.4 \cdot q_t^{0.169}, \tag{6}$$

$$V_s = 103.9 \cdot q_t^{0.058} \cdot f_s^{0.107}. \tag{7}$$

To test the performance of existing and newly derived functions, the computed V_s values are plotted against the measured V_s values in Fig. 6. Regression analyses were performed on each set of results to achieve the best-fit line of the computed/measured ratios of V_s. The linear regression function and corresponding coefficient of determination (R^2) were then obtained. The closer the best-fit line to the perfect-fit line, the higher the R^2 value and the better the correlation function. The R^2 values are presented in Table 4, and the equations of the best-fit lines are presented in Table 5. Because the results of the Ahtri site showed the lowest correlation, the data of this site were analysed separately; the data from the Paldiski and Soodi sites were analysed together. All seven correlations

offered the best results for the Paldiski and Soodi sites. Of the existing functions, the correlation proposed by Trevor et al. [4] showed the best results based on Paldiski and Soodi site data, according to R^2 and the best-fit line. The correlation offered the R^2 value of 0.70. Based on the R^2 and best-fit lines, the correlations presented in this paper provide equivalent results for the Paldiski and Soodi sites. The R^2 value of function (5) is 0.55, function (6) is 0.69 and function (7) is 0.61. However, based on the results from all three sites, all three correlations proposed in this paper offer the best results. Functions (5) and (7) also obtain the highest R^2 value of 0.33 for the data from all three sites. Moreover, functions (6) and (7) provide the lowest COV value of 0.28 for the data from all three sites. The lowest correlation occurred at the Ahtri site, where the R^2 values of all seven correlations were between 0.10 and 0.17. Although the results show great scatter, the correlation proposed in this paper offers close results compared to the measured V_s values at all three sites, as shown in Fig. 4. A significant difference occurred only in CPTu-A1, CPTu-A3 and CPTu-A4 soundings deeper than 14 m at the Ahtri site. The correlations proposed by Hegazy and Mayne [1] and Mayne [3] showed significant flaps at all three study points. However, in the remaining third of the study points, these correlations did not show a good flap. The correlation proposed by Holmsgaard et al. [2] showed a significant flap with only a few study points.
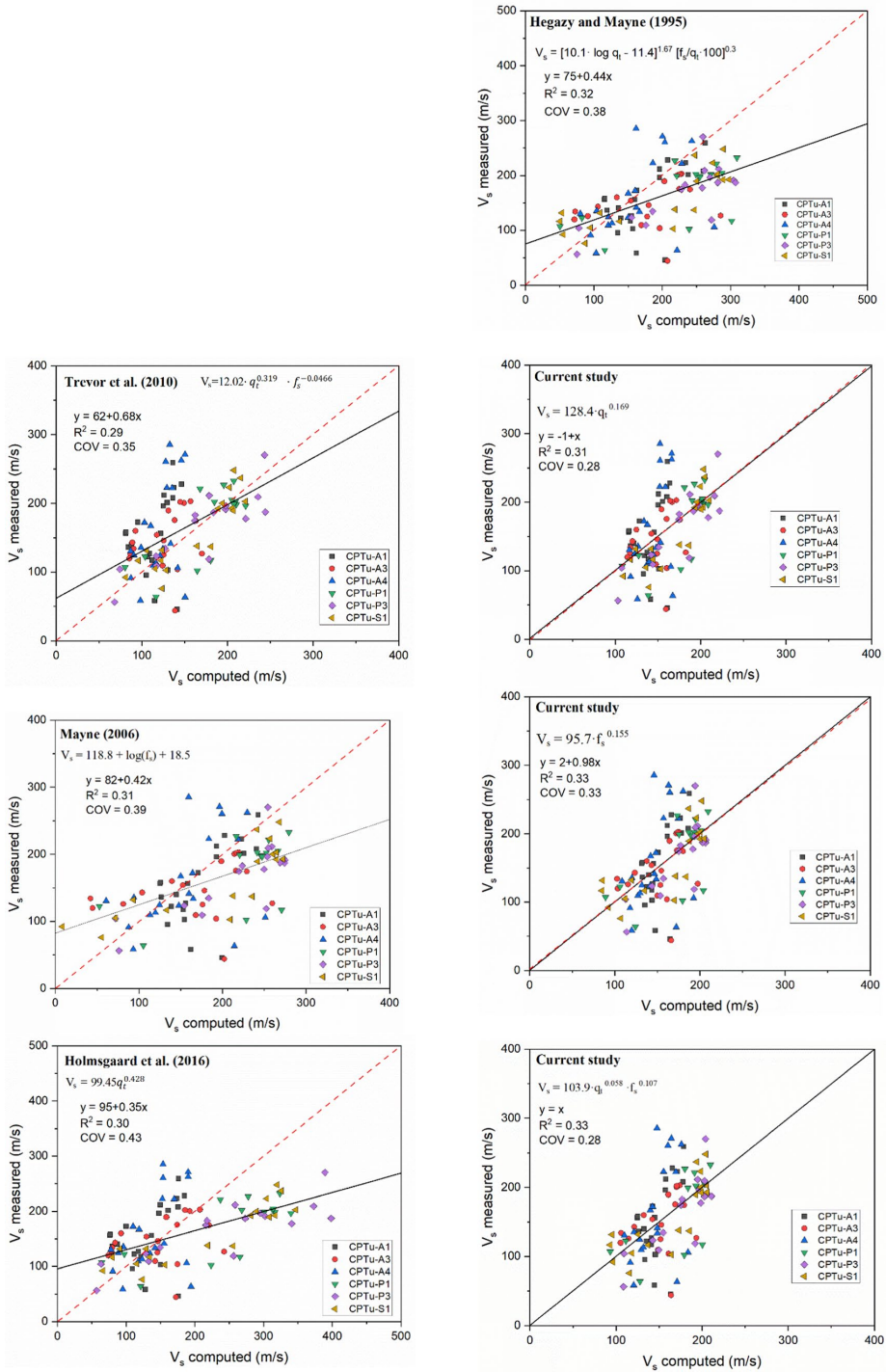
Fig. 6 Evaluation of correlations between computed and measured shear wave velocity V_s for silty soils

Table 4 Coefficient of determination (R^2) for all seven correlations

Name of test sites and number of data points	Hegazy and Mayne [1]	Mayne [3]	Trevor et al. [4]	Holmsgaard et al. [2]	Current correlation based on f_s (5)	Current correlation based on q_t (6)	Current correlation based on q_t+f_s (7)
Ahtri + Paldiski + Soodi ($n=106$)	0.32	0.31	0.29	0.30	0.33	0.31	0.33
Paldiski + Soodi ($n=48$)	0.55	0.51	0.70	0.71	0.55	0.69	0.61
Ahtri ($n=58$)	0.16	0.17	0.10	0.11	0.17	0.11	0.16

Table 5 Coefficients and exponents for (G/G_{max}) V_s. normalised pseudo-strain ($\gamma_f/\gamma_{\text{p-ref}}$) formulation (Eq. 8)

Pile classification (type/installation method)	α1	β1
Bored cast in situ	1.912	0.97
Auger	1.176	1.01
Driven	0.84	1.07
Jacked	0.65	1.25
Screw pile (current study)	0.305	1.68

Estimated Versus Measured Load–Displacement Capacity of the Pile

Using the V_s values measured based on soundings SCPTu-A4, SCPTu-S1, SCPTu-P1 and SCPTu-P2, the G_{max} values were calculated alongside the pile and beneath the pile base with Eq. 2. To determine the mass density of the soil, CPTu readings were applied with Eq. 4. The soil layers adjacent to the pile were counted as a single soil layer in which the increase in the value of G_{max} is a function of depth [11]. Note that the depth-G_{max} figures were compiled from all four soundings and the best-fit line was found (Fig. 7). The soil around the pile base was treated as a second soil layer. G_{max} values were found on the basis of the V_s values measured at the depth of the pile base.

Equation 3 was applied to determine the Q–w relationship of seven screw piles in silty soils. The values $f = 1$ and $g = 0.2$, 0.3 and 0.4 were used in this analysis. The pile types and dimensions are given in Table 2. Piles A-3, P-1 and P-3 were Fundex piles; piles S-1 and S-2 were displacement (DSP) piles; and piles S-3 and S-4 were full displacement (FDP) piles.

Because static pile load tests were not carried to the pile failure, the Q–w curves were extended using Chin's [28] extrapolation. The Q–w curves of all seven piles are presented in Fig. 8. Only the last two to three pile load test values were extrapolated at the Soodi site; most of them were extrapolated from the pile load test of P-1. In piles A-3 and P-1, the last third of the Q–w curve values were extrapolated.

For most analysed piles, the extrapolated results closest to the measured values were taken at $g = 0.4$. For the DSP piles (S-1 and S-2), the value $g = 0.4$ provided a satisfactory alignment with the measured values. For FDP piles (S-3 and S-4), $g = 0.4$ tended to underestimate the bearing capacity of the pile. On two out of three Fundex piles (A-3, P-1 and P-3), the Q–w curves exhibited an adequate alignment with the $g = 0.4$ line. Therefore, it is reasonable to use $g = 0.4$ to derive the Fundex pile Q–w curve in silty soils.

Discussion

In this study, the V_s values ranged between 37 and 352 m/s (Table 3). Poulos [33] proposed that the typical value of V_s for rough estimation is in the range of 85–105 m/s for very soft soils and 276–365 m/s for very stiff soils. For silty soils, Holmsgaard et al. [2] recommended a V_s range of 150–250 m/s. Based on several previous studies, Hussien and Karray [34] presented V_s values for sandy soils in the range of 127–327 m/s for a stress state of $K = 1.0$. As shown in Figs. 1, 2, 3, V_s values of approximately 100 m/s and as small as 37 m/s were measured in sensitive fine-grained, silty sand and sandy silt layers, which were no deeper than 10 m. In deeper layers, the measured V_s values ranging from 150 to 250 m/s agreed with the range proposed by Holmsgaard et al. [2], with small exceptions. Additionally, these measured values fell well within the range presented by Hussien and Karray [34] and Poulos [33]. In the current study, most measured V_s values in depths deeper than 10 m were approximately 200 m/s.

For the analysis of CPTu and V_s correlations, the results obtained at the Ahtri site were treated separately. In the Ahtri site, the soil layers below 14–16 m depth appeared to be more silty than in the two other sites. The results in Fig. 4 illustrate this as, at depths of 14–16 m, the correlations proposed in the present work interlace clearly for all three study points. Other investigated correlations provided satisfying flaps in the range of 14–16-m depths. In the deeper layers, only the correlations from Hegazy and Mayne [1] and Mayne [3] provided an approximate flap. In deeper layers, the soils of complex silt and sand mixtures
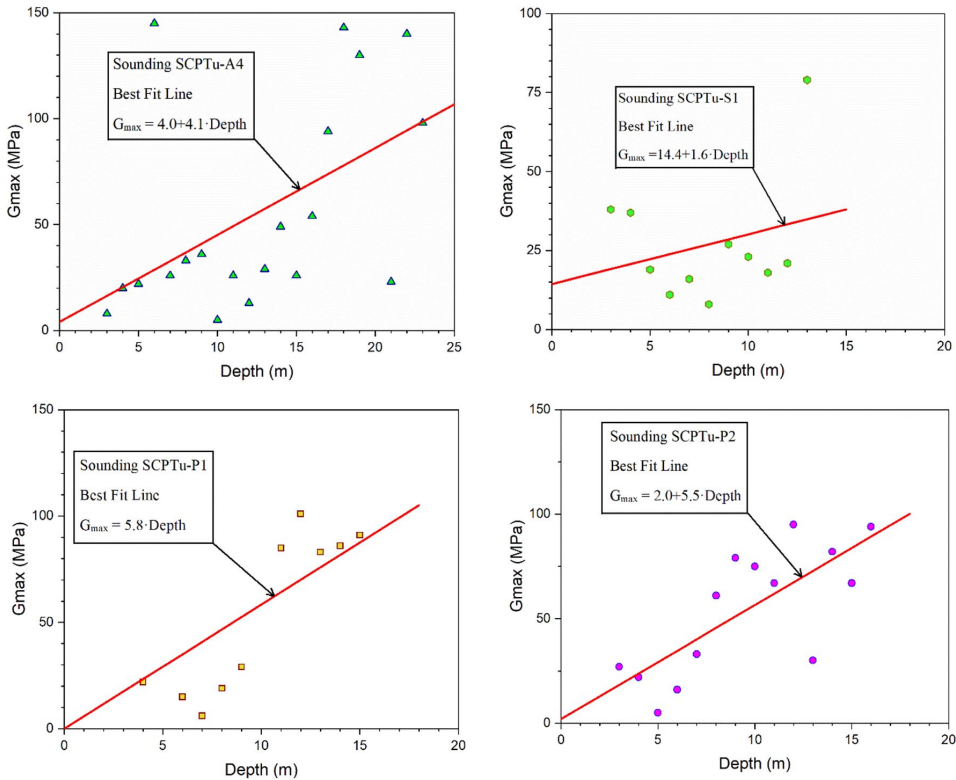
Fig. 7 Depth-G_{max} figures for all four soundings with best-fit lines

rested at the Ahtri site. The beginning of the silt and sand mixtures was well distinguished from the u_2 profile (Fig. 1) between 13 and 16 m, where the value of pore water pressure dropped sharply. For such soils, all correlations reviewed in this paper significantly underestimated the V_s values, apart from the correlations provided by Hegazy and Mayne [1] and Mayne [3].

The correlations proposed using Eqs. 5, 6 and 7 offered the best flap (Fig. 5) for the Paldiski and Soodi sites. The correlation provided by Trevor et al. [4] also showed excellent results. The other three correlations substantially overestimated the V_s value in most soil layers at study points CPTu-P1 and CPTu-P3 at the Paldiski site. At study point CPTu-S1, the same three correlations significantly overestimated the V_s value in several layers and significantly underestimated the V_s value in some layers. This clearly indicates that creating CPTu and V_s correlations for mixed soils is complicated. In mixed soils, universal correlations may not yield good results; hence, a correlation based on a specific soil is necessary. Such mixed soils need further investigation in the future.

As shown in Figs. 4 and 5, the V_s values resulting from the correlations provided by Hegazy and Mayne [1] and Mayne [3] approximated each other at all study points. The correlation provided by Hegazy and Mayne [1] included all CPTu readings, whereas the one provided by Mayne [3] used only f_s values. In addition, Eq. 7 does not offer better results than Eqs. 5 and 6. Therefore, correlations with a single input value may provide good results. This is clear evidence that correlations based on the q_t or f_s values should be used separately. Through this action, it becomes feasible to compare correlation findings derived from separate analyses of the same CPTu soundings.

Measuring the V_s value at the site provides a good opportunity to derive the pile Q–w relationship based on Eqs. 1–3. One of the key constant in the analysis is the exponent parameter g. In this study, the value of $g = 0.4$ was found to be the most suitable for screw piles in silty soils. Based on the results of the seven static pile load tests, back-calculations were performed, resulting in a correlation (8) between normalised operative shear stiffness (G/G_{max}) and normalised pseudo-strain ($\gamma_p/\gamma_{p\text{-ref}}$) with a coefficient
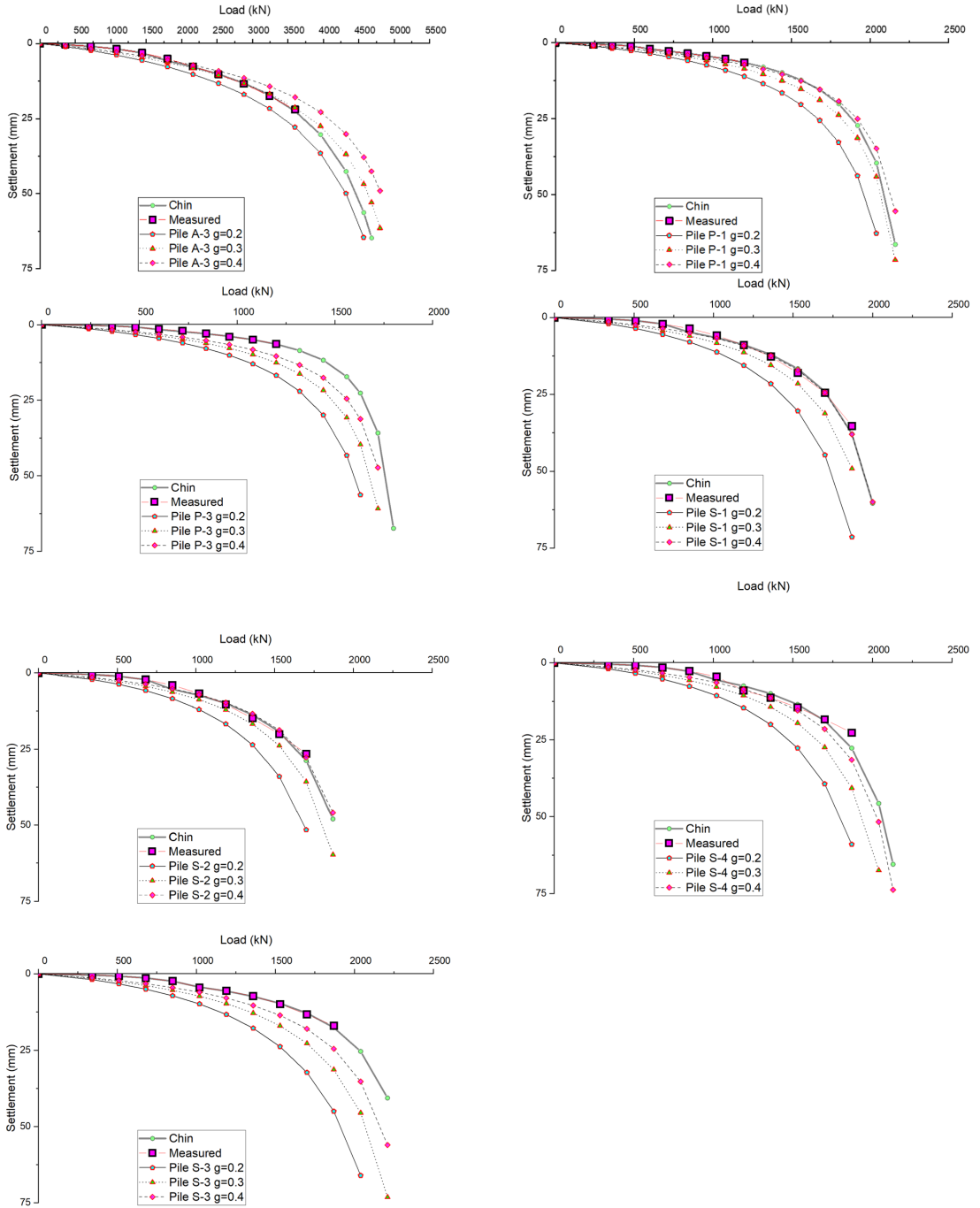
Fig. 8 Estimated pile *Q*–*w* relationships found using Eq. 2 with *g* = 0.2, 0.3 and 0.4 for all seven piles. The results are presented alongside those of the static pile load test curves. The last parts of the pile load test curves were extrapolated using Chin's method

of determination of $R^2 = 0.97$ for $N = 101$ data points. The results are presented in Fig. 9. The values obtained by extrapolation can influence the results in the region of larger strains, which appear in the lower right part of the figure. However, in this part of the graph, the results from the different piles demonstrate minimal scatter. Thus, the presented correlations provide favourable outcomes and deserve attention.

A form of the correlation analysed in the current study was presented by Niazi and Mayne [11], who analysed 299 pile load tests at 61 sites. In their study, a modified hyperbola was introduced based on the curves of Vardanega and Bolton [35]. Niazi and Mayne [11] proposed the following correlation (9), based on stiffness reduction from 299 pile load tests obtained through back-analysis. Coefficient $\alpha 1$ and exponent $\beta 1$ are parameters that identify the pile type and installation methods, as presented in Table 5. Piles are divided into four groups: driven, jacked, auger and bored cast in situ. The values of $\alpha 1$ and $\beta 1$ obtained in the current study are presented in the last line of Table 5. These numbers differ significantly from the values proposed by Niazi and Mayne [11]. It is evident from Fig. 9 that the outcomes of the Niazi and Mayne [11] correlations for various pile categories significantly deviate from the correlation suggested in this study for screw piles in silty soils. Screw piles exhibit the most gradual decrease in shear stiffness within the initial range of per cent γ_p (< 0.3), becoming steeper for high values. Furthermore, it is evident from Fig. 9 that the screw pile exhibits superior load-bearing capacity in comparison to the other referenced pile types, particularly at small strains. This indicates the need for similar correlations to comprise larger numbers of pile types in different soils.
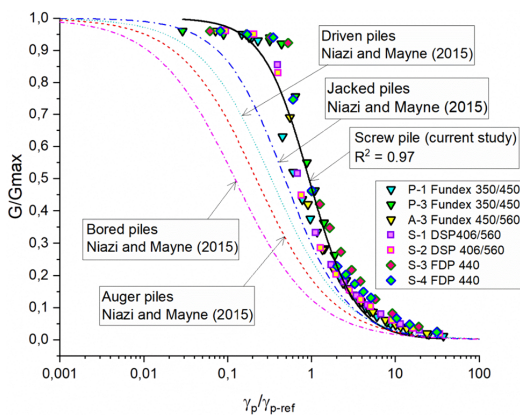
Current study $\quad \dfrac{G}{G_{\max}} = \dfrac{1}{\left[1 + 1.108\left(\frac{\gamma_{\mathrm{ref}}}{\gamma_{\mathrm{p\text{-}ref}}}\right)^{1.58}\right]}.$ (8)

Niazi and Mayne (2015) $\quad \dfrac{G}{G_{\max}} = \dfrac{1}{\left[1 + 3.634\alpha 1\left(\frac{\gamma_{\mathrm{ref}}}{\gamma_{\mathrm{p\text{-}ref}}}\right)^{0.942\beta 1}\right]}.$ (9)

Conclusions

This study examines the potential of SCPTu in evaluating the load-bearing capacity of a pile in silty soils. Since one of the key values of the entire study is V_s reading, the research also analyses the correlations between CPTu readings and V_s. This study analysed four correlations between CPTu and V_s, as presented in the literature. These correlations were denied to a variety of soils [1, 3], particularly silty soils [2, 4]. The best flaps for the selected correlations at all three sites were determined based on Trevor et al.'s [4] correlation. The other three correlations demonstrated significant deviations from the measured results at several study points. Significant flaps for the V_s values for most soil layers were found in all three site specific correlations proposed in the paper. At the Ahtri site, the only approximating flaps with complex silt and sand soil mixtures were found based on the correlations from Hegazy and Mayne [1] and Mayne [3]. This indicates the need to study more mixed soils to produce suitable correlations. Correlations based on q_t of f_s values should be preferred for comparisons of correlation results obtained from independent readings of the same CPTu sounding.

The shear wave velocity V_s values ranged from 37 to 352 m/s in the soils examined in this study. The minimum V_s values and values around 100 m/s were measured in sensitive fine-grained layers, as well as in silty sand and sandy silt layers up to a depth of 10 m. Deeper than 10 m, V_s values of approximately 200 m/s dominated. The range of V_s values measured in this study mostly coincided with the range proposed by Holmsgaard et al. [2] for silty soils and Hussien and Karray [34] for sandy soils. Additionally, the ranges of V_s values measured in this study generally agree with those proposed by Poulos [33] for very soft soils and very stiff soils.

The present study analysed the static load test of seven screw piles in silty soils at three sites. Three Fundex piles, two DSP piles and two FDP piles were included in the study. Because the piles were not tested for their ultimate bearing capacity, Chin's extrapolation was used to complete the Q–w curve. In addition, seven SCPTu soundings were conducted at the three sites. The V_s values obtained from the

Fig. 9 Correlation between normalised operative shear stiffness ($G/G_{\max}$) and normalised pseudo-strain ($\gamma_p/\gamma_{\mathrm{p\text{-}ref}}$), where $\gamma_p = w_t/d$ and $\gamma_{\mathrm{p\text{-}ref}} = 0.01$

soundings were used to determine the soil stiffness (G_{max} or G_0) values. G_{max} was applied in the analytical elastic solution for pile–soil interactions proposed by Randolph and Wroth [14, 15]. Based on this study, $g = 0.4$ (Eq. 1) is the most suitable for screw piles in silty soils. Additionally, correlations between normalised operative shear stiffness (G/G_{max}) and normalised pseudo-strain ($\gamma_p/\gamma_{\text{p-ref}}$) were developed with $R^2 = 0.97$ for $N = 101$ data points based on the back-calculations of the static pile load test results. The results might have been affected by the extrapolation of pile load test results, causing some uncertainty. The results at the Soodi site were the least affected because only a few values were extrapolated. In general, the influence of the extrapolated values on the accuracy of the outcome was found to be negligible. The outcomes of the study were compared with the values proposed by Niazi and Mayne [11] based on 299 pile load tests from 61 sites. The results of the present study differed significantly from these, indicating the need to construct similar correlations for a larger number of pile types in different soils.

Data availability Enquiries about data availability should be directed to the authors.

Declarations

Conflict of interest The authors have no relevant financial or non-financial interest to disclose.

References

1. Hegazy, Y.A., & Mayne, P.W. (1995). Statistical correlations between Vs and CPT data for different soil types. In *Proceedings, Symposium on Cone Penetration Testing* (Vol. 2, pp 173–178), Swedish Geotechnical Society, Linköping, Sweden.

2. Holmsgaard R, Ibsen LB, Nielsen BN (2016) Interpretation of seismic cone penetration testing in silty soil. Electron J Geotech Eng 21(15):4759–4779

3. Mayne PW (2006) The 2nd James K Mitchell Lecture: Undisturbed sand strength from seismic cone tests. Geomechanics and Geoengineering 1(4):239–247

4. Trevor, F.A., Paisley, J.M. & Mayne, P.W. (2010). Cone penetration tests at active earthquake sites. In *Proceedings, 2nd International Symposium on Cone Penetration Testing (CPT'10)* (9–11 May, pp 519–526), Huntington Beach, CA, USA.

5. Cai G, Liu S, Puppala AJ (2012) Reliability assessment of CPTu-based pile capacity predictions in soft clay deposits. Eng Geol 141–142:84–91

6. Eslami, A. (1996). Bearing capacity of piles from cone penetrometer test data. Ph. D. Thesis (p 516), University of Ottawa, Department of Civil Engineering.

7. Moshfeghi S, Eslami A (2016) Study on pile ultimate capacity criteria and CPT-based direct methods. International Journals of Geotechnical Engineering. https://doi.org/10.1080/19386362.2016.1244150

8. Berardi R, Bovolenta R (2005) Pile-settlement evaluation using field stiffness non-linearity. Proceedings, Institution of Civil Engineering, Geotechnical Engineering 158(GE1):35–44

9. Mayne PW, Poulos HG (2001) Approximate displacement influence factors for elastic shallow foundations. ASCE Journal of Geotechnical & Geoenvironmental Engineering 127(1):100–102

10. Niazi FS, Mayne PW (2014) Axial pile response of bidirectional O-cell loading from modified analytical solution and downhole shear wave velocity. Can Geotech J 51(11):1284

11. Niazi FS, Mayne PW (2015) Operational soil stiffness from back-analysis of pile load tests within elastic continuum framework. Geotechnical Engineering Journal of the SEAGS & AGS-SEA 46:1–19

12. Niazi, F.S., Mayne, P.W., & Woeller, D.J. (2010). Case history of axial pile capacity and load-settlement response by SCPTu. In *Proceedings, 2nd International Symposium on Cone Penetration Testing (CPT`10)* (Vol 3, pp 9-16), Huntington Beach, Calif.

13. Cooke RW, Price G, Tarr K (1979) Jacked piles in London clay: A study of load transfer and settlement under working conditions. Géotechnique 29(2):113–147

14. Randolph MF, Wroth CP (1978) Analysis of deformation of vertically-loaded piles. ASCE J Geotech Eng Div 104(GT12):1465–1488

15. Randolph, M.F., & Wroth, C.P. (1979). A simple approach to pile design and the evaluation of pile tests. In *Behavior of Deep Foundations STP 670, ASTM* (pp 484–499), West Conshohocken, PA.

16. Fahey M, Carter J (1993) A finite element study of the pressuremeter using a nonlinear elastic plastic model. Can Geotech J 30(2):348–362

17. Mayne, P.W. (2000). Enhanced geotechnical site characterization by seismic piezocone penetration test. In *Invited lecture, Fourth International Geotechnical Conference* (pp 95–120), Cairo University.

18. Jamiolkowski, M., Lancellotta, R., LoPresti, D.C.F., & Pallara, O. (1994). Stiffness of Toyoura sand at small and intermediate strain. In *Proceedings, 13th International Conference on Soil Mechanics and Foundation Engineering (1)* (pp 169–172), New Delhi.

19. Tatsuoka, F., Jardine, R.J., LoPresti, D.C.F., DiBenedetto, H., & Kodaka, T. (1997). Theme lecture: characterizing the pre-failure deformation properties of geomaterials. In *Proceeedings, 14th International Conf. on Soil Mechanics & Foundation Engineering* (Vol 4, p 35).

20. Burns SE, Mayne PW (1996) Small- and high-strain measurements of in situ soil properties using the seismic piezocone penetrometer. Transp Res Rec 1548:81–88

21. Mayne, P.W. (1995). Application of G/Gmax modulus degradation to foundation settlement analyses. In *Proceedings, U.S.-Taiwan Workshop on Geotechnical Collaboration* (pp 136–148), National Science Foundation/Washington D.C. and National Science Council/Taipei.

22. Mayne, P.W. (2005). Integrated ground behaviour: In-situ and laboratory tests. *Deformation Characteristics of Geomaterials* (2) (155–177.C), Taylor & Francis, UK

23. Mayne, P.W. (2007). In-situ test calibrations for evaluating soil parameters. In *Characterization & Engineering Properties of Natural Soils* (Vol 3, pp 1602–1652), Taylor & Francis Group, London.

24. Mayne, P.W., Peuchen, J., & Bouwmeester, D. (2010). Estimation of soil unit weight from CPTs. In *Proceedings, 2nd International Symposium on Cone Penetration Testing (CPT'10)* (CA, Vol 2, pp 169-176), Huntington Beach.

25. Leetsaar L, Korkiala-Tanttu L, Kurnitski J (2022) CPT, CPTu and DCPT methods for predicting the ultimate bearing capacity of cast in situ displacement piles in silty soils. Geotech Geol Eng. https://doi.org/10.1007/s10706-022-02292-6

26. Leetsaar, L., & Korkiala-Tanttu, L. (2023). Deterministic and probabilistic analyses of the bearing capacity of screw cast in situ displacement piles in silty soils as measured by CPT and SDT. The Baltic Journal of Road and Bridge Engineering. https://bjrbe-journals.rtu.lv/article/view/bjrbe.2023-18.600

27. EN 1997–1:2004. Eurocode 7: Geotechnical Design—Part 1: General Rules (p. 171), Brussels, Belgium, (2004).

28. Chin, F.K. (1970). Estimation of the ultimate load of piles from test not carried to failure. In *Proceedings, Second Southeast Asia Conference on Soil Engineering* (pp 81–90), Singapore.

29. Maertens, J., & Huybrechts, N. (2003). Results of the static pile load tests at the Limelette test site. In *Proceedings, 2nd Symposium on Screw Piles—Belgian Screw Pile Technology—Design and Recent Developments* (pp 167–214), Brussels, Balkema, ISBN: 9058095789.

30. Robertson, P.K. (2010). Soil behaviour type from the CPT: An update. In *2nd International Symposium on Cone Penetration Testing, CPT'10*, Huntington Beach, CA, USA. www.cpt10.com

31. American Society for Testing & Materials (2000) ASTM Book of Standards (vol. 4, Sections 08 and 09), Construction Materials. Soils Rocks, Philadelphia, PA.

32. EN ISO 22476–1:2012 Geotechnical investigation and testing. Field testing. Part 1: Electrical cone and piezocone penetration test. ISO 2012.

33. Poulos HG (2022) Use of shear wave velocity for foundation design. Geotech Geol Eng 40:1921–1938. https://doi.org/10.1007/s10706-021-02000-w

34. Hussien MN, Karray M (2016) Shear wave velocity as a geotechnical parameter: An overview. Can Geotech J 53(2):252

35. Vardanega PJ, Bolton MD (2013) Stiffness of clays and silts: Normalizing shear modulus and shear strain. Journal of Geotechnical and Geoenvironmental Engineering 139(9):1575–1589

BUSINESS +
ECONOMY

ART +
DESIGN +
ARCHITECTURE

SCIENCE +
TECHNOLOGY

CROSSOVER

DOCTORAL
THESES